eCAM
Evidence-Based Complementary and Alternative Medicine

# Evidence-Based ZHENG: A Traditional Chinese Medicine Syndrome 2013

Guest Editors: Shi-Bing Su, Wei Jia, Aiping Lu, and Shao Li

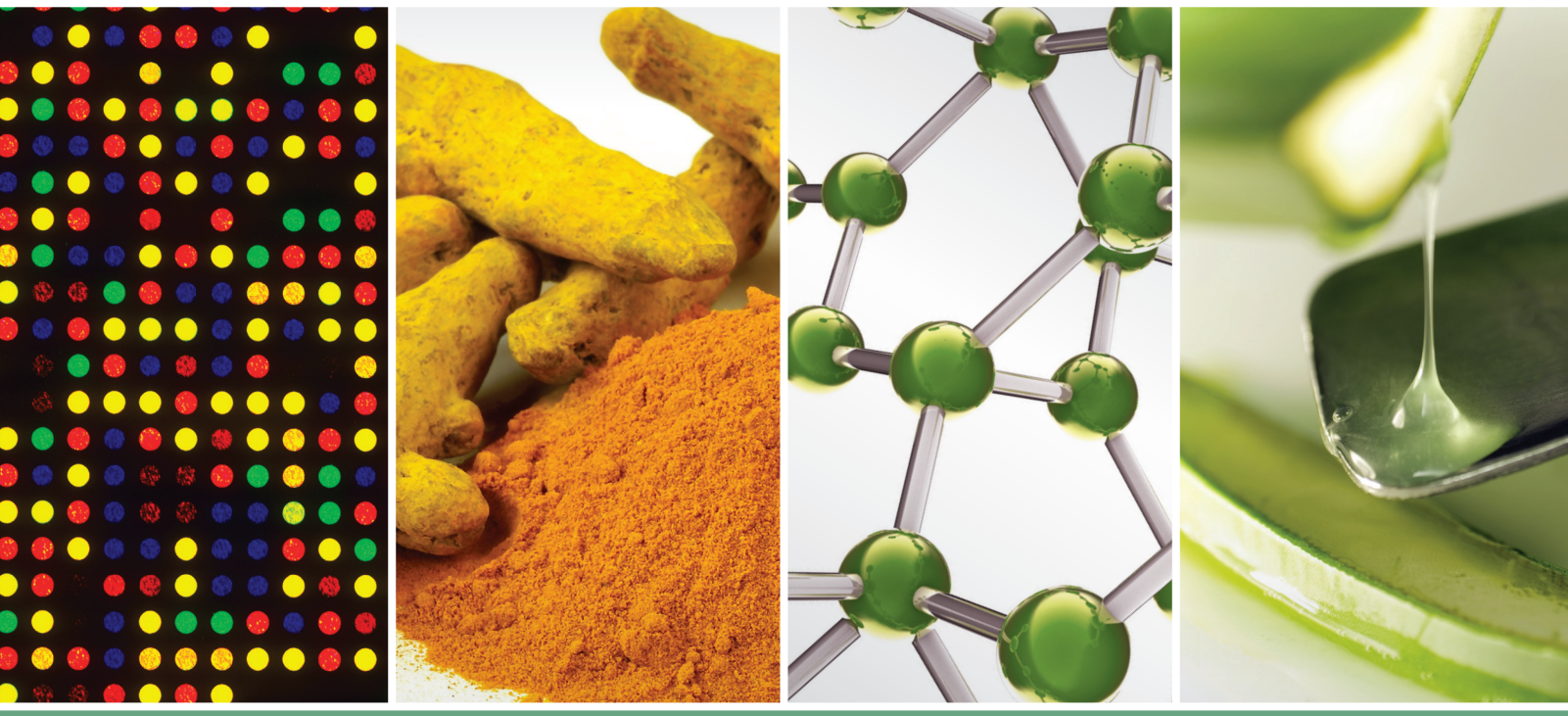

# Evidence-Based ZHENG: A Traditional Chinese Medicine Syndrome 2013

Evidence-Based Complementary and Alternative Medicine

# Evidence-Based ZHENG: A Traditional Chinese Medicine Syndrome 2013

Guest Editors: Shi-Bing Su, Wei Jia, Aiping Lu, and Shao Li

# Editorial Board

# Contents

Hindawi Publishing Corporation
Evidence-Based Complementary and Alternative Medicine
Volume 2014, Article ID 484201, 2 pages
http://dx.doi.org/10.1155/2014/484201

*Editorial*

# Evidence-Based ZHENG: A Traditional Chinese Medicine Syndrome 2013

**Shi-Bing Su,[1] Wei Jia,[2] Aiping Lu,[3] and Shao Li[4]**

[1] *Research Center for Complex System of Traditional Chinese Medicine, Shanghai University of Traditional Chinese Medicine, Shanghai 201203, China*
[2] *University of Hawaii Cancer Center, Honolulu, HI 96813, USA*
[3] *School of Chinese Medicine, Hong Kong Baptist University, Kowloon Tong, Hong Kong*
[4] *Bioinformatics Division, TNLIST and Department of Automation, Tsinghua University, Beijing 100084, China*

Correspondence should be addressed to Shi-Bing Su; shibingsu07@163.com

Received 24 December 2013; Accepted 24 December 2013; Published 6 May 2014



ZHENG, also known as traditional Chinese medicine (TCM) syndrome or TCM pattern, is an integral and essential part of TCM theory. A TCM ZHENG, in essence, is a characteristic profile of all clinical manifestations that can be identified by a TCM practitioner. Clinical treatments of a patient rely on the successful differentiation of a specific ZHENG. Recently, technologies and methods of omics, bioinformatics, bionetwork, and data mining through a system biology approach were applied in ZHENG research, which have significantly facilitated the development of ZHENG theory. Following 2012 Evidence-Based ZHENG special issue, we have further grouped together 15 excellent papers on TCM ZHENG research and put them forward for publication in this special issue.

Firstly, there are 2 research papers in this special issue which addressed the clinical trials based on TCM ZHENG classification and treatment. A paper has evaluated the adaptability of TCM ZHENG diagnosis and found that "Yang-Xu Zheng" of TCM is an early prognostic predictor for patients with severe sepsis and septic shock. Another paper, with a randomized, double-blind clinical study, has evaluated the efficacy of crest herbal toothpaste in "clearing internal heat." Interestingly it has been instructed that the toothpaste (Crest Herbal Crystal) is efficacious through brushing with 1 g toothpaste for 2 minutes each time, 2 times per day in 4 weeks in the internal heat. In addition, the studies of the acupuncture, an efficient therapeutic method originated in ancient China, have also been systematically reviewed.

In TCM, the clinical diagnosis of ZHENG relies on the gathering of clinical information through inspection, auscultation and olfaction, inquiry, and palpation. For ZHENG measurement of the inquiry, 2 research articles of this special issue presented the ZHENG diagnostic methods. A research article discussed the method of objective auscultation of TCM based on wavelet packet fractal dimension and support vector machine. Another paper has investigated ZHENG classification with missing feature values using local-validity approach. This is through the study of the value contributed by symptoms to syndrome diagnosis of chronic hepatitis B, that is, diagnosis weight, constructing symptom-syndrome scale of chronic hepatitis B, and realizing quantitative diagnosis from symptom to syndrome.

Five research articles of this special issue presented the TCM ZHENG classification using profiles of genes, proteins, metabolites, and/or biomarkers. Therein, it has been identified as the relationship between EGF, TGFA, and EGFR gene polymorphisms and ZHENG in gastric cancer, and the curative effects of ZHENG-based Fuzheng-Huayu tablet on hepatitis B caused cirrhosis related to CYP1A2 genetic polymorphism. Moreover, a study of rheumatoid arthritis with deficiency pattern has showed the correlation with cold and hot patterns in gene expression profiles. A new biomarker feature pattern has been identified consisting of TNF-a, IL-10, and IL-8 for blood stasis syndrome corresponding to myocardial ischemia. Additionally, recent advances in metabolomics study of TCM ZHENG have been reviewed.

Bioinformatics and bionetwork are becoming a cutting-edge research field in current TCM ZHENG and ZHENG-based treatment studies. In this special issue, a research article analyzed the characteristics of ZHENG from excessive to deficient syndromes in hepatocarcinoma underlying miRNA array data using bioinformatics and bionetwork techniques. Moreover, a network-based systematic study presented the mechanism of ZHENG related treatment in patients with cough variant asthma, suggesting that the network-based systematic study will be a good way to improve the scientific understanding of mechanism of the treatment of ZHENG.

In TCM, ZHENG experimental models are necessary tools for the mechanistic study of ZHENG and the evaluation of TCM treatment. In this special issue, a review paper summarized the utilization of model organisms in the construction of TCM ZHENG experimental model and highlighted the relevance of modern medicine with ZHENG animal model. Moreover, a paper reported the establishment of an experimental breast cancer ZHENG model and the ZHENG-based curative effect evaluation of a Chinese medicine formula Zuo-Jin Wan. Furthermore, the protective effects of two herbal extract and their metabolic signatures in rat kidney yang deficiency syndrome model have been also presented. More reports on ZHENG experimental models are expected in the near future.

In summary, the concept of TCM ZHENG, as a main diagnostic approach in TCM, would provide invaluable guidance for the therapeutic choices and personalized disease management, not only in traditional medical practices but in modern healthcare systems as well. We look forward to an increasing number and sizes of clinical trials and experimental approaches utilizing TCM ZHENG to be conducted in the future to further promote the development of evidence-based personalized medicine.

*Shi-Bing Su*
*Wei Jia*
*Aiping Lu*
*Shao Li*

Hindawi Publishing Corporation
Evidence-Based Complementary and Alternative Medicine
Volume 2014, Article ID 502348, 11 pages
http://dx.doi.org/10.1155/2014/502348

*Research Article*

# Objective Auscultation of TCM Based on Wavelet Packet Fractal Dimension and Support Vector Machine

**Jian-Jun Yan,[1] Rui Guo,[2] Yi-Qin Wang,[2] Guo-Ping Liu,[2] Hai-Xia Yan,[2] Chun-Ming Xia,[1] and Xiaojing Shen[1]**

[1] *Center for Mechatronics Engineering, East China University of Science and Technology, Shanghai 200237, China*
[2] *Laboratory of Information Access and Synthesis of TCM Four Diagnostic, Shanghai University of Chinese Traditional Medicine, Shanghai 201203, China*

Correspondence should be addressed to Rui Guo; guoruier@sina.com and Yi-Qin Wang; wangyiqin2380@sina.com

Received 18 August 2013; Accepted 5 November 2013; Published 5 May 2014

Academic Editor: Shi-bing Su



This study was conducted to illustrate that auscultation features based on the fractal dimension combined with wavelet packet transform (WPT) were conducive to the identification the pattern of syndromes of Traditional Chinese Medicine (TCM). The WPT and the fractal dimension were employed to extract features of auscultation signals of 137 patients with lung Qi-deficient pattern, 49 patients with lung Yin-deficient pattern, and 43 healthy subjects. With these features, the classification model was constructed based on multiclass support vector machine (SVM). When all auscultation signals were trained by SVM to decide the patterns of TCM syndromes, the overall recognition rate of model was 79.49%; when male and female auscultation signals were trained, respectively, to decide the patterns, the overall recognition rate of model reached 86.05%. The results showed that the methods proposed in this paper were effective to analyze auscultation signals, and the performance of model can be greatly improved when the distinction of gender was considered.

## 1. Introduction

As one of the four diagnostic methods of Traditional Chinese Medicine (TCM), auscultation identifies a syndrome or disease by listening to the speech of patients. Auscultation method was definitely proposed in the Internal Classic of Huang Di [1]. However, it was not until after the Ming and Qing Dynasties that this method attracted attention from the medical field and both its theoretical and clinical application underwent much development. Since then, auscultation has become a distinctive step-by-step diagnostic method. In TCM, auscultation mainly depends on the auditory senses of the physician to accurately identify asthenia, sthenia, and visceral lesions in the patient. Therefore, auscultation is considered a qualitative method that produces unconvincing results.

Objective studies on auscultation have made some progress with the recent developments in computer and signal processing technologies [2]. Frequency spectrum analysis was made on the voice of cough patients making use of digital sonograph [3], but it cannot be quantitatively analyzed and applied for clinical diagnosis. The survey about objective auscultation of TCM was presented in [4], in which the digital technology with respect to auscultation was described and analyzed. The nonlinearity of the vowel /a:/ signals of healthy persons and patients with deficiency syndrome was investigated by using delay vector variance [5], whose studies were an effective attempt on the objective auscultation research. Chiu et al. proposed four novel acoustic parameters, the average number of zero-crossings, the variations in local peaks and valleys, the variations in first and second formant frequencies, and the spectral energy ratio to analyze and identify the characteristics among nondeficiency, Qi-deficiency, and Yin-deficiency subjects [6]. The energy values of wavelet packet coefficients were extracted for the auscultation signals of healthy people and patients with five Zang-organs diseases, and the results were analyzed and discussed [7, 8]. Wavelet packet transform (WPT) and Sample Entropy were combined together to analyze the auscultation signals in TCM. Sample Entropy values for WPT coefficients reflecting the complexity

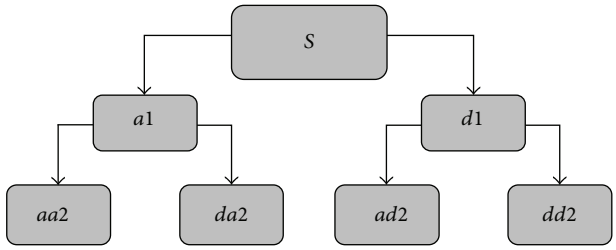


Figure 1: Tree of two-layer WPD.

of the signal in different time-frequency resolutions were computed to quantify the signals from three kinds of samples including Qi-deficiency, Yin-deficiency, and healthy people. The statistical and classification results indicated that the method is useful and effective in auscultation research [9].

These studies provide a good basis for the objective research on its clinical use. However, these studies are still in their initial stages, the experiments are usually carried out in limited conditions, the adopted auscultation signals are not typical and comprehensive enough, and the algorithms are unreliably conducted on a small sample database. Therefore, the creation of a reliable and accurate algorithm remains a challenge in auscultation research.

Speech production is a complex process to analyze through traditional methods as it is influenced by glottis, track, and radiation [10]. The nonlinear characteristics of speech, such as the changes in the voice of the speaker when pronouncing the same phoneme twice, also hinder its analysis. Moreover, the predicted signal cannot accurately match the original speech regardless of the linear production order. Pronunciation includes both the nonlinear libration process and the speech itself. Changes in the shape of the tongue and track, particularly in spirant and explodent speeches, can produce a whirlpool on the track boundary layer that subsequently becomes a chaotic onflow [11]. The time-domain waveform of speech is self-comparable, and it also observes the characteristics of periodicity and randomicity. These findings show that chaos and fractal theories can be used in speech signal analysis [12].

Speech analysis must also be improved. The chaotic and fractal characteristics of speech suggest the combination of the nonlinear fractal dimension and the wavelet packet transform (WPT) to solve the problems in speech signal analysis. This study employed fractal dimension with WPT to analyze the auscultation signals of patients with chronic bronchitis as research object. The patients with chronic bronchitis occurred mostly in the pattern of lung Qi-deficiency and the pattern of lung Yin-deficiency. Therefore, this study analyzed the auscultation signals of patients with lung Qi-deficient pattern, patients with Yin-deficient pattern, and healthy subjects as control. Statistical analysis was made to obtain the effective features, which were used in the multiclass support vector machine (SVM) classifiers. Classification models were constructed to automatically identify the auscultation samples. The classification results are discussed at the end of the study.

Table 1: The group, sex, and age of all subjects in the experiments.

| | Group H | Group Y | Group Q |
|---|---|---|---|
| Subjects | | | |
| Male | 10 | 11 | 47 |
| Female | 33 | 38 | 90 |
| Total | **43** | **49** | **137** |
| Age (mean ± std) | 26.3 ± 6.2 | 53.5 ± 10.6 | 45.2 ± 12.5 |

## 2. Materials and Methods

*2.1. Collected Materials.* Patients who met the diagnostic criteria of chronic bronchitis and provided informed consent were included in the present study. The diagnostic criteria of patients were based on western medicine and TCM. The diagnostic criteria based on western medicine were adopted "the chronic bronchitis clinical diagnosis and curative effect judgment standard" [13]. The diagnostic criteria based on TCM were according to "Guideline for Clinical Study on New Drugs of Traditional Chinese Medicine" [14] and "Clinic Terminology of Traditional Chinese Medical Diagnosis and Treatment-Syndromes" [15], which is the national standard made by the State Bureau of Technical Quality Supervision, as well as the standards in textbooks [16, 17]. Patients with other severe disease, as well as those who cannot express their feelings clearly and did not provide informed consent, were excluded in the present study.

A total of 229 subjects were collected by TCM Syndrome Lab in Shanghai University of Traditional Chinese Medicine. The 186 patients with chronic bronchitis from the affiliated hospital of Shanghai University of TCM were separated into two groups, namely, lung Qi-deficient subjects (Group Q) and lung Yin-deficient subjects (Group Y). Fourty-three healthy subjects from the faculty of the Shanghai University of TCM were in control group (Group H). The detailed information is listed in Table 1. Lung Qi-deficiency and lung Yin-deficiency are TCM specific terms. The pattern of lung Qi-deficiency refers to the condition of declining function of the lung in governing Qi and defending the exterior. Its clinical manifestations are weak cough, panting, spitting of clear and thin phlegm, laziness in speaking, fatigue and a pale complexion, and other signs and symptoms. The pattern of lung Yin-deficiency refers to lung-yin failing to disperse and descend and an internal production of deficient-heat. Its clinical manifestations are dry cough or cough with scanty and sticky sputum or even with blood-streaked sputum, a dry mouth and throat, emaciation, a feverish sensation in the palms, night sweats, red cheeks and a hoarse voice, and other signs and symptoms.

The speech signals of the three groups were recorded using a microphone and were digitized using a 24-bit A/D acquisitive card (Brand CME Xcorpio, with a frequency response range of 20 Hz to 20 kHz and a dynamic range of 100 dB) at a 16 KHz sampling rate with an antialiasing function. The speech signals were recorded at a maintained collecting distance and position. The vowel /a:/ is easy for either patients or healthy people to pronounce. In addition, the vocal organ is not abuttal and there is no obstacle in

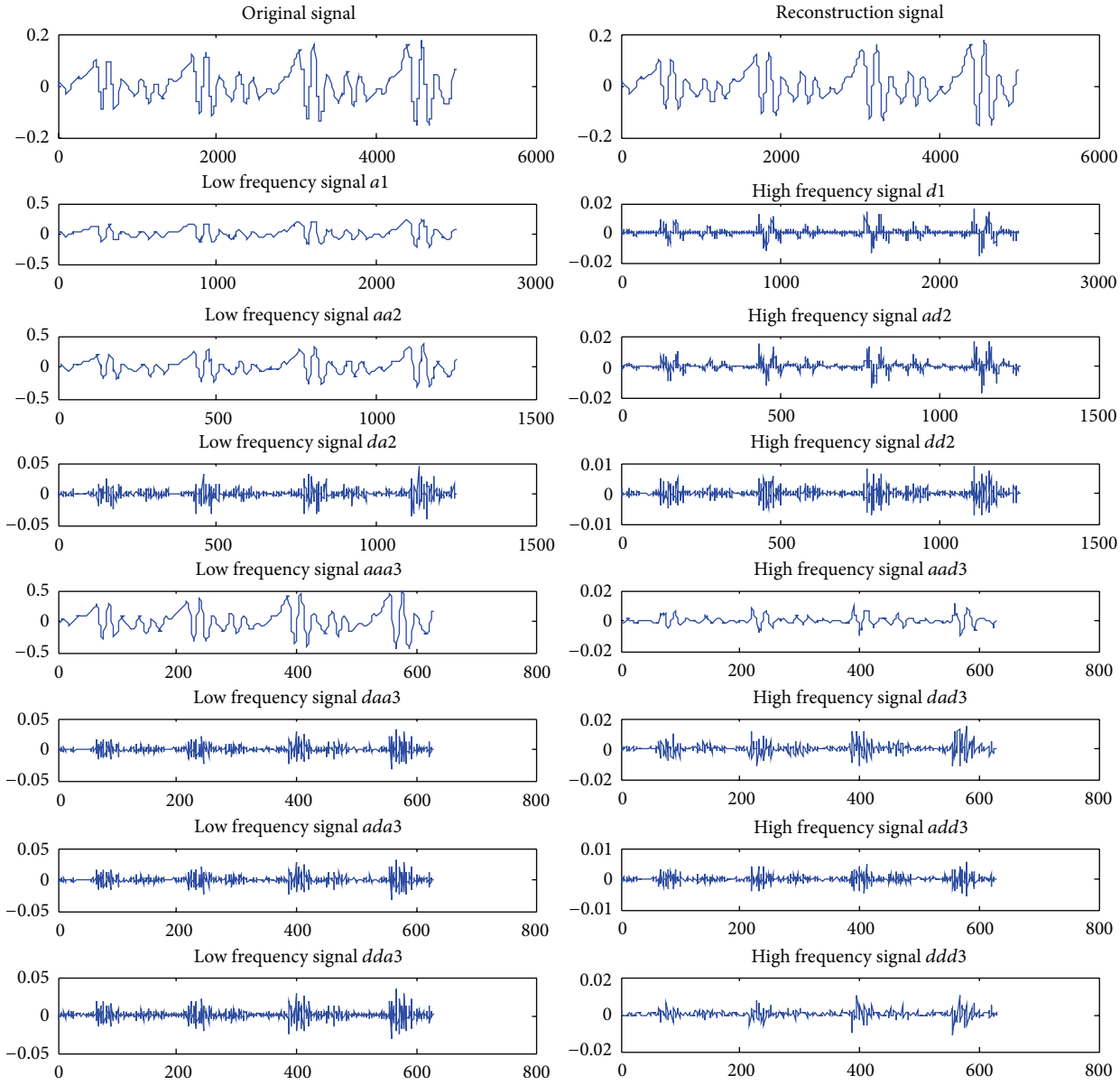


Figure 2: Decomposed and reconstructed waveform of a certain voice signal.

cavity when someone is sending out the vowel [18]. Thus, each patient was asked to utter the vowel /a:/. Each subject produced a sustained stable phonation of vowel /a:/ that lasted for about 1 second.

The research was conducted at Shanghai University of TCM and its affiliated hospital after the approval of the moral and ethical committee of Shanghai University of TCM and informed consent of all subjects had been obtained.

### 2.2. Methods

*2.2.1. Wavelet Packet Decomposition Algorithm.* Wavelet transform is a time-frequency analysis method that uses different scales to obtain the best time-domain and frequency-domain resolutions in different parts of the signal. Resolution analysis conducts further decomposition in the low frequency part only to prevent the subdivision of the high frequency part [19, 20]. WPT provides a more precise decomposition for the signal analysis and carries out further decomposition in the high frequency part to subdivide the frequency bands in the low and high frequency parts synchronously. WPT can also self-adaptively select the signal resolution in different frequency bands to improve the time-frequency resolution [21–23].

A common wavelet function consists of the Harr wavelet, Daubechies wavelet, SymletsA wavelet, Coiflet wavelet, Morlet wavelet, and Mexican Hat wavelet. After comparing the analysis results of db, coif, and sym wavelet functions, the db4 wavelet function with a high energy concentration was ultimately chosen for the analysis of the speech signals of the three sample groups [24]. Figure 1 shows the two-layer WPD tree, and Figure 2 shows the decomposition of a speech

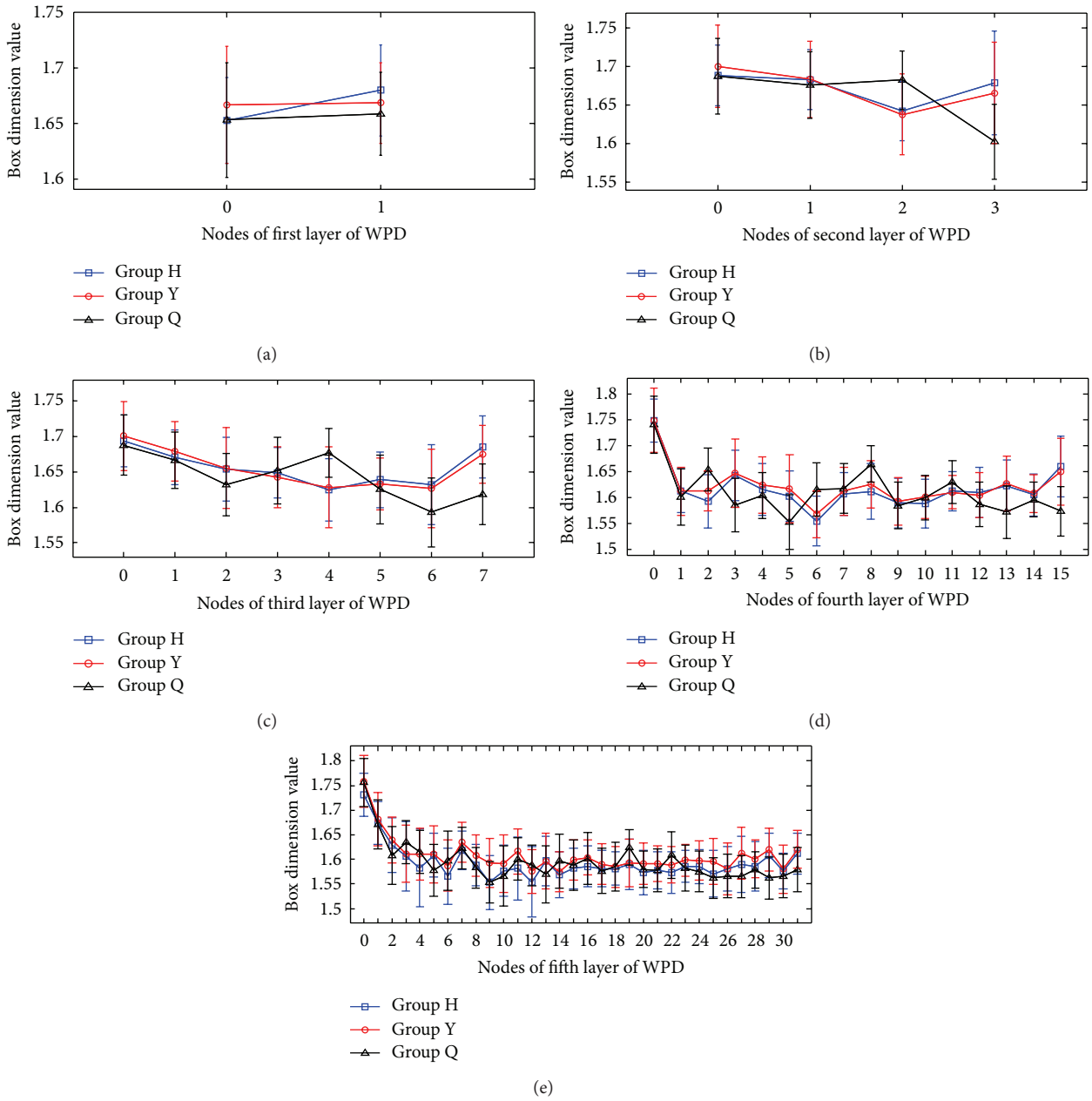


FIGURE 3: Box dimension values of the coefficients of WPT decomposition for all subjects: (a–e) box dimension values for the first to the fifth layer coefficients.

signal at layer 3, where $S$ is the original signal, $a$ represents the approximations (the low frequency components), and $d$ represents the details (the high frequency components).

*2.2.2. Fractal Dimension.* Although the fractal dimension has several definitions [25], the box dimension definition is used in this paper for calculation convenience. Time sequence $A$ of the speech signal is covered with a reticulation grid. $S$ represents the border length, and $N(S)$ denotes the number of mesh grids that contain set $A$ [26]. The box dimension definition is represented by the following equation:

$$D_B = \sum_{s \to 0} \frac{\log N(S)}{\log(1/S)}. \quad (1)$$

The least square method (LSM) is used to approximate the $\log N(s) \sim \log(1/s)$ line. The slope is represented by box dimension $D_B$. The approximation is carried out as follows.

(1) The original speech is unified to a unit square area with a gain signal of $x(t)$, $x(t) \leq 1$.

(2) The square area is divided into the mesh grids, and the $\log N(s)$ and $\log(1/s)$ are calculated. The change in $S$ is recorded, and the corresponding $\log N(s)$ and $\log(1/s)$ are calculated.

(3) Let $x_i = \log(1/s_i)$ and $y_i = \log N(s_i)$, $i = 1, 2, \ldots, M$. $(x_i, y_i)$ is used to approximate line $y = kx + b$ by

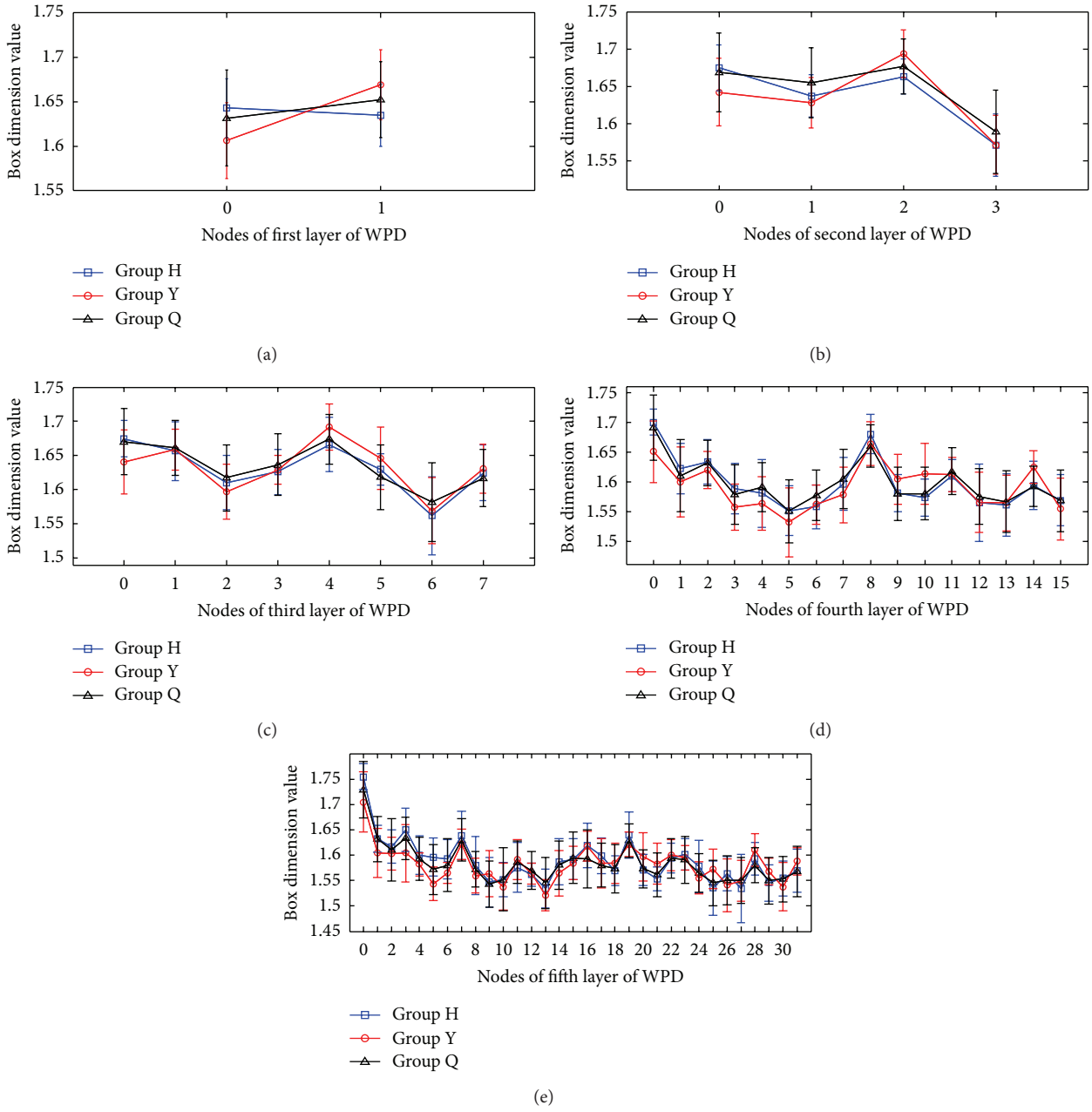


FIGURE 4: Box dimension values of the coefficients of WPT decomposition for male subjects: (a–e) box dimension values for the first to the fifth layer coefficients.

LSM. $k$ represents the box dimension $D_B$, which is calculated as follows:

$$D_B = \frac{\left(\sum_{i=1}^{M} y_i\right)\left(\sum_{i=1}^{M} x_i\right) - M\left(\sum_{i=1}^{M} y_i x_i\right)}{\left(\sum_{i=1}^{M} x_i\right)^2 - M\left(\sum_{i=1}^{M} {x_i}^2\right)}. \quad (2)$$

*2.2.3. Wavelet Packet Fractal Dimension.* Fractal theory is found to be in agreement with the wavelet analysis in terms of self-similarity and understanding things from coarse to fine scales [27]. This paper proposes a wavelet packet fractal theory that uses the WPD of the auscultation signals to compare the box dimension value and its changes in different frequency bands to reflect the irregularity, complexity, and nonstationarity of the signals. The box dimension values of the discrete signals range from 1 to 2, indicating that the more complex the signals are, the greater the box dimension values become.

*2.2.4. Support Vector Machine.* SVMs were first introduced by Vapnik (1998) to perform highly effective classification, regression, and pattern recognition processes [28]. SVM uses a hypothesis space of linear functions in a high-dimensional space and is trained with a learning algorithm

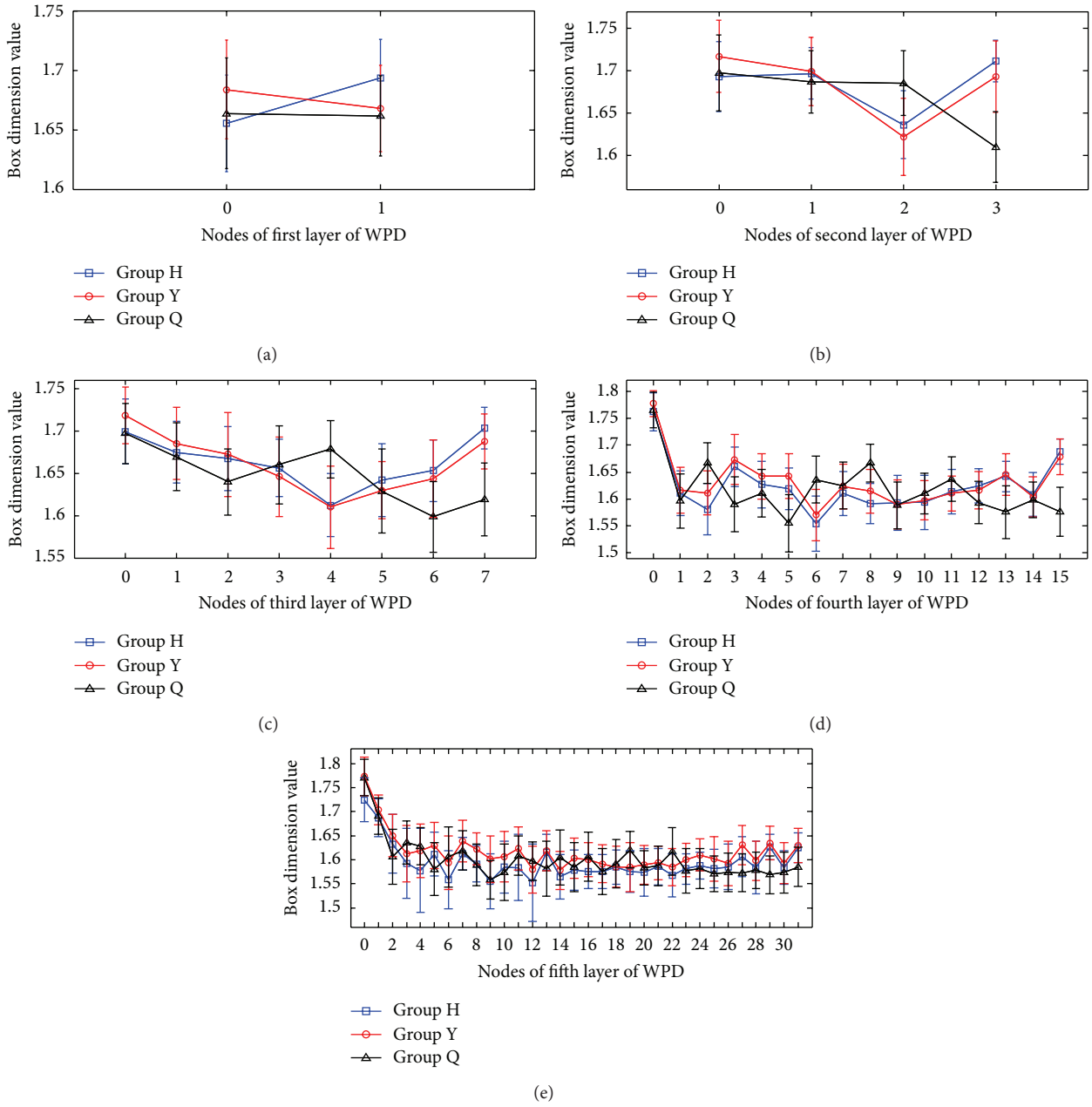


FIGURE 5: Box dimension values of the coefficients of WPT decomposition for female subjects: (a–e) box dimension values for the first to the fifth layer coefficients.

from optimization theory that implements a learning bias from statistical learning theory. SVM uses a linear model to implement nonlinear class boundaries by nonlinearly mapping input vectors into a high-dimensional feature space using kernels [29, 30]. Previous studies suggest using the Radial Basis Function (RBF) kernel as a default kernel. The kernel parameters can be automatically chosen by optimizing a cross-validation-based model selection. One-against-one (1-versus-1) and one-against-rest (1-versus-r) are two popular multi-SVM schemes. In a $k$-class problem, 1-versus-1 forms a training subset for every possible class pair combination and learns an SVM model from each subset. A total of $k \times (k-1)/2$ SVM classifiers are trained for all the combinations. The class for an unseen example is obtained by majority vote of all binary SVM classifiers. The classification result is affected if the same kernel parameters are used in all the SVM classifiers that apply the 1-versus-1 scheme. Therefore, the kernel parameters of each SVM classifier must be separately identified through cross-validation. A multiclass SVM classifier is used to identify the auscultation signals. Each SVM classifier chooses specific RBF kernel parameters through a grid search with a nested cross-validation [31].

Table 2: Significant difference between the box dimension values for the coefficients of the subbands from the first to fifth layers in all subjects.

| Node | Frequency band (KHz) | Group H (mean ± std) | Group Y (mean ± std) | Group Q (mean ± std) |
|---|---|---|---|---|
| 1.1 | 4–8 | $1.680 \pm 0.041^{\#}$ | $1.668 \pm 0.037$ | $1.659 \pm 0.037^{*}$ |
| 2.2 | 4–6 | $1.642 \pm 0.038^{\#}$ | $1.638 \pm 0.053^{\#}$ | $1.683 \pm 0.038^{*\wedge}$ |
| 2.3 | 6–8 | $1.679 \pm 0.067^{\#}$ | $1.666 \pm 0.066^{\#}$ | $1.603 \pm 0.048^{*\wedge}$ |
| 3.0 | 0-1 | $1.694 \pm 0.037$ | $1.701 \pm 0.049^{\#}$ | $1.688 \pm 0.042^{\wedge}$ |
| 3.2 | 2-3 | $1.654 \pm 0.045^{\#}$ | $1.655 \pm 0.057^{\#}$ | $1.632 \pm 0.044^{*\wedge}$ |
| 3.4 | 4-5 | $1.625 \pm 0.044^{\#}$ | $1.628 \pm 0.057^{\#}$ | $1.677 \pm 0.035^{*\wedge}$ |
| 3.6 | 6-7 | $1.632 \pm 0.057^{\#}$ | $1.627 \pm 0.055^{\#}$ | $1.593 \pm 0.048^{*\wedge}$ |
| 3.7 | 7-8 | $1.685 \pm 0.044^{\#}$ | $1.675 \pm 0.041^{\#}$ | $1.618 \pm 0.043^{*\wedge}$ |
| 4.2 | 1–1.5 | $1.593 \pm 0.051^{\#}$ | $1.613 \pm 0.039^{\#}$ | $1.655 \pm 0.041^{*\wedge}$ |
| 4.3 | 1.5–2 | $1.643 \pm 0.049^{\#}$ | $1.647 \pm 0.066^{\#}$ | $1.586 \pm 0.051^{*\wedge}$ |
| 4.4 | 2–2.5 | $1.616 \pm 0.050$ | $1.624 \pm 0.054^{\#}$ | $1.604 \pm 0.044^{\wedge}$ |
| 4.5 | 2.5–3 | $1.603 \pm 0.048^{\#}$ | $1.618 \pm 0.065^{\#}$ | $1.553 \pm 0.053^{*\wedge}$ |
| 4.6 | 3–3.5 | $1.555 \pm 0.048^{\#}$ | $1.568 \pm 0.045^{\#}$ | $1.616 \pm 0.051^{*\wedge}$ |
| 4.8 | 4–4.5 | $1.612 \pm 0.053^{\#}$ | $1.626 \pm 0.045^{\#}$ | $1.665 \pm 0.035^{*\wedge}$ |
| 4.10 | 5.5–6 | $1.613 \pm 0.038^{\#}$ | $1.611 \pm 0.032^{\#}$ | $1.630 \pm 0.041^{*\wedge}$ |
| 4.11 | 6–6.5 | $1.611 \pm 0.048^{\#}$ | $1.605 \pm 0.044^{\#}$ | $1.587 \pm 0.043^{*\wedge}$ |
| 4.12 | 6.5–7 | $1.623 \pm 0.049^{\#}$ | $1.627 \pm 0.052^{\#}$ | $1.573 \pm 0.050^{*\wedge}$ |
| 4.14 | 7.5–8 | $1.661 \pm 0.058^{\#}$ | $1.650 \pm 0.064^{\#}$ | $1.574 \pm 0.048^{*\wedge}$ |
| 5.0 | 0–0.25 | $1.731 \pm 0.044^{\#}$ | $1.758 \pm 0.053$ | $1.757 \pm 0.049^{*}$ |
| 5.2 | 0.5–0.75 | $1.629 \pm 0.056^{\#}$ | $1.639 \pm 0.046^{\#}$ | $1.607 \pm 0.059^{*\wedge}$ |
| 5.3 | 0.75–1 | $1.606 \pm 0.071^{\#}$ | $1.611 \pm 0.058^{\#}$ | $1.635 \pm 0.044^{*\wedge}$ |
| 5.4 | 1–1.25 | $1.583 \pm 0.079^{\#}$ | $1.610 \pm 0.053$ | $1.616 \pm 0.044^{*}$ |
| 5.5 | 1.25–1.5 | $1.608 \pm 0.044^{\#}$ | $1.610 \pm 0.058^{\#}$ | $1.578 \pm 0.053^{*\wedge}$ |
| 5.6 | 1.5–1.75 | $1.566 \pm 0.058^{\#}$ | $1.587 \pm 0.052$ | $1.597 \pm 0.060^{*}$ |
| 5.7 | 1.75–2 | $1.619 \pm 0.039^{\wedge}$ | $1.635 \pm 0.041^{*}$ | $1.623 \pm 0.042$ |
| 5.8 | 2–2.25 | $1.588 \pm 0.042^{\wedge}$ | $1.608 \pm 0.042^{*\#}$ | $1.583 \pm 0.042^{\wedge}$ |
| 5.9 | 2.25–2.5 | $1.553 \pm 0.055^{\wedge}$ | $1.593 \pm 0.050^{*\#}$ | $1.553 \pm 0.043^{\wedge}$ |
| 5.10 | 2.5–2.75 | $1.577 \pm 0.052$ | $1.591 \pm 0.059^{\#}$ | $1.566 \pm 0.061^{\wedge}$ |
| 5.11 | 2.75–3 | $1.582 \pm 0.064^{\wedge}$ | $1.616 \pm 0.046^{*\#}$ | $1.601 \pm 0.043^{\wedge}$ |
| 5.12 | 3–3.25 | $1.554 \pm 0.071^{\#}$ | $1.576 \pm 0.044^{\#}$ | $1.588 \pm 0.042^{*\wedge}$ |
| 5.13 | 3.25–3.5 | $1.597 \pm 0.051^{\#}$ | $1.597 \pm 0.057^{\#}$ | $1.569 \pm 0.057^{*\wedge}$ |
| 5.14 | 3.5–3.75 | $1.569 \pm 0.047^{\#}$ | $1.575 \pm 0.041^{\#}$ | $1.597 \pm 0.055^{*\wedge}$ |
| 5.16 | 4–4.25 | $1.586 \pm 0.042^{\wedge\#}$ | $1.604 \pm 0.035^{*}$ | $1.602 \pm 0.053^{*}$ |
| 5.19 | 4.75–5 | $1.590 \pm 0.051^{\#}$ | $1.593 \pm 0.048^{\#}$ | $1.624 \pm 0.036^{*\wedge}$ |
| 5.21 | 5.25–5.5 | $1.578 \pm 0.038$ | $1.591 \pm 0.036^{\#}$ | $1.578 \pm 0.044^{\wedge}$ |
| 5.22 | 5.5–5.75 | $1.573 \pm 0.043^{\#}$ | $1.589 \pm 0.037^{\#}$ | $1.609 \pm 0.047^{*\wedge}$ |
| 5.23 | 5.75–6 | $1.586 \pm 0.032^{\wedge}$ | $1.599 \pm 0.032^{*\#}$ | $1.582 \pm 0.046^{\wedge}$ |
| 5.24 | 6–6.25 | $1.585 \pm 0.035$ | $1.598 \pm 0.040^{\#}$ | $1.575 \pm 0.041^{\wedge}$ |
| 5.25 | 6.25–6.5 | $1.570 \pm 0.047^{\wedge}$ | $1.595 \pm 0.046^{*\#}$ | $1.562 \pm 0.041^{\wedge}$ |
| 5.27 | 6.75–7 | $1.590 \pm 0.057^{\#}$ | $1.612 \pm 0.053^{\#}$ | $1.565 \pm 0.043^{*\wedge}$ |
| 5.28 | 7–7.25 | $1.586 \pm 0.051$ | $1.601 \pm 0.039^{\#}$ | $1.579 \pm 0.037^{\wedge}$ |
| 5.29 | 7.25–7.5 | $1.608 \pm 0.045^{\#}$ | $1.620 \pm 0.044^{\#}$ | $1.562 \pm 0.043^{*\wedge}$ |
| 5.31 | 7.75–8 | $1.612 \pm 0.041^{\#}$ | $1.620 \pm 0.038^{\#}$ | $1.579 \pm 0.045^{*\wedge}$ |

Compared with Group H, $^{*}P < 0.05$. Compared with Group Y, $^{\wedge}P < 0.05$. Compared with Group Q, $^{\#}P < 0.05$.

## 3. Experimental Results

*3.1. Feature Analysis.* The auscultation signals were processed by a self-developed analytic program under the Matlab environment. The decomposition structure tree at layer 7 was used for the WPD of the auscultation signals in the computer experiment. $2^i$ frequency subbands were observed at the $i$th layer after the WPD of the speech signals. The fractal dimensions of the speech voice in each subband were calculated with a sampling rate of 16,000 Hz and 16 bit precision. The frequency bands for these subbands are as follows: first layer (frequency interval = 4 kHz, $n = 0, 1$),

Table 3: Significant difference between the box dimension values for the coefficients of the subbands from the first to fifth layers in male subjects.

| Node | Frequency band (KHz) | Group H (mean ± std) | Group Y (mean ± std) | Group Q (mean ± std) |
|---|---|---|---|---|
| 2.2 | 4–6 | $1.663 \pm 0.024^{\wedge}$ | $1.694 \pm 0.032^{*}$ | $1.677 \pm 0.037$ |
| 4.0 | 0–0.5 | $1.701 \pm 0.022^{\wedge}$ | $1.651 \pm 0.052^{*\#}$ | $1.691 \pm 0.055^{\wedge}$ |
| 4.4 | 2–2.5 | $1.581 \pm 0.057$ | $1.564 \pm 0.045^{\#}$ | $1.592 \pm 0.042^{\wedge}$ |
| 4.10 | 5–5.5 | $1.573 \pm 0.031$ | $1.614 \pm 0.052^{\#}$ | $1.580 \pm 0.045^{\wedge}$ |
| 4.14 | 7–7.5 | $1.594 \pm 0.041$ | $1.625 \pm 0.028^{\#}$ | $1.592 \pm 0.034^{\wedge}$ |
| 5.1 | 0.25–0.5 | $1.755 \pm 0.026^{\wedge}$ | $1.704 \pm 0.059^{*}$ | $1.729 \pm 0.056$ |
| 5.5 | 1.25–1.5 | $1.596 \pm 0.037^{\wedge}$ | $1.544 \pm 0.033^{*\#}$ | $1.572 \pm 0.049^{\wedge}$ |

Compared with Group H, $^{*}P < 0.05$. Compared with Group Y, $^{\wedge}P < 0.05$. Compared with Group Q, $^{\#}P < 0.05$.

second layer (frequency interval = 2 kHz, $n = 0, 1, 2, 3$), third layer (frequency interval = 1 kHz, $n = 0, 1, 2, \ldots, 7$), fourth layer (frequency interval = 0.5 kHz, $n = 0, 1, 2, \ldots, 15$), and fifth layer (frequency interval = 0.25 kHz, $n = 0, 1, 2, \ldots, 31$). After calculating the box dimensions of vowel /a:/ and observing the fractal dimension trajectory curve, the following findings were made.

(1) The box dimension value in each subband ranges from 1.3 to 1.8, indicating the existence of a regular fractal dimension space distribution for the auscultation signals. This result also indicates that the box dimension value of auscultation signals is completely different from that of noise.

(2) The auscultation signals of male subjects are different from those of female subjects.

(3) Different auscultation signals have different box dimension values, and the box dimension values between the first layer and the second layer of WPD significantly differ. Figures 3 to 5 show different trends in the box dimension values between the first layer and the fifth layer subbands.

*3.2. Statistical Analysis.* The statistical analysis software SPSS 20 was used to analyze the differences between the samples. Age as covariant was included in the statistic model to correct the effect of age. The box dimension values of the WPT coefficients from the first to the fifth layers were analyzed to identify the significant differences between the two groups of samples. Table 2 shows 43 frequency bands with significantly different box dimension values from the first to fifth layers in all subjects. Table 3 shows 7 frequency bands with significantly different box dimension values from the first to fifth layers in the male subjects. Table 4 shows 48 frequency bands with significantly different box dimension values from the first to fifth layers in the female subjects.

*3.3. Classification.* The multiclass SVM was applied as a classifier to discriminate Group Q, Group Y, and Group H by the extracted features of box dimension. The RBF function was chosen as the kernel function. The classification model, in which every binary classifier had its own feature subset and RBF kernel parameters, was constructed to identify the auscultation signals based on the libsvm software [32].

In the process of classification, threefold cross-validation was applied on the classification of auscultation signals. For comparison of recognition accuracy, the experiments were done with different training data. The classification results using multiclass SVM were shown in Table 5. When the auscultation signals of all subjects were trained by SVM to decide the patterns of TCM syndromes, the overall accuracy of all subjects was 79.49%. When auscultation signals of male and female auscultation signals were trained, respectively, to decide the patterns of TCM syndromes, the overall accuracy of male subjects was 91.95% and that of female subjects was 72.07%. And the overall accuracy of male and female subjects was 86.05%, which was the weighted accuracy and the weight was the proportion of subject number of the group with different gender in all samples.

## 4. Discussions

In TCM, the signs and symptoms can be captured through four methods of diagnosis, namely, inspection, auscultation and olfaction, inquisition, and pulse taking. Combined use of four methods is necessary for acquiring full and detailed clinical information as well as disease diagnosis. Auscultation is indispensable part of four methods. The traditional auscultation depends on subjective hearing; however, accurate auscultation is difficult to be done by TCM doctors who lack experience and have decrease in hearing acuity. Therefore, objective research of auscultation is highly desirable, which contributes to quantitatively combined use of four methods, avoiding clinical misdiagnosis or missed diagnosis.

Box dimension $D_B$ can be used for analysis and classification in auscultation research. Independent from $D_B$, the auscultation signal shows a relatively steady fractal dimension value, and the dimension values among the subbands show significant differences. Figures 3(b)–3(d) and Table 2 show that Group H and Group Y share the same variations in their box dimension values. The box dimension values of Group H and Group Y for all subjects are the largest in the low frequency band, then those become lower, and finally the box dimension values of all groups rise to certain extent in the high frequency band. However, the box dimension value of Group Q of all subjects is higher, and then it fluctuates in the other frequency bands. As shown in Figures 4(b)–4(d) and Table 3, Group H has the similar variety of box dimension

Table 4: Significant difference between the box dimension values for the coefficients of the subbands from the first to fifth layers in female subjects.

| Node | Frequency band (KHz) | Group H (mean ± std) | Group Y (mean ± std) | Group Q (mean ± std) |
|---|---|---|---|---|
| 1.0 | 0–4 | $1.656 \pm 0.041^{\wedge}$ | $1.684 \pm 0.042^{*\#}$ | $1.664 \pm 0.047^{\wedge}$ |
| 1.1 | 4–8 | $1.694 \pm 0.033^{\wedge\#}$ | $1.668 \pm 0.036^{*}$ | $1.662 \pm 0.034^{*}$ |
| 2.0 | 0–2 | $1.693 \pm 0.041^{\wedge}$ | $1.717 \pm 0.043^{*\#}$ | $1.698 \pm 0.045^{\wedge}$ |
| 2.2 | 4–6 | $1.636 \pm 0.040^{\#}$ | $1.622 \pm 0.046^{\#}$ | $1.686 \pm 0.038^{*\wedge}$ |
| 2.3 | 6–8 | $1.712 \pm 0.025^{\wedge\#}$ | $1.693 \pm 0.042^{*\#}$ | $1.610 \pm 0.042^{*\wedge}$ |
| 3.0 | 0-1 | $1.699 \pm 0.038$ | $1.718 \pm 0.033^{\#}$ | $1.697 \pm 0.036^{\wedge}$ |
| 3.2 | 2-3 | $1.668 \pm 0.038^{\#}$ | $1.672 \pm 0.050^{\#}$ | $1.640 \pm 0.039^{*\wedge}$ |
| 3.4 | 4-5 | $1.612 \pm 0.037^{\#}$ | $1.610 \pm 0.049^{\#}$ | $1.678 \pm 0.034^{*\wedge}$ |
| 3.6 | 6-7 | $1.653 \pm 0.036^{\#}$ | $1.644 \pm 0.045^{\#}$ | $1.599 \pm 0.042^{*\wedge}$ |
| 3.7 | 7-8 | $1.704 \pm 0.025^{\wedge\#}$ | $1.688 \pm 0.033^{*\#}$ | $1.619 \pm 0.043^{*\wedge}$ |
| 4.2 | 1–1.5 | $1.581 \pm 0.048^{\wedge\#}$ | $1.611 \pm 0.041^{*\#}$ | $1.667 \pm 0.038^{*\wedge}$ |
| 4.3 | 1.5–2 | $1.66 \pm 0.037^{\#}$ | $1.673 \pm 0.046^{\#}$ | $1.590 \pm 0.051^{*\wedge}$ |
| 4.4 | 2–2.5 | $1.627 \pm 0.043^{\#}$ | $1.642 \pm 0.042^{\#}$ | $1.611 \pm 0.044^{*\wedge}$ |
| 4.5 | 2.5–3 | $1.619 \pm 0.038^{\wedge\#}$ | $1.642 \pm 0.042^{*\#}$ | $1.555 \pm 0.053^{*\wedge}$ |
| 4.6 | 3–3.5 | $1.554 \pm 0.051^{\#}$ | $1.570 \pm 0.048^{\#}$ | $1.636 \pm 0.043^{*\wedge}$ |
| 4.8 | 4–4.5 | $1.591 \pm 0.038^{\wedge\#}$ | $1.615 \pm 0.041^{*\#}$ | $1.667 \pm 0.035^{*\wedge}$ |
| 4.10 | 5–5.5 | $1.594 \pm 0.050^{\#}$ | $1.598 \pm 0.036$ | $1.611 \pm 0.038^{*}$ |
| 4.11 | 5.5–6 | $1.613 \pm 0.041^{\#}$ | $1.610 \pm 0.033^{\#}$ | $1.637 \pm 0.041^{*\wedge}$ |
| 4.12 | 6–6.5 | $1.624 \pm 0.032^{\#}$ | $1.616 \pm 0.034^{\#}$ | $1.593 \pm 0.040^{*\wedge}$ |
| 4.13 | 6.5–7 | $1.642 \pm 0.029^{\#}$ | $1.645 \pm 0.038^{\#}$ | $1.576 \pm 0.049^{*\wedge}$ |
| 4.15 | 7.5–8 | $1.688 \pm 0.024^{\#}$ | $1.678 \pm 0.033^{\#}$ | $1.577 \pm 0.046^{*\wedge}$ |
| 5.0 | 0–0.25 | $1.724 \pm 0.046^{\wedge\#}$ | $1.773 \pm 0.040^{*}$ | $1.771 \pm 0.038^{*}$ |
| 5.1 | 0.25–0.5 | $1.687 \pm 0.040^{\wedge}$ | $1.703 \pm 0.031^{*\#}$ | $1.691 \pm 0.038^{\wedge}$ |
| 5.2 | 0.5–0.75 | $1.633 \pm 0.061^{\#}$ | $1.650 \pm 0.044^{\#}$ | $1.606 \pm 0.058^{*\wedge}$ |
| 5.3 | 0.75–1 | $1.593 \pm 0.072^{\#}$ | $1.613 \pm 0.059^{\#}$ | $1.636 \pm 0.045^{*\wedge}$ |
| 5.4 | 1–1.25 | $1.577 \pm 0.087^{\#}$ | $1.619 \pm 0.056$ | $1.628 \pm 0.039^{*}$ |
| 5.5 | 1.25–1.5 | $1.612 \pm 0.046^{\#}$ | $1.630 \pm 0.048^{\#}$ | $1.581 \pm 0.055^{*\wedge}$ |
| 5.6 | 1.5–1.75 | $1.558 \pm 0.061^{\wedge\#}$ | $1.594 \pm 0.056^{*}$ | $1.606 \pm 0.063^{*}$ |
| 5.7 | 1.75–2 | $1.612 \pm 0.034^{\wedge}$ | $1.638 \pm 0.043^{*\#}$ | $1.619 \pm 0.041^{\wedge}$ |
| 5.8 | 2–2.25 | $1.591 \pm 0.037^{\wedge}$ | $1.622 \pm 0.033^{*\#}$ | $1.589 \pm 0.043^{\wedge}$ |
| 5.9 | 2.25–2.5 | $1.555 \pm 0.057^{\wedge}$ | $1.601 \pm 0.049^{*\#}$ | $1.559 \pm 0.040^{\wedge}$ |
| 5.10 | 2.5–2.75 | $1.584 \pm 0.055$ | $1.607 \pm 0.053^{\#}$ | $1.573 \pm 0.059^{\wedge}$ |
| 5.11 | 2.75–3 | $1.584 \pm 0.069^{\wedge}$ | $1.623 \pm 0.045^{*}$ | $1.609 \pm 0.041$ |
| 5.12 | 3–3.25 | $1.552 \pm 0.081^{\#}$ | $1.580 \pm 0.049^{\#}$ | $1.597 \pm 0.041^{*\wedge}$ |
| 5.13 | 3.25–3.5 | $1.616 \pm 0.037^{\#}$ | $1.618 \pm 0.042^{\#}$ | $1.582 \pm 0.057^{*\wedge}$ |
| 5.14 | 3.5–3.75 | $1.564 \pm 0.047^{\#}$ | $1.578 \pm 0.039^{\#}$ | $1.605 \pm 0.057^{*\wedge}$ |
| 5.15 | 3.75–4 | $1.579 \pm 0.042^{\wedge}$ | $1.603 \pm 0.042^{*\#}$ | $1.585 \pm 0.051^{\wedge}$ |
| 5.16 | 4–4.25 | $1.575 \pm 0.036^{\wedge\#}$ | $1.600 \pm 0.036^{*}$ | $1.606 \pm 0.051^{*}$ |
| 5.19 | 4.75–5 | $1.575 \pm 0.043^{\#}$ | $1.585 \pm 0.051^{\#}$ | $1.621 \pm 0.038^{*\wedge}$ |
| 5.22 | 5.5–5.75 | $1.567 \pm 0.044^{\#}$ | $1.585 \pm 0.039^{\#}$ | $1.617 \pm 0.050^{*\wedge}$ |
| 5.23 | 5.75–6 | $1.581 \pm 0.031^{\wedge}$ | $1.600 \pm 0.035^{*\#}$ | $1.577 \pm 0.046^{\wedge}$ |
| 5.24 | 6–6.25 | $1.588 \pm 0.029^{\wedge}$ | $1.610 \pm 0.034^{*\#}$ | $1.581 \pm 0.042^{\wedge}$ |
| 5.25 | 6.25–6.5 | $1.581 \pm 0.040$ | $1.602 \pm 0.047^{\#}$ | $1.571 \pm 0.037^{\wedge}$ |
| 5.27 | 6.75–7 | $1.606 \pm 0.042^{\wedge\#}$ | $1.631 \pm 0.041^{*\#}$ | $1.573 \pm 0.040^{*\wedge}$ |
| 5.28 | 7–7.25 | $1.584 \pm 0.055$ | $1.598 \pm 0.041^{\#}$ | $1.578 \pm 0.038^{\wedge}$ |
| 5.29 | 7.25–7.5 | $1.626 \pm 0.026^{\#}$ | $1.635 \pm 0.035^{\#}$ | $1.569 \pm 0.040^{*\wedge}$ |
| 5.30 | 7.5–7.75 | $1.584 \pm 0.035$ | $1.593 \pm 0.042^{\#}$ | $1.573 \pm 0.042^{\wedge}$ |
| 5.31 | 7.75–8 | $1.625 \pm 0.031^{\#}$ | $1.630 \pm 0.036^{\#}$ | $1.585 \pm 0.041^{*\wedge}$ |

Compared with Group H, $^{*}P < 0.05$. Compared with Group Y, $^{\wedge}P < 0.05$. Compared with Group Q, $^{\#}P < 0.05$.

Table 5: Model recognition accuracies of all subjects, male subjects, and female subjects (%).

| Group | Male | Female | All |
|---|---|---|---|
| Group Q | 93.47 | 100.00 | 97.81 |
| Group Y | 44.44 | 76.71 | 55.39 |
| Group H | 0.00 | 87.88 | 48.89 |
| Total | **91.95** | **72.07** | **79.49** |

values to Group Q instead of Group Y. The box dimension values of all groups for all subjects are higher in the low frequency band. In addition, there is a peak in the frequency band around 4 kHz. However, the change of box dimension values of Group H and Group Y for female subjects in Figure 5 is similar to that in Figure 3. As shown in Tables 2 to 4, most frequency bands with significantly different box dimension values in female subjects, while least frequency bands with significantly different box dimension values in male subjects. It indicates that the female subjects have better class separability in wavelet packet fractal dimensions than the male subjects and all subjects.

The internal information on the auscultation signals shows some irregularities, and the fractal dimension trajectory distinctively varies among the subjects. The differences in the trends are reflected in the diverse internal information of the three groups, and this information can be applied for clinical diagnosis in TCM.

As shown in Table 5, when auscultation signals of all subjects were trained by classification model to decide the patterns of TCM syndromes, the overall accuracy was 79.49%. When those of male subjects were trained by classification model the accuracy was 72.07%, whereas the overall accuracy was up to 91.95% when those of female subjects were trained. Therefore, the overall accuracy of male and female subjects reached 86.05%. The resulted showed that the methods proposed in this paper were effective to analyze auscultation signals, and the performance of model can be greatly improved when distinction of gender was considered.

## 5. Conclusions

This paper selected the vowel /a:/ to be pronounced by each subject to decrease the interference, complexity, and uncertainty of the auscultation signal analysis. The auscultation signals were further processed using combination of box dimension and wavelet packet transform by self-developed analytic program under Matlab environment. Then the box dimension values of the auscultation signals were analyzed and compared in each frequency subband. The differences in the trends are reflected in the diverse internal information of the three groups, and this information was applied for the further classification of auscultation signals. The male and female classification models, if established separately, are applicable and effective in the auscultation analysis of TCM. The clinical subject size must be extended for future studies to verify our proposed methods. Our future research aims to construct an automatic auscultation system to assist in clinical diagnosis.

## Conflict of Interests

The authors declare that they have no financial and personal relationships with other people or organizations that can inappropriately influence their work; there is no professional or other personal interest of any nature or kind in any product, service, and/or company that could be construed as influencing the position presented in, or the review of, the paper.

## Acknowledgment

This work was supported by the National Natural Science Foundation of China under Grant nos. 81302913, 81270050, 30901897, 81173199, and 30701072.

## References

[1] S. G. Zhao, "A modem research overview on the auscultation diagnosis of TCM," *Chinese Journal of the Practical Chinese with Modern Medicine*, vol. 21, no. 14, pp. 1218–1220, 2008.

[2] X. M. Mo, Y. S. Zhang, and J. L. Zhang, "Current situation and prospect of auscultation research in TCM," *Chinese Journal of Basic Medicine in Traditional Chinese Medicine*, vol. 4, no. 1, pp. 54–56, 1998.

[3] X. M. Mo, "Preliminary study on making use of phonograph for the diagnosis of deficiency syndrome of the lung with cough," *Journal of Traditional Chinese Medicine Research*, no. 3, pp. 43–46, 1987.

[4] H. J. Wang, J. J. Yan, and Y. Q. Wang, "Digital technology for objective auscultation in traditional Chinese medical diagnosis," in *Proceedings of the International Conference on Audio, Language and Image Processing (ICALIP '08)*, pp. 1100–1104, July 2008.

[5] J. J. Yan, Y. Q. Wang, H. J. Wang et al., "Nonlinear analysis in TCM acoustic diagnosis using delay vector variance," in *Proceedings of the 2nd International Conference on Bioinformatics and Biomedical Engineering (iCBBE '08)*, pp. 2099–2102, May 2006.

[6] C.-C. Chiu, H.-H. Chang, and C.-H. Yang, "Objective auscultation for traditional Chinese medical diagnosis using novel acoustic parameters," *Computer Methods and Programs in Biomedicine*, vol. 62, no. 2, pp. 99–107, 2000.

[7] J. J. Yan, S. Y. Mao, Y. Q. Wang et al., "Analysis of sound signal of five internal organs based on wavelet packet," in *Proceedings of IEEE International Conference on Bioinformatics & Biomedicine (BIBMW '10)*, pp. 707–711, December 2010.

[8] J. J. Yan, S. Y. Mao, Y. Q. Wang et al., "Wavelet packet based analysis of sound of five internal organs in TCM," in *Proceedings of the 3rd International Conference on Biomedical Engineering and Informatics (BMEI '10)*, pp. 1084–1088, October 2010.

[9] J. J. Yan, Y. Q. Wang, R. Guo et al., "Nonlinear analysis of auscultation signals in TCM using the combination of wavelet packet transform and sample entropy," *Evidence-Based Complementary and Alternative Medicine*, vol. 2012, Article ID 247012, 9 pages, 2012.

[10] G. S. Hu, *Modern Digital Signal Processing*, Tshinghua University Press, Beijing, China, 2004.

[11] C. Thompson, A. Mulpur, and V. Mehta, "Transition to chaos in acoustically driven flows," *Journal of the Acoustical Society of America*, vol. 90, no. 4, pp. 2097–2103, 1991.

[12] P. Maragos, "Fractal aspects of speech signals: dimension and interpolation," in *Proceedings of International Conference on Acoustics, Speech, and Signal Processing (ICASSP '91)*, pp. 417–420, 1991.

[13] Amended in National Clinical Professional Conference of Chronic Bronchitis, "The chronic bronchitis clinical diagnosis and curative effect judgment standard," *Chinese Journal of Tuberculosis and Respiratory Disease*, vol. 3, no. 1, p. 61, 1980.

[14] X. Y. Zheng, *Guideline for Clinical Study on New Drugs of Traditional Chinese Medicine*, China Medicine Science and Technology Press, Beijing, China, 2002.

[15] State Bureau of Technical and Quality Supervision, *Clinic Terminology of Traditional Chinese Medical Diagnosis and Treatment—Syndromes*, Standards Press of China, Beijing, China, 1997.

[16] Y. Q. Wang, *Diagnostics of Traditional Chinese Medicine*, Chinese Medicine Science and Technology Press, Beijing, China, 2004.

[17] W. F. Zhu, *Diagnostics of Traditional Chinese Medicine*, Shanghai Science and Technology Press, Shanghai, China, 2006.

[18] L. Z. Hou and D. M. Han, "Selection of the vowel sound in the throat sound detection," *Journal of Audiology and Speech Diseases*, vol. 10, no. 1, pp. 16–18, 2002.

[19] B. C. Li and J. S. Luo, *Wavelet Analysis and Its Applications*, Electronics Engineering Press, Beijing, China, 2003.

[20] X. H. Tang and Q. L. Li, *Time-Frequency Analysis and Wavelet Transform*, Science Press, Beijing, China, 2008.

[21] S.-Y. Wang, G.-X. Zhu, and Y.-Y. Tang, "Feature extraction using best wavelet packet transform," *Acta Electronica Sinica*, vol. 31, no. 7, pp. 1035–1038, 2003.

[22] G. Antonini and A. Orlandi, "Wavelet packet-based EMI signal processing and source identification," *IEEE Transactions on Electromagnetic Compatibility*, vol. 43, no. 2, pp. 140–148, 2001.

[23] L. Pesu, P. Helisto, E. Ademovic et al., "Classification of respiratory sounds based on wavelet packet decomposition and learning vector quantization," *Technology and Health Care*, vol. 6, no. 1, pp. 65–74, 1998.

[24] A. H. Tewfik, D. Sinha, and P. Jorgensen, "On the optimal choice of a wavelet for signal representation," *IEEE Transactions on Information Theory*, vol. 38, no. 2, pp. 747–765, 1992.

[25] Y. Y. Sun, C. D. Jin, and H. B. Zhang, "Fractal theory and application of fractal dimension," *Forestry Science and Technology Information*, vol. 37, no. 4, pp. 8–9, 2005.

[26] H. Q. Li and F. Q. Wang, *Fractal Theory and Its Application in Molecule Analysis*, Science Press, Beijing, China, 1993.

[27] Y. Y. Zi, Z. J. He, and Z. S. Zhang, "Wavelet fractal technology and its applications to nonstationary fault diagnosis," *Journal of Xi'an Jiaotong University*, vol. 34, no. 9, pp. 83–87, 2000.

[28] V. N. Vapnik, *Statistical Learning Theory*, John Wiley & Sons, New York, NY, USA, 1998.

[29] Z. Q. Bian and X. G. Zhang, *Pattern Recognition*, Tsinghua University Press, Beijing, China, 2nd edition, 2000.

[30] F.-M. Tang, Z.-D. Wang, and M.-Y. Chen, "On multiclass classification methods for support vector machines," *Control and Decision*, vol. 20, no. 7, pp. 746–749, 2005.

[31] J. J. Yan, Q. W. Shen, R. Guo, Y. Q. Wang, C. H. Zhou, and J. T. Ren, "Multi-class learning with specific features for pairwise classes," in *Proceedings of the 4th International Conference on BioMedical Engineering and Informatics*, pp. 2054–2057, 2011.

[32] C. C. Chang and C. J. Lin, "LIBSVM: a library for support vector machines," *ACM Transactions on Intelligent Systems and Technology*, vol. 2, no. 3, article 27, 2011.

Hindawi Publishing Corporation
Evidence-Based Complementary and Alternative Medicine
Volume 2013, Article ID 493626, 6 pages
http://dx.doi.org/10.1155/2013/493626

*Research Article*

# Zheng Classification with Missing Feature Values Using Local-Validity Approach

**Yan Wang[1,2] and Lizhuang Ma[3,4]**

[1] *School of Continuing Education, Shanghai Jiao Tong University, Shanghai 200240, China*
[2] *Provincial Key Laboratory for Computer Information Processing Technology, Soochow University, Suzhou 215006, China*
[3] *Department of Computer Science & Engineering, Shanghai Jiao Tong University, Shanghai 200240, China*
[4] *Center of Traditional Chinese Medicine Information Science and Technology, Shanghai University of TCM, Shanghai 201203, China*

Correspondence should be addressed to Yan Wang; wangyan8383@sjtu.edu.cn and Lizhuang Ma; ma-lz@cs.sjtu.edu.cn

Received 26 July 2013; Revised 15 October 2013; Accepted 15 October 2013

Academic Editor: Shi-bing Su



Zheng classification is a very important step in the diagnosis of traditional Chinese medicine (TCM). In clinical practice of TCM, feature values are often missing and incomplete cases. The performance of Zheng classification is strictly related to rates of missing feature values. Based on the pattern of the missing feature values, a new approach named local-validity is proposed to classify zheng classification with missing feature values. Firstly, the maximum submatrix for the given dataset is constructed and local-validity method finds subsets of cases for which all of the feature values are available. To reduce the computational scale and improve the classification accuracy, the method clusters subsets with similar patterns to form local-validity subsets. Finally, the proposed method trains a classifier for each local-validity subset and combines the outputs of individual classifiers to diagnose zheng classification. The proposed method is applied to the real liver cirrhosis dataset and three public datasets. Experimental results show that classification performance of local-validity method is superior to the widely used methods under missing feature values.

## 1. Introduction

*1.1. The Concept of Zheng Classification.* Traditional Chinese medicine (TCM) is one of the most important complementary medicines used increasingly in the world [1]. Zheng classification enables the doctor to determine the stage that the disease developed and the location of the disease [2]. Zheng classification is the method of recognizing and diagnosing diseases by analyzing patient information based on TCM theories and the doctor's experiences [3].

In an attempt to achieve effective and objective standard of Zheng classification, various data mining approaches are used to construct the classifier on TCM dataset. Figure 1 shows the process of intelligent Zheng classification.

*1.2. Missing Feature Values: The Literature Review.* In clinical practice of traditional Chinese medicine, feature values are often missing and incomplete cases. Missing feature values could be caused by various reasons, such as error of data measure, error of data understanding, erroneous human imputation, or restriction of data collecting [4, 5]. The performance of intelligent Zheng classification model in TCM is strictly related to the rate of missing feature values, but most common methods are short of the ability to solve the missing feature problem [4–6].

At present, the most common strategy for dealing with absent values is essentially to ignore them [7]. The cases with missing feature values are deleted before constructing the Zheng classification model [7]. Although improving the classification performance in some degree, deletion may discard some important information within the missing feature values, especially under the condition of insufficient TCM data. So deleting the data with missing feature values directly is difficult to meet the TCM clinical application.

Considering the shortcomings of the deletion method, imputation solution comes into being. Imputation is the substitution of a missing feature value with a meaningful estimate. Evidence theory is used to predict the missing feature values [8]. However, the evidence function should be learned in advance. The literature [9, 10] fills the missing feature by

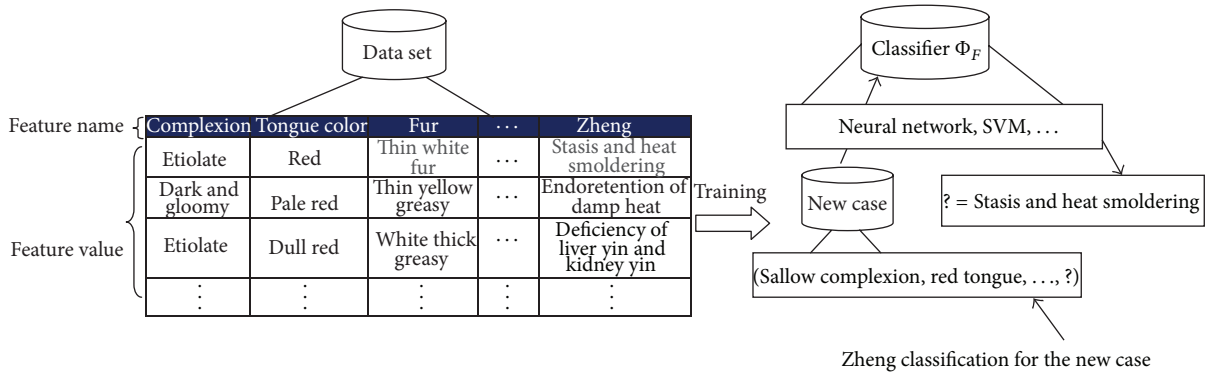


Figure 1: The process of intelligent Zheng classification.

statistics method and Bayesian model, respectively. Nevertheless, these methods need to know probability distribution, which is difficult to be acquired in fact. In some applications, expert experience could be used to form the complete feature values. However, the prediction method for missing data by experts is subjective.

In recent decades, data mining imputation methods are beginning to attract much attention [11]. Logistic regression [12], subspace [4], neural network [13], and rough sets theory [14] have been applied to deal with missing feature values. These methods construct a predictive model to estimate the missing feature values from information within cases. However, imputation method will introduce new noise into cases, and the classification accuracy will decrease subsequently.

When dealing with the missing feature values, deletion and imputation methods will change the original dataset more or less. To avoid the problem of deletion and imputation methods, the literature [15–17] presents a selective Bayes classifier for classifying missing values with a simpler formula for computing gain ratio. Nevertheless, the method needs to satisfy the premise that features should be independent of each other. In TCM clinical practice, it is difficult to guarantee the characteristics of independence.

To overcome the limitation of the methods mentioned above, the proposed local-validity approach need not estimate the missing feature values or remove the deficient cases. It focuses on constructing intelligent Zheng classifier on the original cases directly. Firstly, the method finds the local-validity subset (LVS) within dataset and constructs the Zheng classifier on each LVS. Finally, the performance of each individual classifier is assessed and combined depending on the classification matrix to estimate the final output.

The rest of the paper is organized as follows. Section 2 describes the dataset and the ideas of the proposed local-validity method. The experimental results based on the method are shown in Section 3. Finally, conclusion is given in Section 4.

## 2. Material and Methods

*2.1. Description of Dataset.* 153 liver cirrhosis cases with three different Zheng classifications (i.e., stasis-heat smoldering zheng, damp-heat smoldering zheng, and liver-kidney yin deficiency zheng) have been collected from Shanghai University of Traditional Chinese Medicine. The dataset includes 52 cases with stasis-heat smoldering zheng, 61 cases with damp-heat smoldering zheng and 40 cases with liver-kidney yin deficiency zheng. Each case includes 40 TCM features selected by clinicians as the significant factors to identify the liver cirrhosis zheng.

Features are encoded using the four-value ordinal scales measured by the severity degree:

(i) 1 representing no corresponding symptoms;

(ii) 2 for the normal level;

(iii) 3 for the medium serious level;

(iv) 4 representing the most serious.

Among all features, twenty-three features are missing in varying degrees. In this paper, the missing percentage $\alpha$ is defined as

$$\alpha = \frac{\left|U'\right|}{|U|}, \tag{1}$$

where $|U'|$ denotes the number of cases with missing feature values and $|U|$ denotes the total number of cases.

The list of these features and the corresponding missing percentage are shown in Table 1.

*2.2. The Proposed Local-Validity Approach.* As mentioned above, the local-validity idea overcomes the limitations discussed in the previous section. The flowchart of the proposed approach is shown in Figure 2. The subsequent subsections are organized as follows. First, the TCM zheng classification system with missing feature values is defined. Then, we describe how LVS is selected and how the individual classifier is trained on every LVS. Finally, we present how the individual classification results are combined to boost up the classification performance.

*2.2.1. Definition of Zheng Classification System.* Zheng classification system with missing feature values in TCM can be viewed as a 3-tuple $S = \langle U, F, g \rangle$, where $U$ is a nonempty finite set of cases and $F$ is a nonempty finite set of features.

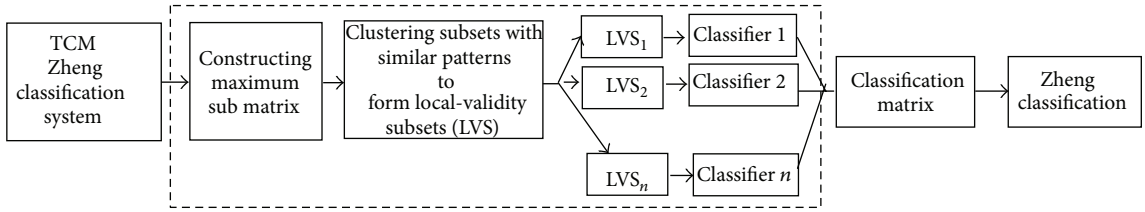


Figure 2: The overall view of the proposed local-validity approach.

Table 1: Description of liver cirrhosis TCM dataset used in the experiment.

| Feature name | $\alpha$ (%) |
|---|---|
| (1) Lassitude and fatigue | 5 |
| (2) Head heaviness | 0.1 |
| (3) Spontaneous sweat | 10 |
| (4) Nocturnal polyuria | 0 |
| (5) Depression | 4 |
| (6) Gingiva bleeding | 0.2 |
| (7) Blurred vision | 3.1 |
| (8) Reduced appetite | 0 |
| (9) Dry and bitter taste | 0 |
| (10) Abdominal pain | 1 |
| (11) Rib-side and flank distention and pain | 2.3 |
| (12) Low limbs puffy swelling | 1.2 |
| (13) Belching | 0 |
| (14) Yellow urine | 0 |
| (15) Scant urine | 3.2 |
| (16) Night sweat | 1.1 |
| (17) Sloppy stool | 0.2 |
| (18) Skin itching | 2.1 |
| (19) Skin bleeding | 0 |
| (20) Insomnia | 0.3 |
| (21) Limp aching lumbar and knees | 0 |
| (22) Tinnitus | 0 |
| (23) Hypochondriac distending pain | 3.8 |
| (24) Abdominal distension | 0.1 |
| (25) Yellow body | 0 |
| (26) Acid regurgitation | 0 |
| (27) Liver palm | 0 |
| (28) Dazzle | 0.1 |
| (29) Chill and cold limbs | 2.1 |
| (30) Constipation | 0 |
| (31) Vexing heat in the five heart | 0.3 |
| (32) Nose bleeding | 0 |
| (33) Rashness impatience and irascibility | 0 |
| (34) Fatigued and heavy limbs | 0 |
| (35) Dry eyes | 4.1 |
| (36) Epigastralgia | 0.1 |
| (37) Foul breath | 0.2 |
| (38) Yellow eyes | 0 |
| (39) Nausea vomit | 0 |
| (40) Spider naïve | 0.1 |

Table 2: A dataset with missing feature values.

| $U$ | $f_1$ | $f_2$ | $f_3$ | $f_4$ |
|---|---|---|---|---|
| $x_1$ | $*$ | $*$ | 1 | 0 |
| $x_2$ | 1 | 1 | $*$ | $*$ |
| $x_3$ | 0 | 1 | 1 | 0 |
| $x_4$ | 1 | 0 | $*$ | 1 |

For $\forall f \in F$ and $x \in U$, $g(x, f)$ denote the value that $x$ holds on feature $f$. Then, in zheng classification system with missing feature values, $\exists x \in U$ and $\exists f \in F$ that satisfies $g(x, f) = *$. Here, we assume that the missing feature values are denoted by "$*$."

An example of zheng classification system with missing feature values is shown in Table 2.

*2.2.2. Finding Local-Validity Subsets.* It is common that the number of missing feature values is $n$ ($n \geq 1$) in TCM clinical application. Based on the maximum sub-matrix theory, the missing feature values are considered as barrier points. The local-validity approach enumerates the maximum feature vector with complete values. Thus, the proposed method starts with a binary matrix $M$ whose element is defined as

$$M_{i,j} = \begin{cases} 1, & g\left(f_i, x_j\right) \neq *, \\ 0, & g\left(f_i, x_j\right) = *. \end{cases} \tag{2}$$

The element $M_{i,j} = 0$ if the $i$th feature is missing in the $j$th case.

The matrix $M$ of the dataset presented in Table 2 is given as follows:

$$M = \begin{bmatrix} 0 & 0 & 1 & 1 \\ 1 & 1 & 0 & 0 \\ 1 & 1 & 1 & 1 \\ 1 & 1 & 0 & 1 \end{bmatrix}. \tag{3}$$

Matrix $M$ finds the maximum feature vector (MFV) that covers the most complete data. Each MFV identifies a local-validity pattern $P$; the formula of $P$ is as follows:

$$\exists x \in U, \quad \forall f_i \in \overline{P} \wedge \forall f_j \in \left(F - \overline{P}\right), \tag{4}$$

satisfing $(g(f_i, x) = *) \wedge (g(f_j, x) \neq *)$ $(i \neq j)$.

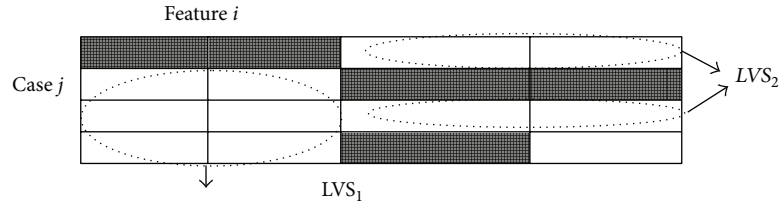


Figure 3: Example of local-validity subset.

Thus, the corresponding local-validity pattern $P$ corresponding to Table 2 is

$$P_1 = \{f1, f2\}, \quad P_2 = \{f3, f4\}, \quad P_3 = \{f1, f2, f3, f4\}, \quad P_4 = \{f1, f2, f4\}. \tag{5}$$

Each pattern $P$ maps the corresponding LVS.

LVS is a collection of the cases that have no missing values for a specific feature subset and the collection of LVS includes all of the cases in the original data. The formula of LVS is as

$$(\forall x \in \mathrm{LVS}_k) \wedge (\forall f_i \in \mathrm{LVS}_k), \tag{6}$$

satisfing $g(f_i, x) \neq *$, where $\mathrm{LVS}_k$ represents the $k$th local-validity subset.

Four LVS can be found from the dataset presented in Table 2 and Figure 3 shows two of them.

The process of finding local-validity subset can be described as follows.

(1) For an original given dataset, generate matrix $M$.

(2) In feature space, traverse matrix $M$ to generate maximum feature vector.

(3) For each feature vector, find the corresponding LVS.

As the feature missing percentage ascends, the number of LVS will increase. The large number of LVS will affect the computation complexity. Then, this problem will be translated into a clustering problem. LVS with the similar pattern will be merged.

*2.2.3. Clustering Local-Validity Subsets with Similar Patterns.* It is desirable to cover the entire data with as few local-validity subsets as possible and obtain the overall best performance.

The preliminary research results [17] show that there are inherent consistencies between mutual information and subset aggregate.

Considering the cross entropy between two local-validity subsets,

$$\mu_{i,k} = -\log\left(\frac{1}{N_i N_k}\sum_{p=1}^{N_i}\sum_{q=1}^{N_k} G\left(x_p - y_q, \sigma^2\right)\right), \tag{7}$$

where $G$ is the Gaussian kernel and $\sigma^2$ is the variance of Gauss function. $N_i$ is the number of cases in subset $\mathrm{LVS}_i$ and $N_k$ represents $\mathrm{LVS}_k$.

Table 3: Performance comparison of three methods on liver cirrhosis dataset.

| Classification accuracy (%) | | |
|---|---|---|
| Deletion | Imputation | Local-validity |
| 68.67 | 70.67 | **80.33** |

The bold values are used to emphasize the best Zheng classification performance.

Then, the mutual information $I(i,k)$ between $\mathrm{LVS}_i$ and $\mathrm{LVS}_k$ can be defined as follows:

$$I(i,k) = \mu_{i,k} \log \frac{N_{i,k}}{N_i + N_k}, \tag{8}$$

where $N_{i,k}$ represents the number of cases that belongs to two subsets at the same time.

The larger $I(i,k)$ is, the stronger the correlation degree between $\mathrm{LVS}_i$ and $\mathrm{LVS}_k$ is. Based on $k$-nearest neighbor algorithm, the subset with strong correlation degree is clustered to form a new subset. In this paper, the $k$th cluster is represented by a set of LVS indices $\Omega_k$.

*2.2.4. Constructing the Zheng Classification Matrix.* Once LVS is chosen, an individual zheng classifier is needed for each $\Omega_k$. In TCM zheng classification previous studies [18], the zheng classification matrix is proposed to merge the outputs of multizheng classifiers under the complete dataset.

Under missing feature values, in order to boost up the zheng classification performance, the complete degree $\lambda_i$ is introduced into the zheng classification matrix $Y$ to estimate the final output. Then, zheng classification matrix $Y$ is updated as

$$Y = \arg\max_{w \in Y} \sum_{i=1}^{k} \lambda_i G_i^w, \tag{9}$$

where $G_i^w$ represents the performance that a new case is diagnosed as $w$ under the $\Omega_i$ local-validity subset.

## 3. Experimental Results

*3.1. Local-Validity versus Other Methods on Liver Cirrhosis Dataset.* To evaluate the performance of the proposed method, we carried out experiments on a real TCM liver cirrhosis dataset with missing data. Description of the dataset is presented in Table 1.

To analyze the improvement in zheng classification accuracy, three different methods are used to deal with the missing values.

Table 4: The performance comparison of three methods on three public datasets.

(a) Lymphography

| $\alpha$ | Diagnosis accuracy (%) | | |
|---|---|---|---|
| | Deletion | Imputation | Local-validity |
| 0 | **85.14** | **85.14** | 83.7 |
| 0.05 | **85.82** | 83.78 | 84.02 |
| 0.10 | 81.21 | 81.08 | **92.16** |
| 0.20 | 78.92 | 77.43 | **88.11** |

(b) SPECT heart

| $\alpha$ | Diagnosis accuracy (%) | | |
|---|---|---|---|
| | Deletion | Imputation | Local-validity |
| 0 | **82.4** | **82.40** | 82.05 |
| 0.05 | **82.28** | 82.02 | 83.06 |
| 0.10 | 82 | 80.52 | **85.25** |
| 0.20 | 80.2 | 78.08 | **86.06** |

(c) Lung cancer

| $\alpha$ | Diagnosis accuracy (%) | | |
|---|---|---|---|
| | Deletion | Imputation | Local-validity |
| 0 | **90.6** | **90.6** | 90.05 |
| 0.05 | 89.25 | **90.12** | 89.17 |
| 0.10 | 86.23 | 83.37 | **87.29** |
| 0.20 | 81.67 | 82.02 | **82.37** |

The bold values are used to emphasize the best Zheng classification performance.

The zheng classification accuracy is first estimated by simply removing the cases with missing values. Then, mean value imputation method is applied to impute missing feature values. Finally, the proposed local-validity approach is applied on the original dataset directly.

Considering the liver cirrhosis data is not sufficient, ten times 10-fold cross-validation is used for the assessment of classification performance. In cross validation, the data is split into ten approximately equal partitions and each in turn is used for testing and the remainder is used for training. That is, use nine-tenths for training and one-tenth for testing and repeat the procedure ten times so that, in the end, every case has been used exactly once for testing [19].

To get a reliable error estimate, the cross-validation process is repeated for 10 times, and the results are averaged [19].

The average classification accuracies are listed in Table 3. The best performance is emphasized using a boldfaced font.

As seen in Table 3, the performance of local-validity approach outperforms the deletion and imputation methods on liver cirrhosis dataset.

It should be pointed out that there are 23 feature values missing in original 40 features. Simply, deletion may introduce substantial biases, and imputation will introduce noise. With the increase of missing rate, problems of deletion and imputation will be more obvious. On the other hand, local-validity method constructs the zheng classification on the original dataset directly. The method can avoid the noise and biases problems.

*3.2. Local-Validity versus Other Methods on Other Datasets.* We also do experiments on three public datasets: lymphography, SPECT heart, and breast cancer.

Because these three datasets are complete, the diagnosis performance can be evaluated effectively. We replace randomly the feature value with "$*$" based on different missing percentages $\alpha = \{0, 0.05, 0.10, 0.20\}$ in these three public datasets. The results are shown in Table 4.

From Tables 4(a), 4(b), and 4(c), it can be seen that the performance of local-validity method is lower than that of deletion and imputation with $\alpha = 0.05$. With $\alpha = 0.1$ and $\alpha = 0.2$, the proposed method performs well than other methods on three datasets. This shows that the performance of local-validity method is more stable than that of the other two methods, and the effect will be more obvious with the number increment of the missing cases.

In summary, the proposed local-validity algorithm is applicable to the dataset with small number of cases and a large percentage of missing values.

## 4. Conclusions

Although various machine-learning algorithms have been used to construct the zheng classification model in TCM, most of them deal with complete feature values. In fact, missing feature values are inevitable in TCM clinical application. Therefore, methods of constructing zheng classifier for missing data deserve more attention.

By analyzing missing data processing methods, this paper presents a local-validity approach for zheng classification with missing feature values. The proposed approach contains the following characteristics.

(1) Instead of deleting or imputing the absent values, the proposed approach discovers the local-validity subsets from the original cases. Therefore, the proposed approach avoids the introduction of noise data.

(2) Our method constructs zheng classifier on the original dataset directly and needs no assumption about the missing mechanism.

(3) During the local-validity subset discovery phase, the formula for computation of the local-validity subset is presented. Then, the zheng classification matrix is described to combine the classification results of multi-individual classifiers.

(4) Through experiments, we can conclude that the proposed method is an appropriate solution to missing feature values problems in TCM zheng classification. The results show that the proposed approach outperforms the deletion and imputation methods as the amount of missing feature values increases.

(5) Further research is under way concerning the relationship between the scale of local-validity subset and classification accuracy in order to get the optimum diagnostic result.

## Conflict of Interests

The authors declare that they have no conflict of interests.

## Acknowledgments

The research is sponsored by Open Research Fund of Jiangsu Provincial Key Laboratory for Computer Information Processing Technology (no. KJS1226) and Biomedical Engineering Cross Funds of Shanghai Jiao Tong University (no. YG2012MS28). The authors gratefully acknowledge all the researchers from the Shanghai University of Traditional Chinese Medicine for the TCM databases.

## References

[1] S. K. Pal, "Complementary and alternative medicine: an overview," *Current Science*, vol. 82, no. 5, pp. 518–524, 2002.

[2] B. Flaws and P. Sionneau, *The Treatment of Modern Western Medical Diseases with Chinese Medicine*, Blue Poppy Press, 2005.

[3] J. Si, L. Sun, N. Dai et al., "Study of sEGF level in chronicatrophic gastritis with either Chinese traditional medicine or Western medicine," *Journal of Zhejiang University Science*, vol. 3, no. 2, pp. 243–246, 2002.

[4] L. Nanni, A. Lumini, and S. Brahnam, "A classifier ensemble approach for the missing feature problem," *Artificial Intelligence in Medicine*, vol. 55, no. 1, pp. 37–50, 2012.

[5] R. Polikar, J. DePasquale, H. S. Mohammed, G. Brown, and L. I. Kuncheva, "Learn++.MF: a random subspace approach for the missing feature problem," *Pattern Recognition*, vol. 43, no. 11, pp. 3817–3832, 2010.

[6] G. Z. Li, S. X. Yan, M. Y. You et al., "Intelligent ZHENG classification of hypertension depending on ML-kNN and information fusion," *Evidence-Based Complementary and Alternative Medicine*, vol. 2012, Article ID 837245, 5 pages, 2012.

[7] H.-B. Qu, L.-F. Mao, and J. Wang, "Method for self-extracting diagnostic rules of blood stasis syndrome based on decision tree," *Chinese Journal of Biomedical Engineering*, vol. 24, no. 6, pp. 709–727, 2005.

[8] M. A. Boujelben, Y. D. Smet, A. Frikha, and H. Chabchoub, "Building a binary outranking relation in uncertain, imprecise and multi-experts contexts: the application of evidence theory," *International Journal of Approximate Reasoning*, vol. 50, no. 8, pp. 1259–1278, 2009.

[9] A. S. Salama, "Topological solution of missing attribute values problem in incomplete information tables," *Information Sciences*, vol. 180, no. 5, pp. 631–639, 2010.

[10] Z. Huang, J. Li, H. Su, G. S. Watts, and H. Chen, "Large-scale regulatory network analysis from microarray data: modified Bayesian network learning and association rule mining," *Decision Support Systems*, vol. 43, no. 4, pp. 1207–1225, 2007.

[11] M. Ghannad-Rezaie, H. Soltanian-Zadeh, H. Ying, and M. Dong, "Selection-fusion approach for classification of datasets with missing values," *Pattern Recognition*, vol. 43, no. 6, pp. 2340–2350, 2010.

[12] D. Williams, X. Liao, Y. Xue, L. Carin, and B. Krishnapuram, "On classification with incomplete data," *IEEE Transactions on Pattern Analysis and Machine Intelligence*, vol. 29, no. 3, pp. 427–436, 2007.

[13] I. A. Gheyas and L. S. Smith, "A neural network-based framework for the reconstruction of incomplete data sets," *Neurocomputing*, vol. 73, no. 16–18, pp. 3039–3065, 2010.

[14] X.-Y. Shao, X.-Z. Chu, H.-B. Qiu, L. Gao, and J. Yan, "An expert system using rough sets theory for aided conceptual design of ship's engine room automation," *Expert Systems with Applications*, vol. 36, no. 2, pp. 3223–3233, 2009.

[15] J. Chen, H. Huang, F. Tian, and S. Tian, "A selective Bayes Classifier for classifying incomplete data based on gain ratio," *Knowledge-Based Systems*, vol. 21, no. 7, pp. 530–534, 2008.

[16] F. Smeraldi, M. Defoin-Platel, and M. Saqi, "Handling missing features with boosting algorithms for protein-protein interaction prediction," *Lecture Notes in Computer Science*, vol. 6254, pp. 132–147, 2010.

[17] Y. Wang, Y. Gao, R. Shen, and F. Yang, "Selective ensemble approach for classification of datasets with incomplete values," *Advances in Intelligent and Soft Computing*, vol. 122, pp. 281–286, 2011.

[18] Y. Wang, L. Ma, and P. Liu, "Feature selection and syndrome prediction for liver cirrhosis in traditional Chinese medicine," *Computer Methods and Programs in Biomedicine*, vol. 95, no. 3, pp. 249–257, 2009.

[19] I. H. Witten and E. Frank, *Data Mining Practical Machine Learning Tools and Techniques*, Morgan Kaufmann Press, San Francisco, Calif, USA, 2005.

Hindawi Publishing Corporation
Evidence-Based Complementary and Alternative Medicine
Volume 2013, Article ID 731071, 13 pages
http://dx.doi.org/10.1155/2013/731071

*Research Article*

# Relationship between *EGF*, *TGFA*, and *EGFR* Gene Polymorphisms and Traditional Chinese Medicine ZHENG in Gastric Cancer

**Junfeng Zhang,[1,2] Zhen Zhan,[1,2] Juan Wu,[2] Chunbing Zhang,[3] Yaping Yang,[2] Shujuan Tong,[1,2] Ruiping Wang,[4] Xuewen Yang,[3] Wei Dong,[2] and Yajun Chen[3]**

[1] *Discipline of Chinese and Western Integrative Medicine, Nanjing University of Chinese Medicine, Nanjing 210023, China*
[2] *College of Basic Medicine, Nanjing University of Chinese Medicine, Nanjing 210023, China*
[3] *Department of Clinical Laboratory, First Affiliated Hospital of Nanjing University of Chinese Medicine, Nanjing 210029, China*
[4] *Department of TCM Oncology, First Affiliated Hospital of Nanjing University of Chinese Medicine, Nanjing 210029, China*

Correspondence should be addressed to Zhen Zhan; zhanzhan5607@sina.com

Received 17 July 2013; Revised 23 October 2013; Accepted 20 November 2013

Academic Editor: Shi-bing Su



In traditional Chinese medicine (TCM), correct syndrome differentiation is the most important principle guiding the prescription of Chinese herbal formulae for the treatment of gastric cancer (GC). We aimed to reveal the genetic mechanisms underlying GC syndrome differentiation (ZHENG) in a population of 387 GC patients. Twenty-nine single nucleotide polymorphisms (SNPs) in *EGF*, *TGFA*, and *EGFR* were investigated. Two SNPs, rs11466285 in *TGFA* and rs884225 in *EGFR*, were significantly associated with the distribution of ZHENG ($P < 0.05$). The rs11466285 TT genotype increased the risk of damp heat with toxin (DHT) and deficiency of both *Qi* and *yin* (DQY) compared with obstruction of blood stasis (OBS). The rs884225 AA genotype could increase the risk of DQY and deficiency of both *Qi* and blood (DQB) compared with *yin* deficiency due to stomach heat (YDSH). Parallel comparison among the SNPs and syndrome types revealed that DQB was distinct from YDSH, disharmony between the liver and stomach, stagnation of phlegm muddiness (SPM), OBS, and other syndromes at several SNP loci ($P < 0.05$). The rs11466285 TT and rs884225 AA genotypes exhibit increased risk of DQB compared with OBS and SPM ($P < 0.05$), respectively. In conclusion, the formation of GC ZHENG was related to *EGF*, *TGFA*, and *EGFR* gene polymorphisms.

## 1. Introduction

Gastric cancer (GC) is the second leading cause of cancer-related death worldwide. Most patients present with an advanced stage of the disease, which has a poor outcome. Evidently, there is a need for the development of new tactics for the treatment of this disease [1]. Traditional Chinese medicine (TCM) takes a holistic approach to medicine with emphasis on the integrity of the human body and the relationship between the human and the social and natural environments and provides a theoretical and practical approach to the treatment of GC [2]. TCM therapy, which has been effective in treating GC and improving patient quality of life, is characterized by treatment based on "syndrome differentiation" (also called ZHENG or TCM pattern) [3–5]. Correct TCM syndrome differentiation is the most important principle guiding the prescription of Chinese herbal formulae, and incorrect classification may result in serious consequences [6]. TCM focuses on treating the disease symptoms. Therefore, the diagnostic process mainly includes the gathering of data on the symptoms experienced by the physician. This evidence gathering is done using four manipulations: inspection, auscultation and olfaction, inquiry, and palpation.

The information obtained from syndrome differentiation, including symptoms, pulse feel, and the appearance of the tongue, is often considered to be subjective. Since the tongue is considered in TCM to be an outer manifestation of

the spleen and stomach, clinical literature suggests that tongue appearance is valuable for TCM diagnosis of malignant gastrointestinal cancers, such as esophageal cancer, GC, hepatic carcinoma, and colorectal cancer [7, 8]. Aspects of tongue appearance include tongue coating, tongue body, and sublingual veins. TCM medical documents indicate that tongue coating is the most valuable parameter of tongue appearance [9] and plays a role in syndrome differentiation of GC [10]. Our previous results indicated that the expression levels of epidermal growth factor (EGF), transforming growth factor alpha (TGF-$\alpha$), and EGF receptor (EGFR) were closely related to the formation of tongue coating [11, 12]. Therefore, we hypothesized that EGF, TGF-$\alpha$, and EGFR can be correlated with the ZHENG of GC.

EGF and TGF-$\alpha$ are members of the EGF super family of cytokines. They function as pleiotropic molecules during many development and pathological processes, such as wound healing and cancer progression. The diverse effects of EGF and TGF-$\alpha$ on dermal fibroblasts are initiated by their interaction with EGFR. The EGFR has a high affinity for its ligands, including EGF and TGF-$\alpha$. EGFR is extensively expressed on the basolateral membrane of intestinal epithelial cells and has multiple physiological effects in the response of the gastric mucosa to wounding *in vivo* [13]. Animal experiments show that some compounds in Chinese herbal medicines could improve the quality of experimental gastric ulcer healing by upregulating the expression of EGF and TGF-$\alpha$ in the tissue around gastric ulcer [14, 15]. Moreover, *Helicobacter pylori* infection can promote EGFR activation, which has an antiapoptotic effect to protect gastric epithelial cells [16]. These results suggest that moderate activation of the EGFR signal pathway plays an important role in the gastrointestinal mucosal repair processes following injury. However, the overactivation of EGFR participates in several essential tumorigenic mechanisms, such as tumor survival, invasion, angiogenesis, and metastatic spread. Clinical research has observed overexpression of EGFR in numerous human tumors, and several studies have demonstrated that overexpression of EGFR correlates with poor prognosis [17]. In GC, EGFR positivity is considered to be a negative prognostic factor in GC, and biomarker analysis shows that EGFR positivity is associated with poor patient outcomes after curative resection of tumor tissue [18]. EGFR overexpression is correlated with advanced tumor stage and a poor clinical outcome [19]. The EGFR pathway is regulated through the generation of ligands that activate the pathway. Therefore, a considerable amount is known about the mechanisms mediating EGF and TGF-$\alpha$ signal transduction [20]. Gene variations (such as single nucleotide polymorphisms (SNPs)) can influence the translation or mRNA degradation [21, 22].

Many studies have suggested that genetic alterations play an important role in the development and progression of GC through gene-environment interactions [23]. In GC, higher levels of EGF, TGF-$\alpha$, and EGFR correlate with advanced tumor stage and a poor clinical outcome [19, 24–26]. Previous studies have reported that the gene variations in *EGF*, *TGFA*, and *EGFR* can lead to deregulation of the EGFR pathway and overexpression of EGF, TGF-$\alpha$, and EGFR proteins [27–30], which are associated with GC and various malignancies [31, 32]. Application of TCM as an adjuvant cancer therapy can enhance quality of life of malignant GC patients and help reduce the adverse effects of chemo- and radiotherapy [33, 34]. ZHENG is an important classification in the subtype for GC TCM therapy. In this study, we hypothesized that genetic variations in *EGF*, *TGFA*, and *EGFR* may affect the formation of ZHENG of GC and form the genetic basis underlying ZHENG. To test this hypothesis, twenty-nine known SNPs in the *EGF*, *TGFA*, and *EGFR* genes were genotyped in a hospital-based population of 387 GC patients broken down into nine types of ZHENG.

## 2. Materials and Methods

*2.1. Study Subjects.* This research protocol was approved by the local ethics committee of Jiangsu Province Hospital of TCM, based on the Declaration of Helsinki. A total of 387 incident GC patients were consecutively recruited from January 2008 to July 2010 in Nanjing, Jiangsu province, eastern China. All subjects were genetically unrelated ethnic Han Chinese. A standard questionnaire was administered by trained interviewers to obtain demographic information and information on related risk factors, including tobacco smoking and alcohol consumption. After signing informed consent documentation, a 3–5 mL venous blood sample was collected from each subject.

*2.2. Diagnostic Criteria.* Diagnoses of all of the patients were confirmed by pathology. Trained interviewers used a uniform questionnaire to collect the TCM diagnostic information from the participants, namely, demographic factors such as age and gender, and known risk factors for GC (such as smoking, drinking, and a family history of digestive tract cancer). The standard criteria used for differentiation of GC ZHENG were as described previously [35]. Nine types of GC ZHENG were used: *Pi Wei Xu Ruo* (spleen and stomach deficiency, SSD), *Wei Re Yin Shang* (*yin* deficiency due to stomach heat, YDSH), *Qi Yin Liang Xu* (deficiency of both *Qi* and *yin*, DQY), *Qi Xue Liang Xu* (deficiency of both *Qi* and blood, DQB), *Gan Wei Bu He* (disharmony between the liver and stomach, DLS), *Shi Re Yun Du* (damp heat with toxin, DHT), *Tan Zhuo Ning Zhi* (stagnation of phlegm muddiness, SPM), *Yu Xue Nei Zu* (obstruction of blood stasis, OBS), and other.

Since many factors may affect the formation TCM syndromes, more than one TCM syndrome was observed in the majority of patients. To ensure a uniform and standard GC ZHENG, the most significant TCM syndromes functioned as units, which were worked out concurrently by two TCM clinical experts. Differentiation criteria for GC are as follows:

SSD: poor appetite, distension of the abdomen, severe distension after eating, epigastric pain with a desire for warmth and pressure, nausea and vomiting, loose stool or defecating with no effort, defecating for a long time, morning diarrhea, lower-extremity edema, listlessness, puffy tongue or teeth imprints on the tongue, whitish tongue coating, thready and weak pulse, or a deep and thready pulse.

YDSH: burning heat, pain after eating, dry mouth, hunger but no desire to eat, dry stool, dysphoria with feverish sensation in the chest, palms, and soles, red or crimson tongue, little or no tongue coating, and a thready and rapid pulse.

DQY: epigastric pain, listlessness, dull complexion, emaciation, shortness of breath after moving, spontaneous perspiration and night sweating, thirst but unwilling to drink, pale tongue with little coating, and a thready and weak pulse.

DQB: emaciation, weakness, low voice, dizziness, pale or yellowish complexion, pale lips and nails, palpitation, shortness of breath, spontaneous perspiration and night sweating, lower-extremity edema, a pale tongue with thin or little coating, and a thready, deep, and weak pulse.

DLS: distended stomach with pain, hypochondriac distention, emotional depression, eructation, acid regurgitation, hiccup, poor appetite, light red or red tongue, thin white or thin yellow tongue coating, and a wiry pulse.

DHT: distended pain and burning heat in the stomach, nausea and vomiting, halitosis, thirst, red tongue with yellowish and greasy coating, and a slippery and rapid pulse.

SPM: distended pain across the abdomen, nausea and vomiting or vomiting of thin and mucous fluid, poor appetite or obstructed sensation after eating, regurgitation of food, tastelessness, no thirst, dizziness, lassitude of the body, loose stool, yellowish complexion and edema, pale tongue with whitish and greasy or slippery coating, and a slippery or moderate to thready pulse.

OBS: stabbing pain or knife-like pain, fixed pain, palpable hard lumps, vomiting with red blood, tarry stool, dark purplish lips and nails, darkish complexion, dark purplish tongue or ecchymosis on the tongue, and an unsmooth pulse.

Other: no obvious syndromes.

*2.3. Inclusion Criteria.* Male and female patients with the following characteristics were included in the study: (a) aged between 20 and 80 years, (b) Han Chinese ethnicity (self-reported), (c) newly histopathologically diagnosed with primary GC, (d) lack of previous malignant tumors in other organs, (e) had not had antitumor therapy before recruitment, including chemotherapy and radiotherapy, and (f) did not have severe heart failure, pulmonary insufficiency, or kidney disease.

*2.4. Genomic DNA Isolation and Genotyping.* After signing informed consent forms, each patient donated 3–5 mL of peripheral blood to be used for genomic DNA extraction. A commercial blood DNA extraction kit (AxyPrep-96 kit, Axygen, CA, USA) was used to extract genomic DNA from the blood samples. Purified DNA samples were stored at −20°C until used for genotyping. Quality of DNA was assessed by agarose gel electrophoresis. The twenty-nine known single nucleotide polymorphisms (SNPs) in the *EGF*, *TGFA*, and *EGFR* genes were searched by the criterion "MAF ≥ 0.05" on the website http://www.ncbi.nlm.nih.gov/snp until July 2010 and are listed as follows: ten SNPs in the *EGF* gene (rs3756261 A/G and rs11568835 A/G in the 5′ near region; rs11568849 A/C, rs11568943 G/A, rs2237051 A/G, and rs11569017 A/T in the nonsynonymous exon region; rs4698803 A/T in the intron region; rs2302135 A/G in the synonymous exon region; rs3733625 A/G in the 3′ untranslated region (UTR); and rs4444903 A/G in the 5′ UTR); eight SNPs in the *TGFA* gene (rs3771527 A/T, rs503314 C/G, rs473698 C/G, rs3732253 C/T, rs538118 A/G, and rs11466285 C/T in the 3′ UTR; rs11466306 A/G in the 3′ near region; and rs2166975 G/A in the synonymous exon region); and eleven SNPs in the *EGFR* gene (rs6965469 C/T and rs884904 A/G in the 5′ near region; rs884225 A/G in the 3′ UTR; rs763317 A/G in the intron region; rs2227983 A/G and rs28384375 T/C in the nonsynonymous exon region; rs17337023 A/T, rs1140475 C/T, rs2293347 G/A, rs2072454 C/T, and rs1050171 G/A in the synonymous exon region).

Polymerase chain reaction-ligation detection reaction (PCR-LDR) was used for genotyping the SNPs, as previously described [29, 36]. In brief, primers were synthesized by Shanghai Sangon Biological Engineering Technology and Services (Shanghai, China). Each set of ligase detection reaction probes comprised one common probe and two discriminating probes for the two types (Table S1 in the Supplementary Matrial available online at http://dx.doi.org/10.1155/2013/731071). After the target DNA sequences were amplified using a multiplex PCR method (Figure S1), the ligation reaction for each subject was carried out in a final volume of 10 $\mu$L containing 1 × NEB Taq DNA ligase buffer, 12.5 pmol of each probe mix, 0.05 $\mu$L Taq DNA ligase, and 1 $\mu$L of multi-PCR product. Probe sequences are shown in Table S2. The fluorescent products of the ligase detection reactions were differentiated by an ABI sequencer 377 (Figure S2). To confirm the accuracy of the PCR-LDR genotyping method, direct DNA sequencing of randomly selected PCR products was performed. The proportion of the sequencing samples was about 5%. The PCR-LDR genotyping results showed complete agreement with the direct DNA sequencing results.

*2.5. Statistical Analyses.* All statistical analyses were conducted using SPSS software, version 16.0 (SPSS Inc., Chicago, IL, USA). The allele and genotype distribution of the SNPs were analyzed by a two-sided $\chi^2$-test among the nine types of GC ZHENG categories. All $P$ values were two-sided, and a $P$ value < 0.05 was considered statistically significant.

## 3. Results

*3.1. Characteristics of the Study Subjects.* A total of 387 GC patients were included in the analysis. Gender, age, and ZHENG distribution of subjects are shown in Table 1. The gender proportion and smoking status among the nine syndrome types of GC were significantly different ($\chi^2$ = 22.342, $P$ = 0.004; $\chi^2$ = 15.844, $P$ = 0.045), but no significant differences were observed between age and smoking status ($P$ > 0.05).

*3.2. Genotyping Distribution and Syndrome Types of GC.* No statistically significant differences were observed for

Table 1: Common characteristics of patients.

| Parameters | Type of ZHENG | | | | | | | | | $\chi^2$ | $P$ |
|---|---|---|---|---|---|---|---|---|---|---|---|
| | SSD | YDSH | DQY | DQB | DLS | DHT | SPM | OBS | Other | | |
| Cases | | | | | | | | | | | |
| *n* (%) | 61 (15.8) | 59 (15.2) | 23 (5.9) | 49 (12.7) | 43 (11.1) | 54 (14.0) | 41 (10.6) | 35 (9.0) | 22 (5.7) | — | — |
| Gender | | | | | | | | | | | |
| Male *n* (%) | 41 (67.2) | 45 (76.3) | 13 (56.5) | 31 (63.3) | 21 (48.8) | 43 (79.6) | 31 (75.6) | 31 (88.6) | 15 (68.2) | 22.342 | 0.004 |
| Female *n* (%) | 20 (32.8) | 14 (23.7) | 10 (43.5) | 18 (36.7) | 22 (51.2) | 11 (20.4) | 10 (24.4) | 4 (11.4) | 7 (31.8) | — | — |
| Age (mean ± S) | | | | | | | | | | | |
| Total cases | 58.3 ± 11.7 | 61.0 ± 10.6 | 57.9 ± 13.2 | 59.8 ± 11.7 | 59.3 ± 13.2 | 61.2 ± 12.8 | 57.3 ± 10.5 | 60.4 ± 9.3 | 55.4 ± 13.1 | 8.472 | 0.389 |
| Male | 61.2 ± 9.3 | 61.6 ± 9.9 | 62.1 ± 6.9 | 60.5 ± 10.9 | 61.9 ± 12.8 | 63.0 ± 12.1 | 59.5 ± 10.2 | 61.5 ± 9.1 | 58.3 ± 11.0 | 4.200 | 0.839 |
| Female | 52.6 ± 14.1 | 59.0 ± 12.8 | 52.4 ± 17.4 | 58.8 ± 13.0 | 57.0 ± 13.5 | 57.0 ± 15.0 | 50.5 ± 8.8 | 52.5 ± 7.8 | 49.3 ± 16.1 | 7.989 | 0.435 |
| <60 | 30 (49.2) | 29 (49.2) | 13 (56.5) | 26 (53.1) | 23 (53.5) | 24 (44.4) | 29 (70.7) | 17 (48.6) | 16 (72.7) | 10.802 | 0.213 |
| >60 | 31 (50.8) | 30 (50.8) | 10 (43.5) | 23 (46.9) | 20 (46.5) | 30 (55.6) | 12 (29.3) | 18 (51.4) | 6 (27.3) | — | — |
| Smoking *n* (%) | | | | | | | | | | | |
| No | 33 (54.1) | 26 (44.1) | 13 (56.5) | 28 (57.1) | 28 (65.1) | 25 (46.3) | 23 (56.1) | 14 (40.0) | 14 (63.6) | 9.392 | 0.310 |
| Yes | 28 (45.9) | 33 (55.9) | 10 (43.5) | 21 (42.9) | 15 (34.9) | 29 (53.7) | 18 (43.9) | 21 (60.0) | 8 (36.4) | — | — |
| Drinking *n* (%) | | | | | | | | | | | |
| No | 29 (47.5) | 24 (40.7) | 9 (39.1) | 34 (69.4) | 25 (58.1) | 25 (46.3) | 16 (39.0) | 13 (37.1) | 10 (45.5) | 15.844 | 0.045 |
| Yes | 32 (52.5) | 35 (59.3) | 14 (60.9) | 15 (30.6) | 18 (41.9) | 29 (53.7) | 25 (61.0) | 22 (62.9) | 12 (54.5) | — | — |

genotype and allele distributions of the ten SNPs in the *EGF* gene among the nine syndrome types of GC ($P > 0.05$) (Table 2). However, in the *TGFA* and *EGFR* genes, two respective SNPs in the 3′ UTR, rs11466285 and rs884225, were significantly different in genotype distribution among the nine GC syndrome types ($\chi^2 = 31.012$, $P = 0.013$, and $\chi^2 = 29.163$, $P = 0.023$) (Tables 3 and 4). The rs11466285 TT genotype distinctly increased the risk of DHT and DQY compared with OBS, and the rs884225 AA genotype could increase the risk of DQY and DQB compared with YDSH. A statistically significant difference was observed in allele distribution, but not the genotype distribution, of the SNP rs884904 A/G in the 5′ near region of the *EGFR* gene among the nine GC syndrome types ($P > 0.05$) (Table 4). Since only the T alleles of SNPs rs28384375 and rs4698803 were detected in this study and the nine types of ZHENG were distinct, a parallel comparison of the genotype and allele distribution of the remaining twenty-seven SNPs between arbitrary pairs of syndrome types linked to polymorphic *EGF*, *TGFA*, and *EGFR* was also conducted. Regarding the relationship between *EGF*, *TGFA*, and *EGFR* gene polymorphisms and GC ZHENG, a parallel comparison of the genotype distribution of the SNPs between either of the two syndrome types linked to polymorphic *TGFA* and *EGFR* was conducted. Fifteen SNPs showed significant differences between random pairs of syndrome types ($P < 0.05$) (Table 5). In these SNPs, four SNPs are in the *EGF* gene, four SNPs are in the *TGFA* gene, and seven SNPs are in the *EGFR* gene. This means that five SNPs (rs3733625, rs3771527, rs3732253, rs11466285, and rs884225) are located in the 3′ UTR, five SNPs (rs11569017, rs2166975, rs17337023, rs1140475, and rs2072454) are located in the exon region, rs763317 is located in the intron region, three SNPs (rs11568835, rs6965469, and rs884904) are located in the 5′ near region, and rs4444903 is located in the 5′ UTR.

More than three SNPs differed among the pairs of syndrome types: DQB versus YDSH, DQB versus DLS, DQB versus SPM, DQB versus OBS, and DQB versus other ($P < 0.05$) (Table 5). First, DQB was significantly different from YDSH in three SNPs (3′ UTR rs884225, 5′ near region rs884904, and exon region rs2072454) (Table 5). Compared with YDSH, the rs884225 AA genotype and A allele and the rs884904 GG genotype and G allele increased the risk of DQB ($P < 0.05$). However, the rs2072454 TT genotype and T allele decreased the risk of DQB ($P < 0.05$) (Table 4). Second, DQB was significantly different from DLS in four SNPs (3′ UTR rs3771527, 5′ near region rs6965469, exon region rs1140475, and intron region rs763317). Compared with DLS, the rs3771527 TT genotype decreased the risk of DQB, the rs6965469 C allele increased the risk of DQB (Table 3), the rs1140475 TC genotype and T allele increased the risk of DQB, and the rs763317 GG genotype and G allele increased the risk of DQB (all $P < 0.05$) (Table 4). Third, DQB was significantly different from SPM in three SNPs (5′ near region rs11568835, exon region rs11569017, and intron region rs763317) ($P < 0.05$). Compared with SPM, the rs11568835 GA genotype increased the risk of DQB though the AA genotype was not detected in DQB. The rs11569017 AA genotype and A allele increased the risk of DQB (Table 2), and the rs763317 A allele decreased the risk of DQB (all $P < 0.05$) (Table 4). Fourth, DQB was significantly different from OBS in three SNPs (5′ UTR rs4444903, 3′ UTR rs884225, and 5′ near region rs884904). Compared with OBS, the rs4444903 A allele increased the risk of DQB (Table 2), the rs884225 AA genotype and A allele increased the risk of DQB, and

Table 2: Relationship between *EGF* gene polymorphisms and the ZHENG of GC.

| SNPs | Genotype | Type of ZHENG *n* (%) | | | | | | | | | $\chi^2$ | *P* |
|---|---|---|---|---|---|---|---|---|---|---|---|---|
| | | SSD | YDSH | DQY | DQB | DLS | DHT | SPM | OBS | Other | | |
| rs11568943 | GG | 37 (60.7) | 34 (58.6) | 13 (56.5) | 31 (64.6) | 25 (58.1) | 32 (59.3) | 17 (42.5) | 24 (68.6) | 14 (63.6) | 15.002 | 0.524 |
| | GA | 21 (34.4) | 19 (32.8) | 9 (39.1) | 14 (29.2) | 17 (39.5) | 18 (33.3) | 23 (57.5) | 9 (25.7) | 7 (31.8) | — | — |
| | AA | 3 (4.9) | 5 (8.6) | 1 (4.3) | 3 (6.2) | 1 (2.3) | 4 (7.4) | 0 (0.0) | 2 (5.7) | 1 (4.5) | — | — |
| | GA/AA | 24 (39.3) | 24 (41.4) | 10 (43.5) | 17 (35.4) | 18 (41.9) | 22 (40.7) | 23 (57.5) | 11 (31.4) | 8 (36.4) | 6.791 | 0.559 |
| | G allele | 95 (77.9) | 87 (75.0) | 35 (76.1) | 76 (79.2) | 67 (77.9) | 82 (75.9) | 57 (71.3) | 57 (81.4) | 35 (79.5) | 3.125 | 0.926 |
| | A allele | 27 (22.1) | 29 (25.0) | 11 (23.9) | 20 (20.8) | 19 (22.1) | 26 (24.1) | 23 (28.8) | 13 (18.6) | 9 (20.5) | — | — |
| rs3733625 | AA | 42 (68.9) | 36 (62.1) | 17 (73.9) | 32 (66.7) | 34 (79.1) | 40 (74.1) | 22 (55.0) | 26 (74.3) | 18 (81.8) | 17.171 | 0.375 |
| | GA | 17 (27.9) | 21 (36.2) | 6 (26.1) | 13 (27.1) | 8 (18.6) | 12 (22.2) | 18 (45.0) | 8 (22.9) | 3 (13.6) | — | — |
| | GG | 2 (3.3) | 1 (1.7) | 0 (0.0) | 3 (6.2) | 1 (2.3) | 2 (3.7) | 0 (0.0) | 1 (2.9) | 1 (4.5) | — | — |
| | GA/GG | 19 (31.1) | 22 (37.9) | 6 (26.1) | 16 (33.3) | 9 (20.9) | 14 (25.9) | 18 (45.0) | 9 (25.7) | 4 (18.2) | 10.233 | 0.249 |
| | A allele | 101 (82.8) | 93 (80.2) | 40 (87.0) | 77 (80.2) | 76 (88.4) | 92 (85.2) | 62 (77.5) | 60 (85.7) | 39 (88.6) | 6.946 | 0.542 |
| | G allele | 21 (17.2) | 23 (19.8) | 6 (13.0) | 19 (19.8) | 10 (11.6) | 16 (14.8) | 18 (22.5) | 10 (14.3) | 5 (11.4) | — | — |
| rs2302135 | AA | 31 (50.8) | 29 (50.9) | 9 (39.1) | 23 (47.9) | 22 (51.2) | 27 (50.0) | 21 (52.5) | 17 (48.6) | 14 (63.6) | 5.218 | 0.995 |
| | GA | 26 (42.6) | 25 (43.9) | 12 (52.2) | 22 (45.8) | 18 (41.9) | 24 (44.4) | 18 (45.0) | 15 (42.9) | 6 (27.3) | — | — |
| | GG | 4 (6.6) | 3 (5.3) | 2 (8.7) | 3 (6.2) | 3 (7.0) | 3 (5.6) | 1 (2.5) | 3 (8.6) | 2 (9.1) | — | — |
| | GA/GG | 30 (49.2) | 28 (49.1) | 14 (60.9) | 25 (52.1) | 21 (48.8) | 27 (50.0) | 19 (47.5) | 18 (51.4) | 8 (36.4) | 2.969 | 0.936 |
| | A allele | 88 (72.1) | 83 (72.8) | 30 (65.2) | 68 (70.8) | 62 (72.1) | 78 (72.2) | 60 (75.0) | 49 (70.0) | 34 (77.3) | 2.26 | 0.972 |
| | G allele | 34 (27.9) | 31 (27.2) | 16 (34.8) | 28 (29.2) | 24 (27.9) | 30 (27.8) | 20 (25.0) | 21 (30.0) | 10 (22.7) | — | — |
| rs2237051 | AA | 24 (39.3) | 21 (36.2) | 12 (52.2) | 19 (39.6) | 17 (39.5) | 22 (40.7) | 19 (47.5) | 19 (54.3) | 9 (40.9) | 15.040 | 0.522 |
| | GA | 29 (47.5) | 33 (56.9) | 9 (39.1) | 26 (54.2) | 25 (58.1) | 30 (55.6) | 18 (45.0) | 14 (40.0) | 9 (40.9) | — | — |
| | GG | 8 (13.1) | 4 (6.9) | 2 (8.7) | 3 (6.2) | 1 (2.3) | 2 (3.7) | 3 (7.5) | 2 (5.7) | 4 (18.2) | — | — |
| | GA/GG | 37 (60.7) | 37 (63.8) | 11 (47.8) | 29 (60.4) | 26 (60.5) | 32 (59.3) | 21 (52.5) | 16 (45.7) | 13 (59.1) | 4.875 | 0.771 |
| | A allele | 77 (63.1) | 75 (64.7) | 33 (71.7) | 64 (66.7) | 59 (68.6) | 74 (68.5) | 56 (70.0) | 52 (74.3) | 27 (61.4) | 4.431 | 0.816 |
| | G allele | 45 (36.9) | 41 (35.3) | 13 (28.3) | 32 (33.3) | 27 (31.4) | 34 (31.5) | 24 (30.0) | 18 (25.7) | 17 (38.6) | — | — |
| rs11568849 | AA | 57 (93.4) | 57 (98.3) | 21 (95.5) | 48 (100.0) | 42 (100.0) | 51 (94.4) | 38 (97.4) | 35 (100.0) | 21 (95.5) | 8.744 | 0.364 |
| | CA | 4 (6.6) | 1 (1.7) | 1 (4.5) | 0 (0.0) | 0 (0.0) | 3 (5.6) | 1 (2.6) | 0 (0.0) | 1 (4.5) | — | — |
| | A allele | 118 (96.7) | 115 (99.1) | 43 (97.7) | 96 (100.0) | 84 (100.0) | 105 (97.2) | 77 (98.7) | 70 (100.0) | 43 (97.7) | 8.616 | 0.376 |
| | C allele | 4 (3.3) | 1 (0.9) | 1 (2.3) | 0 (0.0) | 0 (0.0) | 3 (2.8) | 1 (1.3) | 0 (0.0) | 1 (2.3) | — | — |
| rs3756261 | AA | 40 (65.6) | 36 (62.1) | 13 (56.5) | 32 (66.7) | 28 (65.1) | 33 (61.1) | 18 (45.0) | 21 (61.8) | 15 (68.2) | 13.120 | 0.664 |
| | GA | 17 (27.9) | 17 (29.3) | 9 (39.1) | 13 (27.1) | 14 (32.6) | 18 (33.3) | 21 (52.5) | 12 (35.3) | 7 (31.8) | — | — |
| | GG | 4 (6.6) | 5 (8.6) | 1 (4.3) | 3 (6.2) | 1 (2.3) | 3 (5.6) | 1 (2.5) | 1 (2.9) | 0 (0.0) | — | — |
| | GA/GG | 21 (34.4) | 22 (37.9) | 10 (43.5) | 16 (33.3) | 15 (34.9) | 21 (38.9) | 22 (55.0) | 13 (38.2) | 7 (31.8) | 6.479 | 0.594 |
| | A allele | 97 (79.5) | 89 (76.7) | 35 (76.1) | 77 (80.2) | 70 (81.4) | 84 (77.8) | 57 (71.3) | 54 (79.4) | 37 (84.1) | 4.377 | 0.822 |
| | G allele | 25 (20.5) | 27 (23.3) | 11 (23.9) | 19 (19.8) | 16 (18.6) | 24 (22.2) | 23 (28.8) | 14 (20.6) | 7 (15.9) | — | — |
| rs4444903 | GG | 27 (44.3) | 22 (38.6) | 13 (59.1) | 20 (45.5) | 21 (50.0) | 24 (44.4) | 20 (50.0) | 21 (61.8) | 9 (42.9) | 14.518 | 0.560 |
| | GA | 27 (44.3) | 31 (54.4) | 7 (31.8) | 19 (43.2) | 19 (45.2) | 24 (44.4) | 19 (47.5) | 12 (35.3) | 8 (38.1) | — | — |
| | AA | 7 (11.5) | 4 (7.0) | 2 (9.1) | 5 (11.4) | 2 (4.8) | 6 (11.1) | 1 (2.5) | 1 (2.9) | 4 (19.0) | — | — |
| | GA/AA | 34 (55.7) | 35 (61.4) | 9 (40.9) | 24 (54.5) | 21 (50.0) | 30 (55.6) | 20 (50.0) | 13 (38.2) | 12 (57.1) | 6.682 | 0.571 |
| | G allele | 81 (66.4) | 75 (65.8) | 33 (75.0) | 59 (67.0) | 61 (72.6) | 72 (66.7) | 59 (73.8) | 54 (79.4) | 26 (61.9) | 7.911 | 0.442 |
| | A allele | 41 (33.6) | 39 (34.2) | 11 (25.0) | 29 (33.0) | 23 (27.4) | 36 (33.3) | 21 (26.3) | 14 (20.6) | 16 (38.1) | — | — |
| rs11569017 | AA | 39 (67.2) | 34 (60.7) | 13 (61.9) | 28 (70.0) | 25 (59.5) | 34 (64.2) | 15 (39.5) | 22 (62.9) | 15 (68.2) | 16.137 | 0.443 |
| | TA | 17 (29.3) | 19 (33.9) | 8 (38.1) | 9 (22.5) | 16 (38.1) | 16 (30.2) | 21 (55.3) | 12 (34.3) | 5 (22.7) | — | — |
| | TT | 2 (3.4) | 3 (5.4) | 0 (0.0) | 3 (7.5) | 1 (2.4) | 3 (5.7) | 2 (5.3) | 1 (2.9) | 2 (9.1) | — | — |
| | TA/TT | 19 (32.8) | 22 (39.3) | 8 (38.1) | 12 (30.0) | 17 (40.5) | 19 (35.8) | 23 (60.5) | 13 (37.1) | 7 (31.8) | 10.511 | 0.231 |
| | A allele | 95 (81.9) | 87 (77.7) | 34 (81.0) | 65 (81.3) | 66 (78.6) | 84 (79.2) | 51 (67.1) | 56 (80.0) | 35 (79.5) | 7.348 | 0.500 |
| | T allele | 21 (18.1) | 25 (22.3) | 8 (19.0) | 15 (18.8) | 18 (21.4) | 22 (20.8) | 25 (32.9) | 14 (20.0) | 9 (20.5) | — | — |

Table 2: Continued.

| SNPs | Genotype | Type of ZHENG $n$ (%) | | | | | | | | | $\chi^2$ | $P$ |
|---|---|---|---|---|---|---|---|---|---|---|---|---|
| | | SSD | YDSH | DQY | DQB | DLS | DHT | SPM | OBS | Other | | |
| rs11568835 | GG | 43 (72.9) | 49 (84.5) | 13 (65.0) | 30 (71.4) | 27 (65.9) | 39 (75.0) | 31 (77.5) | 22 (66.7) | 15 (71.4) | 15.005 | 0.524 |
| | GA | 15 (25.4) | 7 (12.1) | 7 (35.0) | 12 (28.6) | 12 (29.3) | 12 (23.1) | 7 (17.5) | 11 (33.3) | 6 (28.6) | — | — |
| | AA | 1 (1.7) | 2 (3.4) | 0 (0.0) | 0 (0.0) | 2 (4.9) | 1 (1.9) | 2 (5.0) | 0 (0.0) | 0 (0.0) | — | — |
| | GA/AA | 16 (27.1) | 9 (15.5) | 7 (35.0) | 12 (28.6) | 14 (34.1) | 13 (25.0) | 9 (22.5) | 11 (33.3) | 6 (28.6) | 6.894 | 0.548 |
| | G allele | 101 (85.6) | 105 (90.5) | 33 (82.5) | 72 (85.7) | 66 (80.5) | 90 (86.5) | 69 (86.3) | 55 (83.3) | 36 (85.7) | 4.717 | 0.787 |
| | A allele | 17 (14.4) | 11 (9.5) | 7 (17.5) | 12 (14.3) | 16 (19.5) | 14 (13.5) | 11 (13.8) | 11 (16.7) | 6 (14.3) | — | — |

the rs884904 GG genotype and G allele increased the risk of DQB (all $P < 0.05$) (Table 4). Finally, DQB was significantly different from other syndromes in four SNPs (3′ UTR rs3771527, 3′ UTR rs884225, 5′ near region rs884904, and exon region rs2072454). Compared with other syndromes, the rs3771527 homozygote (TT and AA) decreased the risk of DQB, but the heterozygote (TA) increased the risk of DQB (Table 3). The rs884225 AA genotype and A allele increased the risk of DQB, the rs884904 GG genotype and G allele increased the risk of DQB, and the rs2072454 AA genotype and A allele decreased the risk of DQB (all $P < 0.05$) (Table 4). In addition, the rs1140475 TC genotype significantly increased the risk of DQB compared with SSD, and the rs884225 AA genotype significantly increased the risk of DQB compared with DHT (Table 4). These results demonstrate that DQB was the most different from the other five types of ZHENG (SPM, DLS, YDSH, OBS, and other).

Several SNPs were different among several pairs of syndromes. The SNP rs884225 was different in six pairs of syndrome types (DQB versus YDSH, YDSH versus DQY, DQB versus DHT, DQB versus SPM, DQB versus OBS, and DQB versus other syndromes), rs11466285 was different in five pairs of syndrome types (DQY vs. DLS, DHT vs. DLS, DHT versus SPM, DQY versus OBS, and DHT versus OBS), and rs884904 was different in five pairs of syndrome types (DQB versus YDSH, YDSH versus DQY, DQB versus SPM, DQB vs. OBS, and DQB vs. other syndromes). There were also two pairs of syndrome types in which the SNPs were different for rs11568835, rs3733625, rs11569017, rs3771527, rs2166975, rs1140475, rs763317, and rs2072454. However, there was only one pair of syndrome types in which the SNPs were distinctly different for rs4444903, rs3732253, rs6965469, and rs17337023 (Table 5). These results are consistent with observation that rs884225 and rs11466285 are significantly correlated to the distribution of ZHENG in GC patients ($P < 0.05$).

## 4. Discussion

The gathering of evidence from the four manipulations plays an important role in correct differentiation of ZHENG. However, it is not clear whether congenital defects can influence the formation of ZHENG, which may be essential to classifying the subtypes of GC based on the symptoms. TCM hypothesizes that congenital endowments are determined by genes. However, genes can mutate due to a variety of factors, including environmental variation. Genetic variation in the human genome is an emerging resource for studying cancer, a complex set of diseases characterized by both environmental and genetic contributions. The most common type of sequence variation in the human genome is the SNP [37]. SNPs are the most abundant class of human polymorphisms, which is the main reason medical researchers are so interested in them, despite their simplicity and limited polymorphic content. SNPs can be used as markers to identify genes that underlie complex diseases and to realize the full potential of pharmacogenomics by facilitating analysis of variable responses to drugs. With the improvement of SNP genotyping technologies, a variety of different SNP typing protocols are available for researchers [38]. Several studies have shown that TCM syndromes are associated with gene SNPs, for example the serotonin transporter gene polymorphism and excess of liver *yang* syndrome [39], ABCA1 gene polymorphism and phlegm syndrome and blood stasis syndrome in coronary heart disease [40], kidney-*yang* deficiency syndrome and linkage disequilibrium SNPs [41], liver Qi stagnation syndrome and gene polymorphism of tryptophan hydroxylase and G-protein $\beta 3$ submission in HBC patients [42], AT1R gene polymorphism and ZHENG in essential hypertension [43], and some cytokine gene (*TNFA*, *TGFB1*, and *IL10*) polymorphisms and TCM syndromes in hepatitis B cirrhosis patients [44–46]. However, there are few studies on the relationship between genetic susceptibility and GC ZHENG.

GC is a complex disease with a high mortality rate. The identification of vast numbers of SNPs should enable us to prevent or alleviate the disease by detecting potential disease-susceptibility alleles and diallelic markers [47]. The study of genetic variation could provide future implications for preventive and early intervention strategies. Many studies have suggested that GC development, treatment, and clinical outcome are associated with variations in several genes, including *EGFR* [48, 49], glutathione-S-transferase M1 and T1 [50], p53 [51], E-cadherin(*CDH1*) [52], and cyclooxygenase-2 [53]. We showed that lifestyle (such as meal duration) and clinical examination (such as the status of glutamic pyruvic transaminase) were significantly associated with GC ZHENG, and rs13689 in *CDH1* is correlated with the GC ZHENG type [54]. To probe the genetic traits of the GC ZHENG, we examined the gene polymorphisms in *EGF*, *TGFA*, and *EGFR* in 387 GC patients by ZHENG.

EGF and TGF-$\alpha$ induce an equipotent stimulation of proliferation because of their homologous structure and

Table 3: Relationship between *TGFA* gene polymorphisms and the ZHENG of GC.

| SNPs | Genotype | Type of ZHENG *n* (%) | | | | | | | | | $\chi^2$ | *P* |
|---|---|---|---|---|---|---|---|---|---|---|---|---|
| | | SSD | YDSH | DQY | DQB | DLS | DHT | SPM | OBS | Other | | |
| rs3771527 | TT | 39 (67.2) | 37 (68.5) | 15 (71.4) | 26 (56.5) | 32 (80.0) | 37 (69.8) | 25 (64.1) | 22 (64.7) | 16 (76.2) | 21.067 | 0.176 |
| | TA | 16 (27.6) | 17 (31.5) | 4 (19.0) | 20 (43.5) | 8 (20.0) | 13 (24.5) | 13 (33.3) | 11 (32.4) | 3 (14.3) | — | — |
| | AA | 3 (5.2) | 0 (0.0) | 2 (9.5) | 0 (0.0) | 0 (0.0) | 3 (5.7) | 1 (2.6) | 1 (2.9) | 2 (9.5) | — | — |
| | TA/AA | 19 (32.8) | 17 (31.5) | 6 (28.6) | 20 (43.5) | 8 (20.0) | 16 (30.2) | 14 (35.9) | 12 (35.3) | 5 (23.8) | 6.740 | 0.565 |
| | T allele | 94 (81.0) | 91 (84.3) | 34 (81.0) | 72 (78.3) | 72 (90.0) | 87 (82.1) | 63 (80.8) | 55 (80.9) | 35 (83.3) | 5.019 | 0.756 |
| | A allele | 22 (19.0) | 17 (15.7) | 8 (19.0) | 20 (21.7) | 8 (10.0) | 19 (17.9) | 15 (19.2) | 13 (19.1) | 7 (16.7) | — | — |
| rs538118 | AA | 27 (45.8) | 24 (41.4) | 13 (56.5) | 27 (56.2) | 24 (58.5) | 27 (50.9) | 21 (52.5) | 17 (48.6) | 9 (40.9) | 11.900 | 0.751 |
| | GA | 26 (44.1) | 28 (48.3) | 6 (26.1) | 15 (31.2) | 15 (36.6) | 23 (43.4) | 16 (40.0) | 15 (42.9) | 12 (54.5) | — | — |
| | GG | 6 (10.2) | 6 (10.3) | 4 (17.4) | 6 (12.5) | 2 (4.9) | 3 (5.7) | 3 (7.5) | 3 (8.6) | 1 (4.5) | — | — |
| | GA/GG | 32 (54.2) | 34 (58.6) | 10 (43.5) | 21 (43.8) | 17 (41.5) | 26 (49.1) | 19 (47.5) | 18 (51.4) | 13 (59.1) | 5.356 | 0.719 |
| | A allele | 80 (67.8) | 76 (65.5) | 32 (69.6) | 69 (71.9) | 63 (76.8) | 77 (72.6) | 58 (72.5) | 49 (70.0) | 30 (68.2) | 3.99 | 0.858 |
| | G allele | 38 (32.2) | 40 (34.5) | 14 (30.4) | 27 (28.1) | 19 (23.2) | 29 (27.4) | 22 (27.5) | 21 (30.0) | 14 (31.8) | — | — |
| rs473698 | CC | 28 (45.9) | 25 (43.1) | 13 (56.5) | 27 (56.2) | 24 (55.8) | 29 (53.7) | 20 (50.0) | 18 (52.9) | 9 (40.9) | 6.733 | 0.978 |
| | GC | 27 (44.3) | 28 (48.3) | 8 (34.8) | 16 (33.3) | 16 (37.2) | 23 (42.6) | 17 (42.5) | 14 (41.2) | 11 (50.0) | — | — |
| | GG | 6 (9.8) | 5 (8.6) | 2 (8.7) | 5 (10.4) | 3 (7.0) | 2 (3.7) | 3 (7.5) | 2 (5.9) | 2 (9.1) | — | — |
| | GC/GG | 33 (54.1) | 33 (56.9) | 10 (43.5) | 21 (43.8) | 19 (44.2) | 25 (46.3) | 20 (50.0) | 16 (47.1) | 13 (59.1) | 4.354 | 0.824 |
| | C allele | 83 (68.0) | 78 (67.2) | 34 (73.9) | 70 (72.9) | 64 (74.4) | 81 (75.0) | 57 (71.3) | 50 (73.5) | 29 (65.9) | 3.766 | 0.878 |
| | G allele | 39 (32.0) | 38 (32.8) | 12 (26.1) | 26 (27.1) | 22 (25.6) | 27 (25.0) | 23 (28.8) | 18 (26.5) | 15 (34.1) | — | — |
| rs3732253 | CC | 33 (54.1) | 25 (43.1) | 10 (43.5) | 25 (52.1) | 18 (41.9) | 19 (35.2) | 16 (40.0) | 20 (57.1) | 11 (50.0) | 15.486 | 0.489 |
| | TC | 23 (37.7) | 27 (46.6) | 8 (34.8) | 19 (39.6) | 22 (51.2) | 31 (57.4) | 20 (50.0) | 14 (40.0) | 8 (36.4) | — | — |
| | TT | 5 (8.2) | 6 (10.3) | 5 (21.7) | 4 (8.3) | 3 (7.0) | 4 (7.4) | 4 (10.0) | 1 (2.9) | 3 (13.6) | — | — |
| | TC/TT | 28 (45.9) | 33 (56.9) | 13 (56.5) | 23 (47.9) | 25 (58.1) | 35 (64.8) | 24 (60.0) | 15 (42.9) | 11 (50.0) | 7.887 | 0.445 |
| | C allele | 89 (73.0) | 77 (66.4) | 28 (60.9) | 69 (71.9) | 58 (67.4) | 69 (63.9) | 52 (65.0) | 54 (77.1) | 30 (68.2) | 7.097 | 0.526 |
| | T allele | 33 (27.0) | 39 (33.6) | 18 (39.1) | 27 (28.1) | 28 (32.6) | 39 (36.1) | 28 (35.0) | 16 (22.9) | 14 (31.8) | — | — |
| rs11466306 | GG | 33 (54.1) | 22 (37.9) | 7 (31.8) | 25 (52.1) | 17 (40.5) | 20 (37.0) | 18 (45.0) | 20 (57.1) | 11 (50.0) | 15.477 | 0.490 |
| | GA | 23 (37.7) | 30 (51.7) | 10 (45.5) | 18 (37.5) | 22 (52.4) | 30 (55.6) | 18 (45.0) | 13 (37.1) | 8 (36.4) | — | — |
| | AA | 5 (8.2) | 6 (10.3) | 5 (22.7) | 5 (10.4) | 3 (7.1) | 4 (7.4) | 4 (10.0) | 2 (5.7) | 3 (13.6) | — | — |
| | GA/AA | 28 (45.9) | 36 (62.1) | 15 (68.2) | 23 (47.9) | 25 (59.5) | 34 (63.0) | 22 (55.0) | 15 (42.9) | 11 (50.0) | 9.743 | 0.284 |
| | G allele | 89 (73.0) | 74 (63.8) | 24 (54.5) | 68 (70.8) | 56 (66.7) | 70 (64.8) | 54 (67.5) | 53 (75.7) | 30 (68.2) | 8.786 | 0.361 |
| | A allele | 33 (27.0) | 42 (36.2) | 20 (45.5) | 28 (29.2) | 28 (33.3) | 38 (35.2) | 26 (32.5) | 17 (24.3) | 14 (31.8) | — | — |
| rs11466285 | TT | 48 (80.0) | 48 (84.2) | 20 (90.9) | 39 (81.2) | 27 (67.5) | 49 (92.5) | 28 (70.0) | 22 (62.9) | 18 (81.8) | 31.012 | 0.013 |
| | TC | 12 (20.0) | 9 (15.8) | 2 (9.1) | 9 (18.8) | 13 (32.5) | 4 (7.5) | 12 (30.0) | 12 (34.3) | 3 (13.6) | — | — |
| | CC | 0 (0.0) | 0 (0.0) | 0 (0.0) | 0 (0.0) | 0 (0.0) | 0 (0.0) | 0 (0.0) | 1 (2.9) | 1 (4.5) | — | — |
| | TC/CC | 12 (20.0) | 9 (15.8) | 2 (9.1) | 9 (18.8) | 13 (32.5) | 4 (7.5) | 12 (30.0) | 13 (37.1) | 4 (18.2) | 19.716 | 0.011 |
| | T allele | 108 (90.0) | 105 (92.1) | 42 (95.5) | 87 (90.6) | 67 (83.8) | 102 (96.2) | 68 (85.0) | 56 (80.0) | 39 (88.6) | 18.86 | 0.016 |
| | C allele | 12 (10.0) | 9 (7.9) | 2 (4.5) | 9 (9.4) | 13 (16.3) | 4 (3.8) | 12 (15.0) | 14 (20.0) | 5 (11.4) | — | — |
| rs503314 | GG | 24 (42.9) | 20 (36.4) | 9 (47.4) | 22 (48.9) | 21 (53.8) | 26 (52.0) | 19 (48.7) | 16 (47.1) | 8 (38.1) | 6.720 | 0.978 |
| | GC | 25 (44.6) | 28 (50.9) | 7 (36.8) | 17 (37.8) | 15 (38.5) | 20 (40.0) | 17 (43.6) | 15 (44.1) | 10 (47.6) | — | — |
| | CC | 7 (12.5) | 7 (12.7) | 3 (15.8) | 6 (13.3) | 3 (7.7) | 4 (8.0) | 3 (7.7) | 3 (8.8) | 3 (14.3) | — | — |
| | GC/CC | 32 (57.1) | 35 (63.6) | 10 (52.6) | 23 (51.1) | 18 (46.2) | 24 (48.0) | 20 (51.3) | 18 (52.9) | 13 (61.9) | 4.793 | 0.780 |
| | G allele | 73 (65.2) | 68 (61.8) | 25 (65.8) | 61 (67.8) | 57 (73.1) | 72 (72.0) | 55 (70.5) | 47 (69.1) | 26 (61.9) | 4.985 | 0.759 |
| | C allele | 39 (34.8) | 42 (38.2) | 13 (34.2) | 29 (32.2) | 21 (26.9) | 28 (28.0) | 23 (29.5) | 21 (30.9) | 16 (38.1) | — | — |
| rs2166975 | GG | 31 (54.4) | 24 (42.1) | 9 (42.9) | 23 (51.1) | 17 (41.5) | 20 (38.5) | 16 (39.0) | 21 (63.6) | 10 (45.5) | 13.479 | 0.637 |
| | GA | 21 (36.8) | 26 (45.6) | 7 (33.3) | 17 (37.8) | 20 (48.8) | 26 (50.0) | 19 (46.3) | 9 (27.3) | 8 (36.4) | — | — |
| | AA | 5 (8.8) | 7 (12.3) | 5 (23.8) | 5 (11.1) | 4 (9.8) | 6 (11.5) | 6 (14.6) | 3 (9.1) | 4 (18.2) | — | — |
| | GA/AA | 26 (45.6) | 33 (57.9) | 12 (57.1) | 22 (48.9) | 24 (58.5) | 32 (61.5) | 25 (61.0) | 12 (36.4) | 12 (54.5) | 8.959 | 0.346 |
| | G allele | 83 (72.8) | 74 (64.9) | 25 (59.5) | 63 (70.0) | 54 (65.9) | 66 (63.5) | 51 (62.2) | 51 (77.3) | 28 (63.6) | 8.268 | 0.408 |
| | A allele | 31 (27.2) | 40 (35.1) | 17 (40.5) | 27 (30.0) | 28 (34.1) | 38 (36.5) | 31 (37.8) | 15 (22.7) | 16 (36.4) | — | — |

Table 4: Relationship between *EGFR* gene polymorphisms and the ZHENG of GC.

| SNPs | Genotype | Type of ZHENG *n* (%) | | | | | | | | | $\chi^2$ | *P* |
|---|---|---|---|---|---|---|---|---|---|---|---|---|
| | | SSD | YDSH | DQY | DQB | DLS | DHT | SPM | OBS | Other | | |
| rs6965469 | CC | 40 (65.6) | 39 (67.2) | 13 (56.5) | 37 (77.1) | 23 (54.8) | 37 (68.5) | 25 (62.5) | 22 (62.9) | 13 (59.1) | 11.629 | 0.769 |
| | TC | 19 (31.1) | 17 (29.3) | 10 (43.5) | 10 (20.8) | 18 (42.9) | 17 (31.5) | 14 (35.0) | 13 (37.1) | 9 (40.9) | — | — |
| | TT | 2 (3.3) | 2 (3.4) | 0 (0.0) | 1 (2.1) | 1 (2.4) | 0 (0.0) | 1 (2.5) | 0 (0.0) | 0 (0.0) | — | — |
| | TC/TT | 21 (34.4) | 19 (32.8) | 10 (43.5) | 11 (22.9) | 19 (45.2) | 17 (31.5) | 15 (37.5) | 13 (37.1) | 9 (40.9) | 6.692 | 0.570 |
| | C allele | 99 (81.1) | 95 (81.9) | 36 (78.3) | 84 (87.5) | 64 (76.2) | 91 (84.3) | 64 (80.0) | 57 (81.4) | 35 (79.5) | 4.996 | 0.758 |
| | T allele | 23 (18.9) | 21 (18.1) | 10 (21.7) | 12 (12.5) | 20 (23.8) | 17 (15.7) | 16 (20.0) | 13 (18.6) | 9 (20.5) | — | — |
| rs17337023 | AA | 24 (40.7) | 12 (20.7) | 9 (39.1) | 16 (33.3) | 14 (32.6) | 21 (38.9) | 11 (27.5) | 10 (28.6) | 6 (27.3) | 18.596 | 0.290 |
| | TA | 18 (30.5) | 35 (60.3) | 9 (39.1) | 24 (50.0) | 19 (44.2) | 23 (42.6) | 20 (50.0) | 16 (45.7) | 7 (31.8) | — | — |
| | TT | 17 (28.8) | 11 (19.0) | 5 (21.7) | 8 (16.7) | 10 (23.3) | 10 (18.5) | 9 (22.5) | 9 (25.7) | 9 (40.9) | — | — |
| | TA/TT | 35 (59.3) | 46 (79.3) | 14 (60.9) | 32 (66.7) | 29 (67.4) | 33 (61.1) | 29 (72.5) | 25 (71.4) | 16 (72.7) | 7.966 | 0.437 |
| | A allele | 66 (55.9) | 59 (50.9) | 27 (58.7) | 56 (58.3) | 47 (54.7) | 65 (60.2) | 42 (52.5) | 36 (51.4) | 19 (43.2) | 5.689 | 0.682 |
| | T allele | 52 (44.1) | 57 (49.1) | 19 (41.3) | 40 (41.7) | 39 (45.3) | 43 (39.8) | 38 (47.5) | 34 (48.6) | 25 (56.8) | — | — |
| rs2227983 | AA | 19 (32.2) | 12 (21.1) | 8 (34.8) | 13 (28.3) | 14 (35.0) | 19 (36.5) | 11 (28.9) | 9 (25.7) | 4 (19.0) | 6.997 | 0.973 |
| | GA | 27 (45.8) | 32 (56.1) | 11 (47.8) | 24 (52.2) | 20 (50.0) | 24 (46.2) | 20 (52.6) | 17 (48.6) | 12 (57.1) | — | — |
| | GG | 13 (22.0) | 13 (22.8) | 4 (17.4) | 9 (19.6) | 6 (15.0) | 9 (17.3) | 7 (18.4) | 9 (25.7) | 5 (23.8) | — | — |
| | GA/GG | 40 (67.8) | 45 (78.9) | 15 (65.2) | 33 (71.7) | 26 (65.0) | 33 (63.5) | 27 (71.1) | 26 (74.3) | 17 (81.0) | 5.687 | 0.682 |
| | A allele | 65 (55.1) | 56 (49.1) | 27 (58.7) | 50 (54.3) | 48 (60.0) | 62 (59.6) | 42 (55.3) | 35 (50.0) | 20 (47.6) | 5.137 | 0.743 |
| | G allele | 53 (44.9) | 58 (50.9) | 19 (41.3) | 42 (45.7) | 32 (40.0) | 42 (40.4) | 34 (44.7) | 35 (50.0) | 22 (52.4) | — | — |
| rs1140475 | CC | 60 (98.4) | 54 (93.1) | 18 (78.3) | 41 (85.4) | 41 (97.6) | 48 (88.9) | 36 (90.0) | 32 (91.4) | 21 (95.5) | 14.620 | 0.067 |
| | TC | 1 (1.6) | 4 (6.9) | 5 (21.7) | 7 (14.6) | 1 (2.4) | 6 (11.1) | 4 (10.0) | 3 (8.6) | 1 (4.5) | — | — |
| | C allele | 121 (99.2) | 112 (96.6) | 41 (89.1) | 89 (92.7) | 83 (98.8) | 102 (94.4) | 76 (95.0) | 67 (95.7) | 43 (97.7) | 13.983 | 0.082 |
| | T allele | 1 (0.8) | 4 (3.4) | 5 (10.9) | 7 (7.3) | 1 (1.2) | 6 (5.6) | 4 (5.0) | 3 (4.3) | 1 (2.3) | — | — |
| rs884225 | GG | 19 (31.1) | 23 (39.7) | 5 (21.7) | 7 (14.6) | 14 (32.6) | 18 (33.3) | 11 (27.5) | 13 (37.1) | 9 (40.9) | 29.163 | 0.023 |
| | GA | 27 (44.3) | 29 (50.0) | 8 (34.8) | 23 (47.9) | 18 (41.9) | 19 (35.2) | 24 (60.0) | 17 (48.6) | 9 (40.9) | — | — |
| | AA | 15 (24.6) | 6 (10.3) | 10 (43.5) | 18 (37.5) | 11 (25.6) | 17 (31.5) | 5 (12.5) | 5 (14.3) | 4 (18.2) | — | — |
| | GA/AA | 42 (68.9) | 35 (60.3) | 18 (78.3) | 41 (85.4) | 29 (67.4) | 36 (66.7) | 29 (72.5) | 22 (62.9) | 13 (59.1) | 11.047 | 0.199 |
| | G allele | 65 (53.3) | 75 (64.7) | 18 (39.1) | 37 (38.5) | 46 (53.5) | 55 (50.9) | 46 (57.5) | 43 (61.4) | 27 (61.4) | 21.924 | 0.005 |
| | A allele | 57 (46.7) | 41 (35.3) | 28 (60.9) | 59 (61.5) | 40 (46.5) | 53 (49.1) | 34 (42.5) | 27 (38.6) | 17 (38.6) | — | — |
| rs884904 | AA | 19 (31.1) | 23 (39.7) | 5 (21.7) | 7 (14.6) | 14 (32.6) | 17 (31.5) | 11 (27.5) | 13 (37.1) | 9 (40.9) | 25.536 | 0.061 |
| | GA | 28 (45.9) | 27 (46.6) | 8 (34.8) | 24 (50.0) | 18 (41.9) | 20 (37.0) | 24 (60.0) | 17 (48.6) | 9 (40.9) | — | — |
| | GG | 14 (23.0) | 8 (13.8) | 10 (43.5) | 17 (35.4) | 11 (25.6) | 17 (31.5) | 5 (12.5) | 5 (14.3) | 4 (18.2) | — | — |
| | GA/GG | 42 (68.9) | 35 (60.3) | 18 (78.3) | 41 (85.4) | 29 (67.4) | 37 (68.5) | 29 (72.5) | 22 (62.9) | 13 (59.1) | 10.953 | 0.204 |
| | A allele | 66 (54.1) | 73 (62.9) | 18 (39.1) | 38 (39.6) | 46 (53.5) | 54 (50.0) | 46 (57.5) | 43 (61.4) | 27 (61.4) | 19.366 | 0.013 |
| | G allele | 56 (45.9) | 43 (37.1) | 28 (60.9) | 58 (60.4) | 40 (46.5) | 54 (50.0) | 34 (42.5) | 27 (38.6) | 17 (38.6) | — | — |
| rs763317 | GG | 37 (61.7) | 36 (62.1) | 13 (56.5) | 36 (75.0) | 20 (46.5) | 34 (63.0) | 22 (55.0) | 22 (62.9) | 14 (63.6) | 12.275 | 0.725 |
| | GA | 21 (35.0) | 20 (34.5) | 9 (39.1) | 10 (20.8) | 21 (48.8) | 20 (37.0) | 16 (40.0) | 12 (34.3) | 8 (36.4) | — | — |
| | AA | 2 (3.3) | 2 (3.4) | 1 (4.3) | 2 (4.2) | 2 (4.7) | 0 (0.0) | 2 (5.0) | 1 (2.9) | 0 (0.0) | — | — |
| | GA/AA | 23 (38.3) | 22 (37.9) | 10 (43.5) | 12 (25.0) | 23 (53.5) | 20 (37.0) | 18 (45.0) | 13 (37.1) | 8 (36.4) | 8.796 | 0.360 |
| | G allele | 95 (79.2) | 92 (79.3) | 35 (76.1) | 82 (85.4) | 61 (70.9) | 88 (81.5) | 60 (75.0) | 56 (80.0) | 36 (81.8) | 7.423 | 0.492 |
| | A allele | 25 (20.8) | 24 (20.7) | 11 (23.9) | 14 (14.6) | 25 (29.1) | 20 (18.5) | 20 (25.0) | 14 (20.0) | 8 (18.2) | — | — |
| rs2293347 | GG | 28 (47.5) | 37 (64.9) | 10 (43.5) | 21 (45.7) | 23 (54.8) | 28 (52.8) | 22 (56.4) | 21 (61.8) | 13 (61.9) | 17.979 | 0.325 |
| | GA | 26 (44.1) | 19 (33.3) | 10 (43.5) | 22 (47.8) | 13 (31.0) | 17 (32.1) | 16 (41.0) | 11 (32.4) | 6 (28.6) | — | — |
| | AA | 5 (8.5) | 1 (1.8) | 3 (13.0) | 3 (6.5) | 6 (14.3) | 8 (15.1) | 1 (2.6) | 2 (5.9) | 2 (9.5) | — | — |
| | GA/AA | 31 (52.5) | 20 (35.1) | 13 (56.5) | 25 (54.3) | 19 (45.2) | 25 (47.2) | 17 (43.6) | 13 (38.2) | 8 (38.1) | 7.544 | 0.479 |
| | G allele | 82 (69.5) | 93 (81.6) | 30 (65.2) | 64 (69.6) | 59 (70.2) | 73 (68.9) | 60 (76.9) | 53 (77.9) | 32 (76.2) | 9.868 | 0.274 |
| | A allele | 36 (30.5) | 21 (18.4) | 16 (34.8) | 28 (30.4) | 25 (29.8) | 33 (31.1) | 18 (23.1) | 15 (22.1) | 10 (23.8) | — | — |

Table 4: Continued.

| SNPs | Genotype | Type of ZHENG *n* (%) | | | | | | | | | $\chi^2$ | *P* |
|---|---|---|---|---|---|---|---|---|---|---|---|---|
| | | SSD | YDSH | DQY | DQB | DLS | DHT | SPM | OBS | Other | | |
| rs2072454 | CC | 20 (32.8) | 14 (24.1) | 10 (43.5) | 24 (50.0) | 13 (30.2) | 20 (37.0) | 12 (30.0) | 12 (34.3) | 5 (22.7) | 15.446 | 0.492 |
| | TC | 27 (44.3) | 31 (53.4) | 8 (34.8) | 19 (39.6) | 21 (48.8) | 24 (44.4) | 22 (55.0) | 18 (51.4) | 10 (45.5) | — | — |
| | TT | 14 (23.0) | 13 (22.4) | 5 (21.7) | 5 (10.4) | 9 (20.9) | 10 (18.5) | 6 (15.0) | 5 (14.3) | 7 (31.8) | — | — |
| | TC/TT | 41 (67.2) | 44 (75.9) | 13 (56.5) | 24 (50.0) | 30 (69.8) | 34 (63.0) | 28 (70.0) | 23 (65.7) | 17 (77.3) | 10.996 | 0.202 |
| | C allele | 67 (54.9) | 59 (50.9) | 28 (60.9) | 67 (69.8) | 47 (54.7) | 64 (59.3) | 46 (57.5) | 42 (60.0) | 20 (45.5) | 11.759 | 0.162 |
| | T allele | 55 (45.1) | 57 (49.1) | 18 (39.1) | 29 (30.2) | 39 (45.3) | 44 (40.7) | 34 (42.5) | 28 (40.0) | 24 (54.5) | — | — |
| rs1050171 | GG | 46 (79.3) | 42 (76.4) | 16 (76.2) | 27 (65.9) | 31 (73.8) | 37 (69.8) | 27 (71.1) | 27 (77.1) | 16 (72.7) | 6.461 | 0.982 |
| | GA | 12 (20.7) | 10 (18.2) | 4 (19.0) | 12 (29.3) | 10 (23.8) | 14 (26.4) | 10 (26.3) | 7 (20.0) | 5 (22.7) | — | — |
| | AA | 0 (0.0) | 3 (5.5) | 1 (4.8) | 2 (4.9) | 1 (2.4) | 2 (3.8) | 1 (2.6) | 1 (2.9) | 1 (4.5) | — | — |
| | GA/AA | 12 (20.7) | 13 (23.6) | 5 (23.8) | 14 (34.1) | 11 (26.2) | 16 (30.2) | 11 (28.9) | 8 (22.9) | 6 (27.3) | 3.288 | 0.915 |
| | G allele | 104 (89.7) | 94 (85.5) | 36 (85.7) | 66 (80.5) | 72 (85.7) | 88 (83.0) | 64 (84.2) | 61 (87.1) | 37 (84.1) | 4.015 | 0.856 |
| | A allele | 12 (10.3) | 16 (14.5) | 6 (14.3) | 16 (19.5) | 12 (14.3) | 18 (17.0) | 12 (15.8) | 9 (12.9) | 7 (15.9) | — | — |

ligation by the same receptor (EGFR). Many reports suggest that EGF and EGFR are critical in cancer progression and their gene polymorphisms are correlated with susceptibility to GC [27, 29, 55]. However, the results are not consistent [31]. Until now, there is no evidence on the relationship between *TGFA* gene polymorphisms and GC risk. In the present study, two polymorphisms, rs11466285 in the *TGFA* gene and rs884225 in the *EGFR* gene, were significantly related to the ZHENG of GC ($\chi^2 = 31.012$, $P = 0.013$ for rs11466285, and $\chi^2 = 29.163$, $P = 0.023$ for rs884225). The rs11466285 TT genotype increased the risk of DHT and DQY compared with OBS, and the rs884225 AA genotype increases the risk of DQY and DQB compared with YDSH. In contrast, no direct association was found between ZHENG of GC and *EGF* gene polymorphisms, though several previous studies have reported that the *EGF* +61 (A/G) in the 5′ UTR (SNP rs4444903) is associated with various carcinomas, including GC [56–59]. We found that the rs4444903 A allele increased the risk of DQB compared with OBS (Table 2). The results suggest that DQB is correlated to patients genetically predisposed to GC, while OBS is correlated to patients environmentally predisposed to GC. There may also be a genetic difference between GC risk and GC ZHENG.

Interestingly, the two SNPs correlated with GC (rs11466285, rs884225) are both located in the 3′ UTR (promoter region). Genetic variants in the 3′ UTR may influence the stability of mRNA and, therefore, the function of a gene. Notably, the SNP rs11466285 appeared to confer a substantially greater effect in DQY compared with DLS and OBS ($\chi^2 = 9.052$, $P = 0.002$ and $\chi^2 = 4.241$, $P = 0.039$) (Table 5). Moreover, the T allele distinctly increased the probability of DQY compared with DLS and OBS. For the 3′ UTR rs884225 in *EGFR*, the AA genotype significantly increased the risk of DQB and DQY compared with YDSH and decreased the risk of OBS and other compared with DQB ($P < 0.05$). Meanwhile, significant differences in gender proportion and smoking and drinking status were also observed among six GC ZHENG: YDSH, DQY, DLS, DQB, OBS, and other (Table 1). Clinical research shows that TGF-$\alpha$ expression in gastric mucosal tissue is significantly positively correlated to ZHENG in patients with chronic gastric disease [60]. Moreover, TCM treatment can decrease the expression of EGFR in gastric mucosal tissue from gastric ulcer patients diagnosed with DLS or syndrome of liver invading the spleen [61]. However, no significant difference was observed between EGF expression and ZHENG in patients with chronic atrophic gastritis (the precursor to GC) [62]. These results suggest that differences in the regulation and gene expression of TGF-$\alpha$ and EGFR in the gastric mucosal tissues may underlie molecular markers in the formation of GC ZHENG. TCM theory hypothesizes that DQB and DQY are typical *Xu* ZHENG (deficient syndrome), YDSH and DLS are typical *Shi* ZHENG (excessive syndrome), and OBS is a typical admixture of *Xu* and *Shi* ZHENG. Therefore, SNPs rs11466285 and rs884225 could be genetic markers of *Xu* and *Shi* ZHENG in GC patients, and the formation of TCM ZHENG could be the result of the interaction between genetics and environment.

A clinical investigation with 325 GC patients showed that DLS always occurs in the early stages of GC with a higher proportion in females [63], which is consistent with the present study (Table 1). This result may attributed to the TCM theory that the liver is often constitutional for females, and relieving *Qi* of the liver is an important principle for treating the female patients with GC. Interestingly, distinct differences were observed in several pairs of syndrome types and the results showed that DQB was different from DLS, SPM, OBS, and other (Table 5). This suggests that DQB in GC patients may have a genetic background. The formation of syndrome types in GC, especially DQB, was significantly correlated with polymorphisms in *EGF*, *TGFA*, and *EGFR*.

*Qi*-blood circulation theory is one of the basic theories of TCM. *Qi* is used to describe the refined nutritious substances constituting the human body and maintaining life activities and is also used to describe functions of the *Zang-Fu* organs. TCM theory hypothesizes that the *Zang-Fu* connection is more important in functional entities than anatomical assumptions. The famous therapeutic principle is a classic example. That is, measures must be taken to strengthen the spleen in the treatment of liver disease because liver disease

Table 5: Parallel comparison of genotype distribution of *EGF*, *TGFA*, and *EGFR* gene SNPs between the arbitrary two types of ZHENG.

| Type of ZHENG | $\chi^2$ $(P)$ | | | | | | | |
|---|---|---|---|---|---|---|---|---|
| | YDSH | DQY | DQB | DLS | DHT | SPM | OBS | Other |
| SSD | 10.731 (0.005)[10a] 5.486 (0.019)[10b] | 10.174 (0.001)[11a] | 6.618 (0.010)[11a] | — | 4.495 (0.034)[11a] | — | — | — |
| YDSH | — | 11.517 (0.003)[12a] 8.588 (0.014)[13a] | — | — | — | — | — | — |
| DQY | — | — | — | 9.502 (0.002)[7a] 6.647 (0.010)[11a] | — | — | 4.241 (0.039)[7a] 6.247 (0.044)[12a] 6.247 (0.044)[13a] | — |
| DQB | 14.410 (0.001)[12a] 8.136 (0.004)[12b] 11.105 (0.004)[13a] 8.136 (0.004)[13b] 8.197 (0.017)[15a] 7.639 (0.006)[15b] | — | — | 5.371 (0.020)[5a] 5.022 (0.025)[9b] 4.118 (0.042)[11a] 4.128 (0.042)[11b] 8.225 (0.016)[14a] 7.777 (0.005)[14b] | 4.828 (0.028)[12a] | 8.616 (0.013)[1a] 4.292 (0.038)[1b] 8.885 (0.012)[4a] 7.341 (0.007)[4b] 3.884 (0.049)[14b] | 4.586 (0.032)[3b] 8.213 (0.016)[12a] 5.632 (0.018)[12b] 7.693 (0.021)[13a] 5.632 (0.018)[13b] | 8.850 (0.012)[5a] 6.527 (0.038)[12a] 5.929 (0.015)[12b] 6.332 (0.042)[13a] 5.929 (0.015)[13b] 6.865 (0.032)[15a] 4.624 (0.032)[15b] |
| DLS | — | — | — | — | — | 7.319 (0.026)[2a] 5.470 (0.019)[2b] | — | — |
| DHT | — | — | — | 9.502 (0.002)[7a] | — | 8.068 (0.005)[7a] | 4.159 (0.041)[6b] 12.092 (0.002)[7a] 11.846 (0.001)[7b] 5.124 (0.024)[8b] | — |
| SPM | — | — | — | — | — | — | 9.027 (0.011)[1a] 5.120 (0.024)[1b] 4.430 (0.035)[8b] | 7.523 (0.023)[2a] 4.459 (0.035)[2b] 6.007 (0.050)[4a] 4.593 (0.032)[4b] |

[1]rs11568835, [2]rs3733625, [3]rs4444903, and [4]rs11569017 are located in the *EGF* gene; [5]rs3771527, [6]rs3732253, [7]rs11466285, and [8]rs2166975 are located in the *TGFA* gene; [9]rs6965469, [10]rs17337023, [11]rs1140475, [12]rs884225, [13]rs884904, [14]rs763317, and [15]rs2072454 are located in the *EGFR* gene. Namely, [2]rs3733625, [5]rs3771527, [6]rs3732253, [7]rs11466285, and [12]rs884225 are located in the 3′ UTR; [4]rs11569017, [8]rs2166975, [10]rs17337023, [11]rs1140475, and [15]rs2072454 are located in the exon region; [14]rs763317 is located in intron region; [1]rs11568835, [9]rs6965469, and [13]rs884904 are located in the 5′ near region; [3]rs4444903 is located in the 5′ UTR.
[a]Comparison of the three genotypes; [b]comparison of wild genotype and mutant genotype.

tends to be transmitted to the spleen. The spleen connects with the stomach to form an exterior-interior relationship. Since patients with GC are always feeling emotionally distressed and the liver controls mental and emotional activities, DLS was a common ZHENG in GC TCM differentiation. Relieving liver *Qi* stagnation can be applied to promote the life quality of GC patients [3].

*Qi* deficiency syndrome is one of the main symptoms described by objective physiological phenomena and indexes, including shortness of breath and spontaneous perspiration. Moreover, *Qi* deficiency can lead to decreasing nutrient concentrations in the interstitial fluid which affects the *ex vivo* hematopoietic process and may lead to lower blood volume (blood deficiency) [64]. In the development of GC, the stomach function declines, which affects food digestion, nutrient absorption, and ultimately hematopoietic capacity. Therefore, DQB is often seen in the advanced stages of GC, which results in a lower quality of life, and often has a high rate of relapse and metastasis [63]. Therefore, it may be inferred that the gene polymorphisms of *EGF*, *TGFA*, and *EGFR* correlate to malignant GC. Parallel correlation between the SNPs and ZHENG showed that the SNPs in the functional region (such as the UTR and near region) regulating the gene expression were the most closely related to ZHENG. This is consistent with previous literature [39, 41, 46]. These results suggest that the transcription and regulation of many genes are involved in the formation of ZHENG. TCM, which treats diseases with prescriptions of Chinese herbal formulae guided by differentiation, could be an effective complementary choice for patients with advanced malignant GC. TCM could alleviate the symptoms [65] and promote quality of life [3–5]. In addition, TCM theory on antitumor therapy can enrich the knowledge and understanding of the prophylaxis and treatment of GC and can provide insights into the potential utility of ZHENG [66]. A growing number of technologies are being used to investigate the nature of ZHENG, such as image processing [67] and metabolomics [68], which may contribute to a better understanding of the standardization and material basis of ZHENG.

Several limitations in the present study need to be addressed: (1) the sample size may not have been large enough to detect SNPs with a low variant frequency, such as rs4698803 and rs28384375; (2) the polymorphisms that were investigated were selected based on known SNPs and may not give a comprehensive view of the genetic variability of the *EGF*, *TGFA*, and *EGFR*; and (3) detailed information about the GC cases was not collected, including patient survival, whether the tumors were of the intestinal or diffuse type, whether or not there was metastasis, and the effectiveness of drug therapy.

To summarize, two promoter region SNPs, rs11466285 in *TGFA* and rs884225 in *EGFR*, were significantly associated with GC ZHENG, but no association was found for *EGF*. Parallel comparison among the SNPs and syndrome types revealed that DQB may have a unique genetic basis in the formation of GC ZHENG, and the rs11466285 TT genotype in *TGFA* and rs884225 AA genotype distinctly increased the risk DQB. A larger sample size of each type of GC ZHENG is required to validate these results and to address the underlying mechanisms.

## Conflict of Interests

The authors have no conflict of interests to declare.

## Acknowledgments

This work was supported by the National Natural Science Foundation of China (30973715 and 81001502), Jiangsu Natural Science Foundation (BK2008461), Priority Academic Program Development of Jiangsu Higher Education Institutions (PAPD), and Research Fund for the Doctoral Program of Higher Education of China (20103237110011).

## References

[1] F. Zagouri, C. A. Papadimitriou, M.-A. Dimopoulos, and D. Pectasides, "Molecularly targeted therapies in unresectable-metastatic gastric cancer. A systematic review," *Cancer Treatment Reviews*, vol. 37, no. 8, pp. 599–610, 2011.

[2] C. J. Li, P. K. Wei, J. Shi, L. Liu, and D. W. Ju, "Ideas and methods in treating gastric cancer by Traditional Chinese Medicine "Tan" (phlegm)," *Zhong Guo Zhong Yi Yao Xin Xi Za Zhi*, vol. 14, no. 8, pp. 84–86, 2007 (Chinese).

[3] X. P. Liu, P. Q. Li, and W. Zhang, "Ideas and methods in preventing and treating peritoneal metastasis of gastric cancer by Traditional Chinese Medicine," *Zhong Yi Za Zhi*, vol. 53, no. 4, pp. 288–290, 2012 (Chinese).

[4] X. Liu and B. J. Hua, "Effect of traditional Chinese medicine on quality of life and survival period in patients with progressive gastric cancer," *Zhong Guo Zhong Xi Yi Jie He Za Zhi*, vol. 28, no. 2, pp. 592–594, 2008 (Chinese).

[5] C. J. Li, P. K. Wei, and B. L. Yu, "Study on the mechanism of Xiaotan Sanjie Recipe for inhibiting proliferation of gastric cancer cells," *Journal of Traditional Chinese Medicine*, vol. 30, no. 4, pp. 249–253, 2010.

[6] H. Bao, J. Gao, T. Huang, Z. M. Zhou, B. Zhang, and Y.-F. Xia, "Relationship between traditional Chinese medicine syndrome differentiation and imaging characterization to the radiosensitivity of nasopharyngeal carcinoma," *Chinese Journal of Cancer*, vol. 29, no. 11, pp. 937–945, 2010.

[7] A. G. Zhou, J. R. Dong, S. Hong, G. Kui, X. Y. Huang, and X. M. Mao, "Advanced research on the tongue image of the patients with malignant tumors," *Zhe Jiang Zhong Yi Za Zhi*, vol. 41, no. 12, pp. 726–728, 2006 (Chinese).

[8] L. Y. Chen and G. Z. Lu, "Analysis of tongue images in 114 patients with gastric cancer," *Zhong Yi Za Zhi*, vol. 52, no. 22, pp. 1935–1938, 2011 (Chinese).

[9] T. Chen, K. Q. Li, M. H. Chen, and R. Liang, "Analysis of tongue diagnosis in 4400 modern well-known doctors' cases of China," *Liao Nin Zhong Yi Za Zhi*, vol. 34, no. 9, pp. 1217–1220, 2007 (Chinese).

[10] D.-Z. Sun, L. Liu, J.-P. Jiao, P.-K. Wei, L.-D. Jiang, and L. Xu, "Syndrome characteristics of traditional Chinese medicine: summary of a clinical survey in 767 patients with gastric cancer," *Zhong Xi Yi Jie He Xue Bao*, vol. 8, no. 4, pp. 332–340, 2010 (Chinese).

[11] Z. Zhan, J. F. Hao, H. Wang, and Y. H. Ma, "Relationship between tongue coating and saliva h-EGF content of tumor

patients," *Nan Jing Zhong Yi Yao Da Xu Xue Bao*, vol. 15, no. 6, pp. 350–351, 1999 (Chinese).

[12] J. Zhang, Y. Fan, J. Hao, S. J. Tong, D. Q. Xu, and Z. Zhan, "Differentially expressed genes in common tongue coatings of cancer patients on cDNA microarrays," *Journal of Chinese Clinical Medicine*, vol. 3, no. 6, pp. 301–311, 2008.

[13] A. J. Wilson and P. R. Gibson, "Role of epidermal growth factor receptor in basal and stimulated colonic epithelial cell migration in vitro," *Experimental Cell Research*, vol. 250, no. 1, pp. 187–196, 1999.

[14] M. Liu, X. R. Chang, J. Yan et al., "Effects of moxibustion on gastric mucosal EGF and TGF-alpha contents and epidermal growth factor receptor expression in rats with gastric mucosal lesion," *Zhen Ci Yan Jiu*, vol. 36, no. 6, pp. 403–408, 2011.

[15] K. Y. Liu, Y. Zhu, and X. Z. Huang, "Effect of Pongamia pinnata root flavonoids on the quality of ulcer healing and expression of EGF and TGF-alpha in the rat model of gastric ulcer induced by acetic acid," *Zhong Guo Ying Yong Sheng Li Xue Za Zhi*, vol. 28, no. 5, pp. 435–438, 2012 (Chinese).

[16] F. Yan, H. Cao, R. Chaturvedi et al., "Epidermal growth factor receptor activation protects gastric epithelial cells from helicobacter pylori-induced apoptosis," *Gastroenterology*, vol. 136, no. 4, pp. 1297–1307, 2009.

[17] E. Mammano, C. Belluco, M. Sciro et al., "Epidermal growth factor receptor (EGFR): mutational and protein expression analysis in gastric cancer," *Anticancer Research*, vol. 26, no. 5 A, pp. 3547–3550, 2006.

[18] M. Terashima, K. Kitada, A. Ochiai et al., "Impact of expression of human epidermal growth factor receptors EGFR and ERBB2 on survival in stage II/III gastric cancer," *Clinical Cancer Research*, vol. 18, no. 21, pp. 5992–6000, 2012.

[19] L. David, R. Seruca, J. M. Nesland et al., "c-erbB-2 expression in primary gastric carcinomas and their metastases," *Modern Pathology*, vol. 5, no. 4, pp. 384–390, 1992.

[20] I. R. Ellis, A. M. Schor, and S. L. Schor, "EGF AND TGF-$\alpha$ motogenic activities are mediated by the EGF receptor via distinct matrix-dependent mechanisms," *Experimental Cell Research*, vol. 313, no. 4, pp. 732–741, 2007.

[21] D. Baulcombe, "DNA events: an RNA microcosm," *Science*, vol. 297, no. 5589, pp. 2002–2003, 2002.

[22] T. Kwan, D. Benovoy, C. Dias et al., "Genome-wide analysis of transcript isoform variation in humans," *Nature Genetics*, vol. 40, no. 2, pp. 225–231, 2008.

[23] D. Compare, A. Rocco, and G. Nardone, "Risk factors in gastric cancer," *European Review for Medical and Pharmacological Sciences*, vol. 14, no. 4, pp. 302–308, 2010.

[24] W. Masiak, A. Szponar, G. Chodorowska, A. Dąbrowski, T. Pedowski, and G. Wallner, "Evaluation of endostatin and EGF serum levels in patients with gastric cancer," *Polish Journal of Surgery*, vol. 83, no. 1, pp. 42–47, 2011.

[25] M. F. Fanelli, L. T. Chinen, M. D. Begnami et al., "The influence of transforming growth factor-alpha, cyclooxygenase-2, matrix metalloproteinase (MMP)-7, MMP-9 and CXCR4 proteins involved in epithelial-mesenchymal transition on overall survival of patients with gastric cancer," *Histopathology*, vol. 61, no. 2, pp. 153–161, 2012.

[26] A. Yamada, N. Saito, S. Kameoka, and M. Kobayashi, "Clinical significance of Epidermal Growth Factor (EGF) expression in gastric cancer," *Hepato-Gastroenterology*, vol. 54, no. 76, pp. 1049–1052, 2007.

[27] G. Yang, L. Rao, L. Tian, and X. Cai, "An association between EGF and EGFR gene polymorphisms with gastric cancer in a Chinese Han population," *Hepatogastroenterology*, vol. 59, no. 120, pp. 2668–2671, 2012.

[28] W. Q. Li, N. Hu, Z. Wang et al., "Genetic variants in epidermal growth factor receptor pathway genes and risk of esophageal squamous cell carcinoma and gastric cancer in a Chinese population," *PLOS ONE*, vol. 8, no. 7, pp. 1–7, 2013.

[29] Z. Zhan, Y. Chen, J. Wu et al., "Functional epidermal growth factor gene polymorphisms and risk of gastric cancer," *Oncology Letters*, vol. 5, no. 2, pp. 631–636, 2013.

[30] S. W. Han, D. Y. Oh, S. A. Im et al., "Epidermal growth factor receptor intron 1 CA dinucleotide repeat polymorphism and survival of advanced gastric cancer patients treated with cetuximab plus modified FOLFOX6," *Cancer Science*, vol. 101, no. 3, pp. 793–799, 2010.

[31] Y. Goto, T. Ando, H. Goto, and N. Hamajima, "No association between EGF gene polymorphism and gastric cancer," *Cancer Epidemiology Biomarkers and Prevention*, vol. 14, no. 10, pp. 2454–2456, 2005.

[32] M. A. Kim, H. S. Lee, H. E. Lee, Y. K. Jeon, H. K. Yang, and W. H. Kim, "EGFR in gastric carcinomas: prognostic significance of protein overexpression and high gene copy number," *Histopathology*, vol. 52, no. 6, pp. 738–746, 2008.

[33] Z. Chen and P. Wang, "Clinical distribution and molecular basis of traditional Chinese medicine ZHENG in cancer," *Evidence-Based Complementary and Alternative Medicine*, vol. 2012, Article ID 783923, 8 pages, 2012.

[34] A. Lu, A. Bensoussan, J. Liu, Z. Bian, and W. C. Cho, "TCM zheng classification and clinical trials," *Evidence-Based Complementary and Alternative Medicine*, vol. 2013, Article ID 723659, 3 pages, 2013.

[35] Y. P. Yang, J. Wu, S. J. Tong et al., "Syndrome description of gastric cancer-in terms of TCM syndrome differentiation," *Shi Zhen Guo Yi Guo Yao*, vol. 23, no. 10, pp. 2565–2567, 2012 (Chinese).

[36] J. Zhang, Z. Zhan, J. Wu et al., "Association among polymorphisms in EGFR gene exons, lifestyle and risk of gastric cancer with gender differences in Chinese Han subjects," *PLOS ONE*, vol. 8, no. 3, pp. 1–12, 2013.

[37] H. C. Erichsen and S. J. Chanock, "SNPs in cancer research and treatment," *British Journal of Cancer*, vol. 90, no. 4, pp. 747–751, 2004.

[38] B. Sobrino, M. Brión, and A. Carracedo, "SNPs in forensic genetics: a review on SNP typing methodologies," *Forensic Science International*, vol. 154, no. 2-3, pp. 181–194, 2005.

[39] J. S. You, S. Y. Hu, and H. G. Zhang, "Study on emotion measurement of liver syndromes in TCM and its correlative study on polymorphism of serotonin (5HT) transporter gene," *Zhong Guo Yi Yao Xue Bao*, vol. 19, no. 11, pp. 669–671, 2004 (Chinese).

[40] Y. F. Wu, Y. C. Zhou, and X.-S. Zhang, "Association between traditional Chinese medicine syndrome of coronary atherosclerotic heart disease and polymorphism of R219K of ABCAI gene in Chinese Han male patients," *Chinese Journal of Clinical Rehabilitation*, vol. 10, no. 7, pp. 7–9, 2006.

[41] W. J. Ding, Y. Z. Zeng, W. H. Li et al., "Identification of linkage disequilibrium SNPs from a Kidney-yang deficiency syndrome pedigree," *American Journal of Chinese Medicine*, vol. 37, no. 3, pp. 427–438, 2009.

[42] Y. B. Liu, W. Zhang, S. B. Su et al., "Association between liver cirrhosis of hepatitis B cases with Ganqi depression pattern and

5HTTLPRVNTRs, TPH A218C, GNB3 C825T polymorphism," *Zhong Xi Yi Jie He Gan Bing Za Zhi*, vol. 20, no. 5, pp. 267–271, 2010 (Chinese).

[43] Q. S. Lu, Y. Lei, and K. J. Chen, "Relationship of the A1166C polymorphism of ATI R gene with TCM syndrome and efficacy of Chinese hypotensor in patients with essential hypertension," *Zhongguo Zhong Xi Yi Jie He Za Zhi*, vol. 25, no. 8, pp. 682–686, 2005.

[44] Z. L. Jiang, W. Zhang, H. Zhang, Y.-B. Liu, and S. B. Su, "Relationship between TNF-$\alpha$, TGF-$\beta$1 and IL-10 genetic polymorphisms and post-hepatitis B cirrhosis," *World Chinese Journal of Digestology*, vol. 17, no. 31, pp. 3263–3268, 2009.

[45] Z.-L. Jiang, W. Zhang, H. Zhang, Y.-B. Liu, Q. Y. Li, and S.-B. Su, "Relationship between gene polymorphisms of interleukin-10 and syndrome types of traditional Chinese medicine in posthepatitis B cirrhosis," *Journal of Chinese Integrative Medicine*, vol. 7, no. 11, pp. 1052–1056, 2009.

[46] Q. Y. Li, Z. Z. Guo, J. Liang et al., "Interleukin-10 genotype correlated to deficiency syndrome in hepatitis B cirrhosis," *Evidence-Based Complementary and Alternative Medicine*, vol. 2012, Article ID 298925, 6 pages, 2012.

[47] H. Huang, Y. Bu, and G. H. Zhou, "Single-tube-genotyping of gastric cancer related SNPs by directly using whole blood and paper-dried blood as starting materials," *World Journal of Gastroenterology*, vol. 12, no. 24, pp. 3814–3820, 2006.

[48] Z. Liu, L. Liu, M. Li et al., "Epidermal growth factor receptor mutation in gastric cancer," *Pathology*, vol. 43, no. 3, pp. 234–238, 2011.

[49] C. Moutinho, A. R. Mateus, F. Milanezi, F. Carneiro, R. Seruca, and G. Suriano, "Epidermal growth factor receptor structural alterations in gastric cancer," *BMC Cancer*, vol. 8, article 10, 2008.

[50] Y. Zhu, Q. He, J. Wang, and H. F. Pan, "The association between GSTM1 polymorphism and gastric cancer risk: a meta-analysis," *Molecular Biology Reports*, vol. 39, no. 1, pp. 685–691, 2012.

[51] K. X. Zhu, Y. M. Li, X. Li, W. C. Zhou, Y. Shan, and T. Liu, "Study on the association of p53 codon 72 polymorphisms with risk of gastric cancer in high incidence Hexi area of Gansu Province in China," *Molecular Biology Reports*, vol. 39, no. 1, pp. 723–728, 2012.

[52] Y. Cui, H. Xue, B. Lin, P. Ni, and J. Y. Fang, "A meta-analysis of CDH1 C-160A genetic polymorphism and gastric cancer risk," *DNA and Cell Biology*, vol. 30, no. 11, pp. 937–945, 2011.

[53] X. Zhang, R. Zhong, Z. Zhang et al., "Interaction of Cyclooxygenase-2 promoter polymorphisms with Helicobacter pylori infection and risk of gastric cancer," *Molecular Carcinogenesis*, vol. 50, no. 11, pp. 876–883, 2011.

[54] J. Zhang, Z. Zhan, J. Wu et al., "Association among lifestyle, clinical examination, polymorphisms in CDH1 gene and Traditional Chinese Medicine syndrome differentiation of gastric cancer," *Journal of Traditional Chinese Medicine*, vol. 33, no. 5, pp. 572–579, 2013.

[55] A. P. Araújo, B. M. Costa, A. L. Pinto-Correia et al., "Association between EGF +61A/G polymorphism and gastric cancer in caucasians," *World Journal of Gastroenterology*, vol. 17, no. 4, pp. 488–492, 2011.

[56] J. Zhu, X. Meng, F. Yan et al., "A functional epidermal growth factor (EGF) polymorphism, EGF serum levels and renal cell carcinoma risk in a Chinese population," *Journal of Human Genetics*, vol. 55, no. 4, pp. 236–240, 2010.

[57] K. Chen, Y. Wei, H. Yang, and B. Li, "Epidermal growth factor +61 G/A polymorphism and the risk of hepatocellular carcinoma in a Chinese population," *Genetic Testing and Molecular Biomarkers*, vol. 15, no. 4, pp. 251–255, 2011.

[58] K. L. Amend, J. T. Elder, L. P. Tomsho et al., "EGF gene polymorphism and the risk of incident primary melanoma," *Cancer Research*, vol. 64, no. 8, pp. 2668–2672, 2004.

[59] Y. Hamai, S. Matsumura, K. Matsusaki et al., "A single nucleotide polymorphism in the 5′ untranslated region of the EGT gene is associated with occurrence and malignant progression of gastric cancer," *Pathobiology*, vol. 72, no. 3, pp. 133–138, 2005.

[60] W. J. Liang, Y. J. Ma, X. Yan, W. D. Zhang, and R.-C. Luo, "Expression of transforming growth factor $\alpha$ and Cyclin E and their correlation in chronic gastric lesion tissues from patients with different TCM types," *World Chinese Journal of Digestology*, vol. 16, no. 12, pp. 1355–1358, 2008.

[61] J. B. Li, X. P. Dai, R. X. Jiang, C. Y. Yu, Y. Li, and W. N. Zhang, "Experimental and clinical study on Jianwei Yuyang Granule in treating relapse of peptic ulcer," *Zhong Guo Zhong Xi Yi Jie He Xiao Hua Za Zhi*, vol. 12, no. 1, pp. 30–33, 2004 (Chinese).

[62] L.-H. Sun, Q. Li, and S. Q. Wang, "Relationship of TCM syndrome type of gastric mucosal epithelial growth factor, vascular endothelial growth factor and proliferative cell nuclear antigen in patients with chronic atrophic gastritis," *Zhong Guo Zhong Xi Yi Jie He Za Zhi*, vol. 28, no. 3, pp. 225–228, 2008 (Chinese).

[63] L. Tao and J. K. Yang, "Univariate analysis of syndrome differentiation in traditional Chinese medicine and clinical correlative factors in gastric cancer," *Zhong Xi Yi Jie He Xue Bao*, vol. 5, no. 4, pp. 398–402, 2007 (Chinese).

[64] W. Yao, H. Yang, and G. Ding, "Mechanisms of Qi-blood circulation and Qi deficiency syndrome in view of blood and interstitial fluid circulation," *Journal of Traditional Chinese Medicine*, vol. 33, no. 4, pp. 538–544, 2013.

[65] Y. Liu, Z. Jia, L. Dong, R. Wang, and G. Qiu, "A randomized pilot study of atractylenolide I on gastric cancer cachexia patients," *Evidence-based Complementary and Alternative Medicine*, vol. 5, no. 3, pp. 337–344, 2008.

[66] R. Wong, C. M. Sagar, and S. M. Sagar, "Integration of Chinese medicine into supportive cancer care: a modern role for an ancient tradition," *Cancer Treatment Reviews*, vol. 27, no. 4, pp. 235–246, 2001.

[67] R. Kanawong, T. Obafemi-Ajayi, T. Ma, D. Xu, S. Li, and Y. Duan, "Automated tongue feature extraction for ZHENG classification in traditional Chinese medicine," *Evid Based Complement Alternat Med*, vol. 2012, Article ID 912852, 12 pages, 2012.

[68] S. Su, J. Duan, W. Cui et al., "Network-based biomarkers for cold coagulation blood stasis syndrome and the therapeutic effects of Shaofu Zhuyu Decoction in rats," *Evid Based Complement Alternat Med*, vol. 2013, Article ID 901943, 15 pages, 2013.

Hindawi Publishing Corporation
Evidence-Based Complementary and Alternative Medicine
Volume 2013, Article ID 324636, 8 pages
http://dx.doi.org/10.1155/2013/324636

*Research Article*

# Characteristic Analysis from Excessive to Deficient Syndromes in Hepatocarcinoma Underlying miRNA Array Data

**Qi-Long Chen,[1,2] Yi-Yu Lu,[1] Gui-Biao Zhang,[1] Ya-Nan Song,[1] Qian-Mei Zhou,[1] Hui Zhang,[1] Wei Zhang,[3] Xin-sheng Tang,[2] and Shi-Bing Su[1]**

[1] *Research Center for TCM Complexity System, Shanghai University of TCM, Shanghai 201203, China*
[2] *College of Life and Environment Science, Huangshan University, Huangshan 245021, China*
[3] *Shanghai Longhua Hospital, Shanghai University of TCM, Shanghai 200126, China*

Correspondence should be addressed to Shi-Bing Su; shibingsu07@163.com

Received 18 August 2013; Accepted 12 November 2013

Academic Editor: Shao Li



Traditional Chinese medicine (TCM) treatment is regarded as a safe and effective method for many diseases. In this study, the characteristics among excessive, excessive-deficient, and deficient syndromes of Hepatocellular carcinoma (HCC) were studied using miRNA array data. We first calculated the differentially expressed miRNAs based on random module $t$-test and classified three TCM syndromes of HCC using SVM method. Then, the weighted miRNA-target networks were constructed for different TCM syndromes using predicted miRNA targets. Subsequently, the prioritized target genes of upexpression network of TCM syndromes were analyzed using DAVID online analysis. The results showed that there are distinctly different hierarchical cluster and network structure of TCM syndromes in HCC, but the excessive-deficient combination syndrome is extrinsically close to deficient syndrome. GO and pathway analysis revealed that the molecular mechanisms of excessive-deficient and deficient syndromes of HCC are more complex than excessive syndrome. Furthermore, although excessive-deficient and deficient syndromes have similar complex mechanisms, excessive-deficient syndrome is more involved than deficient syndrome in development of cancer process. This study suggested that miRNAs might be important mediators involved in the changing process from excessive to deficient syndromes and could be potential molecular markers for the diagnosis of TCM syndromes in HCC.

## 1. Introduction

Hepatocellular carcinoma (HCC) is one of the most common devastating cancer types, ranking sixth in incidence, and the third leading cause of cancer related deaths worldwide [1, 2]. The hepatitis B and hepatitis C infections, idiopathic cirrhosis, and alcoholic liver diseases usually are major risk factors for HCC [3]. For early diagnosis of HCC is difficult, and more than half of the HCC patients are diagnosed too late to benefit from the curative therapies. Furthermore, molecular approaches have revealed many molecular events associated with HCC, yet molecular mechanism of cell proliferation and effective biological markers for driving hepatocarcinogenesis remain largely unknown [4].

Under these circumstances, many failing patients seek to get help from complementary and alternative medicine, especially traditional Chinese medicine (TCM). TCM is an ancient Chinese medicine that evolved through at least three thousand years of uninterrupted clinical practice. The TCM treatment usually uses a traditional diagnosis method to classify the TCM syndromes, which based on clinical symptoms and signs, followed by the use of individualized treatment [5, 6]. For instance, Li et al. established a network balance model to evaluate the imbalanced network underlying TCM syndrome for gastritis patients [7, 8], which demonstrated that cold syndrome patients experience low levels of energy metabolism and immune regulation is intensified in hot syndrome patients.

MicroRNAs (miRNAs) are endogenous, noncoding, single-stranded small RNA molecules of approximately 22 nucleotides, which function as negative regulators that involve posttranscriptional gene expression through binding

to the 3′-untranslated regions (3′-UTRs) of target mRNAs and consequently lead to mRNA cleavage or translational repression [9–11]. Although miRNAs are stable in circulation systems, tissue, and organ [12], they often can be explored in blood under pathological conditions, such as cell turnover and destruction, and pathological injury [13]. In the previous studies, we reported that circulating miR-583 and miR-663 refer to TCM syndrome differentiation in chronic hepatitis B [14] and the progression from excessive to deficient syndromes in chronic hepatitis B using miRNA-target dynamical network [15]. The results implicated that miRNAs are important mediators for TCM syndrome classification as well as CHB development progression and therefore could be potential diagnosis and therapeutic molecular markers.

In this work, we hypothesized that miRNAs expression levels and their target gene expression networks are the important factors for the TCM syndrome classification and the changes from excessive to deficient syndromes in HCC patients. We thus focused on the comparative analysis of the differences and similarities in the three TCM syndromes including liver-gallbladder dampness heat syndrome (LGDHS), liver depression and spleen deficiency syndrome (LDSDS), and liver-kidney yin deficiency syndrome (LKYDS). The aim is to demonstrate the change process of molecular mechanism from excessive syndrome to deficient syndrome at a network level by an integrative and comparative analysis of weighted miRNA-target network in HCC patients.

## 2. Materials and Methods

*2.1. Clinical Specimens.* In this work, clinical serum of 9 HCC patients and 7 healthy donors (Normal) were collected, whose were come from Shanghai Longhua Hospital. Then, these serums were subjected to miRNA microarray analysis. The diagnostic criteria of western medicine for HCC followed the guidelines defined by the Chinese Society of Hepatology and Chinese Society of Infectious Diseases in 2005 [16]. The TCM syndrome system for HCC applied by the 3 senior TCM doctors of each diagnosis was accepted according to the standards of TCM differential syndromes of viral hepatitis defined by the Internal Medicine Hepatopathy Committee of Chinese Traditional Medicine Association in 1991 [17]. This research project was approved by the local ethics committee of Shanghai University of TCM, and all patients were informed and consented for this study.

The differentiation of TCM syndromes in HCC patients was shown in Table 1. There were 3 LGDHSs, 3 LDSDSs, and 3 LKYDSs. In addition, 7 serums of normal control were randomly obtained from 120 individuals who had physically examination at Shanghai Longhua Hospital.

*2.2. Serum Sample Collection and RNA Isolation.* All serum samples were from the peripheral venous blood of HCC patients and healthy donors, which were immediately frozen in liquid nitrogen and then stored at −80°C. The RNAs in serum were extracted using a miRVana PARIS kit (Ambion, Austin, TX, USA) according to the manufacturer's protocol and using the RNase-free DNase (Promega, Madison, WI, USA) to eliminate DNA contamination. The concentration of RNAs isolated from serum ranged from 1.5 to 12 ng/$\mu$L.

Table 1: Differentiation of TCM syndromes in HCC patients.

| Patient ID | Age | Gender | TCM syndromes | TCM syndrome types |
|---|---|---|---|---|
| HCC 1 | 47 | M | LGDHS | Excessive |
| HCC 2 | 63 | M | LGDHS | Excessive |
| HCC 3 | 61 | F | LGDHS | Excessive |
| HCC 4 | 62 | M | LDSDS | Excessive-deficient |
| HCC 5 | 59 | M | LDSDS | Excessive-deficient |
| HCC 6 | 58 | M | LDSDS | Excessive-deficient |
| HCC 7 | 54 | F | LKYDS | Deficient |
| HCC 8 | 52 | M | LKYDS | Deficient |
| HCC 9 | 42 | M | LKYDS | Deficient |

*2.3. miRNA Microarray and Data Analysis.* The profiles of serum miRNAs of 9 HCC patients and 7 normal controls were generated using Agilent Human miRNA microarray V3 (Agilent Technologies Inc, Santa Clara, CA, USA); 60 ng of RNA was labeled and hybridized for each array. Hybridization signals were detected with the Agilent microarray scanner; the data were extracted using Feature Extraction V10.7 (Agilent Technologies, CA, USA). All raw data were transformed into log 2 scale, and then, the expression levels were normalized by having zero mean and unit sample variance.

In order to evaluate the diversity of three TCM syndromes in HCC, we compared the miRNAs expressions of LGDHS, LDSDS, and LKYDS to normal, respectively. The relative miRNA expression levels were further normalized utilizing the median over the all patients, which make the each patient have a median log ration of 0 in normalized expression levels. The weighted differences miRNAs between TCM syndromes were calculated using the random variance model $t$-test and the fold-change >1.5 and $P < 0.05$ were considered significant. Heat-map analysis and hierarchical cluster analysis of expression data were performed using Cluster 3.0 and TreeView programs (the clustering calculation uses one minus correlation metrics and average linkages). Class prediction was performled using a statistical algorithm of the support vector machine (SVM) incorporating miRNA differentially expressed at a univariate parametric significance level of $P = 0.01$. The prediction rate was estimated via 10 fold and 10 times cross-validation and the bootstrap method for small sample data.

*2.4. Identification and Prediction of miRNA Target Genes.* Validated miRNA target genes were selected based on TarBase 6.0, which hosts the largest collection of manually curate experimentally validated miRNA-gene interactions [18]. Furthermore, the unverified miRNA target genes were predicted to regulating by miRNAs based on 10 programs, including DIANAmT, miRanda, miRDB, miRWalk, RNAhybrid, PicTar4, PicTar5, PITA, RNA22, and TargetScan. In

these programs, the miRDB is different from others, which was using SVM learning machine to predict miRNA targets [19]. In order to increase the accuracy of predicted targets, we further screened prediction hits from two ways, that is, (i) random selected two sets from 9 programs (excepted miRDB) and intersected them, respectively, then united these intersection data as Data A; (ii) selected the miRDB data whose score >60, defined this data is Data B. Finally, the intersection between Data A and Data B acts as final data to build miRNA-target network.

*2.5. Enrichment Analysis of Target Genes.* Of the inferred miRNA target genes, those showing a significant ($P < 0.05$) expression difference between normal, LGDHS, LDSDS, and LKYDS samples were analyzed for pathways involving these genes using DAVID online analysis [20, 21], and significance analysis was determined when $P$ values were corrected for false discovery rate (FDR). Gene sets containing less than 5 genes overlapping were removed from the DAVID analysis. In our analysis, GO terms and pathways with an FDR-adjusted $P$ value of less than 0.05 were retained.

*2.6. Weighted miRNA-Target Network Construction.* We built the weighted miRNA-target gene networks for different syndromes of HCC by computing the miRNA and target gene degree distribution based on experimental validated target genes and predicted target genes, thus inferring the miRNA-target network in 3 TCM syndromes of HCC, respectively. In the process of network building, miRNA nodes were weighted by their expression fold changes (absolute value of log 2), while target genes were weighted based on degree distributions between consecutive groups, and thus we obtained a node-weighted miRNA-target interaction network for each stage. In order to validate the veracity of above network, rank all nodes (miRNAs and target genes) of network according to their weights and test the similarity between them [15, 22]; thereafter, obtain deregulated nodes for mapping the network of consecutive TCM syndromes progression. In the weighted miRNA-target network, the nodes represent miRNAs or genes, and the edges represent the connection strength (adjacency).

## 3. Results and Discussion

*3.1. Differential Expressed miRNAs of TCM Syndromes in HCC.* The expressions of miRNAs were calculated and analyzed with random module $t$-test of R package, to search whether there are some significantly differential expressed miRNAs among the consecutive stages form excessive syndromes to deficient syndromes. 35 miRNAs in LGDHS/normal, 61 miRNAs in LDSDS/normal, and 71 miRNAs in LKYDS/normal differentially expressed. Three TCM syndromes of HCC were classified using a supervised learning algorithm (binary tree classification), and SVM act as prediction method. As shown in Figure 1(a), the excessive syndrome (LGDHS) was clearly classified to excessive-deficient combination syndrome (LDSDS) and deficient syndrome (LKYDS) (node 1, score = 82), which implicated that the excessive syndrome was distinctly different for other syndromes in HCC patients. However, we notice that the LDSDS samples first classified two classifications (node 2, score = 86) and then form a parallel branch cluster to LKYDS (node 3, score = 63). Although the topological profiles between LDSDS and LKYDS is clear-cut (Figure 1(a)), the lower SVM score (node 3, score = 63) shows the classification of them is still weakly. This result suggests the relationship between Excessive-deficient combination syndrome and Deficient syndrome is extrinsically closely in HCC patients.

Hierarchical cluster analysis revealed that the expression profiles of the differential miRNAs from each TCM syndrome were roughly classified, respectively. The consecutive heatmaps of differentially expressed miRNAs were shown in Figure 1(b). With the heat-maps, the miRNAs expression profiles of three syndromes were great differences, especially the Excessive syndrome (LGDHS/Normal) has great diversity to other syndromes. It implicates that the mechanism is individual for different typical syndromes of HCC. Interestingly, the hierarchical analysis shows that three LDSDS samples and one normal control (N3) first form a parallel branch and then cluster to other normal samples. This characteristic also was corresponding with the above profiles of LDSDS classification (Figure 1(a)). Because excessive-deficient combination syndrome (LDSDS) is a complicated TCM syndrome that includes both excessive syndrome and deficient syndrome [15], we infer that the LDSDS syndrome might have two features, which is compatible for excessive syndrome and deficient syndrome, and the miRNA-regulated mechanism is more complex than other syndromes in HCC.

*3.2. Overview of the miRNA-Target Networks and Network Connections.* As a gene regulator, a given miRNA usually has multiple different mRNA targets, and multiple miRNAs might target one gene [23]. In this study, using the validation database (Tarbase 6.0) and 10 predicted programs, miRNA target genes of three TCM syndromes were predicted, respectively. The final predictions were obtained by significant differences ($P < 0.05$) in each prediction program. Following the differential expressed miRNAs among LGDHS, LDSDS, and LKYDS in HCC, miRNA-target network for each syndrome was reconstructed based on predicted data. The global profiles of networks were shown in Figure 2(a). Noticeably, the topological profiles are more likely closed to "medusa" architecture [24], which consists of a regulatory core of hub nodes represented most prominently by miRNAs and target genes in network. It implies that the hub nodes (miRNAs or target genes) are much stronger determinants of the realized gene expression profiles, whereas the periphery nodes that should be regulated are not regulating. Furthermore, it also implicates the potential modules are subsistent in the networks, which in biological networks often represent molecular complexes and pathways [22].

To reveal the details of the regulatory core of network, the simplified network was reconstructed through the selected hub nodes. In this work, we defined a hub node that has more than 5 interactions in those TCM syndrome-specific networks, which represent these hub nodes might

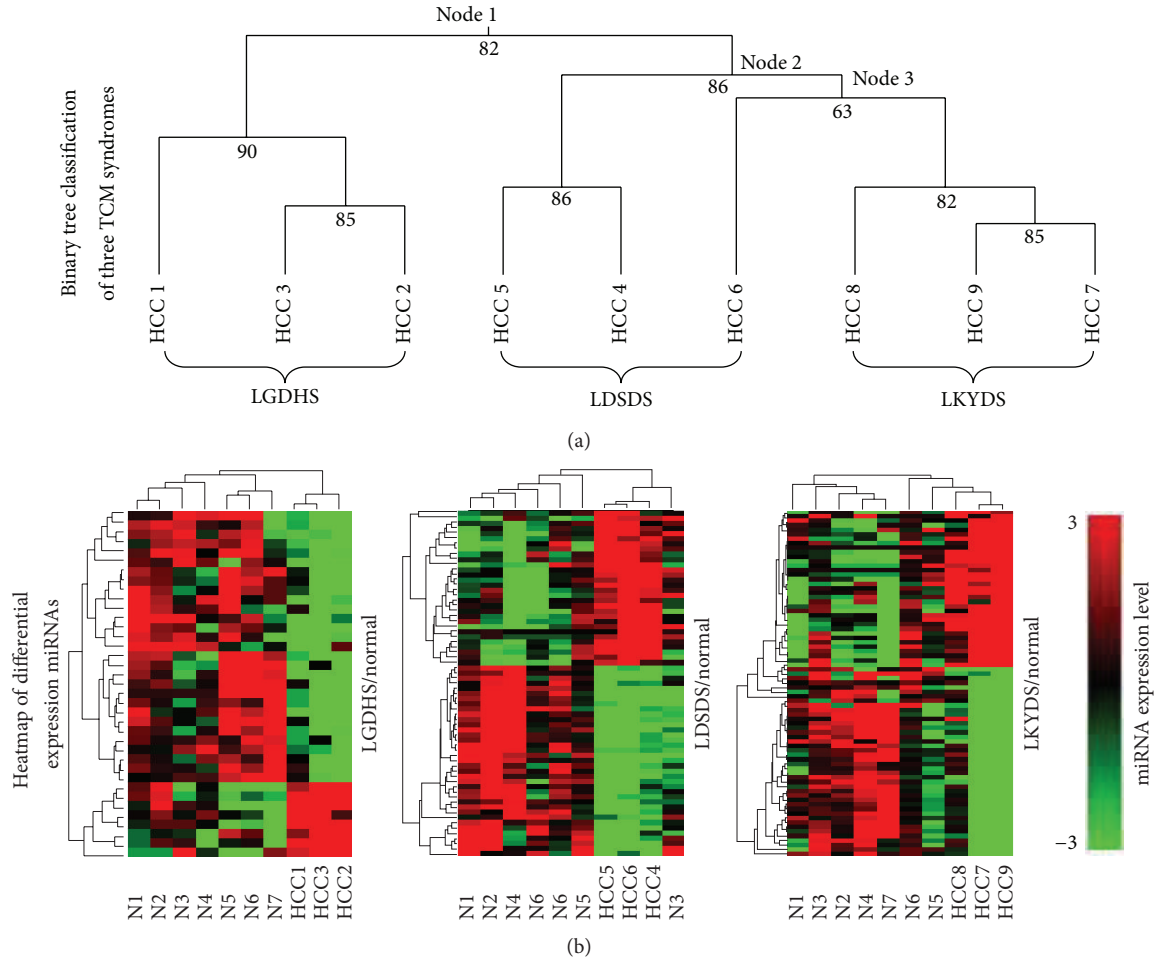


Figure 1: Cluster analysis of differential expression miRNAs in TCM syndromes in HCC. (a) Relationship among three typical syndromes of HCC divided by binary tree classification. (b) Heatmap of differential expressed miRNAs among the LGDHS/normal, LDSDS/normal, and LKYDS/normal.

have highly effects for the topological structure of network. The reconstructed networks were shown in Figure 2(b), including the excessive syndrome (LGDHS/normal) network that consists of 35 miRNAs, excessive-deficient syndrome (LDSDS/normal) network that consists of 61 miRNAs, and Deficient syndromes (LKYDS/normal) network that consists of 71 miRNAs. Furthermore, there were 22 coexpression miRNAs between LGDHS/normal and LDSDS/normal, including 6 upexpression miRNAs. 41 miRNAs overlapped between LDSDS/normal and LKYDS/normal, and 5 miRNAs were upexpression; subsequently, LGDHS/normal shared 22 miRNAs with LKYDS/normal network, and including 12 upexpression miRNAs. The expression levels of overlapping miRNAs were shown in Figure 2(c). Although these overlapping miRNAs were appearance in three TCM syndromes, the difference of expression levels still indicated that they might play different roles form excessive to deficient syndromes in HCC. On the other side, the poor overlapping upexpression miRNAs also show a dramatic difference of deregulation in TCM syndromes, which suggested that LGDHS, LDSDS, and LKYDS have different molecular mechanisms.

*3.3. Networks Prioritized Target Genes and Pathways in TCM Syndromes Progression in HCC.* Because upexpression miRNAs might play roles that are more important in biological process, we divided the up-expression miRNA-target networks from the holistic networks for each TCM syndrome. Figure 3(a) shows the up-expression networks (degree ≥5). We note that the proportion of up-expression miRNAs in LGDHS/normal is 18.8%, which was stringently less than LDSDS/normal (37.0%) and LKYDS/normal (39.7%). This great difference suggests that the molecular mechanism of excessive-deficient syndrome and deficient syndromes is more complex than excessive syndrome for HHC patients. Actually, these hub up-expression miRNAs usually affected the core cellular functions, such as immune responses and cell cycle in the molecular network via inhabited or degraded target genes [15]; furthermore, it also provides a new approach to distinguish the functional processes in disease progression [25, 26].

Because miRNA general inhibit translation or induce mRNA degradation by binding to the 3′-UTRs of target mRNAs [11]; here, we focus to conduct the GO terms and

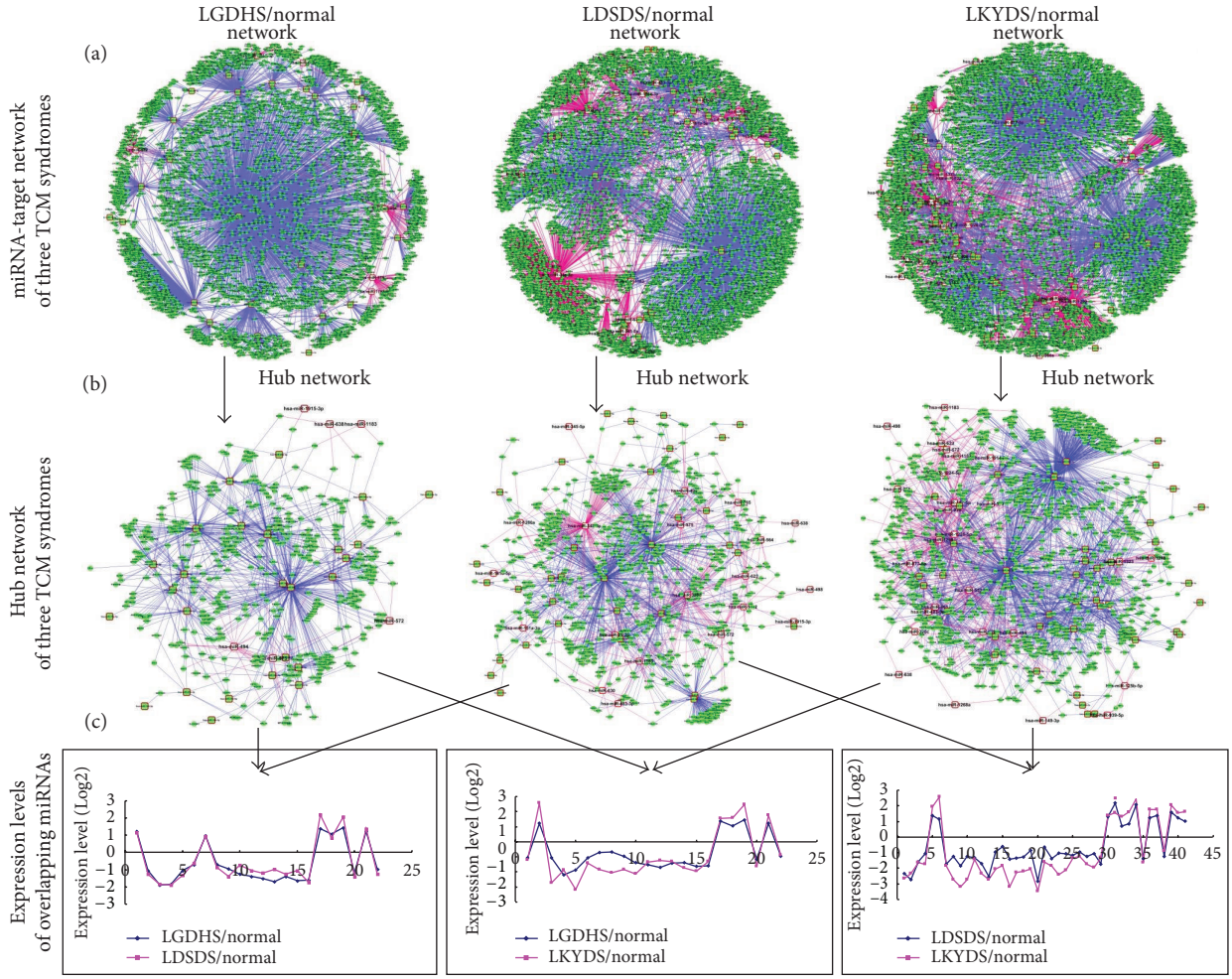


Figure 2: The miRNA-target networks and overlapping miRNA expression in TCM syndromes in HCC. (a) The global profiles of miRNA-target networks in three HCC TCM syndromes. (b) The hub networks of three syndromes from excessive to deficient syndromes. (c) The overlapping miRNA expression levels from the networks of three TCM syndromes.

pathways analysis for the target genes of up-expression miRNAs using DAVID analysis [20, 21]. Significant analysis was determined when $P$ values were corrected for false discovery rate (FDR). Gene sets containing greater than 5 genes overlapping were retained from the DAVID analysis. Analysis results with an FDR-adjusted $P$ value of less than 0.05 were retained.

The representative GO and pathways terms of target genes in each TCM syndrome were shown in Figure 3(b). With the GO analysis, 21 GO terms were overlapping between LGDHS/normal and LDSDS/normal; 18 GO terms are overlapping between LGDHS/normal and LKYDS/normal, while LDSDS/normal and LKYDS/normal have 107 GO terms in common. In order to understand the GO terms holistically, 18 overlapped GO terms among LGDHS, LDSDS, and LKYDS were depth selected from original results based on $P$ value and FDR less than 0.05. The distribution of overlapping GO terms was shown in Figure 3(c). Although these overlapping GO terms were appearance, actually, the FDR-adjusted $P$ value of each GO term is different. For instance, the $P$ values of GO: 0003677 (DNA binding), GO: 0031981 (nuclear lumen), GO: 0044451 (nucleoplasm part), GO: 0048522 (positive regulation of cellular process) and GO: 0070013 (intracellular organelle lumen) in LKYDS are clearly less than LGDHS or LDSDS. These results implicated that these GO terms are more stringently associated with deficient syndrome (LKYDS) and could deregulate the core cellular functions.

The pathway terms (KEGG and BIOCARTA) of target genes were also calculated using DAVID analysis. As shown in Figure 3(b), LKYDS/normal has 15 pathways, LGDHS/normal has 13 pathways, and LGDHS/normal has only 1 pathway. In addition, LGDHS/normal and LDSDS/normal, LGDHS/normal and LKYDS/normal only have one overlapped pathway, respectively, but LDSDS/normal and LKYDS/normal had 7 overlapped pathways. Obviously, this phenomenon suggested the mechanism of Excessive syndrome is different to other syndromes in HCC patients.

The detail of each pathway of three TCM syndromes was represented in Table 2. Compared with KEGG pathway,

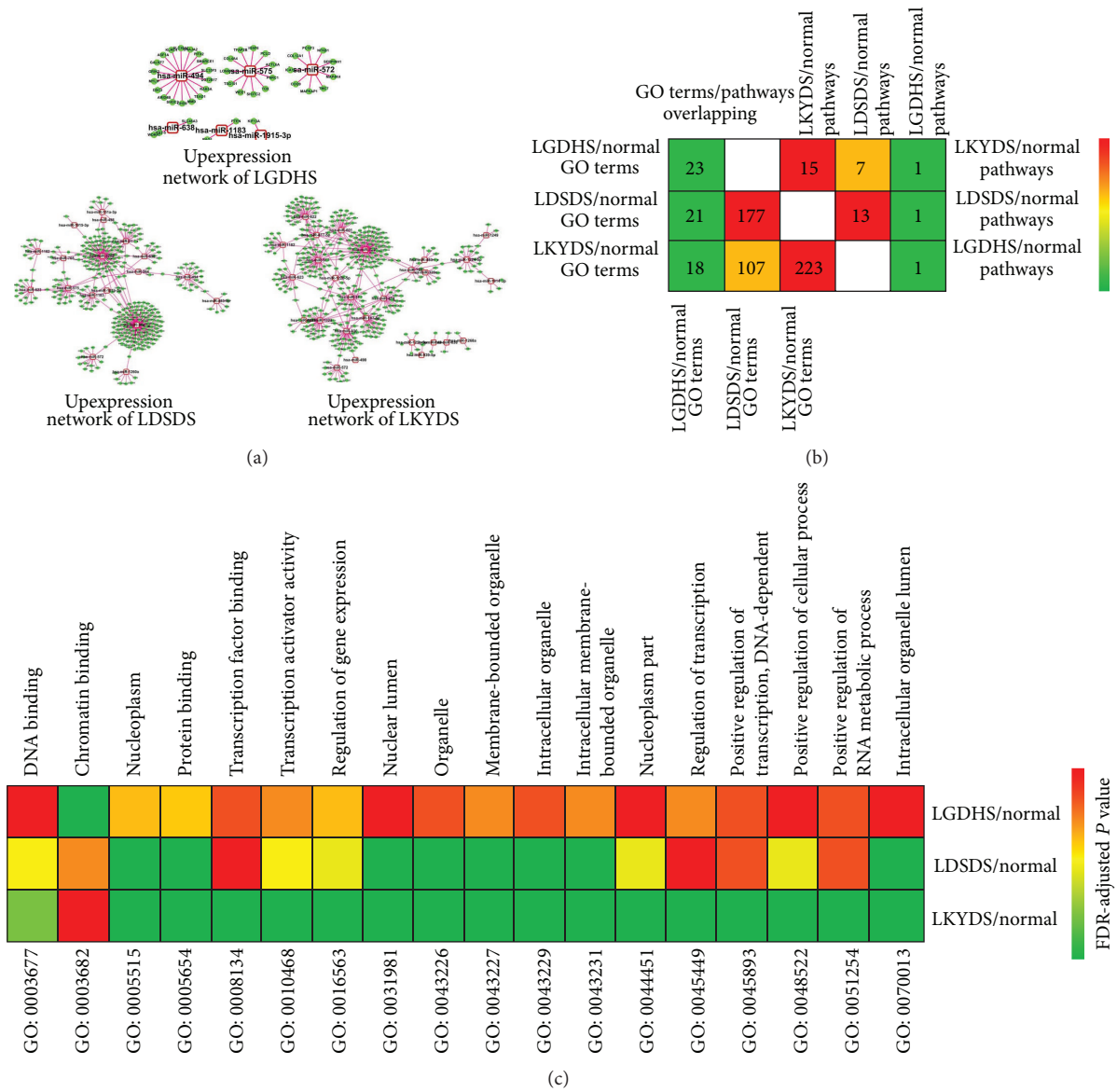


Figure 3: Upexpression miRNA-target networks, GO, and pathway terms in TCM syndromes progression in HCC. (a) Upexpression miRNA-target networks of LGDHS, LDSDS, and LKYDS in HCC. (b) Comparison of GO/pathway terms among the three networks of TCM syndromes. (c) The distribution of overlapping GO terms among the three networks of TCM syndromes. Numbers in the cell represent the number of overlapped GO terms in two networks. Colors were scaled according to the proportion of overlaps.

LGDHS is only related to small cell lung cancer, LDSDS is mainly associated with cell cycle, focal adhesion, endocytosis, and cancer pathways, and apoptosis, chronic/acute myeloid leukemia, and many cancer related pathways are associated with LKYDS. Compared with BIOCARTA pathway, the Deficient syndrome (LKYDS) is mainly associated with transcriptional regulation and map kinase pathways, while excessive-deficient syndrome (LDSDS) was more likely related to cell cycle (G1/S check point), cyclins, and cell cycle regulation. Previous researches have supported that imbalance of G1/S and G2/M phases is associated with dysfunction in hepatocarcinoma [27]. The results implicated that although excessive-deficient and deficient syndromes have similar complex mechanism, excessive-deficient syndrome have more dangers than deficient syndrome involved in the development of cancer process.

## 4. Conclusion

In this study, based on miRNA microarray date of HCC patients and normal controls, we obtained evidence that the miRNA expression profiles of LGDHS, LDSDS and LKYDS are different. The classification results show that the Deficient syndrome (LKYDS) first cluster to Excessive-deficient syndrome (LDSDS), then as a parallel branch cluster to Excessive syndrome (LGDHS). Furthermore, the lower

Table 2: KEGG and BIOCARTA terms distribution of downregulated genes (upexpression level of miRNAs) of TCM syndromes in HCC.

| Category | Term | *P* value | FDR value |
|---|---|---|---|
| LGDHS | | | |
| KEGG | Small cell lung cancer | 0.0159 | 0.0141 |
| LDSDS | | | |
| KEGG | Pathways in cancer | 0.0054 | 0.0022 |
| KEGG | Pancreatic cancer | 0.0142 | 0.0043 |
| KEGG | Glioma | 0.0015 | 0.0157 |
| KEGG | Prostate cancer | 0.0036 | 0.0171 |
| KEGG | Small cell lung cancer | 0.0013 | 0.0313 |
| KEGG | Non-small cell lung cancer | 0.0224 | 0.0113 |
| KEGG | Cell cycle | 0.0017 | 0.0156 |
| KEGG | Endocytosis | 0.0110 | 0.0233 |
| KEGG | Focal adhesion | 0.0476 | 0.0436 |
| BIOCARTA | Influence of Ras and Rho proteins on G1 to S transition | 0.0287 | 0.0144 |
| BIOCARTA | Regulation of BAD phosphorylation | 0.0131 | 0.0291 |
| BIOCARTA | Cyclins and cell cycle regulation | 0.0321 | 0.0323 |
| BIOCARTA | Cell cycle:G1/S check point | 0.0471 | 0.0437 |
| LKYDS | | | |
| KEGG | Prostate cancer | 0.0048 | 0.0001 |
| KEGG | Pathways in cancer | 0.0001 | 0.0005 |
| KEGG | Glioma | 0.0001 | 0.0011 |
| KEGG | Small cell lung cancer | 0.0015 | 0.0013 |
| KEGG | Melanoma | 0.0019 | 0.0025 |
| KEGG | Non-small-cell lung cancer | 0.0020 | 0.0021 |
| KEGG | Pancreatic cancer | 0.0021 | 0.0022 |
| KEGG | Chronic myeloid leukemia | 0.0072 | 0.0813 |
| KEGG | Apoptosis | 0.0145 | 0.0163 |
| KEGG | Acute myeloid leukemia | 0.0436 | 0.0413 |
| BIOCARTA | Y branching of actin filaments | 0.0066 | 0.0771 |
| BIOCARTA | NFAT and hypertrophy of the heart (transcription in the broken heart) | 0.0108 | 0.0122 |
| BIOCARTA | Influence of Ras and Rho proteins on G1 to S transition | 0.0108 | 0.0122 |
| BIOCARTA | Human cytomegalovirus and map kinase pathways | 0.0136 | 0.0151 |
| BIOCARTA | Overview of telomerase RNA component gene hTerc transcriptional regulation | 0.0257 | 0.0268 |

SVM score between LDSDS and LKYDS also suggested that the excessive-deficient syndrome is extrinsically close to deficient syndrome in HCC patients. The topological structure showed that the hub nodes (miRNAs or target genes) of miRNA-target network are much stronger determinants of the realized gene expression profiles, whereas the periphery nodes that should be regulated are not regulating. Obviously, the different topological profiles of networks also involved in the molecular mechanisms are different form Excessive to Deficient syndromes in HCC. GO and pathway analysis of target genes in up-expression networks revealed that the excessive-deficient and deficient syndromes of HCC are more complexity than excessive syndrome. Furthermore, although excessive-deficient and deficient syndromes have similar complex mechanism, excessive-deficient syndrome might have more dangers than deficient syndrome involved in development of cancer process.

## Conflict of Interests

The authors declare that they have no financial and personal relationships with other people or organizations that can inappropriately influence their work; there is no potential conflict of interests including employment, consultancies, stock ownership, honoraria, paid expert testimony, patent applications and registrations, and grants or other funding.

## Acknowledgments

This work was supported by Key Program of National Natural Science Foundation of China (813300416), National S and T Major Project of China (no. 2012ZX10005001-004), Scheming Project of Shanghai Municipal Education Commission (no. 2012JW25), Leading Project of Integrated Traditional and Western Medicine of Shanghai University of Traditional

Chinese Medicine (2013), and Key Science Foundation of Anhui Province (KJ2012A260).

## References


[1] M.-F. Yuen, J.-L. Hou, and A. Chutaputti, "Hepatocellular carcinoma in the Asia pacific region," *Journal of Gastroenterology and Hepatology*, vol. 24, no. 3, pp. 346–353, 2009.

[2] G.-S. Feng, "Conflicting roles of molecules in hepatocarcinogenesis: paradigm or paradox," *Cancer Cell*, vol. 21, no. 2, pp. 150–154, 2012.

[3] H. B. El-Serag, J. A. Davila, N. J. Petersen, and K. A. McGlynn, "The continuing increase in the incidence of hepatocellular carcinoma in the United States: an update," *Annals of Internal Medicine*, vol. 139, no. 10, pp. 817–823, 2003.

[4] H.-C. Hsu, Y.-M. Jeng, T.-L. Mao, J.-S. Chu, P.-L. Lai, and S.-Y. Peng, "$\beta$-catenin mutations are associated with a subset of low-stage hepatocellular carcinoma negative for hepatitis B virus and with favorable prognosis," *The American Journal of Pathology*, vol. 157, no. 3, pp. 763–770, 2000.

[5] W. Jia, W.-Y. Gao, Y.-Q. Yan et al., "The rediscovery of ancient Chinese herbal formulas," *Phytotherapy Research*, vol. 18, no. 8, pp. 681–686, 2004.

[6] Y. N. Song, J. J. Sun, Y. Y. Lu et al., "Therapeutic efficacy of fuzheng-huayu tablet based traditional chinese medicine syndrome differentiation on hepatitis-B-caused cirrhosis: a multicenter double-blind randomized controlled trail," *Evidence Based Complementary Alternative Medicine*, vol. 2013, Article ID 709305, 8 pages, 2013.

[7] R. Li, T. Ma, J. Gu et al., "Imbalanced network biomarkers for traditional Chinese medicine Syndrome in gastritis patients," *Scientific Reports*, vol. 3, article 1543, 2013.

[8] B. Jiang, X. Liang, Y. Chen et al., "Integrating next-generation sequencing and traditional tongue diagnosis to determine tongue coating microbiome," *Scientific Reports*, vol. 2, article 936, 2012.

[9] A. Esquela-Kerscher and F. J. Slack, "Oncomirs—MicroRNAs with a role in cancer," *Nature Reviews Cancer*, vol. 6, no. 4, pp. 259–269, 2006.

[10] D. P. Bartel, "MicroRNAs: target recognition and regulatory functions," *Cell*, vol. 136, no. 2, pp. 215–233, 2009.

[11] J. Hou, L. Lin, W. Zhou et al., "Identification of miRNomes in human liver and hepatocellular carcinoma reveals miR-199a/b-3p as therapeutic target for hepatocellular carcinoma," *Cancer Cell*, vol. 19, no. 2, pp. 232–243, 2011.

[12] G. Chen, J. Wang, and Q. Cui, "Could circulating miRNAs contribute to cancer therapy?" *Trends in Molecular Medicine*, vol. 19, no. 2, pp. 71–73, 2013.

[13] H. Zhang, Q. Y. Li, Z. Z. Guo et al., "Serum levels of microRNAs can specifically predict liver injury of chronic hepatitis B," *World Journal of Gastroenterology*, vol. 18, no. 37, pp. 5188–5196, 2012.

[14] H. Zhang, Y. Guan, Y. Y. Lu et al., "Circulating miR-583 and miR-663 refer to ZHENG differentiation in chronic hepatitis B," *Evidence-Based Complementary and Alternative Medicine*, vol. 2013, Article ID 751341, 8 pages, 2013.

[15] Q. L. Chen, Y. Y. Lu, G. B. Zhang et al., "Progression from excessive to deficient syndromes in chronic hepatitis B: a dynamical network analysis of miRNA array data," *Evidence-Based Complementary and Alternative Medicine*, vol. 2013, Article ID 945245, 10 pages, 2013.

[16] H. Zhuang, "Guideline on prevention and treatment of chronic hepatitis B in China (2005)," *Chinese Medical Journal*, vol. 120, no. 24, pp. 2159–2173, 2007.

[17] "The standards of TCM differential syndromes of viral hepatitis," Internal Medicine Hepatopathy Committee of Chinese Traditional Medicine Association, December 1991.

[18] T. Vergoulis, I. S. Vlachos, P. Alexiou et al., "TarBase 6. 0: capturing the exponential growth of miRNA targets with experimental support," *Nucleic Acids Research*, vol. 40, no. D1, pp. D222–D229, 2012.

[19] X. Wang and I. M. El Naqa, "Prediction of both conserved and nonconserved microRNA targets in animals," *Bioinformatics*, vol. 24, no. 3, pp. 325–332, 2008.

[20] D. W. Huang, B. T. Sherman, and R. A. Lempicki, "Systematic and integrative analysis of large gene lists using DAVID bioinformatics resources," *Nature Protocols*, vol. 4, no. 1, pp. 44–57, 2009.

[21] D. W. Huang, B. T. Sherman, and R. A. Lempicki, "Bioinformatics enrichment tools: paths toward the comprehensive functional analysis of large gene lists," *Nucleic Acids Research*, vol. 37, no. 1, pp. 1–13, 2009.

[22] S. Zheng, W. P. Tansey, S. W. Hiebert, and Z. Zhao, "Integrative network analysis identifies key genes and pathways in the progression of hepatitis C virus induced hepatocellular carcinoma," *BMC Medical Genomics*, vol. 4, article 62, 2011.

[23] A. Krek, D. Grün, M. N. Poy et al., "Combinatorial microRNA target predictions," *Nature Genetics*, vol. 37, no. 5, pp. 495–500, 2005.

[24] Y. Guo, Y. Feng, N. S. Trivedi, and S. Huang, "Medusa structure of the gene regulatory network: dominance of transcription factors in cancer subtype classification," *Experimental Biology and Medicine*, vol. 236, no. 5, pp. 628–636, 2011.

[25] J. A. Miller, S. Horvath, and D. H. Geschwind, "Divergence of human and mouse brain transcriptome highlights Alzheimer disease pathways," *Proceedings of the National Academy of Sciences of the United States of America*, vol. 107, no. 28, pp. 12698–12703, 2010.

[26] D. He, Z. P. Liu, M. Honda et al., "Coexpression network analysis in chronic hepatitis B and C hepatic lesions reveals distinct patterns of disease progression to hepatocellular carcinoma," *Journal of Molecular Cell Biology*, vol. 4, no. 3, pp. 140–152, 2012.

[27] A. Spaziani, A. Alisi, D. Sanna, and C. Balsano, "Role of p38 MAPK and RNA-dependent protein kinase (PKR) in hepatitis C virus core-dependent nuclear delocalization of cyclin B1," *Journal of Biological Chemistry*, vol. 281, no. 16, pp. 10983–10989, 2006.

Hindawi Publishing Corporation
Evidence-Based Complementary and Alternative Medicine
Volume 2013, Article ID 761987, 14 pages
http://dx.doi.org/10.1155/2013/761987

*Review Article*

# Model Organisms and Traditional Chinese Medicine Syndrome Models

**Shuang Ling and Jin-Wen Xu**

*Murad Research Institute for Modernized Chinese Medicine, Shanghai University of Traditional Chinese Medicine, Shanghai 201203, China*

Correspondence should be addressed to Jin-Wen Xu; jinwen.xu88@gmail.com

Received 30 August 2013; Revised 18 October 2013; Accepted 12 November 2013

Academic Editor: Shi-bing Su



Traditional Chinese medicine (TCM) is an ancient medical system with a unique cultural background. Nowadays, more and more Western countries due to its therapeutic efficacy are accepting it. However, safety and clear pharmacological action mechanisms of TCM are still uncertain. Due to the potential application of TCM in healthcare, it is necessary to construct a scientific evaluation system with TCM characteristics and benchmark the difference from the standard of Western medicine. Model organisms have played an important role in the understanding of basic biological processes. It is easier to be studied in certain research aspects and to obtain the information of other species. Despite the controversy over suitable syndrome animal model under TCM theoretical guide, it is unquestionable that many model organisms should be used in the studies of TCM modernization, which will bring modern scientific standards into mysterious ancient Chinese medicine. In this review, we aim to summarize the utilization of model organisms in the construction of TCM syndrome model and highlight the relevance of modern medicine with TCM syndrome animal model. It will serve as the foundation for further research of model organisms and for its application in TCM syndrome model.

## 1. Introduction

It has been found in the early 20th century that the most basic question of life can be answered in the simplest and easiest available biological systems. Simple organisms usually have less cell number and simple distribution of species, which can be observed and manipulated with ease. Since all creatures evolved from a common ancestor, cells have an identity in the basic pattern of development, and the structures and functions of vital genes for life activity are conserved. Therefore, these simple organisms can be used as the models easily to understand the universal law of life world according to their basic biological information. These organisms are commonly referred to as model organisms. As elementary materials for life science, model organisms can not only reveal the fundamental phenomena of life, but also can be an important reference for the exploration of the mechanisms and treatments for human diseases. In recent years, with the completion of genome sequencing, the studies on model organisms have gained a significant development so that human genome research has also entered the "postgenomic era". The functional genes of model organisms could be directly used for drug discovery and development, agricultural industry and medical diagnosis, and treatments with rapid, efficient, and large-scale identification. Comparative medicine and genetic engineering technology also offered the thought and method for the establishment of human genetic disease models in model organisms, which will be beneficial for the study of unknown functional genes and the development of disease therapy.

Although the application and acceptability of traditional Chinese medicine (TCM) increased in Western countries, the modernization of TCM has remained slow. Due to its worldwide application and potential impact on healthcare, a scientific evaluation system of TCM is necessary. Suitable animal models play an important role in the studies on fundamental theory of TCM and herbal pharmacology. In ancient China, animals were used in drug evaluation a long time ago. Domestic animals (horse, cattle, sheep, pig, dog, or chicken) had been used as bone-fracture models to explore

the functions of red copper chippings on bone setting [1]. Broomcorn millet and polished glutinous rice in the absence of vitamins were fed to cats and dogs to observe joint diseases. Rabbits were also used during the study of brain function through acupuncture.

Nowadays, TCM animal model research has become one of the fastest growing areas of modern TCM. It brings positive methodology and modern biological conception and has a positive impact on the development of TCM.

## 2. August Krogh Principle and Model Organisms

Good research system is the key to the success in scientific research. In the field of biomedicine, August Krogh principle [2] interprets that "for such a large number of problems, there will be some animals of choice, or a few such animals, on which it can be most conveniently studied" [3].

The principle requires that scientists should select an appropriate experimental object during studying a scientific problem. Usually, an ideal object in nature is easier to achieve the desired results, or even unexpected discovery when studied on this ideal organism, cell, gene, or protein, thus leading to another concept—model organisms.

Model organisms are special species that have been chosen for certain research aspects. A large amount of information with regards to other species including humans is obtained from model organisms, which will provide valuable data for the analysis of normal human development, gene regulation, genetic diseases, and evolutionary processes. Major model organisms are *Bacteriophage*, *Escherichia coli*, *Saccharomyces cerevisiae*, *Caenorhabditis elegans*, *Drosophila melanogaster*, *Danio rerio*, *Mus musculus,* and *Arabidopsis thaliana*.

## 3. History of Traditional Chinese Medicine Experimental Animal Model [4]

TCM has been practiced for more than 3000 years and has been accepted by a large portion of the population in China as a complementary therapy. *Zheng* (TCM syndrome), the key concept in TCM, refers to the pathological generalization in a certain stage of disease development. Nowadays, TCM is being accepted by more and more Western countries. However, the standards and weak point of fundamental research have restricted its further development. Its safety and pharmacological functions are also uncertain. According to the current status and problems, TCM modernization is highly necessary and urgent.

Since the 17th century, animals have played a vital role in every major medical advance. Experimental studies of TCM animal model started in 1960s in China. Kuang et al. [5] have found that excessive adrenocortical hormone aroused *Yang* asthenia in mice. At the same time, tongue image group of Shanghai Second Medical College has carried out the studies on the pathological change of tongue picture in rabbit models with *Qi*-deficient syndrome (artificial chronic anemia) and *Yin*-deficient syndrome (top digit small intestine side fistula). It is the first time to name TCM symptom. In 1974, abdominal blood coagulation model was used as Blood-Stasis model to explore the pharmacological actions of ectopic pregnancy prescription [6].

After 1976, TCM syndrome model transferring from the disease to *Zheng* was developed. The concept "syndrome differentiation" was focused on the establishment of animal models. In 1977, effects of *Yin*-nourishing drugs and *Yang*-tonifying drugs on *Yin*-deficient syndrome model and *Yang*-deficient syndrome model were explored through histochemistry and molecular biology method. At the same time, Blood-Stasis model and spleen-deficiency syndrome model were also established. These three kinds of models such as Kidney-deficient syndrome, spleen-deficient syndrome and Blood-Stasis syndrome have opened the ancient river of Chinese medicine syndrome [4] model and become the critical research topics for a long time.

In the mid-1980s, a large number of modern technologies such as biochemical immunological techniques, cell culture techniques, DNA analysis, cell fusion techniques, electron microscopy, and image analysis have been used in syndrome model study for achieving objective and standard indexes. Systematic studies of physiological and pathological changes in the syndrome model were conducted *in vitro* and *in vivo* to establish the correlation between modern medicine indexes and Chinese medicine syndrome [7–10].

Through the efforts of more than 40 years, the TCM syndrome model is on the right track and has gradually matured. Nowadays, high throughput genomics, proteomics, and metabolomics provide a new technological platform for the substantial fundamentals of diseases, syndromes, and prescriptions [11, 12].

In recent years, people realized that the unique theory of holistic concept and syndrome differentiation of TCM is coincided with the view of system biology [13]. Due to the combination of theory and technology in modern system biology, the gene expression, protein expression, and metabolic profiles of syndrome can be easily achieved and the relationship between profiles and syndrome can be understood in the aid of bioinformatics techniques, which will provide a proper way to reveal the nature of TCM syndrome.

## 4. TCM Syndrome Model and Disease Model

*Zheng* is a key concept peculiar to disease recognition in TCM. It is an indicator of the integrated reactive state of disease essence; it summarizes the cause, location, nature, and trend of the diseases as well as body's defense in the dynamic evolution process.

The "Disease" and "*Zheng*" recognize the disease essence from different angles [14], but there are also some important differences. A mature disease model always has some accurate special pathological features for distinguishing other diseases. For example, asthma is the common symptom of chronic asthmatic bronchitis and bronchial asthma, but the differences among the age of onset and the history of cough and sputum could distinguish them through the analysis of symptoms.

The characteristic of *Zheng* such as fuzzy, dynamic, complex, and nonspecific determines the complexity and diversity of TCM syndrome models. A disease process can be divided into various types according to syndrome differentiation; and the same TCM syndrome model occurs in many disease processes. For example, angina, called *XIONG BI* (chest impediment and heart pain) can be divided into 7 TCM syndromes such as *Qi* stagnation syndrome, Blood-Stasis syndrome, phlegm-turbid syndrome, congealing cold syndrome and deficiency of heart *Qi*, *Yin,* and *Yang* syndromes. A typical TCM syndrome, Blood-Stasis syndrome, described in TCM theory as a slowing or pooling of the blood, can be observed in many diseases, such as coronary diseases, heart failure, stroke, hyperlipemia, diabetes, rheumatism, endometriosis, and even depression. But above all, disease model and TCM syndrome model are closely related. On the precondition of disease differentiation, syndrome differentiation is more significant in disease diagnosis and treatment and TCM symptomatology study.

TCM syndrome model is the basic tool for the studies on both dynamic development of TCM symptoms and pharmacology of Chinese herbal formula. However, the replication of animal models that can reflect characteristics of *Zheng* is as a premise, which accurately obtains laboratory findings of traditional Chinese medicine. There are five kinds of TCM syndrome animal models: pathogenic models, pathological models, drug-induced models, models of TCM etiology combined with pathology, and models of diseases combined with TCM syndrome. In a variety of ideas developed in TCM syndrome animal models, the models combined with disease and TCM syndrome have both pathological features of Western diseases and characteristics of *Zheng*. On the biological basis of the unclarified *Zheng*, the models combined with disease and TCM syndrome are more appropriate models in the case study.

A major challenge for exploring the mechanisms of human diseases is the selection of an appropriate animal model that accurately reflects the disease. Mechanistic studies in animal models may provide important information on the processes of human disease. Therefore, animal model (Western medical model and TCM syndrome model) is a useful tool for drug development and fundamental research. Nevertheless, TCM syndrome model has its unique applications because of the different philosophical thoughts and medical systems of Western medicine and traditional Chinese medicine. TCM syndrome model is the basic tool for the studies on both dynamic development of TCM symptoms and pharmacology of Chinese herbal formula. A good TCM syndrome model is described, which can bridge the relationship between the essence of relevant TCM syndrome in the clinic and the experimental data to diagnostic criteria of TCM syndrome animal model. Nowadays, the establishment of TCM syndrome model evaluation system is still in the beginning phase. But in the impulse of development of TCM and the government's recognition, there has been made a rapid progress in this field. To date, TCM syndrome animal models have a variety of different evaluation methods, such as macroeconomic performance of the model animal, individual physical and chemical indicators, TCM syndrome differentiation through formula effect assessment, according to modeling factors presumably identified, equivalently corresponding to clinical diagnostic criteria. In view of the close relationship between disease and *Zheng*, some scholars first proposed the 3D establishment and assessment of the combination of disease and TCM syndrome animal model [15]. Based on the clinical syndrome diagnostic criteria, macroscopic indexes of animal model, microscopic indexes of genomics, proteomics and metabonomics, and at last, syndrome differentiation through formula effect assessment will be implemented to confirm this program. The first information gathering workstation of four diagnostic methods is established based on long observation of the animal [16]. It sets up the framework of animal four diagnostic methods and TCM syndrome differentiation. Objectification, standardization, and quantification have been successfully introduced into the realm of TCM symptomatology study.

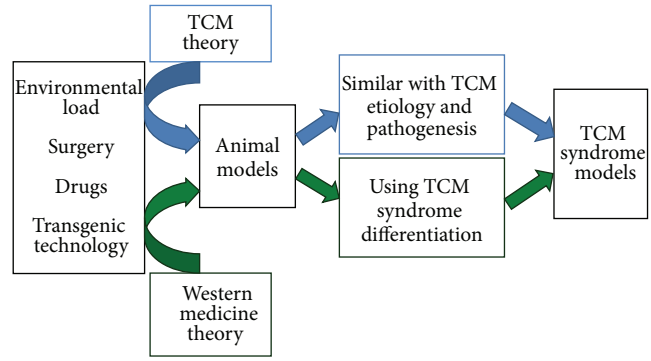


Figure 1: Approaches and applications of current TCM syndrome models.

## 5. Establishment of TCM Syndrome Model

Most essential thoughts of TCM theory are dialectical way, which is stemmed from the ancient Chinese philosophical thoughts, for example, the theories of *Yin-Yang*, Five Elements, *Zang-Fu* (viscera), Channels-collaterals (meridians), *Qi*, and Blood and body fluids. *Zheng* or TCM syndrome is the basic unit in traditional Chinese Medicine. The whole therapeutic system is based on the classification of TCM syndromes, which is a critical strategy to understand and diagnose diseases by TCM. Similarly, under the guidance of a variety of TCM theories and principles, this dialectical approach has been used in animal models with TCM syndromes. TCM syndrome models were usually used in the study of relevant syndrome essence or the function of herbal recipe.

Figure 1 summarizes the current approaches and applications of TCM syndrome models. Part 1, under the guidance of TCM theory, attempts to apply the environmental loading, surgery, hormone, or drug delivery to establish the syndrome animal model. Part 2, on the basis of currently available animal models of diseases in the field of Western medicine with the combination of TCM theory, lists the identified approaches to establish animal models. Due to the similarity

between clinical symptoms and TCM syndromes, these models are usually used directly as a model of syndrome.

TCM syndrome models have common points with modern models. Some TCM syndrome models are exactly same as modern models including stomach ache, cancer, or diabetes. Other TCM syndrome models share similar pathogenic factors or pathological changes with modern models. Currently, the models of disease combined with TCM syndrome have become the mainstream method in the studies of TCM syndrome models. Table 1 summarizes the types, characteristics and application of TCM syndrome models. The animal model of modern disease is in conformity with the clinical practice, in which the evolutionary process of TCM syndrome can be observed.

Furthermore, by studying modern models and TCM syndrome models, researchers can learn a lot regarding human disease and health problems. From a clinical viewpoint, animal models represent the nature of diseases despite the different philosophical thoughts and medical systems. We can take advantage of animal models for basic science study, clinical research, and drug development.

*5.1. TCM Syndrome Model Based on TCM Etiology and Pathogenesis [33].* On the basis of TCM theory, the pure TCM syndrome model is not equal with the modern medical model, such as *Yang*-deficient syndrome, Kidney-deficient syndrome, Blood-Stasis syndrome and *Cold* syndrome.

*5.1.1. TCM Syndrome Models Based on TCM Diagnostic Methods. Zheng* is identified from four main diagnostic TCM methods: observation, listening, questioning, and pulse. Tongue picture with abundant information can be observed easily. Consequently, it is very important to realize the tongue characterization in animal models. For example, red tongue model indicating the *Heat*-syndrome usually can be induced by long-term treatments with *Heat* drug (rats were treated with water extract of ginger, *Radix aconiti, Lateralis preparata,* and *Cinnamomum cassia* for 26 weeks) [17]. Thin white greasy tongue fur implying the impairment of the stomach can be copied with alcohol (50% v/v), overeating, and eating disorders [18].

*5.1.2. TCM Syndrome Model Based on Syndrome Identification of Eight-Principle.* The eight-principle is a general guideline of all kinds of syndrome type methodologies, which generalize the balance of *Yin-Yang*, interior or exterior environments, equilibrium between *Cold* and *Heat*, and deficiency or excess in the *Zheng*. Eight-principle serves the guides for the identification of all syndromes, such as the location or severity of pathological changes, the nature of illness, the condition of body resistance, and pathogenic factors. Different components have specific metabolic features and different susceptibility to certain diseases. For example, *Wind-cold* environment is one of the reasons for *cold* in the exterior syndrome. Excessive exercise after oral administration of *Heat* drugs, such as ginger, *Radix Aconiti, Lateralis preparata,* or *Cinnamomum cassia*, causes *Heat* syndrome due to insufficiency of *Yin*-fluids in animal models (rats were treated with water abstract of *Heat* drugs for 28 days and swimming for 5 min before sacrifice) [19].

*5.1.3. TCM Syndrome Model Based on Qi-Blood-Liquid-Fluid Pattern Identification. Qi*, Blood and Body Fluid are a substantial basis for the functional activities of life in TCM theory. *Qi*-deficiency mice model can be prepared by starvation (controlling forage amount in 125 $g/kg^{-1}\cdot d^{-1}$ for 14 consecutive days) [20]. $^{60}CO$ $\gamma$-ray radiation (3.5 Gy in 4 miles) or cyclophosphamide (120 mg/kg i.p.) can result in the damage of the blood-generating function of bone marrow, which is the representative of blood-deficiency syndrome [21].

*5.1.4. TCM Syndrome Models Based on Viscera Syndrome Types.* The Viscera theory, also named as *Zang-Fu* theory, was formed in the "Shanghan Lun", a famous and authoritative book of Treatise on Febrile and Miscellaneous Diseases in the Han Dynasty. The main point of this book can be traced back in the "Huangdi Neijing" (Inner Canon of Yellow Emperor) in the Spring and Autumn Period of China (400 B. C.). *Zang* and *Fu* are composed of the organs of five *Zang* and six *Fu*. Five *Zang* includes the organs such as heart (including the pericardium), lung, spleen, liver and kidney. Six *Fu* include gall bladder, stomach, large intestine, small intestine, urinary bladder, and Sanjiao (triple energizer). According to the TCM theory, *Zang* and *Fu* are not the simple anatomical concepts and are not equal to the anatomical organs from Western medicine. However, they are the important representation of physiological functions and pathological changes in human body. TCM treatment is characteristic of the analysis of the entire system and has the focuses on the balance of *Yin-Yang* through readjusting the functions of *Zang-Fu* organs. Therefore, a suitable animal model for the classification of viscera syndromes plays an important role in the understanding of visceral connotations, disease prognosis, and corresponding diagnosis and treatment methods.

At present, there are many commonly used models in TCM experimental research. For example, pulmonary *Qi*-deficiency syndrome refers to asthenia syndrome due to the insufficiency of *Qi* and hypofunction of the lung. These symptoms are usually observed in chronic obstructive pulmonary diseases.

Heart-Blood-Stasis syndrome is a more common syndrome differentiation of heart disease. Experimental animals can be established myocardial infarction model by ligation of the anterior descending branch of the left coronary artery or continuous injection with isoprenaline (100 mg/kg) [22, 23].

The clinical symptoms of spleen and stomach diseases in TCM are usually poor appetite, abdominal distension, loose stool, nutrition deficiency, heaviness sensation of arms and legs, lassitude, and emaciation. Low-protein diet with lapactic herbs or subcutaneous injection of reserpine can simulate vague, systemic, chronic, and deficient clinico-pathological features of spleen-deficient syndrome [24].

The kidney is an extremely essential organ in the whole process of life. The most important function of the kidney is

Table 1: Summary of TCM syndrome models.

| Types | Examples | Characteristics | Application |
|---|---|---|---|
| *TCM etiology and pathogenesis* | | | |
| Four diagnostic methods | Red tongue model induced by long-term heat drugs treatment; [17]<br>Thin white greasy tongue fur treated with alcohol, overeating, and eating disorders [18] | *Advantage*:<br>Under the guidance of TCM theory;<br>Simulating the TCM clinical etiology and pathogenesis;<br>Symptoms are similar to human;<br>Much closer to the TCM syndrome model<br>*Disadvantage*:<br>Single intervention factor;<br>TCM syndromes are separated from diseases;<br>Difficult to control the TCM pathogenic factors and TCM syndrome model it causes;<br>Without specific and accurate pathological changes;<br>Lacking stability and poor repeatability | The theory of etiology and pathogenesis of TCM study;<br>TCM therapeutics study |
| Eight-principle | *Heat* syndrome induced with excessive exercise after oral administration of heat drugs [19] | | |
| Qi-Blood-Liquid-Fluid pattern identification | *Qi*-deficiency model induced by starvation [20]<br>Blood-deficiency syndrome treated with $^{60}$CO $\gamma$-ray radiation or cyclophosphamide [21] | | |
| Viscera syndrome types | Heart-Blood-Stasis syndrome induced by coronary artery ligation or continuous injection with isoprenaline [22, 23];<br>Spleen-deficient syndrome induced with low-protein diet and lapactic herbs or subcutaneous injection of reserpine [24]<br>Liver-*Qi* depression model established by bandaging or irritating animals [26–28]<br>Kidney deficiency syndrome induced by excessive adrenocortical hormone [5] | | |
| Based on Western medicine etiology and pathology | Stomach ache induced by formalin or salicylic acid (p.o.) [25];<br>Spleen asthenia syndrome treated with reserpine [24];<br>Blood-Stasis syndrome induced by ameroid constriction of a coronary artery [26]; | *Advantage*:<br>Specific and accurate pathological changes;<br>Indicators are objective, standardized and can be quantified;<br>Highly reproducible;<br>Easy to establish;<br>*Disadvantage*:<br>Without clinical etiology evidence;<br>Lacking relationship with TCM theory;<br>Inappropriate tongue and pulse presentations | Pathology study;<br>Mechanism of drug effect on disease model;<br>Herb screening |

Table 1: Continued.

| Types | Examples | Characteristics | Application |
|---|---|---|---|
| Integrated with traditional Chinese and Western medicine | Heart-Blood-Stasis syndrome model basis on type 2 diabetic animals supplemented with prednisolone and adrenaline injection [27];<br>Congealing-*Cold* with Blood-Stasis syndrome model treated with adrenaline injection plus ice-water bath [28] | *Advantage*:<br>Combine disease and TCM syndrome on the same animal model;<br>Basis on stable and reliable disease model;<br>Highly reproducible;<br>Discussing the relationship between pathophysiology of disease and characteristics of TCM syndrome;<br>Combining TCM theory and experimental method with macrocosm and microcosm unifies in an animal model;<br>To diagnose a disease first then to identify the TCM syndromes<br>*Disadvantage*:<br>Application limitations;<br>Affected by environment, species of animal and animal individual differences | Pharmacodynamics study;<br>Mechanism of drug effect on disease model;<br>A link between TCM theory and clinic;<br>Essential of *Zheng* study |
| Genetically engineered animals | Phlegm-Stasis syndrome (*ApoE* gene knockout mouse) [29];<br>*Chan*-syndrome (Knockout mice of *Nurrl* gene); [30]<br>*Yin*-deficiency and Blood-Stasis syndrome in diabetes (*db*/*db* mutant mouse); [31]<br>Arthromyodynia (*Bi*-syndrome) (Abb knockout/transgenic HLA-DR4 mice) [32] | *Advantage*:<br>Stabilization;<br>High fidelity;<br>Hereditary;<br>High consistency with human disease<br>*Disadvantage*:<br>Limited categories (only mouse);<br>Expensive;<br>Difficult technology and complicated methods; | Pharmacodynamics study;<br>Mechanism of drug effect on disease model;<br>Drug screening;<br>Pathogenesis study of hereditary disease, immunodeficiency disease, tumor, TCM syndrome animal model of insufficient natural endowment; |

the essence storage of life in TCM theory, which is the foundation of the capability for reproduction, growth, and development. Kidney diseases are mainly involved in the deficiency of kidney. Aging, hereditary insufficient, intemperance of sexual life, and disorders of viscera, especially spleen and other reasons lead to asthenia or deficiency of *Qi*, *Yin*, *Yang,* or essence in kidney. Syndromes of Kidney-*Yang* deficiency are usually observed in hypothyroidism, hypoadrenocorticism, hypogonadism, and chronic nephritis. Therefore, excessive administration of hydrocortisone acetate, bendazole, hydroxycarbamide, thyroidectomy, or adrenalectomize can induce Kidney-*Yang* deficiency syndrome in model animals [5]. Syndromes of Kidney-*Yin* deficiency are commonly observed in some chronic consumptive diseases, such as advanced cancer, chronic nephritis, liver cirrhosis, diabetes, and tuberculosis. The administration of adrenocortical hormone and thyroid hormone in large doses or medicinal herbs with heat potency in TCM property, such as aconite, curculigo, orchioides, cinnamon, or epimedium, can induce Kidney-*Yin* deficiency syndrome in the animal model.

Liver disease mainly manifests in abnormal changes in storing- and dispersing- blood and the disorder of Liver-*Qi*. For instance, Liver-*Qi* stagnation may bring irregular menstruation and mental depression. Hyperactivity of Liver-*Qi* may increase your risk of suffering from irritability and anger. The digestive function of spleen-stomach and the excretion of bile are also affected by the syndromes of jaundice and bitter taste. Dizziness, tremor of limbs, numbness of hands, shaking head, and even sudden coma or hemiplegia is associated with the abnormal function of the liver. Liver-*Qi* depression model can be established by bandaging or irritating animals [34–36]. In TCM diagnosis, the 2K2C (two-kidney two-clip) renovascular hypertensive model is similar to the process of Liver-*Yang* Forming *Wind*-Syndrome (LYFWS), which refers to Wind syndrome due to the hyperactivity of Liver-*Yang*, usually observed in hypertension, cerebral hemorrhage, cerebrovascular accident sequela, Parkinson's disease, epilepsy, and injury of spinal cord [37]. Chronic hepatic injury induced by carbon tetrachloride (hypodermic injection of 40% oil solution, 0.3 mL/100 g body weight for 6 weeks) plus heat herbal compound prescription (rats were treated with water extract of ginger, *Radix aconiti, Lateralis preparata,* and *Cinnamomum cassia* for 2 weeks) can decrease body weight and increase heart rate and temperature of experimental rats [38], which is consistent with clinical signs of Liver-*Yin* deficiency syndrome.

*5.2. TCM Syndrome Models Based on the Etiology and Pathology of Western Medicine.* According to TCM theory, a part of diseases such as cancer, stroke, myocardial infarction, and diabetes share similar etiology and pathogenesis identified by modern medicine. Thus, the models usually used by Western medicine seem to be directly applicable.

For instance, liver cancer can be induced by chemical carcinogens such as diethylnitrosamine (DEN), dimethylamino-azobenzene (DBA), *o*-aminozaotoluene (OAAT), 2-acetamidobenzoic acid (2AAT), and aflatoxin in rats. Stomach ache, a common syndrome of stomach disease, is usually observed in acute gastric ulcer induced by oral administration of 1% formalin or salicylic acid [25]. The usual clinical symptoms of lung disease include cough, dyspnea, and lung distension. Pneumonia, emphysema, and pulmonary fibrosis can be induced by infusing bacteria, papain, and bleomycin through tracheal intubation, respectively. Streptozotocin (STZ) plus high calorie and high sugar diet cause diabetes, so called emaciation-thirst disease during TCM diagnosis. Whether strokes by middle cerebral artery occlusion or thoracic obstruction by the left anterior descending coronary artery ligation, both present Blood-Stasis syndrome. For example, chronic myocardial ischemia model generated by ameroid constriction of a coronary artery shows typical Blood-Stasis syndrome with clinical signs of dark purple tongue, arrhythmia, coronary stenosis or obstruction, and increased blood viscosity [26]. This kind of model is highly reproducible and easy to establish. It is an ideal model for the study of TCM theory through the thought of Western medicine.

*5.3. TCM Syndrome Models Integrated with Traditional Chinese and Western Medicine.* Another ideal model called combination of disease and syndrome mode (CDSM) is usually used to evaluate the preclinical validity of TCM. *Zheng* is induced according to the pathogenesis of TCM theory on the basis of Western medicine disease models.

For example, type 2 diabetic animals supplemented with 0.1% prednisolone (0.1 mL for 13 days) and 0.1% adrenaline injection (0.1 mol for the last day) for increasing blood lipid and intimal thickening, and causing early plaque formation, higher hematocrit, and cardiovascular morphological changes, can reveal a success Heart-Blood-Stasis syndrome model [27]. Moreover, subcutaneous injection with large dose of 0.1% adrenaline (0.08 mL/100 g body weight) causes peripheral circulatory disturbance, and then animals are placed in an ice-water bath to simulate the syndrome of Congealing-*Cold* with Blood-Stasis [28]. On the other hand, in order to build an animal model of Heart-*Qi* deficiency syndrome, a commonly used method is dietary restriction combined with forced load swimming and propranolol (0.5 mL, 1 mg/mL) or pituitrin injection (0.2 mL, 5 U/mL), resulting in the myocardial damage [39]. To sum up, CDSM promotes the understanding of diseases, *Zheng,* and relationship between *Zheng* and diseases, which is beneficial to the application in clinical discipline of Chinese and Western integrative medicine.

*5.4. TCM Syndrome Models from Genetically Engineered Animals.* With the development of functional genomics and model organisms, genetically engineered animal model is one of the most powerful research systems in the area of life science. Genetic engineering technology, including gene targeting, gene silencing, and transgenic technique, has been used to induce a variety of genetically engineered animals.

Mouse is the closest mammalian model organism to humans. The application of transgenic technology to modify the mouse genes has become commonplace. Transgenic animals also offer the opportunity for pharmaceutical research of TCM. Mutations of *Adenomatous polyposis coli* (*Apc*)

gene are important in sporadic colorectal tumorigenesis. The first mutant in *Apc* gene in mice came from a colony of randomly mutagenized mice. The mutant model of mouse tumor suppressor genes can cause similar symptoms with human cancer. The *Apc* mutant model mouse provides an *in vivo* environment to evaluate the validity of drugs.

From clinical symptoms, based on TCM theory, gene knockout mice can be considered as the model for naturally inherited insufficiency and hypoplasia. For example, *ApoE* gene knockout mice were used as Phlegm-Stasis syndrome model in atherosis and dementia [29]. Knockout mice of *Nurrl* gene, a transcription factor, are associated with Parkinson's disease that is a common degenerative disorder of the central nervous system in the elderly. The *Nurrl* knockout mouse model can be used in the studies on *Chan-Zheng*, a clinical syndrome of TCM characterized by tremors, muscle rigidity, and flaccid [30]. *db/db* mutant mouse is a kind of diabetic model, because $\text{Lepr}^{db}$ is an autosomal-recessive mutation on chromosome 4 and displays the characteristics of obesity, hyperglycemia, high insulin secretion, polyphagia, and polyuria, which are similar to non-insulin-dependent diabetes in humans. The *db/db* mutant mouse also provides an ideal model of diabetic microvascular disease, which presents the characteristics of a typical *Yin*-deficiency and Blood-Stasis syndrome. The tongue color of C57BL/6J-HBV transgenic mice, a chronic hepatitis animal model, is mostly purple due to microcirculation disturbance. The change of tongue color implies the severity of illness and the degree of Blood-Stasis syndrome [31]. The APP transgenic mice exhibit many pathological changes of Alzheimer's disease include extracellular A$\beta$ deposition, synaptic and cognitive defects, reactive astrocyte hyperplasia and dystrophic neurons, which are also commonly used in the study on senile dementia in TCM [40]. HLA-DR4 is associated with rheumatoid arthritis and multiple sclerosis. The Abb knockout/transgenic HLA-DR4 mice are susceptible to arthritis and connective tissue diseases, which is similar to arthromyodynia (or *Bi* syndrome), a pathological phenomenon of Cool-Dampness of joints according to TCM theory and used to analyze the correlation between TCM syndromes and rheumatoid arthritis [32].

## 6. Diagnostic Criteria for TCM Syndrome Animal Models and Biomarkers

There is a difference between animal models of TCM syndromes and Western medicine, which is established on the basis of clear pathological changes; on the contrary, dynamic *Zheng* is the soul of TCM syndrome animal models. *Zheng* is the external manifestation of diseases in some stages with a dynamic evolution; however, the mechanisms are still not clear. Because Chinese medicine is personalized medicine, the majority of the diagnostic criteria are still in the initial stage of the establishment and evaluation of animal models according to TCM syndromes and also lack widely accepted "gold standard"; therefore, the replication and effective evaluation of these animal models are still limited. During the evaluation of the syndrome model, several aspects of these works are still to be improved.

*6.1. Establishment of TCM Syndrome Diagnostic Criteria.* Macrosyndrome differentiation is a traditional method of Chinese medicine diagnosis through macroscopic information from observation, auscultation, smelling, asking, and pulse. This method is influenced by subjective factors, which can be applied to the evaluation of TCM syndrome animal models. Currently, a growing emphasis on microsyndrome differentiation considered by Western idea to identify diseases through detectable or quantifiable disease-related laboratory indicators as a basis for judging TCM syndromes or diagnostic criteria is present. The development of genomics, proteomics, and metabolomics technology plays a catalytic role for the exploration of TCM essence. The application of these methods can provide "TCM syndromes-related biomarkers" to improve the diagnostic criteria of syndrome animal models.

For example, the study [41] on patients with diabetes indicated that glucose, inositol D, C4 sugar 2, and C4 sugar 1 may be the new biomarkers for diabetes. However, the changes in level of xylose and C4 sugar 2 present the opposite results in diabetic patients with deficiency- or excess-syndrome, which they can serve as biomarkers to distinguish between deficiency- or excess-syndrome. Furthermore, compared with *cold* syndrome and *heat* syndrome in gastritis, Rui Li and his colleagues [42] found that leptin is a biomarker of *cold* syndrome, suggesting a low energy metabolism. On the contrary, CCL2/MCP1 is a biomarker of *heat* syndrome, showing increased inflammation, body temperature, metabolism, and immune regulation. These biomarkers will help for distinguishing *cold* from *heat* syndromes in gastritis model. Some studies have also reported [43, 44] that different types of Phlegm-Stasis syndrome induced by hyperlipidemia and atherosclerosis, dividing into 3 subtypes of phlegm-syndrome, Blood-Stasis-syndrome, and phlegm-and-Blood-Stasis-syndrome, have specific changes in plasma proteins; for example, (1) the levels of fibrinogen B-chain and apolipoprotein AI precursors can be used for distinguishing Phlegm-Stasis syndrome; (2) fibrinogen C-chain, albumin, and apolipoprotein AI precursors can be used as biomarkers to distinguish phlegm-syndrome and phlegm-and-Blood-Stasis-syndrome; (3) the application of indicators such as haptoglobin precursor, adrenomedullin-binding protein precursor, albumin, and complement C4 are able to distinguish phlegm-and-Blood-Stasis-syndromes. The variation of these biomarkers can result in the changes in protein expression, thus leading to the changes in the Phlegm-Stasis syndrome among different types.

*6.2. Established Evaluation Methods for the Syndrome Characteristics of Animal Models.* At present, a large number of scholars have studied and summarized the characterisyics of the TCM syndrome animal model; for example, some people [45, 46] think that there are differences in rat/mouse models in physique and characterization of TCM syndromes. To this end, through noninvasive information collection and analysis on the characterization of small animals, the

implementation of individualized diagnosis and treatment of small animals has initially achieved the standardization, objectivity, and quantification of diagnostic methods. The application of intelligent diagnostic techniques, such as, digital cameras, photoelectric blood stream plethysm, infrared imaging, colorimeter detection, and computer image processing, can observe the changes in animal hair luster, body weight, body temperature, heart rate, claw color, tongue color, excrement and urine, secretion and crissum color, and behavior changes including burnout, curled up, keeping warm together, decreased activity, trembling, drowsiness, and carpenter, which is used to judge the types of syndromes of model animals. Some studies [47] have established the scoring criteria and quantification table, a diagnostic scale for the model of liver-depression-and-spleen-deficiency caused by chronic restraint stress including a total of 26 indexes such as the appearance of characterization, stress response, feces situation, and general indicators (body weight, eating, drinking, body temperature, and so on).

*6.3. Syndrome Differentiation through Formula Effect Assessment.* The application of pharmacological effects was a widely accepted formula that disproves symptoms lesions and locations of the established animal models, which is also a way to improve the diagnosis. For example, on the above model [48], caused by chronic restraint stress to result in liver-depression-and-spleen-deficiency syndrome, after administration of "Xiaoyao San", a formula with the function of dispersing stagnated liver *Qi* and relieving *Qi* stagnation, nourishing spleen to harmonize with nutrient *Qi* can significantly improve animals' symptoms and result in the reduction of various metabolites from some biomarkers such as lactic acid, choline, N-acetyl-glycoprotein, saturated fatty acids, blood sugar, as well as the enhancement of unsaturated fatty acids and high density lipoprotein, which reveal clinically similar therapeutic effects, suggesting that it is generally successful to establish animal model of TCM symptoms. Moreover, Professor Shen [49] has systematically investigated the essence of kidney-*Yang*-deficiency and believes that the regulation center of kidney-*Yang* deficiency is the hormone axis from the hypothalamus to the top. To this end, he used "Yougui Yin", a classic formula for nourishing kidney-*Yang*-deficiency, to confirm his hypothesis. Experimental results show that "Yougui Yin" can specifically improve the mRNA expression of hypothalamic corticotropin-releasing factor and enhance the role of neuronal excitability.

In TCM animal models, despite numerous efforts, however, the ambiguity and complexity of TCM syndrome differentiation formed different standards of animal models, thus leading to the lack of comparability. This was largely hindered the development of Chinese medicine research; therefore, the establishment of a unified, objective diagnostic criteria is highly urgent.

Currently, the disease and syndrome integrated with animal model have become the mainstream model of the TCM syndrome. First, according to Western diagnostic criteria established disease model, and according to TCM clinical diagnostic criteria to collect animal information characterized by TCM syndromes; then, further application of genomics, proteomics, and metabolomics technology can exert the exploration of microlaboratory diagnostic criteria (such as biomarkers) at the molecular level. After obtaining the objective and reliable data, the application of data mining technology can be used to deal with a huge number and complicated data analysis and to understand their intrinsic linkages and rules; finally, the approval of classic formula can form an evaluation criteria of the diseases and syndrome integrated with animal models.

## 7. Application of TCM Models on Drug Screening and Mechanism Research

Unlike Western medical model, TCM symptom model is based on the guidance of TCM theory with certain characteristics of *Zheng* and human diseases. For this reason, some small mammals such as rats and mice are the most appropriate model organisms [7]. Guinea pig, rabbit, cat, dog, monkey, or mini-pig are also popularly used. Compared with mammals, lower model organisms such as yeast, worms, drosophila, and zebra fish are not suitable because of lacking the carrier for diagnosis and TCM syndrome differentiation. In contrast, due to their similarity with human genes and sharing common biochemical mechanisms or certain disease characteristics, the simple model organisms are still suitable for the use of high throughput screening for bioactive components in Chinese herbals and the exploration of disease mechanisms.

### *7.1. Model Organisms in Drug Discovery*

*7.1.1. Antiaging Drug.* From lower model organisms to higher primates and even human itself, longevity is limited by the interaction of genetic and environmental factors. Regulatory pathways and physiology are relatively conserved because the genetic mechanism of life span is dependent on species. The studies regarding longevity mechanisms have stepped into functional genome stage along with the advancement of technology and development of genome theory. According to long-term clinical practices in TCM, a unique theory of longevity has already achieved; for example, Kidney deficiency is considered as the basic cause of aging. Many antiaging drugs have recorded in ancient herbs, and most of which are Kidney-reinforcing formula. Therefore, the nourishing strategies of kidney combined with other viscera such as invigorating spleen and replenishing *Qi*, or promoting circulation and removing Blood-Stasis according to different syndromes is an ideal antiaging strategy.

Animal model for antiaging drug screening is a promising approach for drug discovery. The characters of *Caenorhabditis elegans* and *Drosophila melanogaster* make them useful for antiaging research because of short generation time, big progeny size, highly detailed genetic maps, and cheap breeding in the laboratory. "Erzhi Pill" and Chuanxiong Extract selected from drug screening on *C. elegans* could prolong the lifespan of the animals from more than 30 kinds of TCM [50]. "Erzhi Pill" is a liver-and-kidney-nourishing formula and Chuanxiong Extract reveals the obvious *Qi*-replenishing

and *Blood*-activating effects. Although both formulas have the regulatory functions for insulin/IGF-1 signaling pathway, "Erzhi Pill" can be involved in neuroendocrine genes and clock genes, while Chuanxiong Extract reveals an obvious effect on energy metabolism. In addition to delaying the aging process, Kidney-*Yang*-tonifying herb, *Epimedium*, can also promote the reproductive peak of *C. elegans* [51], as well as kidney-*Yin*-nourishing herb, *Cordyceps militaris*, on *Drosophila melarogaster* [52].

*7.1.2. Cardiovascular Drugs.* Zebra fish is a popular model for high throughout drug screening. In recent years, the transgenic zebra fish [Tg (flil: EGFP)] has become an important model of angiogenesis research, which is characterized by the expression of green fluorescent protein in endothelial cells of vascular system. The significant effects of the drug on blood vessels can be directly observed. Generally, herbal extract or corresponding components with *Qi*-tonifying and blood-promoting functions can promote angiogenesis in zebra fish model. The antiangiogenesis drugs commonly strengthen healthy *Qi* to eliminate pathogens, which are tested and validated in mammalian models even in clinics. For example, *Qi*-tonifying drug such as *Astragalus* polysaccharide can repair the injured vessel by increasing KDR-l, KDR, and Flt-1 mRNA expression [53], and curcumol can activate blood stasis by VEGFA and VEGFR2 [54]. Water-soluble components of *Angelica sinensis* can also be used in chronic diabetic foot ulcer and angiogenesis [55]. On the contrary, *Angelica sinensis* oil may suppress angiogenesis, induce apoptosis, and activate p38 and ERK1/2 signaling pathway [56]. *Qi*-activating drug such as tangerine peel and blood-cooling drug such as indirubin can inhibit angiogenesis by inducing HUVEC apoptosis and G0/G1 arrest [57].

*7.2. Mechanisms of TCM Treatments on Neurodegenerative Diseases.* Neurodegenerative diseases including Alzheimer's disease, Parkinson's disease, Huntington's disease, and amyotrophic lateral sclerosis refer to the progressive loss of structure or function of neurons in the central nervous system. The current treatment of neurodegenerative diseases is limited. Establishing a neurodegenerative disease animal model for drug screening and mechanism study is of significance.

*7.2.1. Parkinson's Disease.* Parkinson's disease (PD) is an age-related movement disorder. There are two most prevalent PD pathological markers: the formation of proteinaceous inclusions in PD patient brains and selective loss of dopamine (DA) in neurons. Nonmammalian organisms have been developed to explore cellular mechanisms and the discovery of new drugs. For example, zebra fish larvae are sequentially exposed to neurotoxin, 1-methyl-4-phenyl-1,2,3,6-tetrahydropyridine (MPTP), and Chinese herbal extract. The extract of *Fructus alpinia oxyphylla* and *Flos eriocauli* can prevent and reverse the degeneration of dopamine neurons and improve the deficiency of behaviors. The expression of human $\alpha$-synuclein gene in *Drosophila* may be the model of Parkinson's disease with proteinaceous inclusions and locomotor dysfunction. The organic pesticide rotenone has been found to cause DA neurotoxicity. Both the polysaccharides from *Cordyceps militaris* and the extract of *Acanthopanax senticosus* have shown the protective effect against rotenone-induced oxidative damage in *Drosophila melanogaster* [58, 59].

*7.2.2. Alzheimer's Disease.* Alzheimer's disease (AD) is a chronic neurodegenerative disorder characterized by cognition impairment and progressive decline in memory, neuronal loss, formation of neurofibrillary tangles (NFTs), and senile plaques. The major relevant gene includes A$\beta$ precursor protein (APP), Presenilin1 (PS1), and Presenilin2 (PS2) genes, tau protein and ApoE gene. In order to study AD pathogenesis *in vivo*, the model systems such as *C. elegans* and *Drosophila* will facilitate to high throughout genetic screening. In addition, the gradual loss of brain cells and A$\beta$ secretion to the extracellular compartment in *Drosophila* with AD were observed. Its pathological features are similar to AD in human. Therefore, the metabolic process of APP and the toxicity of A$\beta$ as well as retinal neuron disease and amyloid deposition can be observed. Turmeric, an ancient Chinese herb used in promoting blood circulation and removing *Ji*-syndromes (a syndrome of *Qi*-Stagnation and Blood-Stasis), has been proved to inhibit the formation of A$\beta$ oligomers and the transformation of A$\beta$ oligomer into fibrils [60].

*7.3. Safety Evaluation of TCM.* Zebra fish has been widely used in embryo, environmental, pathological, and drug toxicological studies. When drugs are added to the living water of zebra fish, and the death rate can be evaluated after 24 h administration, which can be used for the rapid screening and toxicity evaluation of traditional Chinese herbs on zebra fish [61]. A metabolite of mothballs, 1,4-naphthoquinone, can inhibit the activity of apoptotic protein CED-3, thus correspondingly inhibiting cell apoptosis. These findings suggest that mothballs as a daily necessity have carcinogenic tendency [62].

## 8. Conclusion and Prospect

Model organisms play an irreplaceable important role in fundamental studies of modern life science. In the last decades, important scientific discoveries achieved through model organisms are constantly emerging. Now the life science has entered the era of functional genomics. Functional genes of model organisms can be obtained and identified in a large-scale, fast, and efficient way, and can be used directly for drug discovery, disease diagnosis, and disease treatment. Model organism obtained through gene engineering technology and modern comparative medicine has the advantages for exploring the functions of new genes, verifying cellular metabolism or signaling pathways, and improving the development of disease diagnosis and management. Compared with the rapid development of Western medicine, the technology of traditional Chinese medicine lag behind, which has restricted the development of traditional Chinese medicine.

Different constitution types have specific metabolic features and susceptibility to certain diseases. Some studies

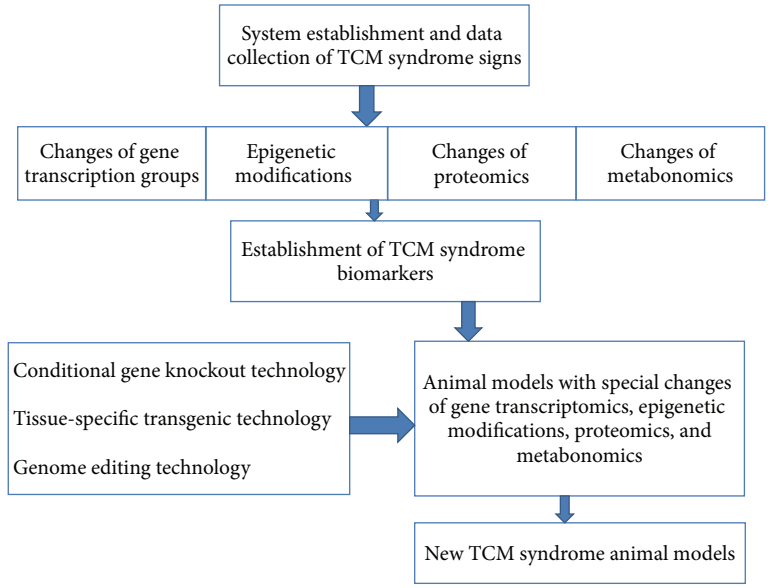


Figure 2: Assumptions regarding the establishment of new animal models for TCM syndromes.

have shown that a part of TCM syndrome has the genetic [63, 64], proteomic [65, 66], and metabolomic [67, 68] basis according to such constitution classification, which is closely correlated with syndrome types. We need to make full use of achievements in modern science and technology to establish *Zheng* model according to TCM theory, which will be helpful to reveal the essence of TCM syndrome and to promote theoretical creativity. The application of technologies for gain-function or loss-function can benefit for establishing a stable and heritable animal model in accordance with the demand of TCM syndrome. Nowadays, conditional gene knockin, knockout, or transgenic technologies are already mature in the production of model animals. These technologies can be used to determine the temporal and spatial expression pattern on a specific period and in a specific tissue and organ [69–71]. Although previous knockout of rats has difficulty in achieving successful results, recent studies have shown that TALEN approach is a widely applicable technology for targeted-genome editing that can result in the conditional gene knockout in rats [72–74]. This technology is an efficient and rapid method to gain the prospect of conditional knockout rats. Therefore, these technologies can be used to explore specific function or role of genes in specific tissues and organs under certain conditions. Likewise, these technologies also can provide a good prospect for manufacturing of TCM syndrome model that has the requirement of altered gene expression at a given time and specific organs or tissues. The studies on TCM syndromes require animal models with specific genotypes to achieve good reproducibility, uniformity, and stability. These assumptions are shown in Figure 2. These technologies are expected to become an effective way for TCM modernization.

However, due to the difference between animals and humans, the TCM syndrome animal model is complex, and some important symptoms and signs are difficult to reproduce in an animal model, such as tongue pictures, pulse conditions, and emotional symptoms. Transgenic technology is still facing some problems, such as low productivity, long production cycle, inefficient integration of genes, and high cost. Meanwhile, transgenic animals have high mortality and fertility rate. Moreover, there are technical issues also involved in ethical, legal, security, and other issues. How to improve the performance of model organisms and integrate with TCM research still needs further consideration and exploration.

## Acknowledgments

This work was financially supported by Grants from the Natural Science Foundation of China (81274130), the Youth Fund of Natural Science Foundation of China (81102532), the Specialized Research Fund for the Doctoral Program of Higher Education of China (20113107110006), the Innovation Program of Shanghai Municipal Education Commission of China (12ZZ122), the Shanghai 085 Project of Higher Education Connotation Construction (085ZY1202), and the Program for Young Teachers in Shanghai Universities of Shanghai Municipal Education Commission of China (shzy033).

## References

[1] C. Chen, *Supplement To Medica*, Anhui Science and Technology Press, Anhui, China, 2004.

[2] A. Krogh, "The progress of physiology," *American Journal of Physiology*, vol. 90, no. 2, pp. 243–251, 1929.

[3] H. A. Krebs, "The August Krogh Principle: or many problems there is an animal on which it can be most conveniently studied," *Journal of Experimental Zoology*, vol. 194, no. 1, pp. 221–226, 1975.

[4] X. Y. Chen, "Overview and progress in animal model of syndrome of traditional Chinese medicine," *Laboratory Animal Science*, vol. 8, no. 3, pp. 9–12, 1991.

[5] A. K. Kuang, Y. X. Wu, and T. Ding, "Effect of yang-tonifying drugs on system exhaustion induced by large dosage cortical hormone," *Chinese Journal of Internal Medicine*, vol. 11, no. 2, p. 113, 1963.

[6] Ectopic pregnancy research laboratory of Shanxi Medical College, "Pathological observation of abdominal blood clots absorption for effect of decoction of ectopic pregnancy on rabbit," *Shanxi Medical Journal*, vol. 12, pp. 61–64, 1974.

[7] L. Tong, J. H. Chen, S. J. Wu et al., "The effect of multiple factors on erythrocyte immunity function in dampness-heat model rats of epidemic febrile disease," *Chinese Journal of Immunology*, vol. 15, no. 8, pp. 1–4, 1999.

[8] T. M. Mao and J. H. Lin, "Preliminary survey of an experimental model on blood stagnation," *Journal of Peking University*, vol. 17, no. 4, pp. 246–248, 1985.

[9] S. J. Wu, Y. G. Yang, Q. H. Yang et al., "Preparation on the wetness-heat animal model of seasonal febrile disease and discussion on the mechanism of clearing heatness and removing wetness method," *Chinese Journal of TCM and Technology*, vol. 6, no. 2, pp. 65–67, 1999.

[10] C. E. Ben and B. K. Ye, "Preliminary study of blood-deficient animal model," *Shanghai Journal of TCM*, vol. 6, pp. 38–39, 1981.

[11] S. Zhang and H.-C. Shang, "Correlation between traditional Chinese medicine syndromes and omics: a literature review," *Journal of Chinese Integrative Medicine*, vol. 9, no. 12, pp. 1286–1291, 2011.

[12] P. Liu, P. Wang, G. Chen et al., "Research thinking and method of application of metabonomics in complicated theory system of traditional Chinese medicine," *China Journal of Traditional Chinese Medicine and Pharmacy*, vol. 26, no. 5, pp. 993–998, 2011.

[13] W. Jia, L. P. Zhao, and Z. Chen, "Systems biomedicine—the convergence of western medicine and traditional Chinese medicine," *World Science and Technology Modernization of Traditional Chinese Medicine and Materia Medica*, vol. 9, no. 2, pp. 1–5, 2007.

[14] Y. G. Wu, "Conception of disease, zheng, syndrome and their relationship in traditional chinese medicine," *Journal of Yunnan College of Traditional Chinese Medicine*, vol. 29, no. 2, pp. 1–7, 2006.

[15] H. H. Zhao, S. W. Guo, and W. Wang, "Establishment of judgement criteria in animal model combined disease and syndrome," *Journal of Beijing University of Traditional Chinese Medicine*, vol. 32, no. 6, pp. 365–373, 2009.

[16] Z. Q. Fang, Z. Q. Pan, W. L. Lu et al., "Main model organisms of Syndrome study—rat/mouse," *China Journal of Basic Medicine in Traditional Chinese Medicine*, vol. 15, no. 5, pp. 352–353, 2009.

[17] X. Y. Chen and S. J. Zou, "SEM observation of rat tongue with long-term heat-syndrome model," *Guangxi Journal of Traditional Chinese Medicine*, vol. 21, no. 2, pp. 42–44, 1998.

[18] S. J. Wang, Y. L. Chen, X. Y. Chen et al., "SEM observation of rat tongue with long-term Spleen-deficiency syndrome model," *Shaanxi Journal of Traditional Chinese Medicine*, vol. 23, no. 2, pp. 181–183, 2002.

[19] Y. S. Zhou, Y. L. Fan, Y. P. Zhang et al., "Development of animal model of heat syndrome due to insufficiency of Yin fluids," *China Journal of Basic Medicine in Traditional Chinese Medicine*, vol. 7, no. 9, pp. 23–26, 2001.

[20] M. S. Zhou and Q. L. Li, "Study on Qi-deficiency syndrome animal model," *Journal of Traditional Chinese Medicine*, vol. 30, no. 9, pp. 41–43, 1989.

[21] L. H. Jiao, L. M. Ren, and S. K. Zhao, "Comparison of four types of Blood deficiency model in mice," *Lishizhen Medicine and Materia Medica Research*, vol. 17, no. 6, p. 1001, 2006.

[22] J. Wang and J. P. Hu, "Preliminary study on animal's model of Qi-deficiency and blood-stasis in ischemia stroke," *Journal of Anhui TCM College*, vol. 18, no. 2, pp. 46–49, 1998.

[23] L. He, W.-Y. Jiang, and T.-M. Mao, "Preliminary exploration on establishing a simulated model of acute and chronic after-qi-stagnation blood stasis by adrenaline injection," *Chinese Journal of Integrated Traditional and Western Medicine*, vol. 24, no. 3, pp. 244–246, 2004.

[24] X. Y. Chen, "Method and thought on establishing primarily standardized animal model of the spleen Qi deficiency syndrome," *Chinese Journal of Basic Medicine in Traditional Chinese Medicine*, vol. 9, no. 1, pp. 3–5, 2003.

[25] H. Y. He, X. Y. Liu, W. P. Xiao et al., "Therapeutic effect of Weiweifang (WWF) on gastric ulcer and on serum IL-2 in experimental rats," *Lishizhen Medicine and Materia Medica Research*, vol. 20, no. 9, pp. 2141–2143, 2009.

[26] L. Liu, W. Wang, S. Z. Guo et al., "Research on collection of four diagnostic information from swine model with chronic myocardial ischemia," *Chinese Archives of Traditional Chinese Medicine*, vol. 26, no. 7, pp. 1438–1440, 2008.

[27] H. M. Tian, *Animal model research of heart blood stasis syndrome in type 2 Diabetic rats [M.S. thesis]*, Hunan University of Traditional Chinese Medicine, 2006.

[28] J. X. Teng and H. B. Liu, "Effect of Jiuqiniantong capsule on cold—stagnation and blood—stasis syndrome model," *New Journal of Traditional Chinese Medicine*, vol. 30, no. 11, pp. 32–33, 1998.

[29] Y. D. Hong, H. H. Mo, H. Y. Zhu et al., "Relationship of phlegm and blood-stasis syndrome in coronary heart disease with ApoE serum level and its gene polymorphism," *Journal of New Chinese Medicine*, vol. 41, no. 2, pp. 42–44, 2009.

[30] X. T. Wang, "Ideal animal model of anti-Parkinson's disease using the traditional Chinese medicine-*Nurr*1 Knockout (*Nurr*1 +/-) mice," *Chinese Archives Traditional Chinese Medicine*, vol. 25, no. 6, pp. 1117–1119, 2007.

[31] J. L. Li, T. Y. Wang, and L. Z. Wang, "Establishment of "disease and syndrome combined" rat model of type 2 diabetes mellitus," *Chinese Journal of Comparative Medicine*, vol. 17, no. 8, pp. 473–475, 2007.

[32] J. F. Hu, "Clinical observation on 69 cases of rheumatoid arthritis treated with combination of traditional Chinese and Western medicine," *China Journal of Traditional Chinese Medicine and Pharmacy*, vol. 7, no. 6, pp. 115–116, 2007.

[33] H. Zhang, W. B. Yang, L. Y. Wang et al., "Application of animal model in syndrome study," *Lishizhen Medicine and Materia Medica Research*, vol. 22, no. 6, pp. 1478–1479, 2011.

[34] Y. Li, X. M. Zhao, D. Li et al., "Changes of multiple organ function in rats with liver-qi stagnation syndrome," *Journal of Chinese PLA Postgraduate Medical School*, vol. 32, pp. 860–862, 2011.

[35] F. W. Li, H. R. Xu, W. Q. Zhang et al., "Clinical and experimental study on liver-depression and Qi-blood stagnation," *Journal of Traditional Chinese Medicine*, vol. 10, pp. 46–48, 1991.

[36] Z. P. Lv, "Lipid peroxidation and protection of xiaoyaosan in liver-Qi syndrome model rats," *Journal of Shandong College of TCM*, vol. 19, no. 3, pp. 199–201, 1995.

[37] S. P. Hu, G. Y. Lv, P. Y. Yu et al., "Evaluation to hypertension model of hyperaction of liver yang," *Journal of Zhejiang Chinese Medical University*, vol. 32, no. 5, pp. 698–701, 2008.

[38] Q. C. Ouyang and L. J. Shi, "Studies of the syndrome of liver yin deficiency in model rats," *Journal of Hunan College of Traditional Chinese Medicine*, vol. 19, no. 2, pp. 25–27, 1999.

[39] S. Z. Li, W. F. Zhu, X. P. Huang et al., "Establishmend of heart-Qi deficiency syndrome animal model," *China Journal of Basic Medicine in Traditional Chinese Medicine*, vol. 6, no. 7, pp. 46–52, 2000.

[40] L. T. Liu and H. Li, "Application of APP transgenic mouse models of dementia in TCM field," *Chinese Journal of Information on Traditional Chinese Medicine*, vol. 16, no. 9, pp. 7–8, 2009.

[41] T. Wu M Wang, H. F. Wei et al., "Application of metabolomics in traditional chinese medicine differentiation of deficiency and excess syndromes in patients with diabetes mellitus," *Evidence-Based Complementary and Alternative Medicine*, vol. 2012, Article ID 968083, 11 pages, 2012.

[42] R. Li, T. Ma, J. Gu et al., "Imbalanced network biomarkers for traditional Chinese medicine syndrome in gastritis patients," *Scientific Reports*, vol. 3, article 1543, 2013.

[43] J. L. Liu, J. N. Song, Y. Lei et al., "Differential plasma protein profiles in patients with hyperlipidemia and atherosclerosis of different patterns of phlegm-stasis syndrome," *Chinese Journal of Integrative Medicine*, vol. 30, no. 5, pp. 482–487, 2010.

[44] J.-N. Song, J.-L. Liu, X.-Z. Fang et al., "Relationship between plasma protein expression profiles and states of Zang-Fu organs in patients with phlegm or blood stagnation syndromes due to hyperlipidemia and atherosclerosis," *Journal of Chinese Integrative Medicine*, vol. 6, no. 12, pp. 1233–1237, 2008.

[45] Z. Q. Pan, Z. Q. Fang, X. L. Fu et al., "Evolution of typical syndromes and the characteristics of hind paw images in tumor-bearing mice," *Shanghai Journal of TCM*, vol. 38, no. 6, pp. 62–64, 2004.

[46] Z. Q. Fang, Z. Q. Pan, W. C. Tang et al., "Construction and operational standard of four diagnostic methods workstation for mice," *Acta Universitatis Traditionis Medicalis Sinensis Pharmacologiaeque Shanghai*, vol. 20, no. 1, pp. 42–46, 2006.

[47] L. F. Yue, J. Ding, J. X. Chen et al., "Establishment and review of rat model of syndrome of liver depression with spleen insufficiency," *Journal of Beijing University of TCM*, vol. 31, no. 6, pp. 396–400, 2008.

[48] H. G. Luo, *Studies of prescriptions corresponding to syndromes of "Xiaoyao San" decoction based on metabonomics [Ph.D. thesis]*, Beijing University of Traditional Chinese Medicine, 2007.

[49] D. F. CAI, Z. Y. Shen, L. J. Zhang et al., "Inhibition of, "Yougui Yin" on rat's model of hypothalamus—pituitary—adrenal—thymus axis," *Chinese Journal of Immunology*, vol. 10, no. 7, pp. 236–239, 1994.

[50] X. Y. Wang, *Study of the anti-aging effects of TCMs that could promote Qi and activate blood or nourish kidney and liver on* C. elegans *and the underlying molecular mechanisms [Ph.D. thesis]*, China Academy of Traditional Chinese Medicine, 2007.

[51] W. J. Cai, *Life extension of C. elegans caused by epimedium flavoniods treatment [M.S. thesis]*, Fudan University, 2008.

[52] B. G. Wang, G. Y. Zhang, and L. Y. Zhao, "The effect of cordyceps on *Droxophila melarogaster* longevity," *Chinese Journal of Gerontology*, vol. 22, no. 2, pp. 148–150, 2002.

[53] G. Hu, G. B. Mahady, S. Li et al., "Polysaccharides from astragali radix restore chemical-induced blood vessel loss in zebrafish," *Vascular Cell*, vol. 4, no. 1, pp. 1–8, 2012.

[54] L. L. Tian, *Curcuma oil active substances in angiogenesis screening, mechanism and safety [M.S. thesis]*, Wenzhou Medical College, 2011.

[55] H.-W. Lam, H.-C. Lin, S.-C. Lao et al., "The angiogenic effects of *Angelica sinensis* extract on HUVEC *in vitro* and zebrafish *in vivo*," *Journal of Cellular Biochemistry*, vol. 103, no. 1, pp. 195–211, 2008.

[56] J.-C. Yeh, T. Cindrova-Davies, M. Belleri et al., "The natural compound n-butylidenephthalide derived from the volatile oil of *Radix Angelica sinensis* inhibits angiogenesis *in vitro* and *in vivo*," *Angiogenesis*, vol. 14, no. 2, pp. 187–197, 2011.

[57] I. K. Lam, D. Alex, Y. H. Wang et al., "*in vitro* and *in vivo* structure and activity relationship analysis of polymethoxylated flavonoids: identifying sinensetin as a novel antiangiogenesis agent," *Molecular Nutrition & Food Research*, vol. 56, no. 6, pp. 945–956, 2012.

[58] D. Alex, I. K. Lam, Z. Lin, and S. M. Y. Lee, "Indirubin shows anti-angiogenic activity in an *in vivo* zebrafish model and an *in vitro* HUVEC model," *Journal of Ethnopharmacology*, vol. 131, no. 2, pp. 242–247, 2010.

[59] Z. Chen and T. L. Li, "Study of Acanthopanax senticosus on Rotenone-induced Parkinson's disease," *Chinese Journal of Traditional Medical Science and Technology*, vol. 18, no. 5, p. 410, 2011.

[60] J. D. Sun, J. Hou, and Y. Yang, "Protective effect of selenium-enriched polysaccharides from cordyceps militaris against rotenone-induced oxidative damage in Drosophila melanogaster," *Food Science*, vol. 34, no. 7, pp. 266–269, 2013.

[61] I. Caesar, M. Jonson, K. P. R. Nilsson, S. Thor, and P. Hammarström, "Curcumin promotes a-beta fibrillation and reduces neurotoxicity in transgenic Drosophila," *PLoS ONE*, vol. 7, no. 2, Article ID e31424, 2012.

[62] B. Shu, Y. J. Wei, L. Y. Zhang et al., "Acute toxicity of triptolide, matrine and emodin on zebrafish," *Journal of Yunnan University of Traditional Chinese Medicine*, vol. 33, no. 1, pp. 35–37, 2010.

[63] D. Kokel, Y. Li, J. Qin, and D. Xue, "The nongenotoxic carcinogens naphthalene and para-dichlorobenzene suppress apoptosis in Caenorhabditis elegans," *Nature Chemical Biology*, vol. 2, no. 6, pp. 338–345, 2006.

[64] Y. Wu, Y. Cun, J. Dong et al., "Polymorphisms in PPARD, PPARG and APM1 associated with four types of traditional chinese medicine constitutions," *Journal of Genetics and Genomics*, vol. 37, no. 6, pp. 371–379, 2010.

[65] W. J. Ding, Y. Z. Zeng, W. H. Li et al., "Identification of linkage disequilibrium SNPs from a kidney-yang deficiency syndrome pedigree," *The American Journal of Chinese Medicine*, vol. 37, no. 3, pp. 427–438, 2009.

[66] Y.-Q. Wang, F.-F. Li, W.-J. Wang, L.-Y. Zhao, L. Guo, and H.-F. Wang, "Serum proteomics study of chronic gastritis with dampness syndrome in traditional Chinese medicine," *Journal of Chinese Integrative Medicine*, vol. 5, no. 5, pp. 514–516, 2007.

[67] C.-L. Lu, X.-Y. Qv, and J.-G. Jiang, "Proteomics and syndrome of Chinese medicine," *Journal of Cellular and Molecular Medicine*, vol. 14, no. 12, pp. 2721–2728, 2010.

[68] X. Lu, Z. Xiong, J. Li, S. Zheng, T. Huo, and F. Li, "Metabonomic study on 'Kidney-Yang Deficiency syndrome' and intervention effects of Rhizoma Drynariae extracts in rats using ultra performance liquid chromatography coupled with mass spectrometry," *Talanta*, vol. 83, no. 3, pp. 700–708, 2011.

[69] Y. Wang, S.-Z. Guo, C. Li et al., "Analysis of plasma metabonomics of mini-swines with qi deficiency and blood stasis

syndrome due to chronic myocardial ischemia," *Journal of Chinese Integrative Medicine*, vol. 9, no. 2, pp. 158–164, 2011.

[70] K. Stankunas, J. H. Bayle, J. E. Gestwicki, Y.-M. Lin, T. J. Wandless, and G. R. Crabtree, "Conditional protein alleles using knockin mice and a chemical inducer of dimerization," *Molecular Cell*, vol. 12, no. 6, pp. 1615–1624, 2003.

[71] M. Lewandoski, "Conditional control of gene expression in the mouse," *Nature Reviews Genetics*, vol. 2, no. 10, pp. 743–755, 2001.

[72] S. Ristevski, "Transgenic studies in the mouse. Improving the technology towards a conditional temporal and spatial approach," *Methods in Molecular Biology*, vol. 158, pp. 319–334, 2001.

[73] A. J. Brown, D. A. Fisher, E. Kouranova et al., "Whole-rat conditional gene knockout via genome editing," *Nature Methods*, vol. 10, pp. 638–640, 2013.

[74] J. K. Joung and J. D. Sander, "TALENs: a widely applicable technology for targeted genome editing," *Nature Reviews Molecular Cell Biology*, vol. 14, no. 1, pp. 49–55, 2013.

Hindawi Publishing Corporation
Evidence-Based Complementary and Alternative Medicine
Volume 2013, Article ID 130702, 8 pages
http://dx.doi.org/10.1155/2013/130702

*Research Article*

# A New Biomarkers Feature Pattern Consisting of TNF-$\alpha$, IL-10, and IL-8 for Blood Stasis Syndrome with Myocardial Ischemia

**Shuzhen Guo,[1] Jianxin Chen,[1] Wenjing Chuo,[1] Lei Liu,[1,2] Xuanchao Feng,[1] Hongjian Lian,[1] Lei Zheng,[1] Yong Wang,[1] Hua Xie,[1] Liangtao Luo,[1] Chenglong Zheng,[1] Bangze Fu,[1] and Wei Wang[1]**

[1] *School of Preclinical Medicine, Beijing University of Chinese Medicine, Beijing 100029, China*
[2] *Department of Health Care, General Military Hospital of Beijing PLA, Beijing 100700, China*

Correspondence should be addressed to Wei Wang; wangwei@bucm.edu.cn

Received 18 July 2013; Revised 12 October 2013; Accepted 12 October 2013

Academic Editor: Shi-bing Su



*Objective*. To explore new diagnostic patterns for syndromes to overcome the insufficiency of obtainable macrocharacteristics and specific biomarkers. *Methods*. Chinese miniswines were subjected to Ameroid constrictor, placed around the proximal left anterior descending branch. On the 4th week, macrocharacteristics, coronary angiography, echocardiography, and hemorheology indices were detected for diagnosis. IL-1, IL-6, IL-8, IL-10, TNF-$\alpha$, and hsCRP in serum were detected, and Decision Tree was built. *Results*. According to current official-issued standard, model animals matched the diagnosis of blood stasis syndrome with myocardial ischemia based on findings, including >90% occlusion, attenuated left ventricular segmental motion, dark red or purple tongues, and higher blood viscosity. Significant decrease of IL-10 and increase of TNF-$\alpha$ were found in model animals. However, in the Decision Tree, besides IL-10 and TNF-$\alpha$, IL-8 helped to increase the accuracy of classification to 86%. *Conclusions*. The Decision Tree building with TNF-$\alpha$, IL-10, and IL-8 is helpful for the diagnosis of blood stasis syndrome in myocardial ischemia animals. What is more is that our data set up a new path to the differentiation of syndrome by feature patterns consisting of multiple biomarkers not only for animals but also for patients. We believe that it will contribute to the standardization and international application of syndromes.

## 1. Introduction

Treatments based on syndrome differentiation are essential to Traditional Chinese Medicine (TCM). Syndromes were named from different aspects and always including information of property or location of the disease, such as blood stasis syndrome and Qi deficiency in heart. It is widely accepted that disease and syndrome were the different aspects to the same pathological changes of a patient. When we focused on a particular disease, syndromes of TCM worked more like the criteria to further divide patients into different subtypes. These subtypes were the aims of Chinese herbal recipe and acupuncture for a long history. These subtypes were differentiated according to the major pathogenesis, and the latter was concluded from a group of symptoms and signs which are called macrocharacteristics. For the collecting of macrocharacteristics, looking, listening, question, and feeling the pulse were considered as the main methods.

Different from TCM, western medicine traditionally focused on the general character of a disease and the standardized treatment for all patients. But recently, it began to pay more attention to the differences between patients and look for the causes from genomics. Thus, the new strategy which emphasized on the diversification of treatment according to patients' gene background was known as personalized medicine. However, macrocharacters or pathologic changes are mostly decided by the function of multiple genes instead of single one. What is more, genotypes may give some clues of the differences of patients, but acquired factors contributed a lot to the phenotypes as well. Differentiating by macrocharacteristics will still be one of the most efficient ways to subtype patients for clinical purpose.

Experimental animals are the most important tool of translational medicine as well as TCM. The only difference is that the syndrome of animals should be taken into account to meet the therapeutic principles of herbal recipes besides diseases. However, most of those macrocharacteristics for patients' syndrome differentiation are difficult to get from animals. Standards and easily accessible biomarkers are desperately needed to overcome this huge gap between humans and experimental animals. Moreover, due to their poor specificities and/or sensitivities, many biomarkers for syndromes differentiation were discovered and then abandoned when used singly in the past decades. Considering the facts that a group of symptoms and signs together was used for patients' diagnosis, we believe that some kind of feature patterns consisting of several biomarkers will work better than single one.

Currently, coronary artery disease is one of the most widespread diseases, and blood stasis syndrome is the most common subtype of it. Blood stasis syndrome always performs as dark-purple tongue, pain in a fixed position, stagnated blood under skin, astringent pulse, angiemphraxis, abnormal hemorheology indices, and so forth.

Previous researches had shown that inflammation was one of the most important path physiological processes involved in blood stasis syndrome with coronary artery disease or myocardial ischemia [1, 2]. In this study, we try to explore feature patterns of blood stasis syndrome by screening biomarkers from the most easily detected and widely reported inflammation related cytokines, including interleukin-1 (IL-1), interleukin-6 (IL-6), interleukin-8 (IL-8), interleukin-10 (IL-10), tumor necrosis factor-a (TNF-$\alpha$), and high-sensitivity C-reactive protein (hsCRP).

## 2. Material and Methods

This study was reviewed and approved by Fuwai Hospital Animal Care and Use Committee and met the criteria of the National Institutes of Health for animal research. The surgery and model evaluation were conducted in Animal Research Center at Fuwai Cardiovascular Hospital, and laboratory analysis was conducted in our laboratory.

*2.1. Surgery.* In this study, Chinese miniswines from Animal Breeding Center of China Agricultural University (Beijing, China), weighing between 20 and 30 kg, were included. Anesthesia was induced with ketamine intramuscularly and maintained by diazepam and ketamine together. Chronic myocardial ischemia was produced by placing an Ameroid constrictor (Research Instruments, SW) around the proximal left anterior descending branch (LAD) after left thoracotomy. Thoracotomy without Ameroid constrictor placing was performed in sham group. 4 weeks later, examination and evaluation were performed.

*2.2. Observation of Macrocharacteristics.* According to a scale for macrocharacteristics of swine as we reported previously, details of animals' macrocharacteristics were observed in the morning [3]. Without any disturbance, overall performances of animals were observed, including general state, activity, daily food intake, daily water intake, and urine and stool property. And a video was recorded for further analysis. Then, animals were fixed by experienced breeders in a way veterinarian commonly used. After animal calmed down, its tongue, nose, and skin of fore and hind hoofs were observed, and the description of these characteristics was written down. Hereafter, photos of these areas were taken in the natural light by a camera (Nikon D70, Japan), and Casmatch Color Card (BEAR Medic Corporation, Japan) was used as reference. To standardize the condition of photos, the same angle and same distance were set and photos were taken by the same researcher.

*2.3. Echocardiography.* In the 4th week after surgery, transthoracic echocardiography was performed with standard left ventricular short axis and apical four chamber views under anesthesia (Agilent SONOS 5500, USA). Left ventricular volumes at the ends of systole and diastole, ejection factor (EF), fractional shortening (FS), and the wall motion index were calculated according to the method previously described by the American Society of Echocardiography [4].

*2.4. Coronary Angiography.* Four weeks after surgery, selective left coronary angiography was performed (Cardicav GE OEC 9800, USA) under the guidance of manufactory to document coronary flow to the LAD. Then TIMI of LAD was analyzed.

*2.5. Hemorheology Indices.* Whole blood was collected on the 28th day after surgery from the femoral vein. Analyses of hemorheology indices were performed in 6 hours after blood collection. High shear specific viscosity and low shear specific viscosity of whole blood and reduced blood, plasma specific viscosity, hematocrit, erythrocyte deformation index, and erythrocyte aggregation index were determined by using a rotary whole blood viscometer and plasma viscometer (LG-R-80 and LG-B-190, China) in the Laboratory of Dongzhimen hospital (Beijing, China). All measurements were carried out at 37°C according to the international guidelines for the measurements of hemorheologic parameters [5].

*2.6. ELISA Analysis.* Whole blood was collected on the 28th day after surgery from the femoral vein. Serum samples were collected, and concentrations of IL-1, IL-6, IL-8, IL-10, TNF-$\alpha$, and hsCRP were measured by enzyme-linked immunosorbent assay (ELISA) (Kangyuan Ruide Biological Technology Co., Ltd, China) according to the manufacturer's instructions.

*2.7. Statistical Analysis.* All continuous data are expressed by mean ± SEM. Independent sample $t$-test was used to compare the means between groups. All statistical analyses were performed by using SPSS 17.0 for Windows. And $P < 0.05$ was considered as significant.

*2.8. Classification by Decision Tree.* The program of Decision Tree in SPSS 17.0 was used as the classification method. IL-1, IL-6, IL-8, IL-10, TNF-$\alpha$, and hsCRP were included as independent variables, while blood stasis syndrome as dependent

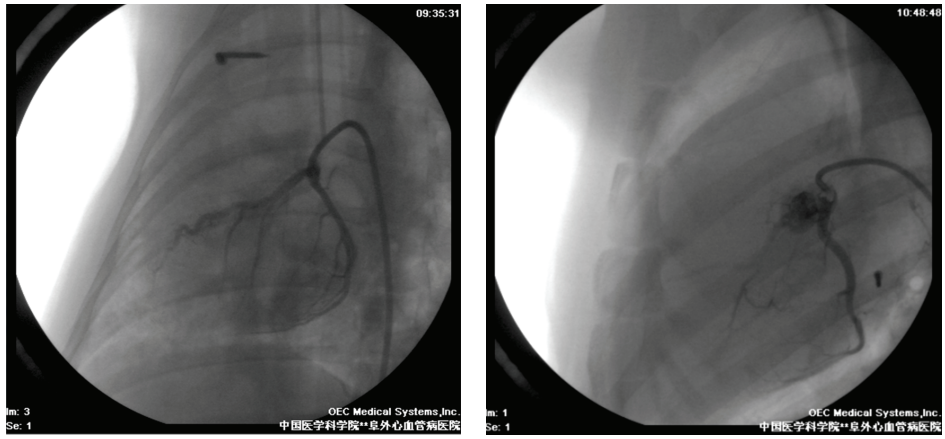


(a) Control group (b) Model group

Figure 1: Coronary angiography.

variable. CRT was selected as growing method. Minimum Cases in parent and children Node were set to 10 and 5, respectively. 3-folds crossvalidation was used.

## 3. Results

25 animals alive in 4th week were used in further analysis, including 15 animals for model group and 10 for sham group. These 10 sham-operated animals were used in the diagnosis of blood stasis syndrome, including analysis of angiography, echocardiography, macrocharacteristics, and hemorheology indices. Since no difference was found between sham-operated animals and healthy ones, for the sake of increasing specificity, we used 18 health animals together with 10 sham-operated animals in the control group when we analyzed the inflammation related cytokines and built the Decision Tree.

*3.1. Coronary Angiography.* Ex vivo angiography showed that more than 90% occlusion or even complete block of the left anterior descending artery by the Ameroid was found in model animals in the 4th week after surgery. TIMI flow grade I or II was observed in most of the model animals. There was good filling in the left anterior descending artery with TIMI flow grade III in Sham-operated animals. Results were shown in Figure 1.

*3.2. Echocardiography.* The structure and function of left ventricular were evaluated by echocardiography. Compared with sham operated animals, there was great increase of left ventricular volume and diameter at both end-systolic and end-diastolic volume ($P < 0.01$) in model animals. Anterior wall thickness of both papillary muscle and apex level was decreased at end-diastolic and end-systolic in model animals ($P < 0.01$). Interventricular septal depth was decreased at end-diastolic and end-systolic in model animals ($P < 0.05$ and $P < 0.01$). Meanwhile, papillary muscles level and the apex of the left ventricular anterior systolic wall thickening decreased ($P < 0.05$ and $P < 0.01$, resp.). In addition, septal thickness at the end-systolic decreased ($P < 0.05$). All the results above showed a segmental dysfunction of the left ventricular. There were no significant changes in ejection faction (EF) and fraction of shortening (FS), which suggested that cardiac function was still in compensatory period. Results were given in Table 1.

*3.3. Observation of Macrocharacteristics.* Model animals showed mental stress, irritation, fear, violent behaviors, strong self-defense, disorderly fur lack of luster, slightly dark red or purple tongue, and so forth, while sham-operated animals' performances gradually returned to normal, with increased appetite, neat and shiny fur, and light red or light white tongue.

*3.4. Hemorheology Indices.* As data displayed in Table 2, the whole blood viscosity and reduced blood viscosity of model animals increased significantly at a shear rate of middle (1/38) and low (1/5) ($P < 0.05$) when compared with sham-operated animals. No other changes were observed.

*3.5. Changes of Inflammation Related Cytokines.* In model group, IL-10 was decreased and TNF-$\alpha$ was increased dramatically ($P < 0.01$). No significant changes were found in IL-1, IL-6, IL-8, and hsCRP. Data were summarized in Table 3.

*3.6. Decision Tree Building with Inflammation Related Cytokines.* Results were depicted in Figures 2 and 3. The number of nodes was 7, number of terminal nodes was 4, and the depth of tree was 3. TNF-$\alpha$ and IL-10 were two of the most important parameters for the blood stasis syndrome classification (improvement = 0.110 and 0.092, resp.). IL-8 takes some part of responsibility of this classification (improvement = 0.033) unless there were no big differences between two groups when compared by $t$-test. IL-1, IL-6, and hsCRP were not as important as other parameters above. The first node of classification was TNF-$\alpha$. Most of the animals with lower than 1.150 ng/mL TNF-$\alpha$ were control group (16/17). And not

Table 1: Changes of heart function evaluated by echocardiography (Mean ± SEM).

| | Control ($N = 10$) | Model ($N = 15$) | $P$ value |
|---|---|---|---|
| LVEDd (cm) | 3.208 ± 0.124** | 3.895 ± 0.076 | 0.000 |
| LVEDs (cm) | 2.041 ± 0.043** | 2.657 ± 0.072 | 0.000 |
| ESV (mL) | 8.559 ± 0.940** | 16.115 ± 1.217 | 0.003 |
| EDV (mL) | 22.542 ± 2.117** | 36.371 ± 1.628 | 0.000 |
| IVSDs (cm) | 1.185 ± 0.199** | 0.833 ± 0.032 | 0.004 |
| IVSDd (cm) | 0.692 ± 0.029* | 0.592 ± 0.020 | 0.024 |
| LVAWTs (cm) | | | |
| Mitral valve level | 1.029 ± 0.055 | 1.004 ± 0.027 | 0.665 |
| Papillary muscles level | 1.153 ± 0.032** | 0.849 ± 0.044 | 0.001 |
| Apex level | 1.145 ± 0.045** | 0.623 ± 0.044 | 0.000 |
| LVAWTd (cm) | | | |
| Mitral valve level | 0.728 ± 0.025 | 0.739 ± 0.017 | 0.754 |
| Papillary muscles level | 0.794 ± 0.034* | 0.648 ± 0.027 | 0.012 |
| Apex level | 0.808 ± 0.040** | 0.546 ± 0.032 | 0.000 |
| Wall thickening (%) | | | |
| Mitral valve level | 41.748 ± 6.016 | 36.317 ± 2.498 | 0.350 |
| Papillary muscles level | 47.325 ± 7.038 | 30.136 ± 3.268 | 0.023 |
| Apex level | 42.564 ± 3.194** | 12.072 ± 1.887 | 0.000 |
| FS (%) | 35.818 ± 1.752 | 30.835 ± 2.780 | 0.372 |
| EF (%) | 61.770 ± 2.067 | 56.299 ± 2.020 | 0.189 |

Model versus Control group, $^{*}P < 0.05$; $^{**}P < 0.01$.
LVEDd: left ventricular end-diastolic dimension; LVEDs: left ventricular end-systolic dimension; ESV: end-systolic volume; EDV: end-diastolic volume; IVSDs: interventricular end-systolic septal depth; IVSDd: interventricular end-diastolic septal depth; LVAWTs: left ventricular end systolic anterior wall thickness; LVAWTd: left ventricular end diastolic anterior wall thickness; FS: fractional shortening; EF: ejection fraction.

Table 2: Hemorheology indices (Mean ± SEM).

| | Control ($N = 10$) | Model ($N = 15$) | $P$ value |
|---|---|---|---|
| Whole blood viscosity 1/150 (mPa.s) | 5.224 ± 0.149 | 5.275 ± 0.091 | 0.795 |
| Whole blood viscosity 1/38 (mPa.s) | 8.758 ± 0.234 | 9.563 ± 0.163* | 0.025 |
| Whole blood viscosity 1/10 (mPa.s) | 3.727 ± 0.112 | 3.608 ± 0.068 | 0.395 |
| Whole blood viscosity 1/5 (mPa.s) | 12.590 ± 0.362 | 13.987 ± 0.253* | 0.012 |
| Reduced viscosity 1/150 (mPa.s) | 10.091 ± 0.300 | 10.438 ± 0.191 | 0.350 |
| Reduced viscosity 1/38 (mPa.s) | 18.861 ± 0.600 | 20.593 ± 0.385* | 0.026 |
| Reduced viscosity 1/10 (mPa.s) | 6.189 ± 0.189 | 6.272 ± 0.128 | 0.725 |
| Reduced viscosity 1/5 (mPa.s) | 28.835 ± 0.921 | 31.328 ± 0.621* | 0.047 |
| Plasma viscosity (mPa.s) | 1.843 ± 0.054 | 1.899 ± 0.042 | 0.465 |
| Hematocrit (%) | 43.545 ± 0.928 | 42.727 ± 0.717 | 0.550 |
| Erythrocyte aggregation index | 2.651 ± 0.069 | 2.534 ± 0.042 | 0.163 |
| Aggregation index of integral area | 498.500 ± 15.307 | 498.500 ± 8.502 | 1.000 |
| Erythrocyte deformability index | 0.367 ± 0.007 | 0.382 ± 0.006 | 0.208 |
| Deformation index of integral area | 191.800 ± 5.736 | 190.848 ± 3.289 | 0.889 |

Model versus Control group, $^{*}P < 0.05$; $^{**}P < 0.01$.

only model animals (14/26) but also part of control animals (12/26) shared a higher TNF-$\alpha$ concentration (>0.115 ng/mL). Then IL-10 was used as the second node; higher IL-10 (>1.506 pg/mL) most frequently appeared in control group (7/8). When TNF-$\alpha$ was higher than 0.115 ng/mL and IL-10 was less than 1.506 pg/mL, IL-8 turned up as the third classification node; most model animals were assigned to >55.022 pg/mL group (11/13). When TNF-$\alpha$, IL-10, and IL-8 were used together as classification nodes, the total predicted accuracy was 86%. Accuracy was much higher in control group (92.9%) than in model group (73.7%) (see Table 4).

## 4. Discussion

*4.1. Evaluation of Myocardial Ischemia.* Ameroid constrictor is a widely used instrument in myocardial ischemia models. It results in chronic ischemia due to gradual occlusion. In our study, in the 4th week after surgery, more than 90% occlusion

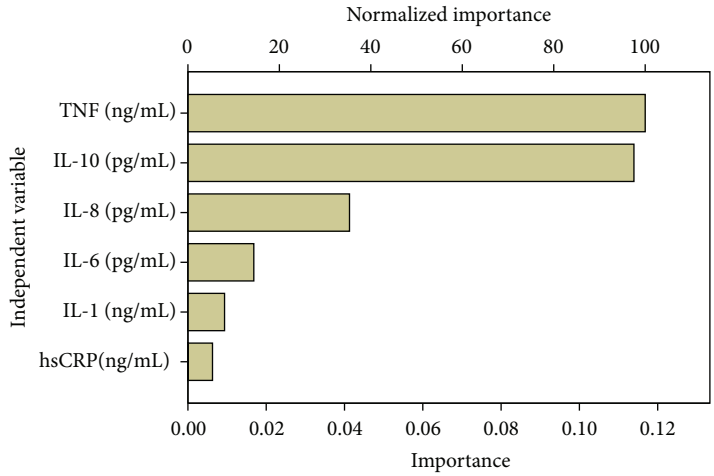


Figure 2: Importance of inflammation related cytokines in the Decision Tree of blood stasis syndrome. Growing method: CRT. Dependent variable: blood stasis in heart.

Table 3: Changes of inflammation related cytokines (Mean ± SEM).

| | Control ($N = 28$) | Model ($N = 15$) | $P$ value |
|---|---|---|---|
| IL-1 (ng/mL) | 0.279 ± 0.021 | 0.308 ± 0.036 | 0.466 |
| IL-6 (pg/mL) | 288.037 ± 15.161 | 307.662 ± 27.806 | 0.542 |
| IL-8 (pg/mL) | 97.436 ± 6.673 | 86.832 ± 10.958 | 0.387 |
| IL-10 (pg/mL) | 1.467 ± 0.129 | 0.962 ± 0.142* | 0.018 |
| TNF-$\alpha$ (ng/mL) | 1.266 ± 0.117 | 1.769 ± 0.147* | 0.012 |
| hsCRP (ng/mL) | 10.591 ± 0.839 | 12.936 ± 1.324 | 0.126 |

Model versus Control group, $^{*}P < 0.05$; $^{**}P < 0.01$.

Table 4: Prediction accuracy of the Decision Tree.

| Observed | Predicted | | |
|---|---|---|---|
| | Control | Model | Percent correct |
| Control | 26 | 2 | 92.9% |
| Model | 4 | 11 | 73.3% |
| Overall percentage | 69.8% | 30.2% | 86.0% |

or even complete block of the left anterior descending artery was confirmed by angiography. Significant changes were found in the structure of left ventricle and its anterior wall, such as LVEDd, LVEDs, ESV, EDV, LVAWTs, and LVAWTd at both papillary muscles and apex level. Segmental motion deficiency was found at both papillary muscles and apex level, but no big difference was found in EF or FS. At this time of point, model animals met the criteria of myocardial ischemia. These results were similar to other reports [6].

*4.2. Differentiation of Blood Stasis Syndrome.* This was the most controversial and difficult part of this study. Traditionally, syndromes were differentiated by symptoms and signs in clinic. Most parts of them were difficult to obtain from animals. Even if some macrocharacteristics were obtained from animals, diagnostic values have to be elucidated carefully by comparing their similarity with patients. In this study we used the principles we had published previously [3]. Comprehensive observation of macrocharacteristics was explored at multiple time points to reduce bias. Since there was no officially-issued standard for animal blood stasis syndrome, we used the diagnostic criteria of blood stasis syndrome issued by the Chinese Association of Integrative Medicine as the reference [7]. And according to the similarity of clinic property, the macrocharacteristics of patients in the criteria were translated to animals ones carefully. Different from the traditional blood stasis syndrome diagnostic criteria, biological indices were included as diagnostic items. Although relative changes instead of testing threshold were used for biological indices, it was still a big progress during the history of syndromes' objectification and standardization. Besides purple tongue and other macrocharacteristics, occlusion of blood vessels and changes of hemorheology indices were both considered as characters of blood stasis syndrome. Due to this big progress, differentiation of animals' syndrome began to be more feasible. Animals in the 4th week after surgery were found with angiemphraxis in coronary artery and dark purple tongue, which met 2 of the major defining characteristics and abnormal hemorheological indices, which met one of the laboratory evidences. According to these criteria, the chronic myocardial ischemia swine we established met the diagnosis of blood stasis syndrome, which was consistent with our previous report [8].

*4.3. Exploring a Method of Syndrome Differentiation for Individual Animal Models.* In clinic, patients were diagnosed individually based on symptoms and signs as well as inspection items with testing threshold. However, the comparison between model and control group was the only element used in the syndrome differentiation due to the shortage of diagnostic researches in animals. Moreover, even sharing the most pure genetic background, individual animal performed differently to the same treatment in the window of both macrocharacteristics and biomarkers. Thus, some samples

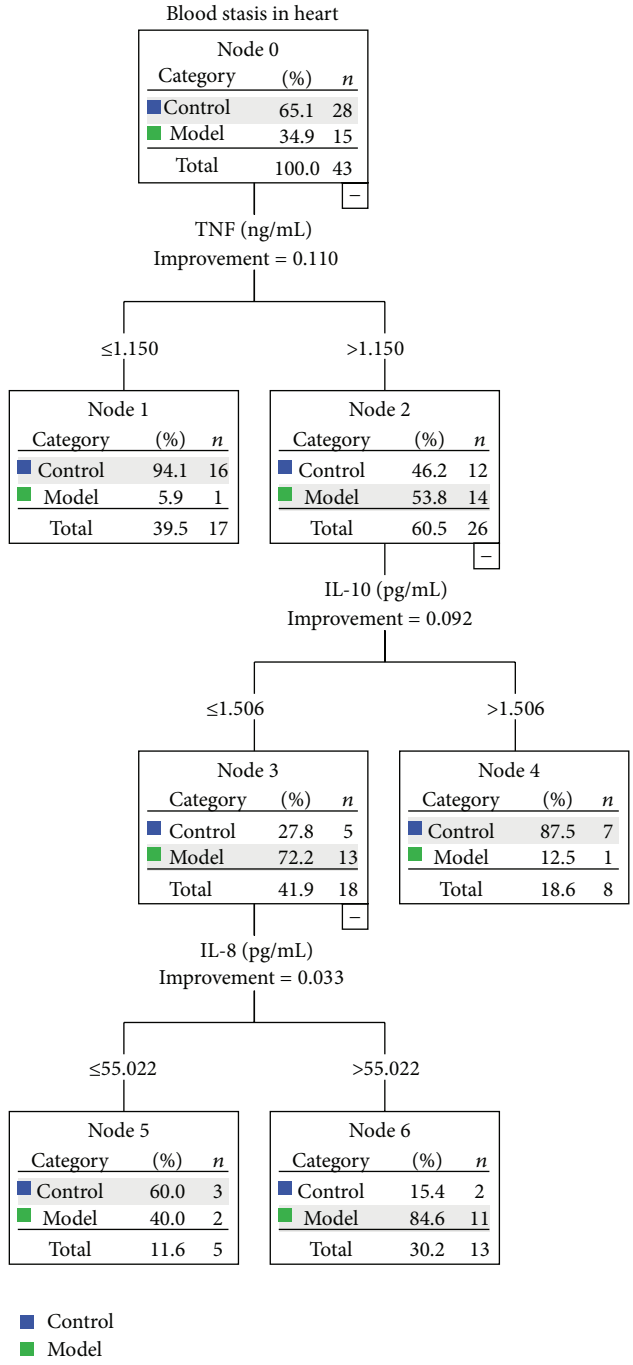


Figure 3: Decision Tree of blood stasis syndrome building by inflammation related cytokines.

have to be excluded to get more accurate results in many conditions. As the result, we believed that it will be better to perform individual differentiation instead of group statistic test in animal syndrome diagnosis. Since available animal macrocharacteristics are still limited, objective diagnostic items and their testing threshold were desperately needed.

A lot of researches suggested that syndrome was complicated and difficult to be distinguished by single biomarkers efficiently. It was widely accepted that a group of specific symptoms and signs are essential for the particular syndrome differentiation. We believe that a group of biological biomarkers working together may improve the sensitivity and specialty of syndrome differentiation. Nonetheless, fewer biomarkers with higher accuracy will be more efficient. What's more, for the sake of practical consideration, simple methods with good repeatability were always chosen for diagnosis use. That is to say, the balance had to be made between accuracy and practice.

Decision Tree was one of the best methods to classify samples according to several independent variables. It cannot only select the most important variables for classification but also provide the cutoff of every independent variable.

When we were seeking the possible biomarkers from multiple pathophysiological processes involved in blood stasis syndrome with myocardial ischemia, inflammation related cytokines came to our sight. A lot of researches showed that inflammation was one of the most important changes in blood stasis syndrome. Meanwhile, there are many inflammation related cytokines which were related to ischemia and/or blood stasis syndrome. Interleukin-1 (IL-1) was considered as one of the most patent prototypic inflammatory cytokines with adverse effects [9]. On the contrary, IL-10 and IL-8 played positive roles in left ventricular dysfunction and remodeling [10, 11]. Elevated IL-6 and CRP were both considered as biomarkers for adverse cardiovascular events [12, 13]. Interestingly, TNF-$\alpha$ played an ambivalent (detrimental versus beneficial) role depending on its dose and/or time [14]. And it was reported that some of these inflammation-related cytokines were involved in blood stasis syndrome [15]. All these inflammation related cytokines may be the most hopeful candidates for the biomarkers pattern.

We try to explore whether several parameters together will be better for blood stasis syndrome differentiation. And here we identified that higher TNF-$\alpha$ and lower IL-10 were closely related to it. Both TNF-$\alpha$ and IL-10 played the most important role in the Decision Tree. Interestingly, IL-8 helped to increase the accuracy of differentiation which did not change dramatically in model animals. It may become a new trend to discover biomarkers of syndromes as a feature pattern instead of single gold biomarker. Moreover, ELISA was a simple and reproductive method which is widely used in most labs, while serum is an easily obtained material from both animal and human. It is certain that after this feature pattern is validated in larger samples, it may not only become a new method for diagnosis of blood stasis with myocardial ischemia animals but also be helpful for objective diagnosis of blood stasis syndromes in patients.

## 5. Limitations

Due to the similarity of its heart with human, we chose mini swine in this research. But it was too expensive and difficult to raise many swines at the same time. If more samples were used, our findings may be more accurate and valuable for future usage.

## 6. Conclusions

We explored a new pattern of biomarkers for blood stasis syndrome with myocardial ischemia, which was a Decision Tree building with TNF-$\alpha$, IL-10, and IL-8. This feature pattern may not only help the syndromes differentiation of individual animals but also provide a new window of syndrome diagnosis in clinic. Feature pattern may become a new hopeful way for externalizing and standardizing of the diagnosis of syndromes in traditional Chinese Medicine. Further large scale trial is needed before it becomes a new diagnostic method of animal models or patients.

## Nonstandard Abbreviations and Acronyms

| | |
|---|---|
| IL-1: | Interleukin-1 |
| IL-6: | Interleukin-6 |
| IL-8: | Interleukin-8 |
| IL-10: | Interleukin-10 |
| TNF-$\alpha$: | Tumor necrosis factor |
| hsCRP: | High super C reactive protein |
| LAD: | Left anterior descending branch |
| ELISA: | Enzyme-linked immunosorbent assay |
| LVAWTd: | Left ventricular end diastolic anterior wall thickness |
| LVAWTs: | Left ventricular end systolic anterior wall thickness |
| LVEDd: | Left ventricular end-diastolic dimension |
| LVEDs: | Left ventricular end-systolic dimension |
| IVSDs: | Interventricular end-systolic septal depth |
| IVSDd: | Interventricular end-diastolic septal depth |
| EDV: | End-diastolic volume |
| ESV: | End- systolic volume |
| EF: | Ejection fraction |
| FS: | Fractional shortening. |

## Conflict of Interests

The authors declare that they have no conflict of interests.

## Authors' Contribution

Shuzhen Guo, Jianxin Chen, and Wenjing Chuo collaborated equally to the present work.

## Acknowledgments

The work described in this paper was supported by the Natural Science Foundation of Beijing (Grant no. 7112077), the Drug Discovery Initiative (Grant no. 2012ZX09103201-011), the National Natural Science Foundation of China (Grant no. 81102839), the new century excellent talent support plan of the ministry of education (Shuzhen Guo and Jianxin Chen), Beijing Nova Program (Grant no. xx2013032), and the foundation of Beijing university of Chinese medicine basic scientific research business expenses (Grant no. 2011-CXTD-06). The authors quite appreciate the Animal Research Center of Fuwai Hospital for their support and help in animal surgery and management.

## References

[1] H. Zhao, W. Wang, and S. Guo, "Proteomics study on unstable angina pectoris patients with blood stasis syndrome," *Chinese Journal of Arteriosclerosis*, vol. 16, no. 7, pp. 545–549, 2008.

[2] S. Guo, L. Liu, W. Xu, W. Wang, J. Han, and X. Chai, "Research on the plasma proteomic characteristics of blood stasis syndrome with myocardial ischemia by using an integrated animal model of mini swine," *Chinese Archives of Traditional Chinese Medicine*, vol. 28, no. 10, pp. 2063–2066, 2010.

[3] L. Liu, W. Wang, S. Guo, W. Xu, and Y. Yu, "Research on collection of four diagnostic information from swine model with

chronic myocardial ischemia," *Chinese Archives of Traditional Chinese Medicine*, vol. 26, no. 7, pp. 1438–1441, 2008.

[4] M. H. Picard, D. Adams, S. M. Bierig et al., "American Society of Echocardiography recommendations for quality echocardiography laboratory operations," *Journal of the American Society of Echocardiography*, vol. 24, no. 1, pp. 1–10, 2011.

[5] O. K. Baskurt, M. Boynard, G. C. Cokelet et al., "New guidelines for hemorheological laboratory techniques," *Clinical Hemorheology and Microcirculation*, vol. 42, no. 2, pp. 75–97, 2009.

[6] D. Caillaud, J. Calderon, P. Réant et al., "Echocardiographic analysis with a two-dimensional strain of chronic myocardial ischemia induced with ameroid constrictor in the pig," *Interactive Cardiovascular and Thoracic Surgery*, vol. 10, no. 5, pp. 689–693, 2010.

[7] Chinese Association of Integrative Medicine, "Diagnostic criteria of blood stasis syndrome," *Chinese Journal of Integrative Medicine*, vol. 7, no. 3, pp. 129–131, 1987.

[8] W.-Y. Xu, W. Wang, S.-Z. Guo, T. Liu, L. Liu, and Y.-X. Yu, "Duplication of an animal model of myocardial ischemia with blood stasis syndrome in mini-swines," *Journal of Chinese Integrative Medicine*, vol. 6, no. 4, pp. 409–413, 2008.

[9] A. Abbate, B. W. van Tassell, G. Biondi-Zoccai et al., "Effects of interleukin-1 blockade with anakinra on adverse cardiac remodeling and heart failure after acute myocardial infarction [from the Virginia Commonwealth University-Anakinra Remodeling Trial (2) (VCU-ART2) pilot study]," *The American Journal of Cardiology*, vol. 111, no. 10, pp. 1394–1400, 2013.

[10] P. Krishnamurthy, M. Thal, S. Verma et al., "Interleukin-10 deficiency impairs bone marrow-derived endothelial progenitor cell survival and function in ischemic myocardium," *Circulation Research*, vol. 109, no. 11, pp. 1280–1289, 2011.

[11] A. Li, S. Dubey, M. L. Varney, B. J. Dave, and R. K. Singh, "IL-8 directly enhanced endothelial cell survival, proliferation, and matrix metalloproteinases production and regulated angiogenesis," *Journal of Immunology*, vol. 170, no. 6, pp. 3369–3376, 2003.

[12] D. Su, Z. Li, X. Li et al., "Association between serum interleukin-6 concentration and mortality in patients with coronary artery disease," *Mediators of Inflammation*, vol. 2013, Article ID 726178, 7 pages, 2013.

[13] A. S. Sheikh, S. Yahya, N. S. Sheikh, and A. A. Sheikh, "C-reactive protein as a predictor of adverse outcome in patients with acute coronary syndrome," *Heart Views*, vol. 13, no. 1, pp. 7–12, 2012.

[14] P. Kleinbongard, G. Heusch, and R. Schulz, "TNF$\alpha$ in atherosclerosis, myocardial ischemia/reperfusion and heart failure," *Pharmacology and Therapeutics*, vol. 127, no. 3, pp. 295–314, 2010.

[15] Y. Hong, Y. Huang, H. Wu, Y. Chen, F. Li, and H. Mo, "Clinical studies on relationship between TCM syndromes of coronary heart disease and inflammatory factors," *Journal of Guangzhou University of Traditional Chinese Medicine*, vol. 22, no. 2, pp. 81–86, 2005.

Hindawi Publishing Corporation
Evidence-Based Complementary and Alternative Medicine
Volume 2013, Article ID 324732, 6 pages
http://dx.doi.org/10.1155/2013/324732

*Research Article*

# Establishment of an Experimental Breast Cancer ZHENG Model and Curative Effect Evaluation of Zuo-Jin Wan

**Jia Du, Yang Sun, Xiu-Feng Wang, Yi-Yu Lu, Qian-Mei Zhou, and Shi-Bing Su**

*Research Center for Traditional Chinese Medicine Complexity System, Shanghai University of Traditional Chinese Medicine, 1200 Cailun Road, Pudong, Shanghai 201203, China*

Correspondence should be addressed to Shi-Bing Su; shibingsu07@163.com

Received 18 August 2013; Accepted 22 October 2013

Academic Editor: Aiping Lu



Herbal formulas based on the traditional Chinese medicine (TCM) syndrome (ZHENG) have been used as alternative treatments for breast cancer. However, there is a lack of the experimental animal ZHENG model for the evaluation of the herbal formulas. In this study, we have established 4T1 mouse breast cancer with Liver Fire Invading Stomach Syndrome model (4T1 LFISS mice) and investigated the effects of the herbal formula, Zuo-Jin Wan (ZJW). Our results showed that 4T1 LFISS mice have the features of LFISS including irritability, loss of appetite, yellow urine, chow, and a tail hot. Compared to untreated 4T1 LFISS mice, ZJW significantly reduced tumor weight and volume ($P < 0.05$), although it was weaker than Cisplatin. However, ZJW significantly increased the body weight and food intake of 4T1 LFISS mice and decreased serum ALT, AST, Cr, and BUN levels and ZHENG score ($P < 0.05$), while Cisplatin reduced the food intake, and body weight and increased serum ALT, AST, Cr, and BUN levels in 4T1 LFISS mice. Our study has provided a mouse breast cancer ZHENG model and showed that ZJW suppresses tumor growth and improves LFISS and kidney and liver functions in the 4T1 LFISS mice.

## 1. Introduction

Breast cancer is the most common cancer among women; 1.38 million women were diagnosed with breast cancer in 2008. Its incidence rates vary considerably, with the highest rates in Europe and the lowest rates in Africa and Asia [1]. Its incidence rate in China is also increasing rapidly, and the number of cases increased by 38.5% from 2000 to 2005 [2]. However, there currently is a lack of clinically safe and effective drugs for prevention and treatment of breast cancer. In traditional Chinese medicine (TCM), some herbal formulas originating from natural products have been used as alternative treatments for breast cancer [3].

In order to experimentally evaluate the effectiveness and safety of treatment based-ZHENG (TCM syndrome) for cancer, an animal ZHENG model is necessary. However, there is a lack of an experimental animal ZHENG model in cancer research. Recently, Chen et al. [4] have established mouse xenograft pancreatic cancer models with dampness-heat, spleen-deficiency, and blood-stasis syndromes and found that they correlated with the treatment response of herbal medicine. An animal ZHENG models for breast cancer needs to be established for the evaluation of Chinese herbal formula.

Zuo-Jin Wan (ZJW, also called Zuo-Jin pill) is a Chinese herbal formula. In the clinical practices of TCM, the efficacy of ZJW is based on Liver Fire Invading Stomach Syndrome (LFISS, a ZHENG), which is characterized by a choking sensation in the chest and irritability, loss of appetite, yellow urine, red tongue, and more in patients with cancer. Moreover, in recent studies, ZJW has been identified experimentally to have anticancer activity in recent studies in gastric cancer [5], liver cancer [6] and colorectal cancer [7],

Table 1: Semiquantitative evaluation of symptoms and signs.

| Symptoms | Light (1 point) | Middle (2 points) | Heavy (3 points) |
|---|---|---|---|
| Irritability | Angry, irritable, and occasional mood swings | Angry, easily irritable, but can be controlled | Often be agitated and angry, and difficult to control |
| Loss of appetite | Poor appetite, amount eaten decreases by less than a third of original amount | Appetite reduction, amount eaten decreases by more than a third | No appetite, eat less than half |
| Yellow urine | Slightly yellow urine | Yellow urine | Deep yellow urine |
| Claws and tail hot | Claws and tail slightly hot | Claws and tail hot | Claws and tail very hot |

and multiple cancer cell lines, and it has suggested that the anti-cancer activities are due to induction of mitochondria-dependent apoptosis pathway [8]. However, whether ZJW has inhibitory activities against tumor growth without the side effects in breast cancer is unknown.

In this study, we have established 4T1 mouse breast cancer with Liver Fire Invading Stomach Syndrome model (4T1 LFISS mice) and investigated the effects and safety of Zuo-Jin Wan (ZJW) compared to Cisplatin on 4T1 LFISS mice. Our results showed that ZJW inhibits the tumor growth and improves LFISS and kidney and liver functions in the 4T1 LFISS mice.

## 2. Materials and Methods

*2.1. Cell Culture.* The mouse 4T1 mammary tumor cell line was purchased from Shanghai Cell Bank, Chinese Academy of Sciences (Shanghai, China), and was cultured in DMEM medium (Gibco, San Francisco, CA, USA) supplemented with 10% heat-inactivated (56°C, 30 min) fetal calf serum (PAA, A-4061, Pasching, Austria), penicillin (100 U/mL), and streptomycin (100 $\mu$g/mL). The cell culture was maintained at 37°C with 5% $CO_2$ in a humidified atmosphere.

*2.2. 4T1 LFISS Mice.* Female BALB/c mice (5 weeks old) were purchased from SLAC Laboratory Animal (Shanghai, China) and bred in the Laboratory Animal Center at Shanghai University of traditional Chinese medicine. The mice were housed in pathogen-free condition throughout the experimental duration and given free access to commercial rodent chow and water. 4T1 cells ($3 \times 10^6$, suspended in 100 $\mu$L of PBS), were injected into mammary fat pads of female BALB/c mice.

*2.3. Preparation of Zuo-Jin Wan and Cisplatin.* Zuo-Jin Wan is formulated by mixing the herbs, Rhizoma Coptidis and Fructus Euodiae as 6 : 1 ratio. The herbs were purchased from Shanghai Kangqiao Chinese Traditional Medicine Co., Ltd. (Shanghai, China). The aqueous extracts of these herbs was prepared and the quality control was performed as described previously [4]. The extract was stored at −20°C, and its preparations were standardized, regulated, and quality controlled according to the guidelines defined by the Chinese State Food and Drug Administration. Cisplatin injection was purchased from Nanjing Pharmaceutical Factory Co., Ltd. (Nanjing, China).

*2.4. Treatment Protocol.* One day after tumor cell inoculation, the mice were randomly divided into four groups ($n = 8$ per group; normal, $n = 6$). ZJW-treated group (1.8 g/kg, once a day) was received by gavages, and Cisplatin-treated group (5 mg/kg, next day at a time), the positive control, was received by intraperitoneal injection as a positive control. Untreated groups were divided into a normal group and a model group. The model group was received with physiological saline as a sham control. The treatments lasted for 3 weeks. The mouse body weight, food intake, tumor weight, and volume were measured at different time points following tumor implantation. The tumor volume ($V$) was calculated by $V = a$ (long diameter) $\times b$ (short diameter) $2 \div 2$.

*2.5. Liver and Kidney Functions Tests.* After obtaining blood samples by picked eyeballs of the mice, it was centrifuged at 3000 rpm for 10 minutes in order to separate and collect the serum. Serum alanine transaminase (ALT), aspartate transaminase (AST), serum creatinine (Cr), and blood urea nitrogen (BUN) were measured using the colorimeter testing kit (Kangcheng, Nanjing, China). According to the manufacturer's instructions, serum samples were measured at 510 nm, 510 nm, 510 nm, and 520 nm, respectively.

*2.6. Evaluation of ZHENG in Mice.* The LFISS, a ZHENG, in 4T1 mice was diagnosed by its characteristic symptoms and signs, which include irritability, loss of appetite, yellow urine and claws, and a tail hot. It was given a semiquantitative evaluation as shown in Table 1, according to the established methodology and criteria for ZHENG animal models [9].

*2.7. Efficacy Evaluation of ZHENG.* The efficacy evaluation of ZHENG in mice was done according to the "Guideline for Clinical New Drug Research in Chinese Herbal Medicine" [10]. The standard of ZHENG outcome was scored as follows: ZHENG score as none: 0; light: 1 point; middle: 2 points; heavy: 3 points (Table 1). The calculation formula was as follows: the efficacy index of ZHENG ($N$) = [(before treatment score − after treatment score)/before treatment score] × 100%. The efficacy evaluation standard of ZHENG was the following: experimental cure: $N \geq 90\%$; excellent: $N < 90\%$ to 60%; effective: $N \leq 60\%$ to >30%; invalid: $N \leq 30\%$ [11].

*2.8. Statistical Analyses.* All data was expressed as means ± SD. Comparisons between groups were performed by

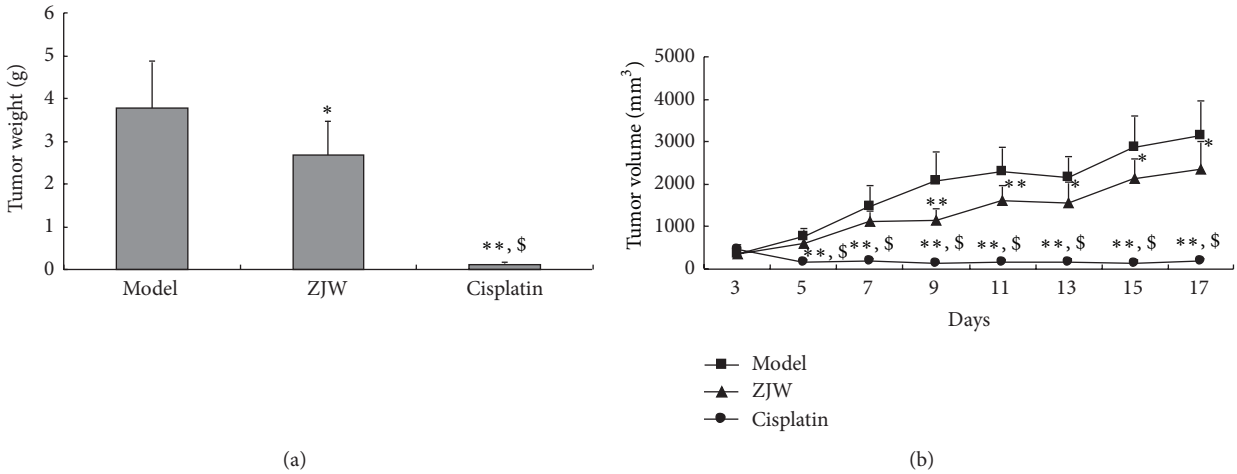


Figure 1: ZJW reduced tumor weight and volume in 4T1 LFISS mice. Tumor weights (a) and volumes (b) in 4T1 LFISS mice with ZJW and Cisplatin in treatments were measured, respectively. $^{*}P < 0.05$, $^{**}P < 0.01$, versus model group; $^{\$}P < 0.05$, versus ZJW-treated group.

Student's $t$-test and one-way analysis of variance (ANOVA). The level of significance was set at $P < 0.05$.

## 3. Results

*3.1. ZJW Reduced Tumor Weight and Volume in 4T1 LFISS Mice.* To determine whether ZJW could suppress the tumor growth of breast cancer, we tested the ability of ZJW to reduce tumor weight and volume in 4T1 LFISS mice. The tumor weights were significantly reduced in the ZJW-treated group ($P < 0.05$) and the Cisplatin-treated group ($P < 0.01$) compared to the model group, respectively (Figure 1(a)). Moreover, the tumor volumes were significantly reduced in the ZJW-treated group on days 9 and 11 ($P < 0.01$) and on days 13, 15, and 17 ($P < 0.05$). It significantly reduced on 5 to 17 days ($P < 0.01$) in the Cisplatin-treated group compared to the model group (Figure 1(b)). There were significant differences between the ZJW-treated group and the Cisplatin-treated group ($P < 0.05$). Together, these results suggested that ZJW can suppress the tumor growth, although it was weaker than Cisplatin in 4T1 LFISS mice.

*3.2. Effects of ZJW on Body Weight in 4T1 LFISS Mice.* In order to detect whether ZJW has any side effects, we measured the body weight of 4T1 LFISS mice once each day. As shown in Figure 2(a), there were no significant differences of the body weight among normal group, model groups and ZJW-treated group ($P > 0.05$). However, starting from 3rd day, there were significant differences between Cisplatin-treated group ($P < 0.01$) and the other groups.

*3.3. Effects of ZJW on ALT, AST, Cr, and BUN in 4T1 LFISS Mice.* We further tested whether ZJW has any effect on liver and kidney functions. The results showed that ALT (Figure 3(a)), AST (Figure 3(b)), Cr (Figure 3(c)), and BUN (Figure 3(d)) significantly increase in model group compared to normal group ($P < 0.05$). ALT (Figure 3(a)) and Cr

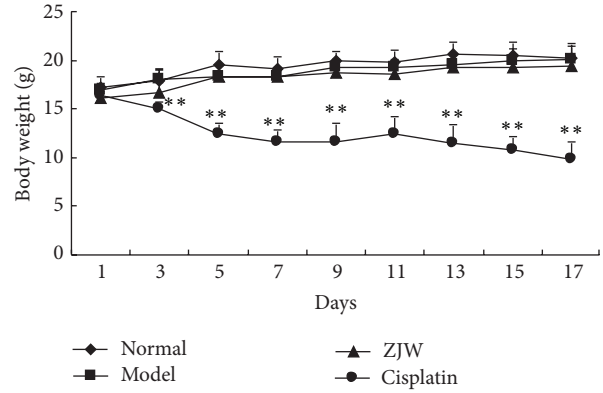


Figure 2: Effects of ZJW on body weight in 4T1 LFISS mice. Mice were treated by ZJW and Cisplatin. The body weights of 4T1 LFISS mice at different time points were measured. $^{**}P < 0.01$, versus model group.

(Figure 3(c)) were significantly decreased in ZJW-treated group compared to model group ($P < 0.05$), but there were no significant changes in the level of AST (Figure 3(b)) and BUN (Figure 3(d)) ($P < 0.05$). ALT (Figure 3(a)), AST (Figure 3(b)), Cr (Figure 3(c)), and BUN (Figure 3(d)) significantly increased in Cisplatin-treated group compared to model group ($P < 0.05$). Moreover, there were significant differences between ZJW-treated group and Cisplatin-treated group ($P < 0.01$). Together, these results suggested that ZJW has no side effects and improves liver and kidney functions while Cisplatin reduces body weight and increases ALT, AST, Cr, and BUN in 4T1 LFISS mice.

*3.4. ZJW Increased Food Intake in 4T1 LFISS Mice.* In order to detect whether ZJW increased food intake, we measured the food intake of 4T1 LFISS mice once every 2 days. As shown in Figure 4, the food intake of 4T1 LFISS mice was significantly decreased in model group compared to normal

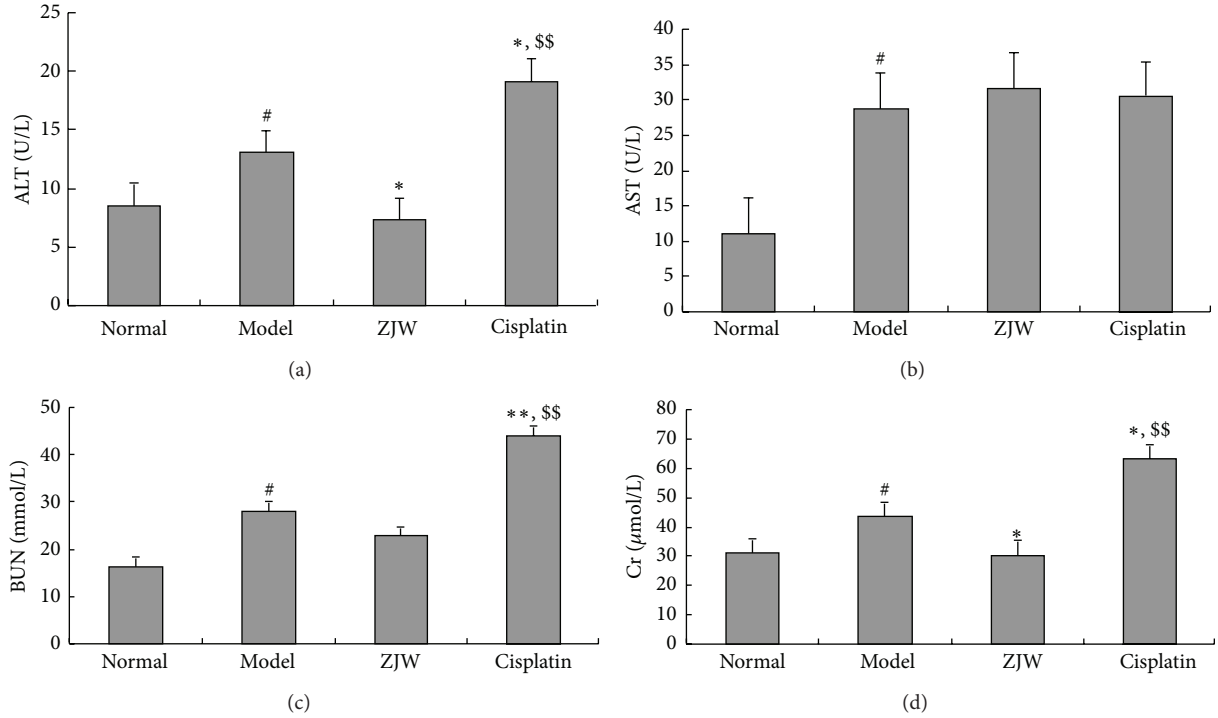


Figure 3: Effects of ZJW on kidney and liver functions in 4T1 LFISS mice. Mice were treated by ZJW and Cisplatin. (a) ALT, (b) AST, (c) BUN, and (d) Cr were measured using the colorimeter testing kit. $^{*}P < 0.01$, versus model group; $^{\#}P < 0.05$, versus normal group; $^{\$\$}P < 0.01$, versus ZJW-treated group.

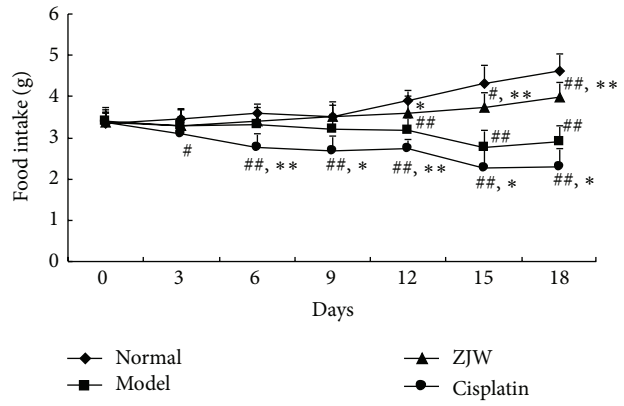


Figure 4: Effect of ZJW on food intake in 4T1 LFISS mice. The food intake in 4T1 LFISS mice with ZJW and Cisplatin treatments was measured. $^{*}P < 0.05$, $^{**}P < 0.01$, versus model group; $^{\#}P < 0.05$, $^{\#\#}P < 0.01$, versus normal group; $^{\$}P < 0.05$, $^{\$\$}P < 0.01$, versus ZJW-treated group.

group on days 12, 15, and 18, respectively ($P < 0.05$). Moreover, the food intake was significantly increased in ZJW-treated group compared to model group ($P < 0.05$ or $P < 0.01$) from the 15th day after treatment, but the food intake in Cisplatin-treated group was not only less than model group but was also significantly different from ZJW-treated group and normal group ($P < 0.01$). The results suggest that ZJW increased food intake while Cisplatin reduces food intake in 4T1 LFISS mice.

*3.5. ZJW Decreased ZHENG Score in 4T1 LFISS Mice.* To detect whether ZJW impacted the quality of life of the animals compared to Cisplatin treatment, we measured the ZHENG score of 4T1 LFISS mice once every 2 days. As shown in Figure 5, the ZHENG scores were significantly decreased in ZJW-treated group compared to model group ($P < 0.05$ or $P < 0.01$) from the 12th day after treatment, but Cisplatin-treated group was not significantly different from model group ($P < 0.05$), and the ZHENG scores were significantly decreased in Cisplatin-treated group compared to ZJW-treated group at day 15 and day 18, respectively ($P < 0.01$). The efficacy index of ZHENG is 53% in ZJW-treated group and 6.2% in Cisplatin-treated group, indicating that the ZJW treatment was effective and Cisplatin treatment was invalid. The results suggest that ZJW improves the quality of life of 4T1 LFISS mice through the decrease of ZHENG score while Cisplatin is unable to reduce ZHENG score in 4T1 LFISS mice.

## 4. Discussion and Conclusions

Treatment based on ZHENG differentiation, also called "Bian Zheng Shi Zhi", is the comprehensive analysis of clinical information that is used to guide the choice of treatment with TCM herbal formulae [11, 12]. It is the main approach in the clinical practice to increase the effectiveness and safety of TCM treatment in the clinical practice. Following the revaluation of herbal formulas-based ZHENG, the development of new drugs and the discovery of the mechanisms

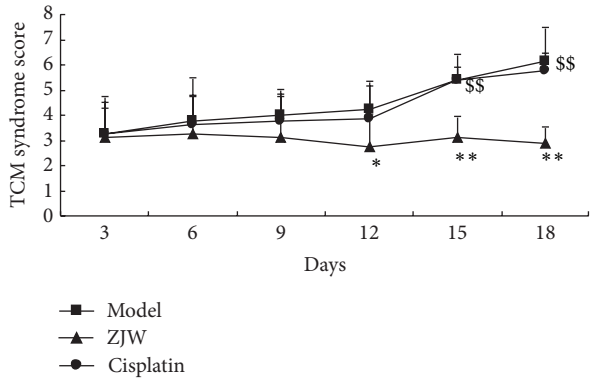


Figure 5: ZJW decreased ZHENG score in 4T1 LFISS Mice. The ZHENG scores in 4T1 LFISS mice with ZJW and Cisplatin treatments were measured. $^{*}P < 0.05$, $^{**}P < 0.01$, versus model group; $^{\$\$}P < 0.01$, versus ZJW-treated group.

all need an experimental animal model. Therefore, making the experimental animal ZHENG model as well as an animal disease model is important to breast cancer research.

The animal ZHENG model is necessary for ZHENG research; however, there is a lack of the experimental animal ZHENG model in mice. Recently, Chai et al. have established a Deficiency of both Qi and Yin Syndrome (DQYS) model with the clinical features and one key pathological factor in mice [13]. Previous studies have also established mouse pancreatic cancer models for evaluation of the molecular mechanisms underlying ZHENG and tumor growth [14], and the administration of herbal medicine to the ZHENG model modified the tumor microenvironment [4]. In this study, a mouse breast cancer ZHENG model was established. It was 4T1 mouse mammary cancer ZHENG (LFISS) model, that is, 4T1 LFISS mice. The symptomatic features of 4T1 LFISS mice were irritability and loss of appetite, yellow urine, hot tails and/or claws, along with increase in tumor size (Figure 1), decrease in body weights (Figure 2), and liver and kidney functions disorders (Figure 3). Furthermore, it was found that the ZHENG of 4T1 LFISS mice responds to the ZJW treatment and does not responded to Cisplatin treatment, indicating that the established 4T1 mouse breast cancer LFISS model is useful for the evaluation of the efficacy of herbal formulas.

Cisplatin is a common chemotherapy drug for breast cancer therapy, but its side effects such as nephrotoxicity [15], myelotoxicity [16], and neurotoxicity [17] limit its use. In this study, although Cisplatin treatment significantly suppressed tumor growth better than ZJW (Figure 1), it resulted in a decrease in body weight (Figure 2), liver and kidney functions disorders (Figure 3), and reduction in food intake (Figure 4). On the contrary, although the effect on inhibitory tumor is less than that of Cisplatin, ZJW increased body weight and food intake (Figures 2 and 4), improved liver and kidney functions (Figure 3), and improved the quality of life by reducing the ZHENG score (Figure 5) in 4T1 LFISS mice. It suggested that ZJW may be useful the as alternative treatment for breast cancer. Further research will investigate the effects of ZJW combined with Cisplatin.

Recurrently, the use of natural Chinese herbal medicine with antitumor effects is receiving to the treatment of breast cancer [18]. It is a holistic approach through multilevel, multitarget and multi-channel control, which focuses on reducing the side effects of chemotherapy, reversing drug resistance, and improving the quality of life and survival of patients. Therefore, these unique advantages have gradually made the TCM approach more promising in combating breast cancer [3, 19, 20]. Previous studies have shown that some herbal formulas have been used for the treatment of breast cancer including PC-SPESII extract [21] and Sangu decoction [20]. Although ZJW has been first found to have the antitumor effects on breast cancer in this study, the underlying mechanisms remain unknown.

ZJW consists of a combination of two Chinese herbs, Rhizoma Coptidis and Fructus Evodiae, in the ratio of 6 : 1 (w/w) [4, 22, 23], which contains high levels of active antineoplastic compounds such as berberine and evodiamine [24]. It has been reported that Rhizoma Coptidis and Fructus Evodiae synergistically inhibit s180 tumors in vivo [23], and the synergy of berberine and evodiamine enhances apoptosis of human hepatocellular carcinoma SMMC-7721 cells [24]. Moreover, it has been reported that evodiamine induces some cancer cell apoptosis, such as in human melanoma A375-S2 cells [25], human colorectal carcinoma COLO-205 cells [26], and human breast cancer MDA-MB-231 cells [25]. In addition, previous studies have shown that ZJW can inhibit the expression of inflammatory mediators [27] and modulate the monoaminergic neurotransmitter system [28] and catecholamine secretion [22]. These results indicated that the effects of ZJW may be involved in the induction of cancer cell apoptosis and the adjustment of the nerve, endocrine, and immune systems.

In conclusion, the present study is aiming to establish a 4T1 mouse breast cancer ZHENG model and investigate the antitumor effects of the herbal formula, ZJW. Our study has established a mouse breast cancer ZHENG model and showed that ZJW suppresses tumor growth and improves the quality of life through reducing ZHENG score, improving the kidney and liver functions and without obvious side effects in the 4T1 LFISS mice. The results indicated that ZJW may be useful as alternative treatment for breast cancer. However, further research is needed to investigate the mechanisms of ZJW efficacy and safety.

## Conflict of Interests

All authors declared that there is no conflict of interests.

## Authors' Contribution

Jia Du and Yang Sun equally contributed to this research.

## Acknowledgments

This study was supported by the National Natural Science Foundation (81073134), "085" First-Class Discipline

Construction Innovation Science and Technology Support Project of Shanghai University of TCM (085ZY1206) and the E-institutes of Shanghai Municipal Education Commission (E 03008).

## References

[1] J. Ferlay, H. R. Shin, F. Bray et al., *GLOBOCAN, 2008 V1. 2, Cancer Incidence and Mortality Worldwide: IARC Cancer Base No. 10 [Internet]*, International Agency for Research on Cancer, Lyon, France, 2010, http://globocan.iarc.fr/.

[2] L. Yang, L. Li, Y. Chen, and D. M. Parkin, "Cancer incidence and mortality estimates and prediction for year 2000 and 2005 in China," *Chinese Journal of Health Statistics*, vol. 22, no. 4, pp. 218–222, 2005.

[3] Y. He, X. Zheng, C. Sit et al., "Using association rules mining to explore pattern of Chinese medicinal formulae (prescription) in treating and preventing breast cancer recurrence and metastasis," *Journal of Translational Medicine*, vol. 10, supplement 1, p. S12, 2012.

[4] Z. Chen, L. Y. Chen, P. Wang et al., "Tumor microenvironment varies under different TCM ZHENG models and correlates with treatment response to herbal medicine," *Evidence-Based Complementary and Alternative Medicine*, vol. 2012, Article ID 635702, 10 pages, 2012.

[5] Q. F. Tang, X. Liu, Y. Ge et al., "Experimental study on inhibiting proliferation and inducing apoptosis of zuo jin wan alcohol extracts on human gastric cancer cells infected by Helicobacter pylori," *Chongqing Medicine*, vol. 41, no. 15, pp. 1462–1464, 2012.

[6] D. C. Chao, L. J. Lin, S. T. Kao et al., "Inhibitory effects of Zuo-Jin-Wan and its alkaloidal ingredients on activator protein 1, nuclear factor-$\kappa$B, and cellular transformation in HepG2 cells," *Fitoterapia*, vol. 82, no. 4, pp. 696–703, 2011.

[7] H. Sui, X. Liu, B. H. Jin et al., "Zuo Jin Wan, a traditional Chinese herbal formula, reverses P-gp-mediated MDR in vitro and in vivo," *Evidence-Based Complementary and Alternative Medicine*, vol. 2013, Article ID 957078, 13 pages, 2013.

[8] Xu, Y. Qi, L. Lv et al., "In vitro anti-proliferative effects of Zuojinwan on eight kinds of human cancer cell lines," *Cytotechnology*, 2013.

[9] Z. Q. Fang, Z. Q. Pan, and W. L. Xu, "Methodology and purposes of establishing mouse and rat models for syndrome differentiation and treatment," *Zhong Xi Yi Jie He Xue Bao*, vol. 7, no. 10, pp. 907–912, 2009.

[10] X. Zheng, *Guideline for Clinical New Drug Research in Chinese Herbal Medicine*, vol. 5, Chinese Medical Science and Technology Press, Beijing, China, 2002.

[11] Y. N. Song, J. J. Sun, Y. Y. Lu et al., "Therapeutic efficacy of Fuzheng-Huayu tablet based traditional Chinese medicine syndrome differentiation on hepatitis-B-caused cirrhosis: a multicenter double-blind randomized controlled trail," *Evidence-Based Complementary and Alternative Medicine*, vol. 2013, Article ID 709305, 8 pages, 2013.

[12] S. B. Su, "Recent advance in ZHENG differentiation research in traditional Chinese medicine," *International Journal of Integrative Medicine*, vol. 1, no. 7, p. 2013, 2013.

[13] C. Chai, J. Kou, D. Zhu et al., "Mice exposed to chronic intermittent hypoxia simulate clinical features of deficiency of both Qi and Yin syndrome in traditional Chinese medicine," *Evidence-Based Complementary and Alternative Medicine*, vol. 2011, Article ID 356252, 7 pages, 2011.

[14] H. Y. Dai, P. Wang, L. Feng et al., "The molecular mechanisms of traditional Chinese medicine ZHENG syndromes on pancreatic tumor growth," *Integrative Cancer Therapies*, vol. 9, no. 3, pp. 291–297, 2010.

[15] R. P. Miller, R. K. Tadagavadi, G. Ramesh, and W. B. Reeves, "Mechanisms of cisplatin nephrotoxicity," *Toxins*, vol. 2, no. 11, pp. 2490–2518, 2010.

[16] T. Boulikas, "Clinical overview on LipoplatinŮ: a successful liposomal formulation of cisplatin," *Expert Opinion on Investigational Drugs*, vol. 18, no. 8, pp. 1197–1218, 2009.

[17] S. R. McWhinney, R. M. Goldberg, and H. L. McLeod, "Platinum neurotoxicity pharmacogenetics," *Molecular Cancer Therapeutics*, vol. 8, no. 1, pp. 10–16, 2009.

[18] I. Cohen, M. Tagliaferri, and D. Tripathy, "Traditional Chinese medicine in the treatment of breast cancer," *Seminars in Oncology*, vol. 29, no. 6, pp. 563–574, 2002.

[19] A. K. Mukherjee, S. Basu, N. Sarkar, and A. C. Ghosh, "Advances in cancer therapy with plant based natural products," *Current Medicinal Chemistry*, vol. 8, no. 12, pp. 1467–1486, 2001.

[20] W. L. Hsiao and L. Liu, "The role of traditional Chinese herbal medicines in cancer therapy from TCM theory to mechanistic insights," *Planta Medica*, vol. 76, no. 11, pp. 1118–1131, 2010.

[21] X. F. Wang, J. Du, T. L. Zhang et al., "Inhibitory effects of PC-SPESII herbal extract on human breast cancer metastasis," *Evidence-Based Complementary and Alternative Medicine*, vol. 2013, Article ID 894386, 11 pages, 2013.

[22] F.-R. Zhao, H.-P. Mao, H. Zhang et al., "Antagonistic effects of two herbs in Zuojin Wan, a traditional Chinese medicine formula, on catecholamine secretion in bovine adrenal medullary cells," *Phytomedicine*, vol. 17, no. 8-9, pp. 659–668, 2010.

[23] X. Wang, L. Xu, J. Peng, K. Liu, L. Zhang, and Y. Zhang, "In vivo inhibition of s180 tumors by the synergistic effect of the chinese medicinal herbs coptis chinensis and evodia rutaecarpa," *Planta Medica*, vol. 75, no. 11, pp. 1215–1220, 2009.

[24] X. N. Wang, X. Han, L.-N. Xu et al., "Enhancement of apoptosis of human hepatocellular carcinoma SMMC-7721 cells through synergy of berberine and evodiamine," *Phytomedicine*, vol. 15, no. 12, pp. 1062–1068, 2008.

[25] J. Yang, L. Wu, S. Tashino, S. Onodera, and T. Ikejima, "Critical roles of reactive oxygen species in mitochondrial permeability transition in mediating evodiamine-induced human melanoma A375-S2 cell apoptosis," *Free Radical Research*, vol. 41, no. 10, pp. 1099–1108, 2007.

[26] Z. G. Yang, A. Q. Chen, and B. Liu, "Antiproliferation and apoptosis induced by evodiamine in human colorectal carcinoma cells (COLO-205)," *Chemistry and Biodiversity*, vol. 6, no. 6, pp. 924–933, 2009.

[27] Q. Wang, Y. Cui, T. Dong, X. Zhang, and K. Lin, "Ethanol extract from a Chinese herbal formula, "zuojin Pill", inhibit the expression of inflammatory mediators in lipopolysaccharide- stimulated RAW 264.7 mouse macrophages," *Journal of Ethnopharmacology*, vol. 141, no. 1, pp. 377–385, 2012.

[28] Q. S. Wang, S. L. Ding, and H. P. Mao, "Antidepressant-like effect of ethanol extract from Zuojin Pill, containing two herbal drugs of Rhizoma Coptidis and Fructus Evodiae, is explained by modulating the monoaminergic neurotransmitter system in mice," *Journal of Ethnopharmacology*, vol. 148, no. 2, pp. 603–609, 2013.

Hindawi Publishing Corporation
Evidence-Based Complementary and Alternative Medicine
Volume 2013, Article ID 956967, 10 pages
http://dx.doi.org/10.1155/2013/956967

*Review Article*

# Understanding Acupuncture Based on ZHENG Classification from System Perspective

**Junwei Fang, Ningning Zheng, Yang Wang, Huijuan Cao, Shujun Sun, Jianye Dai, Qianhua Li, and Yongyu Zhang**

*Center for Traditional Chinese Medicine and Systems Biology,*
*Shanghai University of Traditional Chinese Medicine, Shanghai 201203, China*

Correspondence should be addressed to Yongyu Zhang; dryyz@sina.com

Received 30 July 2013; Revised 24 September 2013; Accepted 14 October 2013

Academic Editor: Shi-bing Su



Acupuncture is an efficient therapy method originated in ancient China, the study of which based on ZHENG classification is a systematic research on understanding its complexity. The system perspective is contributed to understand the essence of phenomena, and, as the coming of the system biology era, broader technology platforms such as omics technologies were established for the objective study of traditional chinese medicine (TCM). Omics technologies could dynamically determine molecular components of various levels, which could achieve a systematic understanding of acupuncture by finding out the relationships of various response parts. After reviewing the literature of acupuncture studied by omics approaches, the following points were found. Firstly, with the help of omics approaches, acupuncture was found to be able to treat diseases by regulating the neuroendocrine immune (NEI) network and the change of which could reflect the global effect of acupuncture. Secondly, the global effect of acupuncture could reflect ZHENG information at certain structure and function levels, which might reveal the mechanism of Meridian and Acupoint Specificity. Furthermore, based on comprehensive ZHENG classification, omics researches could help us understand the action characteristics of acupoints and the molecular mechanisms of their synergistic effect.

## 1. Introduction

Acupuncture is an efficient therapy method that originated in ancient China. It uses thin metal needles to pierce through skin into acupoints to regulate the flow of Qi around the whole body, and its effect is validated primarily by the evidence of its beneficial practice while the mechanism awaits understanding. Acupuncture effect is complicated, which is determined by the complexity of human body and disease and is manifested by the properties that acupuncture acting factors possess multielement, multilevel, and nonlinearity [1]. But one of the problems in acupuncture research is how to study the action mechanism of acupuncture and evaluate its efficacy at molecular level based on scientific methods under the guidance of TCM theory. Reductionism study is unable to embody the integration and complexity of acupuncture effect; therefore, it is limited to reveal the rule of acupuncture effect without the guidance of systems theory.

As the most important part of TCM, acupuncture develops its therapeutic effect by stimulating acupoints, which could form a complex regulating network system through the flowing and changing of energy and information in meridians and collaterals [2]. The study of acupuncture should be based on the understanding of the complexity in TCM. ZHENG classification (also referred to as syndrome differentiation) is the essence of TCM which attaches importance to various factors, at the same time it emphasizes on the interaction and relation in integration, which is confronted with nonlinear phenomenon [3, 4]. The acupuncture research based on ZHENG classification is the systematic research which is under the guidance of TCM theory and could bring the complexity of acupuncture effect to light, so the acupuncture research on the foundation of ZHENG classification should be taken as the breakthrough point to reveal the acupuncture mechanism and its efficacy.

ZHENG is the specific pattern to identify disease and is the essence of ZHENG classification and treatment (Bianzheng lunzhi) in TCM [5], Sun et al. [6] use metabonomic methods to differentiate ZHENG types and evaluate the therapeutic efficiency of Fuzhenghuayu tablet in hepatitis-B-caused cirrhosis. The efficiency of FZHY treatment based on ZHENG differentiation indicated that accurately ZHENG differentiating could guide the appropriate TCM treatment in HBC. ZHENG is a relational model of dysfunctions in whole which is produced by logical reasoning based on practical experiences [7], and the nature of ZHENG may be the substances imbalance of multisystem and multilevel in spatiotemporal distribution and relation combination [8]. The idea of system biology is comprehensive, integrated, and global, which is in correspondence with the holistic and systemic approaches of TCM. As the coming of the system biology era, the system perspective provides us an important approach to understand the essence of phenomenon [9], and broader technology platforms were established for the objective study of TCM. Omics technologies could dynamically determine molecular components of various levels and creates the feasible conditions to explore the material basis of ZHENG. Lu et al. [10, 11] used genechip analytical techniques to distinguish between cold syndrome and heat syndrome of female rheumatoid arthritis (RA) patients; the results showed that the genes referred with cold or heat ZHENG were different from those genes with RA and further suggested that ZHENG in TCM has solid foundation in gene profile. Liu et al. [12] used proteomics technology to get the preliminary evidence in functional protein level that the transfer of phlegm and blood stasis syndrome is mainly from phlegm syndrome to blood stasis syndrome and ultimately formed phlegm accumulating with stagnation syndrome. In omics researches of ZHENG, system models have been used to analyze the interrelation between various factors in the whole. Xu et al. [13] explored a strategy of classifying five TCM syndromes in diabetes based on plasma fatty acid metabolic profiles, lipid metabolism indicators, and chemometrics methods. Compared with orthogonal signal correction-partial least squares (OSC-PLS) method, better clustering results were demonstrated with the application of the uncorrelated linear discriminant analysis (ULDA), a new method which was used to analyze the various factors in a joint way. By finding out the relationship between various response parts, omics researches can show us a systematic understanding of the microenvironment, based on the results of genomics research and literature data mining. Li et al. [14] successfully established a heat and cold ZHENG model.

Omics provides integral, systemic, and dynamic technology platforms for the study of TCM, the study by which has effectively revealed the essence and connotation of TCM phenomena such as ZHENG at molecular level. In the study of acupuncture, omics researches are helpful to understand the entire effect of acupuncture; moreover, based on ZHENG classification, holistic study can investigate the action characteristics of acupoints and the molecular mechanism of their synergistic effect under the guidance of TCM theory. So the present paper reviewed the omics researches of acupuncture. We hope that the review will help to understand the entire effect of acupuncture and the special effects of meridians and acupoints with combining the theory of TCM and help promote acupuncture to be more properly used clinically.

## 2. Omics Researches of Acupuncture Based on the Cognition of Diseases

Acupuncture stimulation could cause synchronous changes of body systems [1]. If we ignore the relation of the body systems and study the action mechanisms of acupuncture separately, we may offend against the view of holism and overlook the effective links. While the development of omics and bioinformation analysis technologies provide a global, systematical, and dynamic technology platform for TCM research, by dynamically detecting molecular components of various levels, omics researches of acupuncture can show us the entire effect of acupuncture.

*2.1. Entire Effect of Acupuncture.* Meridian is the "channel" which runs Qi and Xue (the theory of blood in TCM) and connects Zangfu (the viscera in TCM), body surface, and other parts of human body, regulating the body function. When a single acupoint in the "channel" is stimulated by acupuncture, an entire effect would be produced through the interactions during the transmit process of meridian Qi and pathopoeia factors [1]. As a global approach and a primary method of investigating biological phenotypes, omics could be utilized to explore the mechanism of acupuncture from the perspective of effect by revealing the overall alterations of molecular after stimulating on certain acupoints.

The omics researches on acupuncture are based on the researchers' understanding of diseases. On the basis of different disease knowledge and study purposes, various samples and omics methods are selected. Different omics researches reflect the integral cognition for study subjects from different aspects. Due to the variety of sample resources and omics methods, the conclusion of mechanism study on the same disease may differ.

*2.1.1. Researches by Different Omics Approaches.* Genomics, proteomics, and metabolomics had been applied in the study of acupuncture. The microarrays of either cDNA or oligonucleotide probes were used to screen for potential candidate genes to mediate acupuncture responses. The proteomic technologies of two-dimensional electrophoresis (2-DE) and mass spectrum (MS) analysis have been extensively used in acupuncture studies. Metabolic analysis has to deal with a highly diverse range of biomolecules which is different from genome and proteome analysis; recent advances in the two analytical platforms of mass spectrometry (MS) and nuclear magnetic resonance (NMR) spectroscopy have driven forward the discipline of metabolomics, but every platform covers only part of metabolomic [15]. In order to make metabolomic analysis to be a comprehensive research method as the genomic and proteomic assays, a community effort is required to develop the tools and databases and provide integration of these different tools and databases [16].

In a study reported by Gao et al. [17] the pain relieving effect of acupuncture may be mediated by endogenous opioid peptides in central nervous system. Sung et al. [18] analyzed the protein expression profile in hypothalamus by two-dimensional electrophoresis, which is different from the result of genomics research by Gao et al. Proteomics evidence indicated that the mechanism of analgesia by needling Zusanli was associated with inflammation, enzyme metabolism, and signal transduction.

The researches indicated that experimental results based on high-flux omics studies may be false positive or false negative unavoidably, thus impacting further researches on acupuncture. In addition, it is still difficult to analyze the variance results of different samples and different omics methods and to systematically integrate these results. On the basis of omics studies, creating system models which could be driven by clinical data would help us to better understand the molecular mechanism integrally [19].

*2.1.2. Researches with Different Sample Sources.* In the genomics study on the treatment effect of acupuncturing on GB34 (Yanglingquan) and LR3 (Taichong) with 1-methyl-4-phenyl-1,2,3,6-tetrahydropyridine (MPTP) induced Parkinson's disease animal models, Choi et al. analyzed the genetic changes in spinal cord [20] and Corpus Striatum [21] before and after acupuncture treatment based on gene chips technology and validate the results by reverse transcription-polymerase chain reaction (RT-PCR). It was proved that beneficial regulation on genes was developed by acupuncture, which showed their treatment effect by protecting nerves and inhibiting degradation of Corpus Striatum, respectively.

In a genomic study [22] on the pain relieving effect of electroacupuncture on Zusanli, the RNA changes in spinal nerves before and after acupuncture treatment were analyzed based on cDNA microarray technology. Signal transduction, gene expression, and an algesia pathway regulation were involved in the mechanism, which is different from the research by Gao et al. [17].

The effect of acupuncturing on specific acupoints is not only related to diseases but also to body conditions. In the genomics study [23] about acupuncture treatment on allergic coryza, gene expression profile in respect of positive/negative Phadiatop (Ph) test reaction [Ph(+) and Ph(−)] was analyzed before and after acupuncture treatment. Distinct physiological responses in Ph(+) and Ph(−) groups could be differentiated in the profiles. Another study [24] on the pain relieving effect of acupuncturing on the Hegu based on Genomics also indicated that individual differences of the pain relieving effect existed when specific acupoints were stimulated, and these differences were related to inheritance. The function of human body is mobilized fully to prevent and cure diseases by stimulating acupoints in the therapy of acupuncture, as the complexity of human body and disease determined the complexity of the acupuncture efficacy, analyzing the connections between effectors molecules and integrating that the omics results are the foundation of holistic understanding and evaluating acupuncture effect.

Omics studies on the acupuncture effects on Parkinson's disease [21, 22, 25, 26], rhinitis [24, 27], osteoarthritis [28], spinal injury [29, 30], pain [18, 19, 23, 25], aging [31, 32], ischemia (ischemic stroke) [33, 34], parturition [35] functional dyspepsia [36, 37], and so forth indicated that the mechanism of acupuncture is involved in the regulation of many body systems and is mainly associated with NEI system (Figure 1). The nerve, endocrine, and immune systems are distributed over the body widely. What is more, the three systems can regulate mutually through the common information molecules and receptors; thus the complex regulation network is formed and the other body systems are regulated. The body defense, growth, and development are regulated by the complex system (Figure 1(a)). Acupuncture may treat diseases by regulating the NEI network and then develop effects such as anti-inflammation, neuroprotection, and antioxidative stress (Figure 1(b)). Needling specific acupoints, the change of NEI network can reflect acupuncture effect systematically.

*2.2. Special Effect of Meridian and Acupoint.* Treatment by stimulating acupoints is the key point to distinguish acupuncture treatment from other therapies, and the special structure and function of the acupoints are the efficiency basis of acupuncture therapy. Wu et al. [37, 38] investigated the effects of acupuncture at Yangming meridian points and other meridian points using plasma and urine metabonomics approach based on $^1$H NMR and analyzed whether Yangming meridian points have common or different metabolic characteristics from other meridian points by pattern recognition. This study suggested that Yangming meridian points have different characteristics from those of both Yanglingquan and Weizhong.

The treatment rules of acupuncture are very complicated but regular, which mainly depend on acupoints location, meridians attribution, and category [38]. The manifestations of acupoints specificity are diversified and compared with other specificities such as anatomy; efficiency specificity has more practical value and is more coincident with clinical requirements, which is regarded as the breakthrough point of acupoints specificity research. Omics researches show the global effect of acupuncture which possesses relative specificity; that is, needling different acupoints could treat the same disease and different diseases could be treated by needling the same acupoints.

*2.2.1. Same Acupoints for Different Diseases.* Needling a specific acupoint could develop a widely biological effect; in the omics study of acupuncture, needling Zusanli could develop the effects such as immunity regulating [36, 39], pain relieving [18, 19, 23], and anti-inflammation [40], thus treating many diseases and developing more effects by synergy of other acupoints. While in TCM, the major effects by needling Zusanli are germinating Wei (the theory of stomach in TCM) Qi and drying Pi (the theory of spleen in TCM) dampness.

Omics researches showed that acupuncture could treat diseases by regulating the NEI network, and the information molecules and their receptors shared by nervous, endocrine, and immune systems were associated with the occurrence and development of several diseases. Li et al. [14] found that

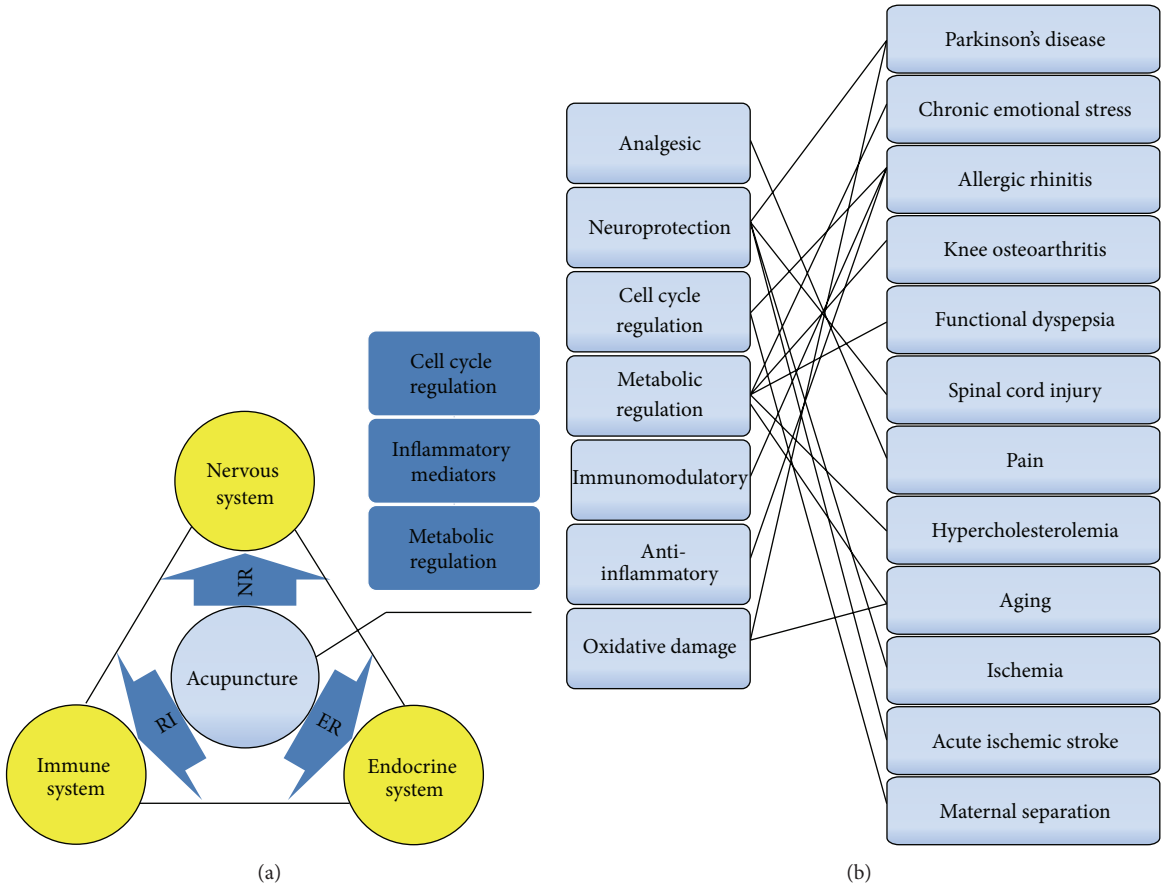


Figure 1: The entire effect of acupuncture is associated with the regulation of NEI which plays an extensive role in disease treatment. The nerve, endocrine, and immune systems are distributed over the body widely and the three systems can regulate mutually; thus the complex regulation network is formed and the other body systems are regulated. The body defense, growth, and development are regulated by the complex system (a). Acupuncture may treat diseases by regulating the NEI network and then develop effects such as anti-inflammation, neuroprotection, and antioxidative stress in disease treatment (b). Needling specific acupoints, the change of NEI network can reflect acupuncture effect systematically.

heat and cold ZHENG were associated with the disorder of different NEI regulation models, which were able to respond to different TCM ZHENGs. Based on NEI network, they successfully establish heat and cold ZHENG model. Needling specific acupoints could treat several different diseases, from which the entire effect of acupuncture may be consistent with the regulation of certain TCM ZHENGs.

*2.2.2. Same Disease with Different Acupoints.* Functional dyspepsia (FD) is a set of common symptoms including abdominal pain or discomfort. A plasma metabolomics research based on $^{1}$H NMR technology was designed to investigate the metabolic difference between FD patients and healthy volunteers, and a series of differential metabolites were sought out [41, 42] (Figure 2(b)). The pathway analysis indicated that FD was related to some disorders in energy metabolism and especially with the NEI dysfunction (Figure 2(c)). And the corresponding ZHENGs of FD were mainly regarded as Pi-Wei weakness or Gan (the theory of liver in TCM) depression and Pi deficiency [43] (Figure 2(d)).

When the Wei and its Back-Shu and Front-Mu points [42] as well as the specific acupoints of Yang-mingjing were needled [43], both of them had beneficial and regulative effects on the metabolites associated with FD. And the regulative intensity was greater and the range was wider compared with that of the nonacupoints. Moreover, the longer the treatment time of acupuncture was, the more obvious positive regulative effects it would have. Therefore both methods had therapeutic effect on FD. As disease is complex and the practitioners may treat disease from different angles, they may select different acupoints when treating disease. There were differential regulative effects on potential biomarkers and key metabolites of FD when the stomach and its Back-Shu and Front-Mu points as well as the specific acupoints of Yang-mingjing were needled, so the regulative effects to FD-related NEI network were different; thus different point selection may make certain regulative effects on different TCM ZHENGs (Figure 2). The location of FD in TCM is in Pi and Wei, and the main therapeutic effects by needling the back shu points and the front mu points are in diseases of Zangfu.

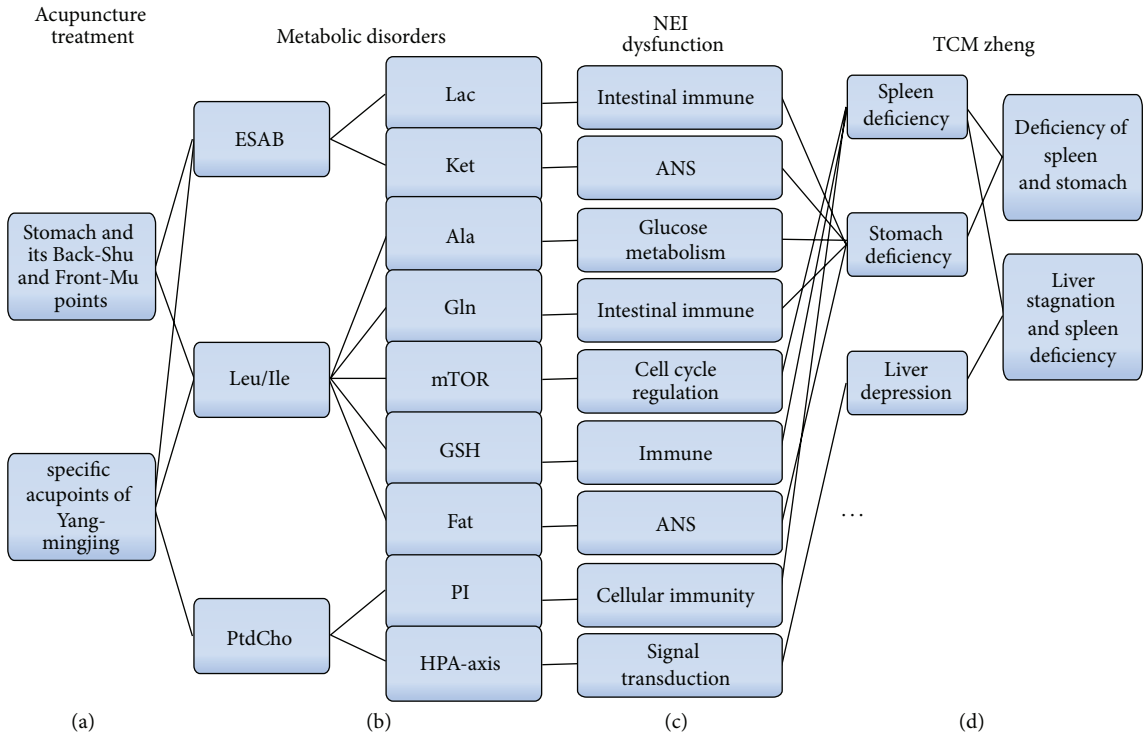


Figure 2: Special effect of meridian and acupoint. A plasma metabolomics investigation was designed to investigate the metabolic difference between FD patients and healthy volunteers, and a series of differential metabolites were sought out (b). The pathway analysis indicated that FD is related to some disorders in energy metabolism and especially to the NEI dysfunction (c) and the corresponding ZHENGs of FD are mainly regarded as Pi-Wei weakness or Gan depression and Pi deficiency (d). When the Wei and its Back-Shu and Front-Mu points as well as the specific acupoints of Yang-mingjing were needled, both of them have beneficial regulative effects on the metabolites associated with FD (a). The corresponding changes of NEI network reflect that different points selection methods may have certain regulative effects on different TCM ZHENGs, which might be the mechanism of Meridian Specificity.

The $^{1}$H NMR metabolomics studies of FD with acupuncture treatment showed that needling the acupoints could regulate Qi, Xue, yin, and yang of the Zangfu, helping to restore normal physiological function of Zangfu. Acupuncture with selecting acupoints along meridians is the most important point selection method in the treatment of FD [44]. Meridians and collaterals are the channels of transporting the Qi and Xue, contacting Zangfu and body surface as well as all parts of the body, and it is the regulatory system of body function. When the specific acupoints of Yang-mingjing were needled, the treatment effect of selected acupoints along meridians was a whole regulation which was showed by $^{1}$H NMR metabolomics studies of FD. The stimulations acted on acupoints, and the acupoints were connected with meridians, so Yin and Yang, deficiency, and excess could be regulated through restoring Qi-Xue transportation.

Biology molecular alterations before and after acupuncture intervention could reflect the ZHENG information at certain structure and function level, which embodies different ZHENG classification of acupuncture. ZHENG is a complicated nonlinear system which emphasizes the interaction and relation of various factors, and it could be described as a model with dysfunctional relationship. Clinical ZHENG will present different interfaces by observing the disease appearance with different methods and points of view, which is called different ZHENG classification of TCM [45]. Needling specific acupoints is guided by meridian theories which could beneficially regulate the corresponding biology molecular of TCM ZHENG from the level of disease location or pathogenesis, which might be the mechanism of Meridian Specificity.

The specificity rules of meridians and acupoints which are illustrated by researching are helpful to select acupoints for treatment in clinic and to make acupoints selection methods more in line with ZHENG classification.

## 3. Omics Researches of Acupuncture Based on ZHENG Classification

ZHENG classification of acupuncture reflects the comprehensive and systematic understanding of disease. It is the theoretical basis of guiding acupoints selection, improving the clinical efficacy as well as studying the acupuncture. Omics researches of acupuncture based on clinical ZHENG classification could reveal the effect mechanism of acupuncture at molecular level integrally by ignoring the anatomic location of specific tissues and organs. By analyzing the connections among the ZHENG relevant biological molecules in the omics studies, biology network models had been established

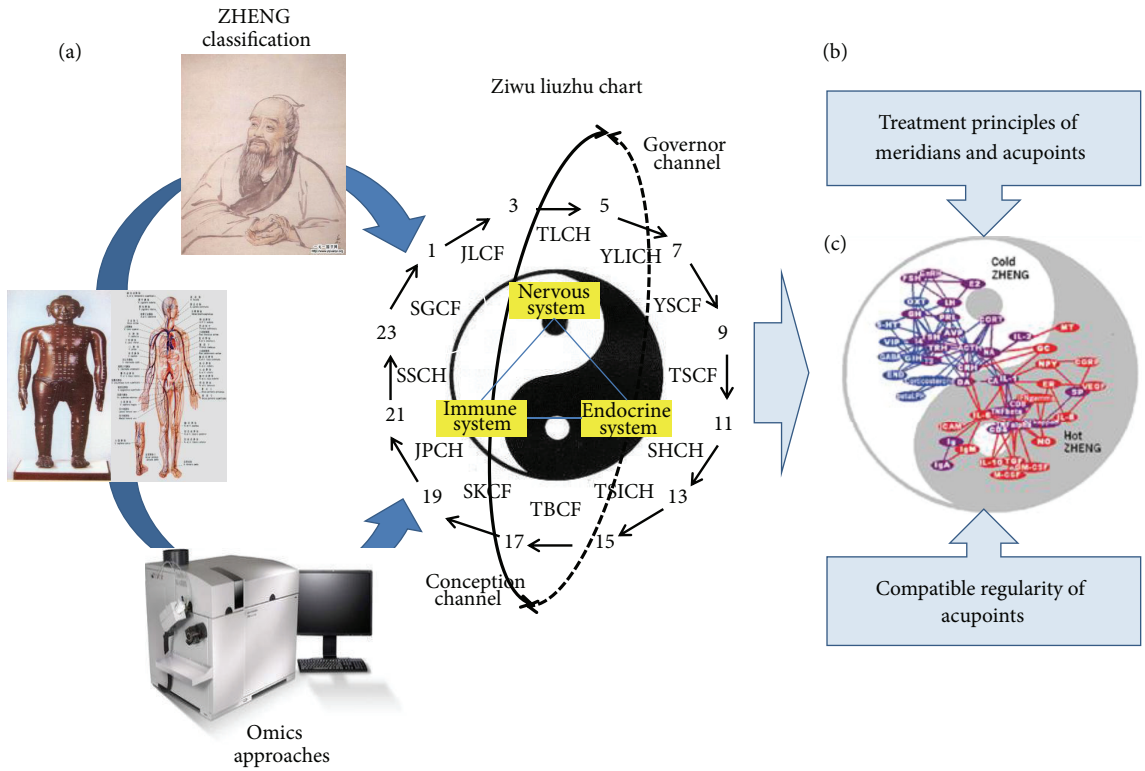


Figure 3: Understanding acupuncture with omics researches based on ZHENG classification. The omics researches of acupuncture based on ZHENG classification are the systematic research which are under the guidance of TCM theory and could bring the complexity of acupuncture effect and theory to light (a). By analyzing the connections among the ZHENG-related biological molecules in the omics studies of acupuncture, biology network models had been established for the further study of ZHENG. Studying the structure changes of biology network models would help us understand the action characteristics of acupoints and the molecular mechanism of their synergistic effect (b). (c) cited from [14].

for the further study of ZHENG. Researching and analyzing the structure changes of biology network models, it would make objective evaluation for health status, ZHENG changes and treatment efficacy and it will help us understand the action characteristics of acupoints and the molecular mechanism of their synergistic effect (Figure 3).

*3.1. Treatment Principles of Meridian and Acupoint.* In the imparting and inheriting history of acupuncture, a theoretical system of ZHENG classification and treatment with its own characteristics which guide the diagnosis and treatment of acupuncture comprehensively and systematically was formed. Meridian theory is the key of the theory of acupuncture. It is the ZHENG classification according to meridian theories that clinical acupuncture ZHENG classification takes as the "main body," ZHENG classification according to location as the "key," ZHENG classification according to eight principles as the "guidance," and ZHENG classification according to visceral theory as the "supplement" [46]. Omics researches based on different ZHENG classification can reflect the features and functions of acupoints in disease treatment.

Osteoarthritis (OA) belongs to "bone impediment" in TCM whose characteristics are deficiency in origin and excess in superficiality. According to the pathological sites of OA, by topical ZHENG classification, left and right Xiyan which is near knee joint were selected as treatment acupoints. Changes in gene expression of patients who were response to warm acupuncture before and after treatment were analyzed by gene chip technology; the result showed that genes related to inflammation were changed, which may be the direct treatment effect of needling left and right Xiyan in improving the relevant symptoms of OA [47].

Kidney-yang is the foundation of yang Qi. Kidney-yang deficiency is very common in clinic which mainly manifests as deficiency and cold of the whole body. According to the theory of TCM, the kidney masters the bones which has close relationship with the pathogenesis of OA. Previous studies also showed that kidney-yang deficiency was the highest incidence of TCM ZHENG pattern in OA [48]. With the analysis of etiology and pathogenesis of kidney-yang deficiency pattern by viscera ZHENG classification, the acupoints of Guanyuan and Qihai as well as warm needling method were selected to treat OA. Shen [49] thought that kidney-yang deficiency pattern was an overall performance of multisystems and organs dysfunction which are mainly related to the dysfunction of nervous system, endocrine system, and immune system.

Ding et al. and Yang et al. [50, 51] found that signal transduction abnormalities among cells may play a key role

in the development and progression of OA with kidney-yang deficiency. Various common signal molecules and receptors in nervous, endocrinology, and immune system are the molecule structure basis of NEI network. Genomics research about OA with deficiency cold by warm acupuncture treatment demonstrated that the genes of signal transduction were significantly expressed [47]. Taking Guanyuan, Qihai, and Zusanli as master points, traditional warm needling technique could stimulate Yang Qi of kidney and recover the physiological function of kidney by regulating NEI network so that the meridians are dredged and the symptoms of OA could be improved.

Quadriceps atrophy is caused by knee pain and joint dysfunction and vice versa. The Wei meridians being circulated through quadriceps, Yang-mingjing is rich in Qi and Xue; it nourishes the ancestral sinew [52]. Deficiency of Qi and Xue could lead to emptiness of meridians, which could be the reason of osteoarthritis. Based on the meridian differentiation, Zusanli was selected as the treatment acupoint. The modern research showed that Pi and Wei in TCM are closely related to immune theory in modern medicine [53]. The researches of genome [29, 53] showed that the pathogenesis of osteoarthritis are involved in abnormal expression of immune-related genes. Further studies conducted by Yang et al. [51, 54] showed that osteoarthritis belonging to Kidney-Yang deficiency is involved in 13 immune-related gene expression abnormalities. Needling Zusanli could induct or repress the expression of immune-related genes in order to restore the physiological function of Wei meridian of Foot-Yangming, which could develop the therapeutic effect on osteoarthritis by playing a regulative role in enriching the Qi, Xue, and meridians to make the therapeutic effect on OA.

By improving corresponding symptoms, different point selection methods have a direct or indirect therapeutic effect on disease treatment, taking a temporary solution and effecting a permanent cure.

*3.2. Compatible Regularity of Acupoints.* Different methods of ZHENG classification are overlapping at some extent in the clinical use of acupuncture while each method has its own merit and characteristic, so different ZHENG classification methods are irreplaceable in clinic [55]. By integrating data of omics researches guided by systems theory of ZHENG, it would help us understand the molecular mechanisms of acupoints compatibility.

Genomics research showed that the mechanism of warm acupuncture treatment for OA with Kidney-Yang Deficiency may be related to the recovery of energy metabolism, inflammation, immune function, and signaling systems. Among them, the therapeutic effect of needling the left and right Xiyan and Yanglingquan may associate with the regulation of inflammation and immune-related genes. Needling Qihai and Guanyuan with the method of traditional warm acupuncture could beneficially regulate the metabolic changes of OA by affecting the NEI network. While the normal function of NEI network is dependent on the regular of synthesis, secretion and transport of the whole system, TCM theory holds that the transport and transformation of various substances in the body depend on the normal Pihealth movement. Thus, the warming acupuncture on Zusanli could enhance the overall regulative effect.

Acupuncture treatment is reasonably compatible according to the action laws of acupoints based on the comprehensive ZHENG classification. Acupuncture genomics studies showed that characterized acupoints which develop specific regulative effect on disease-related NEI network may form a new system through the interrelating and interacting of the network to treat diseases integrally.

## 4. Summary and Prospect

The effects of acupuncture are complex and it is unilateral to explore the mechanism of acupuncture in accordance with reductionism at the molecular levels due to the limitation of science. However, as the development of science, the essence of acupuncture may be uncovered at atom or electron levels [56]. At the molecular levels, omics researches of acupuncture based on ZHENG classification provided a wealth of information such as molecular structure information for the further systemic study of acupuncture.

Clinical ZHENG is a complex and nonlinear system which is consistent with the complicated and various properties of disease. While it is too complex for data processing which limits the further study of the ZHENG quantization and mechanism, and even through omics experiments, only small subsets of ZHENG correlated variables could be observed and most variables are still hidden which must be defined by computing [57], while the relative deficiency of data processing makes the omics data not easily be fully interpreted [58]. Therefore, in the omics researches of acupuncture based on ZHENG classification, we must decompose the ZHENG legitimately according to its property for further study [59].

With the application of bioinformatics and other science technologies, biological networks which connect and interact with each other should be established on the foundations of genomics, proteomics, and metabolomics in acupuncture study. With the researches on the relationship between different ZHENG classifications and the spatiotemporal distribution rule of nonspecific substances based on biological networks, the combination of omics technologies and different ZHENG classification will be truly achieved, and the molecular mechanism of the acupuncture will be understood in system levels.

TCM can be regarded as traditional systems biology, and it is more important to discover the behavior of the system compared with the understanding of the structure of biological systems. System biology introduced the concept of perturbation as an artificial tool to control the state [60]. Under the artificial controlled state, dynamic characteristics of specific life system in different conditions and different times are studied. The integrated effect of acupuncture treatment is actually one of the manifestations of systems biology perturbation which is based on the endogenous substances, and as acupuncture is an important part of TCM, the omic

study of acupuncture based on ZHENG classification has certain guidance and reference for the study and development of systems biology.

## Abbreviations

Ala: Alanine
CNS: Central nervous system
ER: Endocrine regulation
ESAB: Energy supply and application bottleneck
Gln: Glutamine
GSH: Glutathione
HPA: Hypothalamic pituitary adrenal
Ile: Isoleucine
IR: Immune regulation
JLCF: Jueyin liver channel of foot
JPCH: Jueyin pericardium channel of hand
Ket: Ketone body
Lac: Lactate
Leu: Leucine
mTOR: Mammalian target of rapamycin
NR: Neuroregulation
Ph: Phadiatop
PI: Phosphatidylinositol
Pro: Proline
PtdCho: Phosphatidylcholine
SGCF: Shaoyang gallbladder channel of foot
SHCH: Shaoyin heart channel of hand
SKCF: Shaoyin kidney channel of foot
SSCH: Shaoyang Sanjiao channel of hand
TBCF: Taiyang bladder channel of foot
TLCH: Taiyin lung channel of hand
TSCF: Taiyin spleen channel of foot
TSICH: Taiyang small intestine channel of hand
YLICH: Yangming large intestine channel of hand
YSCF: Yangming stomach channel of foot.

## Conflict of Interests

The authors declared that they have no conflict of interests regarding this work. And they did not have a direct financial relation with the commercial identity mentioned in this paper.

## Authors' Contribution

Junwei Fang and Ningning Zheng contributed equally to this work and should be considered as cofirst authors.

## Acknowledgments

This paper was supported by Shanghai Interdisciplinary Cultivation Platform of Outstanding and Innovative Postgraduates and Shanghai "085" Science and Technology Innovation Supporting Project for Top-grade Discipline Construction.

## References

[1] T. T. Ma and F. R. Liang, "Acupuncture and its sophisticated effects," *World Science and Technology*, vol. 10, no. 2, pp. 42–45, 2008.

[2] Y. Tang, S. G. Yu, X. G. Liu, Y. Li, H. Y. Yin, and F. R. Liang, "Discussion on research methods and ideas of meridians and acupoints specificity," *Journal of Chengdu University of TCM*, vol. 30, no. 2, pp. 3–4, 2007.

[3] S. Li, Y. Y. Wang, L. Ji, and Y. D. Li, "A discussion and case study of complexities in Traditional Chinese Medicine," *Journal of System Simulation*, vol. 14, no. 11, pp. 1429–1403, 2002.

[4] S. Li and Q. C. Zhang, "A second study on the relationship between TCM Qi and entrop theory," *Journal of Beijing University of TCM*, vol. 20, no. 5, pp. 9–11, 1997.

[5] M. Zhang, "The influence of traditional culture on the formation of ZHENG theories in traditional Chinese medicine," *Henan Zhong Yi*, vol. 31, no. 8, pp. 839–840, 2011.

[6] S. J. Sun, J. Y. Dai, and W. Y. Wang, "Metabonomic evaluation of ZHENG differentiation and treatment by Fuzhenghuayu tablet in hepatitis-B-caused cirrhosis," *Evidence-Based Complementary and Alternative Medicine*, vol. 2012, Article ID 453503, 8 pages, 2012.

[7] C. J. Li, Z. D. Gong, and J. H. Yan, "Researches on the essence of TCM ZHENG from the perspective of ZHENG model," *Journal of Traditional Chinese Medicine*, vol. 52, no. 15, pp. 1267–1268, 2011.

[8] C. X. Li, "Discuss the essence of ZHENG," *Journal of Sichuan of Traditional TCM*, vol. 29, no. 7, pp. 36–38, 2011.

[9] C. Auffray, Z. Chen, and L. Hood, "Systems medicine: the future of medical genomics and healthcare," *Genome Medicine*, vol. 1, article 2, 2009.

[10] C. Lu, L. H. Zhao, C. Xiao et al., "Comparison of gene profile of peripheral CD4+ lymphocytes in rheumatoid arthritis," *Chinese Journal of Rheumatology*, vol. 10, no. 7, pp. 438–439, 2006.

[11] C. Lu, C. Xiao, L. H. Zhao et al., "Comparison of gene profile of peripheral CD4+ lymphocytes in rheumatoid arthritis with cold and heat syndrome," *Chinese Journal of Basic Medicine in Traditional Chinese Medicine*, vol. 12, no. 2, pp. 130–133, 2006.

[12] J. L. Liu, J. N. Song, Y. Lei et al., "Differential plasma protein profiles in patients with hyperlipidemia & atherosclerosis of different patterns of phlegm-stasis syndrome," *Chinese Journal of Integrated Traditional and Western Medicine*, vol. 30, no. 5, pp. 482–487, 2010.

[13] W. J. Xu, L. X. Zhang, Y. H. Huang, Q. X. Yang, H. B. Xiao, and D. Q. Zhang, "Plasma fatty acid metabolic profiles for traditional Chinese medicine syndrome differentiation in diabetic patients using uncorrelated linear discriminant analysis," *Chinese Journal of Chromatography*, vol. 30, no. 9, pp. 864–869, 2012.

[14] S. Li, Z. Q. Zhang, L. J. Wu, X. G. Zhang, Y. D. Li, and Y. Y. Wang, "Understanding ZHENG in traditional Chinese medicine in the context of neuro-endocrine-immune network," *IET Systems Biology*, vol. 1, no. 1, pp. 51–60, 2007.

[15] C. Birkemeyer, A. Luedemann, C. Wagner, A. Erban, and J. Kopka, "Metabolome analysis: the potential of in vivo labeling with stable isotopes for metabolite profiling," *Trends in Biotechnology*, vol. 23, no. 1, pp. 28–33, 2005.

[16] W. B. Dunn, A. Erban, R. J. M. Weber et al., "Mass appeal: metabolite identification in mass spectrometry-focused untargeted metabolomics," *Metabolomics*, vol. 9, no. 1, pp. 44–66, 2013.

[17] Y.-Z. Gao, S.-Y. Guo, Q.-Z. Yin, T. Hisamitsu, and X.-H. Jiang, "An individual variation study of electroacupuncture analgesia in rats using microarray," *American Journal of Chinese Medicine*, vol. 35, no. 5, pp. 767–778, 2007.

[18] H. J. Sung, Y. S. Kim, I. S. Kim et al., "Proteomic analysis of differential protein expression in neuropathic pain and electroacupuncture treatment models," *Proteomics*, vol. 4, no. 9, pp. 2805–2813, 2004.

[19] Y. Y. Cai, Z. S. Liu, and B. Y. Liu, "Explore the issues of acupuncture research in clinical based on the result of systematic review," *Journal of Nanjing University of TCM*, vol. 26, no. 4, pp. 245–248, 2010.

[20] Y.-G. Choi, S. Yeo, Y.-M. Hong, and S. Lim, "Neuroprotective changes of striatal degeneration-related gene expression by acupuncture in an MPTP mouse model of Parkinsonism: microarray analysis," *Cellular and Molecular Neurobiology*, vol. 31, no. 3, pp. 377–391, 2011.

[21] Y.-G. Choi, S. Yeo, Y.-M. Hong, S.-H. Kim, and S. Lim, "Changes of gene expression profiles in the cervical spinal cord by acupuncture in an MPTP-intoxicated mouse model: microarray analysis," *Gene*, vol. 481, no. 1, pp. 7–16, 2011.

[22] J. Ko, S. N. Doe, H. L. Young et al., "cDNA microarray analysis of the differential gene expression in the neuropathic pain and electroacupuncture treatment models," *Journal of Biochemistry and Molecular Biology*, vol. 35, no. 4, pp. 420–427, 2002.

[23] H.-S. Shiue, Y.-S. Lee, C.-N. Tsai, Y.-M. Hsueh, J.-R. Sheu, and H.-H. Chang, "Gene expression profile of patients with phadiatop-positive and -negative allergic rhinitis treated with acupuncture," *Journal of Alternative and Complementary Medicine*, vol. 16, no. 1, pp. 59–68, 2010.

[24] Y. Chae, H.-J. Park, D.-H. Hahm, S.-H. Yi, and H. Lee, "Individual differences of acupuncture analgesia in humans using cDNA microarray," *Journal of Physiological Sciences*, vol. 56, no. 6, pp. 425–431, 2006.

[25] S.-T. Kim, W. Moon, Y. Chae, Y. J. Kim, H. Lee, and H.-J. Park, "The effect of electroaucpuncture for 1-methyl-4-phenyl-1,2,3,6-tetrahydropyridine-induced proteomic changes in the mouse striatum," *Journal of Physiological Sciences*, vol. 60, no. 1, pp. 27–34, 2010.

[26] S. Jeon, J. K. Youn, S.-T. Kim et al., "Proteomic analysis of the neuroprotective mechanisms of acupuncture treatment in a Parkinson's disease mouse model," *Proteomics*, vol. 8, no. 22, pp. 4822–4832, 2008.

[27] H.-S. Shiue, Y.-S. Lee, C.-N. Tsai, Y.-M. Hsueh, J.-R. Sheu, and H.-H. Chang, "DNA microarray analysis of the effect on inflammation in patients treated with acupuncture for allergic rhinitis," *Journal of Alternative and Complementary Medicine*, vol. 14, no. 6, pp. 689–698, 2008.

[28] C. Tan, J. Wang, W. Feng, W. Ding, and M. Wang, "Preliminary correlation between warm needling treatment for knee osteoarthritis of deficiency-cold syndrome and metabolic functional genes and pathways," *Journal of Acupuncture and Meridian Studies*, vol. 3, no. 3, pp. 173–180, 2010.

[29] X.-Y. Wang, X.-L. Li, S.-Q. Hong, Y.-B. Xi-Yang, and T.-H. Wang, "Electroacupuncture induced spinal plasticity is linked to multiple gene expressions in dorsal root deafferented rats," *Journal of Molecular Neuroscience*, vol. 37, no. 2, pp. 97–110, 2009.

[30] W.-J. Li, S.-Q. Pan, Y.-S. Zeng et al., "Identification of acupuncture-specific proteins in the process of electroacupuncture after spinal cord injury," *Neuroscience Research*, vol. 67, no. 4, pp. 307–316, 2010.

[31] X. Ding, J. Yu, T. Yu, Y. Fu, and J. Han, "Acupuncture regulates the aging-related changes in gene profile expression of the hippocampus in senescence-accelerated mouse (SAMP10)," *Neuroscience Letters*, vol. 399, no. 1-2, pp. 11–16, 2006.

[32] Y. Tang, L. L. Guo, and Q. Zhang, "Effect on electric acupuncture to $^{1}$H-NMR spectrogram of senescence accelerated mouse/prone8 kidney," *Journal of Chengdu University of TCM*, vol. 32, no. 2, pp. 1–4, 2009.

[33] J.-C. Guo, H.-M. Gao, J. Chen et al., "Modulation of the gene expression in the protective effects of electroacupuncture against cerebral ischemia: a cDNA microarray study," *Acupuncture and Electro-Therapeutics Research*, vol. 29, no. 3-4, pp. 173–186, 2004.

[34] S. Pan, X. Zhan, X. Su, L. Guo, L. Lv, and B. Su, "Proteomic analysis of serum proteins in acute ischemic stroke patients treated with acupuncture," *Experimental Biology and Medicine*, vol. 236, no. 3, pp. 325–333, 2011.

[35] H. J. Kim, H. J. Park, M. S. Hong et al., "Effect by acupuncture on hypothalamic expression of maternally separated rats: proteomic approach," *Neurological Research*, vol. 32, no. 5, pp. 69–73, 2010.

[36] Q. F. Wu, S. Mao, C. Wei et al., "Effects of electroacupuncture of Weishu (BL 21) and Zhongwan (CV 12) on serum large molecular metabolites in functional dyspepsia rats," *Acupuncture Research*, vol. 35, no. 4, pp. 287–292, 2010.

[37] Q. F. Wu, S. Z. Xu, S. G. Yu et al., "Metabonomics and pattern recognition study on the specificity of foot-Yangming Meridian Points," *Shanghai Journal of Acupuncture and Moxibustion*, vol. 29, no. 9, pp. 552–555, 2010.

[38] Y. F. Luo, *Fundamentals of Acupuncture*, Sichuan University Press, 2008.

[39] S.-H. Sohn, S. K. Kim, E. Ko et al., "The genome-wide expression profile of electroacupuncture in DNP-KLH immunized mice," *Cellular and Molecular Neurobiology*, vol. 30, no. 4, pp. 631–640, 2010.

[40] Y. Chae, M.-S. Hong, G.-H. Kim et al., "Protein array analysis of cytokine levels on the action of acupuncture in carrageenan-induced inflammation," *Neurological Research*, vol. 29, no. 1, pp. S55–S58, 2007.

[41] S. Y. Zhou, *A$^{1}$H NMR-Based metabonomics study with the Back-Shu and Front-Mu acupoints of Stomach for treating Functional Dyspepsia [M.S. thesis]*, Chengdu University of Traditional Chinese Medicine, 2011.

[42] Q. F. Wu, *A$^{1}$H NMR-Based metabonomics study on the acupoint specificity effect of Foot-Yangming Meradian in treating Functional Dyspepsia [M.S. thesis]*, Chengdu University of Traditional Chinese Medicine, 2010.

[43] M. Fan, "Functional Dyspepsia of traditional Chinese medicinal research," *TCM Research*, vol. 20, no. 11, pp. 61–64, 2007.

[44] F. Zeng, *Acupuncture for functional dyspepsia at acipoints on involved meridian: a multi-center, randomized, controlled trial and PETT-CT study [Ph.D. thesis]*, Chengdu University of Traditional Chinese Medicine, 2010.

[45] L. Guo, Y. Y. Wang, and Z. B. Zhang, "Interpretation of the concept of ZHENG," *Journal of Beijing University of TCM*, vol. 26, no. 2, pp. 5–8, 2003.

[46] F.-R. Liang, F. Zeng, and Y. Tang, "Thinking about building a clinical syndrome differentiation system of acupuncture and moxibustion," *Chinese Acupuncture & Moxibustion*, vol. 28, no. 8, pp. 551–553, 2008.

[47] C. E. Tan, M. Q. Wang, and M. Lu, "Differential gene expression profile of therapeutic effect of warm needling treatment on knee osteoarthritis with kidney-yang deficiency," *Journal of Yunan University of Traditional Chinese Medicine*, vol. 34, no. 4, pp. 4–10, 2011.

[48] J. H. Yang, H. Y. Cao, Z. K. Feng, and X. Q. Liu, "Epidemiological studies of Traditional Chinese Medicine Syndrome in Primary osteoarthritis," *The Journal of Traditional Chinese Orthopedics and Traumatology*, vol. 17, no. 7, pp. 19–22, 2005.

[49] Z. Y. Shen, *The Sequel of Renal Research*, Shanghai science and Technology Press, Shanghai, China, 1990.

[50] H. R. Ding, C. E. Tan, W. Z. Feng, and M. Q. Wang, "Analyse of differentially expressed genes associated with signal transduction of patients who suffered from Osteoarthritis of Deficiency of Kidney-Yang," *Liaoning Journal of Traditional Chinese Medicine*, vol. 33, no. 10, pp. 1217–1220, 2006.

[51] L. P. Yang, M. C. Wang, M. Q. Wang, and W. G. Liu, "Effect of acupuncture on expression of Immuno-related genes in patients of Kidney-Yang Deficiency Osteoarthritis through gene microarray," *Liaoning Journal of Traditional Chinese Medicine*, vol. 33, no. 3, pp. 257–258, 2006.

[52] R. Zhang, F. Li, H. Li, H. F. Wang, and Y. H. Song, "Analyzing of point selection features by acupuncture in treatment on Knee Osteoarthritis," *Chinese Journal of Rehabilitation Medicine*, vol. 22, no. 4, pp. 357–358, 2007.

[53] H. R. Wang and P. X. Li, "Research progress of the relation between stomach theory and Immunity doctrine," *Hunan Journal of Traditional Chinese Medicine*, vol. 28, no. 3, pp. 164–165, 2012.

[54] L.-P. Yang, M.-C. Wang, W.-G. Liu, and M.-Q. Wang, "Effects of warming-needle therapy on gene expression pathways in the patient with knee osteoarthritis of deficiency-cold syndrome," *Chinese Acupuncture & Moxibustion*, vol. 27, no. 9, pp. 677–680, 2007.

[55] J. P. Zhao and S. Chen, "Eligible selection of syndrome differentiation methods based on discrimination and treatment in acupuncture clinic," *Journal of Beijing University of Traditional Chinese Medicine*, vol. 19, no. 5, pp. 1–6, 2012.

[56] J. Han, "Meridian is a three-dimensional network from bioelectromagnetic radiation interference: an interference hypothesis of meridian," *Cell Biochemistry and Biophysics*, vol. 62, no. 2, pp. 297–303, 2012.

[57] P. Baldi and S. Brunak, *Bioinformatics: The Machine Learning Approach*, MIT Press, 2nd edition, 2001.

[58] W. Liu, Y. P. Zhu, and F. C. He, "Integration of various "omics" data in biological systems," *Chinese Journal of Biochemistry and Molecular Biology*, vol. 23, no. 12, pp. 971–976, 2007.

[59] Z. B. Zhang, Y. Y. Wang, A. P. Lv, L. Guo, and Y. Wang, "On combined syndrome differentiation of essential elements of syndrome and syndrome target point corresponding syndromes," *Journal of Traditional Chinese Medicine*, vol. 47, no. 7, pp. 483–485, 2006.

[60] T. Ideker, V. Thorsson, J. A. Ranish et al., "Integrated genomic and proteomic analyses of a systematically perturbed metabolic network," *Science*, vol. 292, no. 5518, pp. 929–934, 2001.

Hindawi Publishing Corporation
Evidence-Based Complementary and Alternative Medicine
Volume 2013, Article ID 595924, 15 pages
http://dx.doi.org/10.1155/2013/595924

*Research Article*

# A Network-Based Systematic Study for the Mechanism of the Treatment of Zhengs Related to Cough Variant Asthma

**Di Chen,[1] Fangbo Zhang,[2] Shihuan Tang,[2] Yan Chen,[3] Peng Lu,[1,2] Shaoxin Wen,[1] Hongchun Zhang,[3] Xi Liu,[1] Enxiang Chao,[3] and Hongjun Yang[2]**

[1] *Institute of Automation, Chinese Academy of Sciences, Beijing 100190, China*
[2] *Institute of Chinese Materia Medica, China Academy of Chinese Medical Sciences, Beijing 100700, China*
[3] *China-Japan Friendship Hospital, Beijing 100029, China*

Correspondence should be addressed to Enxiang Chao; chaoenxiang@163.com

Received 8 July 2013; Revised 10 September 2013; Accepted 12 September 2013

Academic Editor: Shao Li



Traditional Chinese medicine (TCM) has shown significant efficacy in the treatment of cough variant asthma (CVA), a special type of asthma. However, there is shortage of explanations for relevant mechanism of treatment. As Zhengs differentiation is a critical concept in TCM, it is necessary to explain the mechanism of treatment of Zhengs. Based on TCM clinical cases, this study illustrated the mechanism of the treatment of three remarkably relevant Zhengs for CVA: "FengXieFanFei," "FeiQiShiXuan", and "QiDaoLuanJi." To achieve this goal, five steps were carried out: (1) determining feature Zhengs and corresponding key herbs of CVA by analyses of clinical cases; (2) finding out potential targets of the key herbs and clustering them based on their functional annotations; (3) constructing an ingredient-herb network and an ingredient network; (4) identifying modules of the ingredient network; (5) illustrating the mechanism of the treatment by further mining the latent biological implications within each module. The systematic study reveals that the treatment of "FengXieFanFei," "FeiQiShiXuan," and "QiDaoLuanJi" has effects on the regulation of multiple bioprocesses by herbs containing different ingredients with functions of steroid metabolism regulation, airway inflammation, and ion conduction and transportation. This network-based systematic study will be a good way to boost the scientific understanding of mechanism of the treatment of Zhengs.

## 1. Introduction

Traditional Chinese medicine (TCM), as a system of ancient medical practice which differs in substance, methodology, and philosophy from modern medicine, involves a broad range of empirical testing and refinement and plays an important role in the health maintenance for people. During the long history of TCM clinical practices, much treatment experience for a myriad of diseases has been accumulated [1]. The clinical cases of TCM, especially those from experienced TCM doctors, are precious sources for the understanding and development of TCM.

Doctors diagnose whether a patient is suffering from certain types of diseases or not based on a comprehensive analysis of the patient's symptoms. In the field of TCM, it is especially important to identify patients' Zhengs based on the four diagnostic methods, which include inspection, listening and smelling, inquiry, and pulse taking. According to Zhengs, TCM practitioners will prescribe proper formulas to patients in order to heal their disorders [2, 3]. Herbal medicines, a powerful tool of TCM, can heal different kinds of Zhengs by combinations [4–6]. Although there are substantial records of TCM clinical cases and corresponding analyses of the clinical information [7–9], there is still shortage of scientific explanations for corresponding mechanism.

With the development of bioinformatics and system biology [10–12], it is possible to analyze the molecular mechanism of drugs. Some system biology tools, with extremely high efficiency and molecular level representation, have been invented (e.g., MetaDrug (http://www.genego.com/)). They are widely used for the understanding of the complex functions of compounds [13–15]. With the help of system biology tools, herbal functions and the mechanism of treatment of Zhengs can be interpreted in some degree.

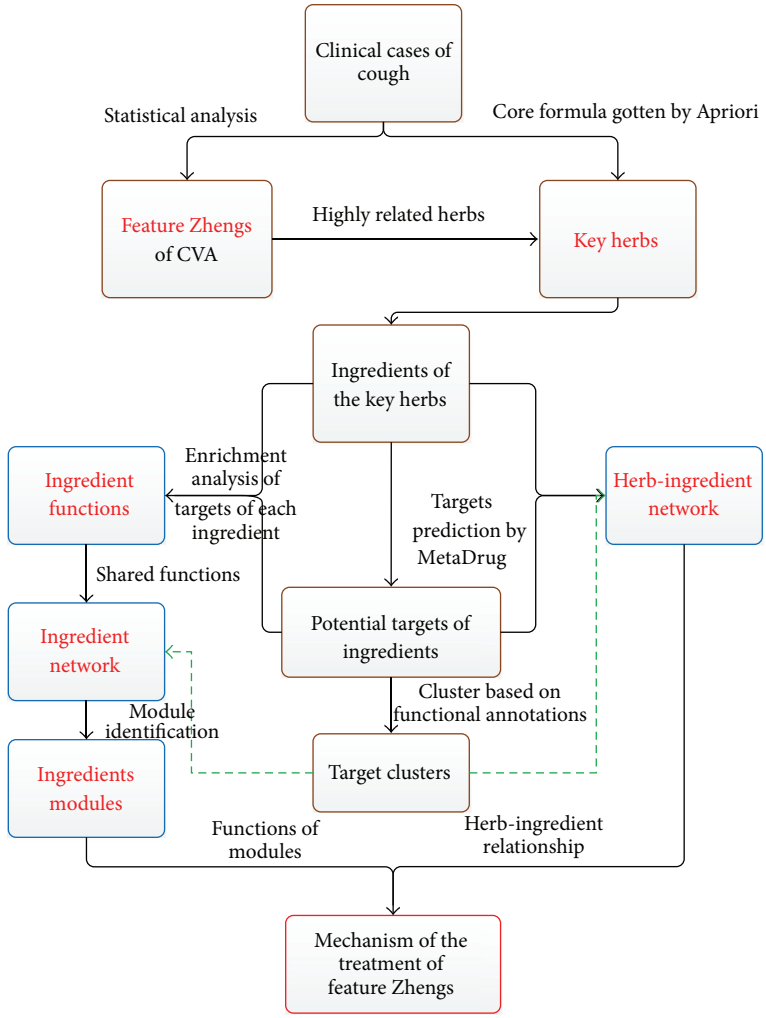


Figure 1: The flow diagram of the systematic study.

Cough variant asthma (CVA), a type of asthma with main symptom of a dry, nonproductive cough [16–18], is affecting many people's health. It is sometimes called chronic cough to describe a cough that has lasted longer than six to eight weeks. Together with lung disease and other symptoms such as tachycardia and dyspnea [19–22], CVA is one major health burden in the area of respiratory medicine. In the field of TCM, CVA is usually related with the Zheng of "FengXie (wind-evil)" and is named as "FengKe" in Chinese.

Although TCM has shown remarkable curative effects for CVA, the latent mechanism is still unknown. Current studies on TCM have provided few insights into the biological mechanism. The obscurity of the mechanism will hinder the development and clinical popularizing of TCM theory. A systematic study on the mechanism of the treatment of TCM Zhengs from the aspects of herb ingredients, ingredient targets, and their functions, as well as the complex relationships among them is extremely necessary. Besides, explanations for the mechanism of the treatment of CVA-related Zhengs can help us validate the reasonability of TCM theory and develop a deep understanding of the mechanism which is beneficial to new herbal medicine design. This study tried to illustrate the biological mechanism of the treatment of Zhengs related with CVA by analyzing the clinical cases.

## 2. Materials and Methods

We have identified the potential mechanism of the herbs for the treatment of three distinguished Zhengs of CVA by a network-based systematic study (as shown in Figure 1) of the TCM clinical cases. Our approach proceeds as follows.

(1) Determine feature Zhengs and corresponding key herbs of CVA by analyzing clinical cases.

(2) Find out potential targets of key herbs and cluster them based on their functional annotations.

(3) Construct an ingredient-herb network and an ingredient network to study the relationship between ingredients and herbs.

(4) Identify modules in the ingredient network.

(5) Illustrate the mechanism of the treatment by mining the latent biological implications (pathways and GOs [23]) within each module.

### 2.1. Analysis of TCM Clinical Cases

*2.1.1. Identification of Feature Zhengs of CVA.* The information of the clinical cases was collected from June 2009 to July 2012, by the *Famous TCM Doctor Inheritance Studio of Chao Enxiang*, who has engaged in medical work for more than forty years and has accumulated many successful experiences of treating CVA [24, 25], and the data were exported from the *Traditional Chinese Medicine Inheritance Support Plat* [26]. These cases were recorded in standard format, so it is convenient to do analysis about them. These clinical cases contain the information of Zhengs, disease name, the principle and method of therapy, herbal formulae, patient's age, and gender, and so on. By statistical analyses of the clinical cases, we have identified some highly related Zhengs for CVA. These Zhengs are distinguished from others for they occur remarkably more times than the others in the clinical cases. These Zhengs, which represent the main feature of CVA, were defined as feature Zhengs of CVA.

*2.1.2. Identification of the Key Herbs.* The clinical cases list the herbs which constitute the formulas. It is easy to find that similar Zhengs are treated by similar formulas as discussed in [27, 28]. Although formulas of patients with the same Zhengs can vary with individuals' conditions, there are always several herbs prescribed changelessly for the same Zhengs. The clinical cases from Professor Chao included 2414 cases and 948 records of formulas. These cases provided abundant information about the herb combination laws and treatment rules. As it is difficult to elaborate the mechanism of the treatment of Zhengs directly, we tried to illustrate the latent mechanism by finding the functions of the herbs alternatively. The conditional probability of an herb appeared in the cases given certain Zheng can be used to represent the correlation degree between an herb and a Zheng. In our study, more than one Zheng was identified as feature Zhengs; the conditional probability given these Zhengs is as below:

$$p(h \mid Z) = \frac{\sum_i c(h, z_i)}{\sum_i c(z_i)}, \quad (1)$$

where $h$ represents an herb, $Z$ represents the set of feature Zhengs, $c(h, z_i)$ represents how many times herb $h$ and Zheng $z_i$ appear in the same case, and $c(z_i)$ is the times Zheng $z_i$ appears in the clinical cases. $p(h \mid Z)$ represents the probability of an herb that appeared given the feature Zhengs.

Herbs with high conditional probability are more related to the feature Zhengs. However, as TCM pays attention to the rules of composition, it is not suitable to consider each herb separately without consideration of their combination rules [29–31]. Apriori's algorithm [32] was used here to find out core formulas, and the minimum support was set at 0.4. Then herbs with high conditional probability and appearing in the core formulas at the same time were defined as the key herbs which were highly related to the feature Zhengs. By analyzing the mechanism of the key herbs, it will help to understand the mechanism of the treatment of feature Zhengs.

### 2.2. Potential Targets of Key Herbs

*2.2.1. Finding Out the Potential Targets.* A drug target is a key molecule involved in particular metabolic or signaling pathways which are specific to a disease condition or pathology [33–35]. In order to find out the bioprocesses that may be affected by the herbs, we need to find out the potential targets of key herbs. If some targets are targeted by most of the key herbs, it is probable that these targets play key roles in the treatment of the feature Zhengs.

To find out the potential targets of key herbs, we need to seek out the compounds of each herb at first. The targets of the ingredients of an herb were considered as the targets of this herb. In our study, we used MetaDrug, which is a system biology tool developed by the Gene GO company [14, 15], to find the potential targets of each compound. This tool uses the known targets of similar compounds to predict the possible targets of a compound. The similarity is referred to as the chemical structure similarity defined by Tanimoto's coefficient [36]. In order to achieve relatively reliable results, we set the lower and upper values of the coefficient to 0.9 and 1.0 to do the similarity search.

*2.2.2. Clustering the Potential Targets Based on Functions.* Because of the great number of compounds of an herb and the multiple targets of each compound, the total number of the targets of all the key herbs is substantial. The great amount of targets makes it difficult to understand the biological meaning, so we clustered the targets according to their functional annotations. The clustering was done by DAVID [37], a tool widely used in the studies about genes or proteins. Targets in the same cluster share similar functional annotations, and different clusters represent different functions.

### 2.3. Network-Based Analysis

*2.3.1. Herb-Ingredient Network.* An herb-ingredient network is a bipartite network constructed by simply connecting an herb and its ingredients together. It can shed light on the relationship of different herbs' ingredients and supply some latent lines of evidence for the combination rules of herbs at the same time.

*2.3.2. Ingredient Network.* We constructed an ingredient network based on the shared functions of ingredients.

(1) Ingredient functions.

Since an ingredient achieves its effects by acting on certain targets, functions of an ingredient can be derived by the functions of its targets. However, one ingredient can have effects on multiple targets of which the functions are complex. We obtained the detailed functions of an ingredient by enrichment analyses of its targets in respect to GO processes, GO molecular functions, GO localizations, and pathways. The enrichment results were gotten from MetaDrug with

a $P$ value less than $1 \times 10^{-4}$, and all of the four aspect functions are in standardized items. At last, each ingredient was assigned a standardized functional item set.

(2) Ingredient network construction.

According to the ingredient functions gotten from enrichment analyses of targets, the relationship between two ingredients can be represented by the intersection of their functional item sets. The weight of an edge on the ingredient network is defined as below:

$$w\left(c_i, c_j\right) = \frac{1}{4} \cdot \sum_{k \in E} \frac{\left|F_{c_i}^k \cap F_{c_j}^k\right|}{\left|F_{c_i}^k \cup F_{c_j}^k\right|}, \quad (2)$$

where $c_i$, $c_j$ are two ingredients; $E$ represents four different enriched aspects: $E = \{$*GO processes, GO molecular functions, GO localizations, pathways*$\}$; $F_{c_i}^k$ represents the set of enriched functions of $c_i$ in the aspect of $k$; $|\cdot|$ represents the size of a set; and $\cap$, $\cup$ represent intersection and union of two sets as usual.

We constructed an ingredient network in our study by only considering edges with a weight larger than the threshold of 0.2 and with $P$ value (Fisher's exact test) less than 0.01. Besides, we also assigned the intersection of two sets of functional items: $F_{c_i} \cap F_{c_j}$ to each edge $(c_i, c_j)$ as its functional implications for further analysis, where $F_{c_i}$ represents the united set of functional items of four aspects.

*2.3.3. Network Visualization.* All of the networks were visualized by Cytoscape [38], a widely used network visualization tool. Targets, ingredients, and herbs in the networks are represented by nodes, and interactions are represented by edges.

*2.4. Modules of Ingredient Network.* To figure out the latent mechanism, just finding out functional relationship between ingredients by a network is not enough. We should also find out whether these ingredients collaborate with each other to achieve certain main functions or not. Modules [38, 39] are densely related parts of a network, so modules in the ingredient networks can stand for the functional related ingredients. We used MCODE [40], an effective network module identification plugin of Cytoscape, to identify the modules from the ingredient network.

*2.5. Module Functions.* Modules of the ingredient network can suggest which ingredients have similar functions. To explore the biological meaning hidden in each module, we employed the functional implications assigned to the edges, as discussed in Section 2.3.2. By counting the functional items of edges in each module, we got the frequent items whose frequencies were larger than half of the biggest counts of all items within a module to reveal the main functions of the module.

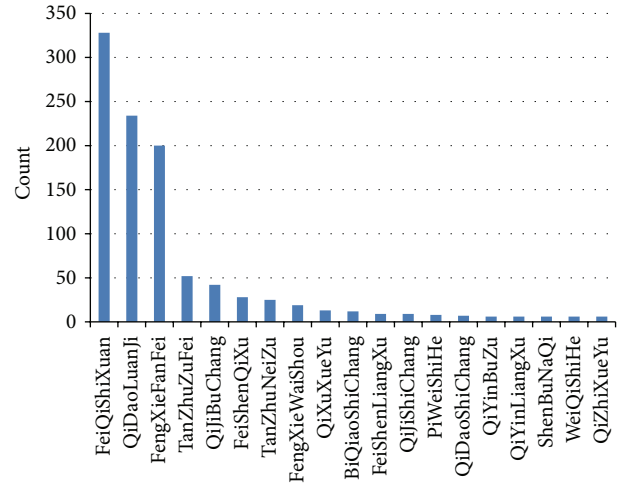


Figure 2: Count of Zhengs in the clinical cases. Among the clinical cases, there were 133 Zhengs in total. This histogram only shows the Zhengs with a count larger than 3. The horizontal axis represents different Zhengs, and the vertical axis represents the counts of one Zheng in the clinical cases.

## 3. Results and Discussion

For thousands of years, TCM holds a great promise for medical treatments in China and now is considered as a complementary medical system in many Western countries [41]. Despite the fact that many positive outcomes have been observed in TCM clinical cases, the underlying mechanism of the treatment of Zhengs is unclear. An herbal formula usually incorporates several herbs which are chosen based on the patients' Zhengs, so we can catch sight of the underlying Zheng treatment mechanism by analyzing the related herbs indirectly. In this study, we applied our method to the clinical cases of Professor Chao to find out the biological mechanism.

*3.1. Feature Zhengs Derived from Clinical Cases.* We collected 2414 clinical cases of CVA-related diseases, and the final statistics showed that among all of the 133 different Zhengs recorded, "FengXieFanFei (wind-evil invading lung)," "FeiQiShiXuan (lung Qi obstruction)," and "QiDaoLuanJi (twin acute airway)" were three most frequent CVA-related Zhengs. As shown in Figure 2, these Zhengs were not only frequent, but also possessed an apparent advantage over all other Zhengs. These three Zhengs occupied 67% of all the Zhengs recorded in the clinical cases while the other 130 Zhengs occupied 33% of the cases. This manifested that most of the CVA cases were related to these three Zhengs. Consequently, "FeiQiShiXuan," "QiDaoLuanJi," "FengXieFanFei," three most typical Zhengs for CVA, were determined as the feature Zhengs of these CVA-related clinical cases.

*3.2. Key Herbs of the Feature Zhengs*

*3.2.1. Conditional Probability of Each Herb Given the Feature Zhengs.* To seek out the key herbs which are highly associated

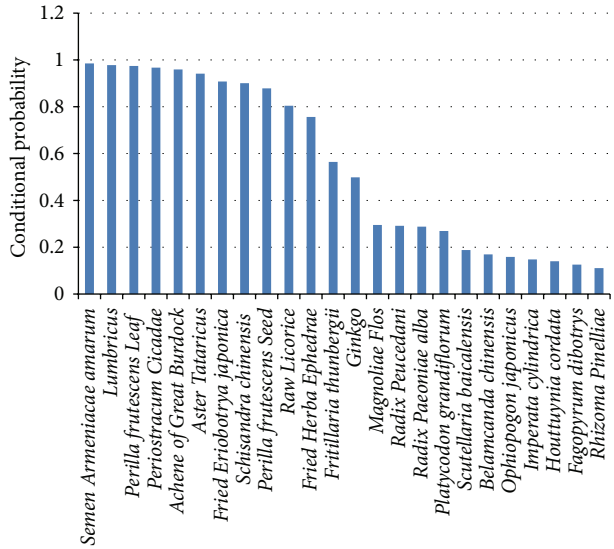


Figure 3: Conditional probability of an herb given feature Zhengs. This figure shows the conditional probability of an herb given feature Zhengs ("FeiQiShiXuan," "FengXieFanFei," and "QiDaoLuanJi"). Herbs with probability less than 0.1 are ignored.

with the feature Zhengs, we calculated the probability as shown in (1) and got the results as shown in Figure 3.

As shown in Figure 3, the probabilities of the first 11 herbs—*Semen Armeniacae amarum* (SAA), *Lumbricus* (Lum), *Perilla frutescens Leaf* (PFL), *Periostracum cicadae* (PC), *Achene of Great Burdock* (AGB), *Aster tataricus* (AT), *Fried Eriobotrya japonica* (FEJ), *Schisandra chinensis* (SC), *Perilla frutescens seed* (PFS), *Raw Licorice* (RL), and *Fried Herba ephedrae* (FHE) were larger than 0.7. The probabilities of these 11 herbs are apparently higher than other herbs for the treatment of "FeiQiShiXuan," "FengXieFanFei," and "QiDaoLuanJi"; they must play key roles in the treatment of these feature Zhengs.

*3.2.2. Core Formula.* Furthermore, we applied Apriori's algorithm to determine the frequent herb combinations as the core formula for the treatment of feature Zhengs. The combinations found out by the algorithm (the support rate was set at 0.4) were SAA, Lum, PFL, PC, AGB, AT, FEJ, SC, PFS, RL, and FHE.

The result showed that these 11 herbs were frequently prescribed together to heal CVA. Considering the high conditional probability of the 11 herbs as discussed in Section 3.2.1 and their frequent combination, these two results testified that not only do the 11 herbs play key roles by isolation analysis, but also they can combine with each other to achieve therapeutic effects. It is reasonable to define these 11 herbs as the key herbs of the feature Zhengs. There are also many studies that prove the effectiveness of the 11 herbs for the treatment of CVA [42–48], and nine of them are the ingredients of "Suhuangzhike" granules, a Chinese patent medicine which has shown significant clinical effects [49–51].

Table 1: The number of compounds and potential targets.

| Herb name | Number of compounds | Number of potential targets |
|---|---|---|
| SAA | 19 | 494 |
| Lum | 23 | 447 |
| PFL | 15 | 303 |
| PC | 25 | 381 |
| AGB | 6 | 350 |
| AT | 6 | 8 |
| FEJ | 13 | 104 |
| SC | 29 | 29 |
| PFS | 4 | 428 |
| RL | 87 | 501 |
| FHE | 19 | 160 |
| Number of nonrepetitive objects in total | 223 | 954 |

### 3.3. Potential Targets of Key Herbs

*3.3.1. Targets of the Herbs.* There were 306 compounds collected for the 11 key herbs. The potential targets for the compounds were obtained by the targets prediction function of MetaDrug. The potential targets of an herb were considered as the sum of the targets of its compounds. The number of compounds and potential targets for each herb is listed in Table 1. This testifies the multicompounds and multitargets characteristics of Chinese herbs. There are 954 different targets for all 11 key herbs, and 372 of them are the targets of more than 7 compounds. To make our study more reliable and to show that Chinese medicine achieve the therapeutic effects by combination of compounds, we used the 372 targets which were targeted by more than 7 compounds for the following analyses.

*3.3.2. Target-Compound Network.* We got the interaction networks of compounds and their potential targets as shown in Figure 4. As we can see from the network, multiple compounds act on the same targets. This is different from Western medicine which usually employs only one compound to act on one certain target.

*3.3.3. Clustering Targets Based on Functional Annotations.* However, the number of targets is so big and the promiscuity of the targets restrains the understanding of the mechanism. To make clear the main functions of the key herbs, we clustered these targets by the functional annotations clustering function of DAVID. We got 18 clusters in total, and the main clusters are shown in Table 2. Clusters 1 to 3 are three biggest clusters; Clusters 4 and 5 are the clusters with OMIM [52] genes of asthma and cough, two similar diseases of CVA.

To find out the mechanism of the herbs, functions of these targets are of crucial roles. As the clustering process is based on functional annotations of each gene, different clusters must correspond to different functions. The functions

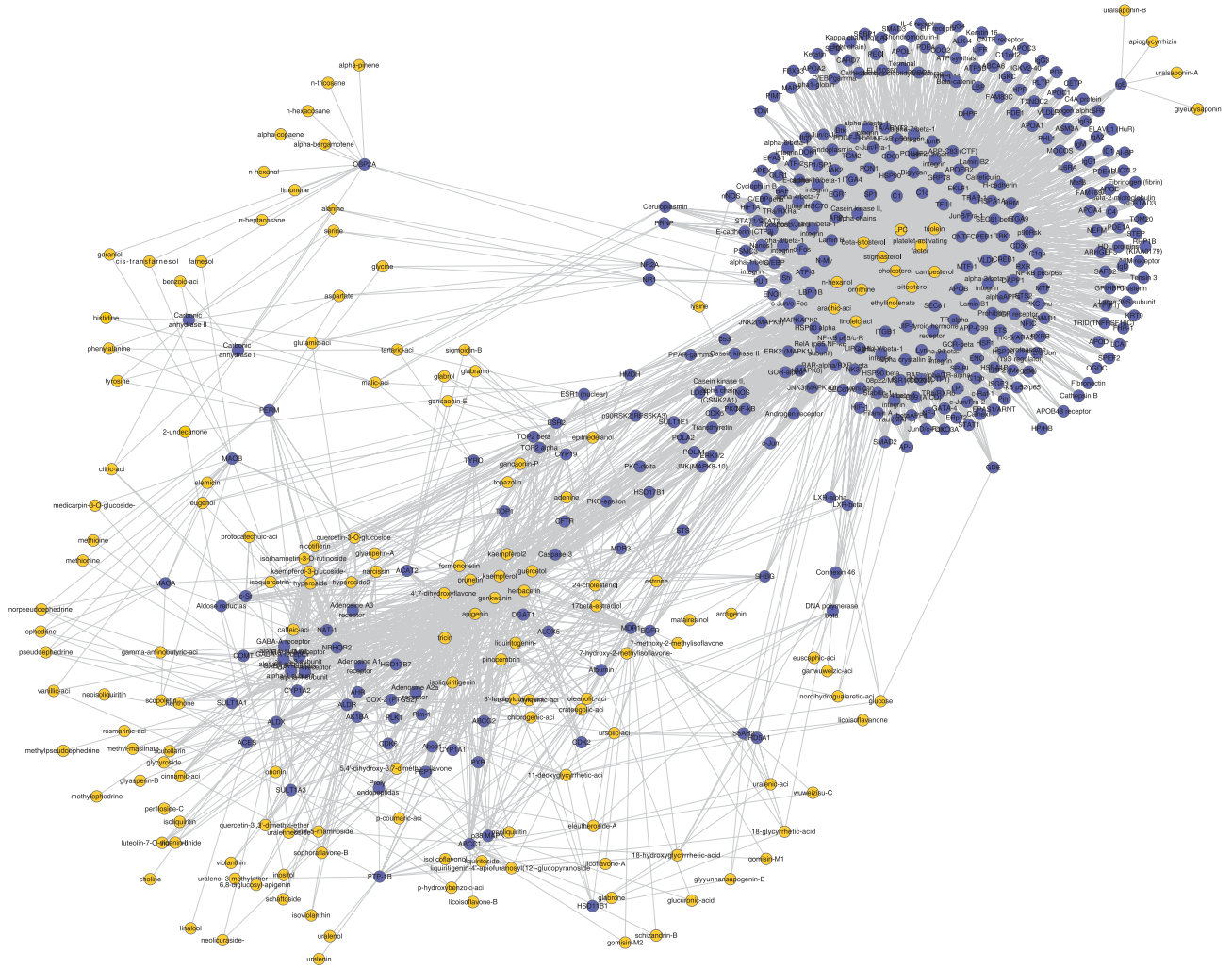

Figure 4: The interactions between potential targets and compounds. Yellow nodes represent the compounds, and the blue ones are potential targets.

of the biggest clusters correspond to the main functions of the key herbs. The genes in Cluster 1 are connected with hormone stimulus. Activated estrogen receptors (ER, Cluster 1) via ER$\alpha$ or ER$\beta$ stimulate NO production in airway epithelium; estrogen-induced NO and its impairment may contribute to altered bronchodilator in women with asthma [53]. Peroxisome proliferator-activated receptor $\gamma$ (PPAR$\gamma$, Cluster 1) ligands, such as rosiglitazone and pioglitazone, inhibit proliferation and inflammatory cytokine production from airway smooth muscles through a PPAR$\gamma$-independent mechanism [54]. The genes in Cluster 2 are associated with cellular metabolic process. Mitogen-activated protein kinase-1 (MAPK1, Cluster 2) controls a vast array of physiological processes. Inflammatory cytokines and environmental stresses may activate p38 MAPKs, which contributes to diseases like asthma and autoimmunity [55]. Pim kinases are a family of serine/threonine kinases that are induced by cytokines and involved in allergy and asthma. The inhibition of Pim1 kinase (Cluster 2) effectively prevents the development of airway hyperresponsiveness, airway inflammation, and cytokine production in allergen-sensitized and allergen-challenged mice [56]. Most studies of chronic cough or bronchial asthma deal with IgE responsiveness. Different serum IgG1, IgG2, and IgG3 (Immunoglobulin, Cluster 3) levels together with different numbers of peripheral blood eosinophil and CD8 lymphocytes represent different pathways of immune regulation of bronchial asthma [57].

The three biggest clusters are all related to the treatment of asthma or cough by regulating the hormone stimulus, airway inflammation, and immune regulations. Except for these three clusters, two clusters (Clusters 4, 5) have OMIM genes (Genes IDs: 718, 1080) of asthma or cough in the cluster, and we define the two clusters as disease-related target clusters. The genes in Cluster 4 are mainly related to complement system. The activation of the complement system could have a role in treating cough by promoting inflammation and enhancing airway hyperresponsiveness. C5a is usually elevated at the site of inflammation in patients with asthma [58]. The genes in Cluster 5 are related to transport function across cell membrane. ATP-binding

Table 2: Gene functional clustering result.

| Gene ID | Name | Gene ID | Name | Gene ID | Name |
|---|---|---|---|---|---|
| | | | Cluster 1 | | |
| 6257 | RXRb | 1958 | EGR1 | 4520 | MTF-1 |
| 10062 | LXR-alpha | 5468 | PPAR-gamma | 7376 | LXR-beta |
| 367 | Androgen receptor | 7342 | LBP-1B | 2626 | GATA-4 |
| 2100 | ESR2 | 10661 | EKLF1 | 5914 | RAR-alpha |
| 8856 | PXR | 6667 | SP1/SP3 | 6595 | BRM |
| 9971 | FXR | 6688 | PU.1 | 2908 | GCR-beta |
| 2099 | ESR1 | 6256 | RXR-beta | 4782 | CTF |
| 7067 | TR-alpha | 5458 | POU4F2 | 2354 | JunB |
| 1386 | ATF-2 | | | | |
| | | | Cluster 2 | | |
| 6196 | p90RSK3 | 3706 | IP3KA | 29110 | TBK1 |
| 1459 | CSNK2A2 | 5599 | MAPK8 | 5581 | PKC-epsilon |
| 8986 | MSK2 | 1432 | MAPK14 | 6195 | p90RSK1 |
| 1017 | CDK2 | 5594 | MAPK1 | 5292 | Pim-1 |
| 5587 | PKC-mu | 80271 | ITPKC | 5602 | MAPK10 |
| 5580 | PKC-delta | 1021 | CDK6 | 5347 | PLK1 |
| 9252 | MSK1 | 253430 | IMPK | 695 | Btk |
| 5601 | MAPK9 | 6197 | p90Rsk | 9261 | MAPKAPK2 |
| | | | Cluster 3 | | |
| 28916 | IGKV2-40 | 3500 | IgG1 | 3502 | IgG3 |
| 3501 | IgG2 | 3494 | IgA2 | 3514 | IGKC |
| 3497 | IgE | 3493 | IgA1 | 3535 | IgD |
| 3503 | IgG4 | | | | |
| | | | Cluster 4 | | |
| 718 | C3 | 720 | C4A protein | 713 | C1qb |
| 3078 | FHR-1 | 1191 | clusterin | 712 | C1qa |
| | | | Cluster 5 | | |
| 9429 | ABCG2 | 5243 | MDR1 | 1080 | CFTR |
| 225 | ALD2 | 5244 | MDR3 | 23460 | ABCA6 |
| 4363 | ABCC1 | | | | |

cassette (ABC) transporters are a family of transmembrane proteins which can transport numerous substrates across biological membranes in an energy-dependent pattern. Many ABC transporters such as P-glycoprotein (P-gp), multidrug resistance-associated protein 1 (MRP1), and breast cancer resistance protein (BCRP) are highly expressed in bronchial epithelium. These three ABC transporters are well known to play an important role in lung functioning. Mutations in the cystic fibrosis transmembrane conductance regulator (CFTR) gene can cause cystic fibrosis. The role of altered function of ABC transporters in asthma has hardly been investigated so far [59].

The multiple functions of the targets prove that TCM aims not only to antagonize specific pathogenic targets, but also to correct maladjustments and restore the self-regulatory ability of the body.

*3.4. Herb-Ingredient Network.* To understand the mechanism of herb combinations, it is necessary to know whether ingredients of an herb have similar functions or different herbs share similar compositions. The herb-ingredient network, as shown in Figure 5, in which different colors represent different functions, provides a way to make clear the composition characteristics of herbs.

It is obvious to see from the herb-ingredient network that different key herbs used for CVA basically do not have same ingredients with only a few expectations, and nearly every herb has targets (targets with blue or purple color) of the disease-related target clusters. By combination of different herbs, more ingredients can collaborate with each other to achieve the same therapeutic effects, for ingredients of different herbs share similar functions.

*3.5. Ingredient Network*

*3.5.1. Ingredient Network Construction.* We constructed an ingredient network (Figure 6) to do further analysis of the relationship between herbs and ingredients. The edges of this network were decided by the intersection of the functional items enriched by the targets of two ingredients instead

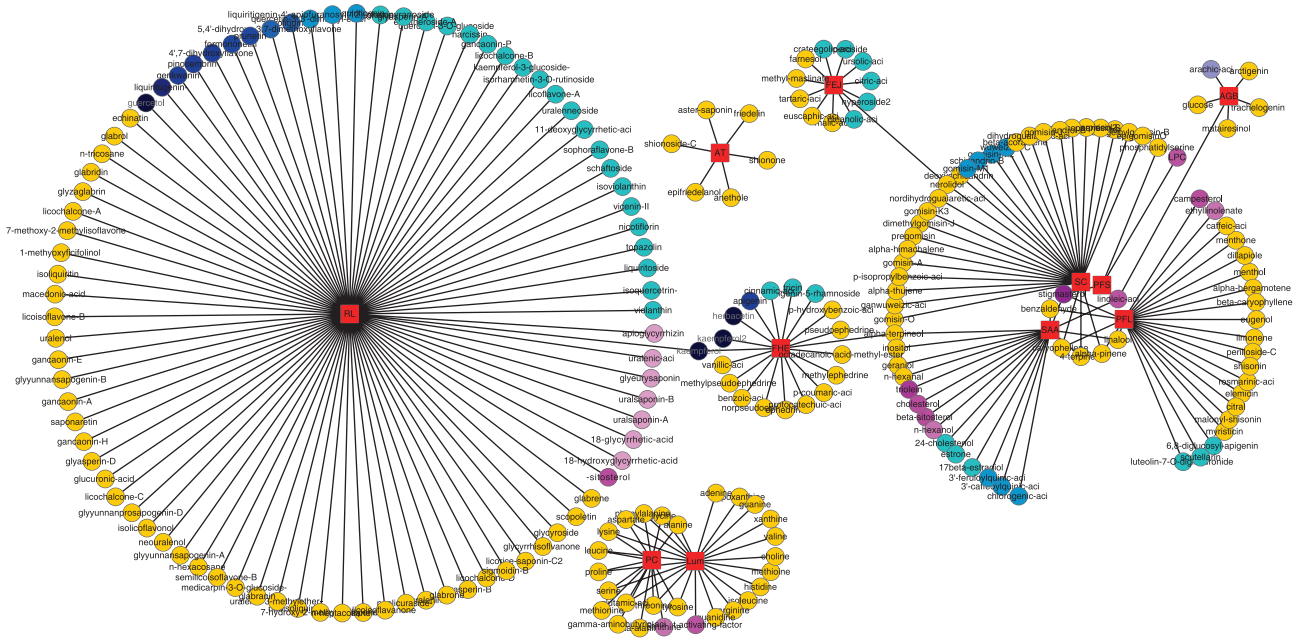


FIGURE 5: Herb-ingredient network. In this network, circular nodes are ingredients, square nodes are herbs, and an edge represents that an ingredient is a composition of an herb. Different colors stand for different target clusters. The shades of the colors represent the relation intensity of an ingredient to a disease-related target cluster. To be more specific, if the number of targets in Cluster 4 is larger than targets in Cluster 5, the ingredient is assigned purple, and the ingredient is assigned blue if the number of targets in Cluster 5 is larger. The shade of the color is proportional to the absolute value (ranging from 1 to 7) of the difference of the number of targets in Cluster 4 and Cluster 5. The only ingredient, with an absolute value of zero, was colored as bluish violet. Ingredients with targets which are not in disease-related target clusters are yellow, and those ones without any targets are not shown in this network. As the ingredients were hardly collected, they are not the overall compositions, but they can elucidate the problem in some degree.

of the intersections of simple targets of two ingredients, because different targets, which can share similar functions by involving in the same processes or different pathways, do not stand for different functions of ingredients.

By construction of ingredient network, not only did we know whether there were interactions between ingredients, but also we obtained the implications of their interactions as partly shown in Table 3. For example, there is an interaction between the ingredients schaftoside and glycyroside, and the targets of two compounds share part of the enriched GOs and pathways, like the GO processes of "cellular aldehyde metabolic process," GO molecular functions of "alcohol dehydrogenase (NADP+) activity," and the pathway of "triacylglycerol metabolism p.1." That is to say, ingredients schaftoside and glycyroside act on the targets with similar functions, in the same biological processes and in the same localizations of human body. Above all, each edge has corresponding functional annotations, which can reveal the interactions of two ingredients, with respect to GO processes, GO molecular functions, and GO localizations and pathways.

*3.5.2. Modules of Ingredient Network.* Six modules (as shown in Figure 7) were identified from the ingredient network by the MCODE method; each module represents a densely related ingredient set. By visual observation, it is evident to see that ingredients of two types of functions (blue ones and purple ones, resp., act on targets in two disease-related target clusters) are mainly located in different modules.

Since each edge of the network has its corresponding biology items in respect to GO processes, GO molecular functions, and GO localizations and pathways calculated by MetaDrug, that is to say, each interaction has its corresponding biology implications, ingredients of the same module must share certain GOs or pathways. We did analysis of these implications within each module to mine the underlying biology functions of the ingredient set. At last, the main functions of 3 largest modules were given out (as shown in Table 4). Take for example Module 2; most of the ingredients in this module have effects on the targets located in soluble fraction, cell projection, with the molecular functions of regulatory region nucleic acid binding, transcription factor binding, and protein binding, interfere with the processes of developmental process, regulation of cell death, and so on, and act on the main pathway of EGFR signaling pathways, IL-17 signaling pathways, Immune response_C5a signaling, and so on.

To make clear the main functions of the ingredients, we need to consider the three biggest modules. According to the colors of the nodes in these three modules, we can deduce that Module 1 is composed of some ingredients whose targets are in the disease-related target Cluster 5 and some ingredients whose targets are not in the disease-related target clusters, so it achieves therapeutic effects by influencing some processes

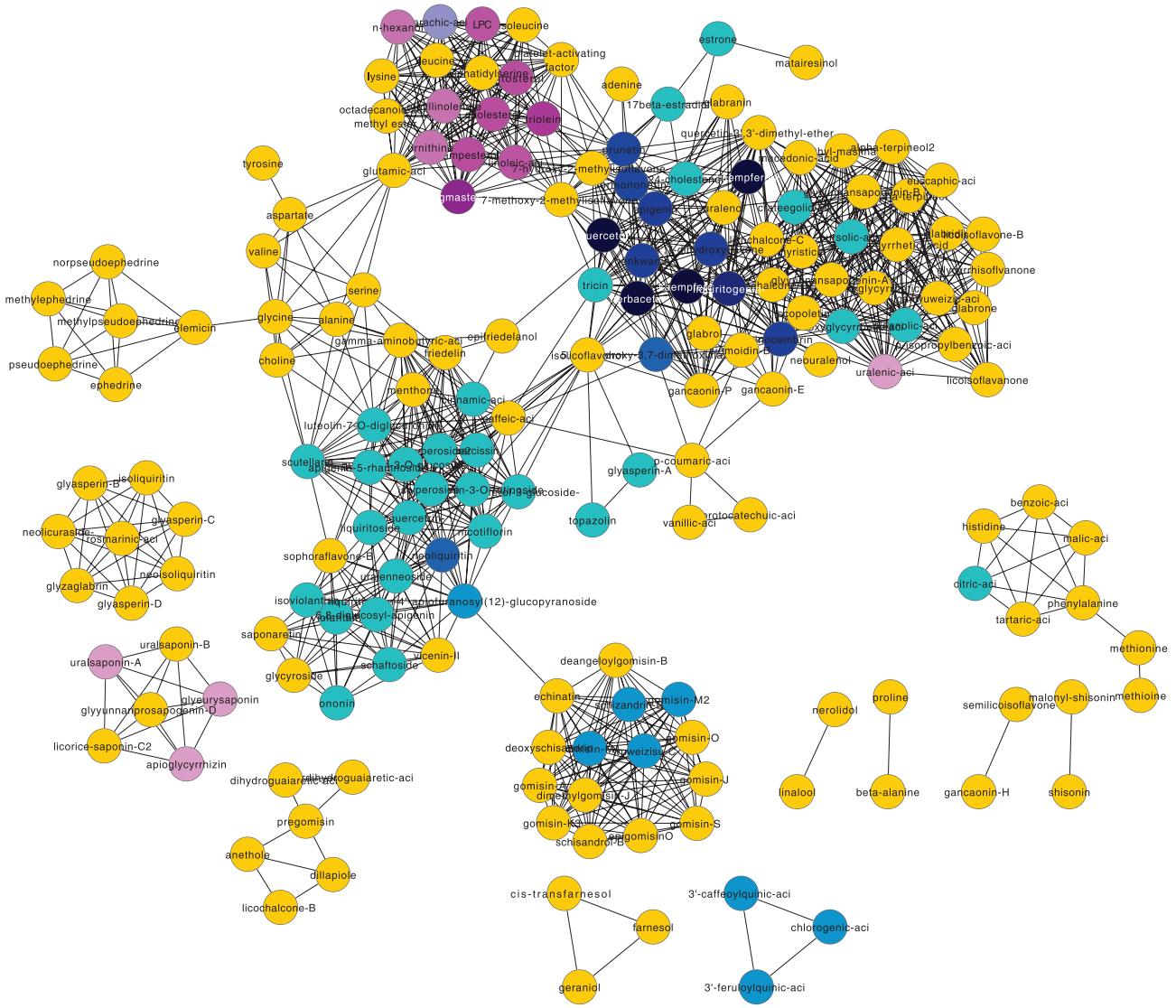


Figure 6: Ingredient network. The meanings of colors are the same as in Figure 5, the same in Table 3.

Table 3: Ingredients interactions.

| Ingredient 1 | Ingredient 2 | GO processes | GO molecular functions | GO localizations | Pathways |
|---|---|---|---|---|---|
| Schaftoside | Glycyroside | Cellular aldehyde metabolic process, antibiotic metabolic process, and so forth | Alcohol dehydrogenase (NADP+) activity, Alditol:NADP+ 1-oxidoreductase activity, and so forth | None | Triacylglycerol metabolism p.1 |
| Liquiritoside | Schaftoside | Aminoglycoside antibiotic metabolic process, daunorubicin metabolic process, and so forth | Alditol:NADP+ 1-oxidoreductase activity, oxidoreductase activity, and so forth | | Triacylglycerol metabolism p.1 |
| n-Hexanol | Glutamic-aci | Regulation of programmed cell death, regulation of multicellular organismal process, and so forth | Binding, regulatory region nucleic acid binding, and so forth | Neuron projection, axon, dendrite, and so forth | Immune response_CD40 signaling, Development_EGFR signaling pathway, Immune response_IL-3 activation and signaling pathway, and so forth |

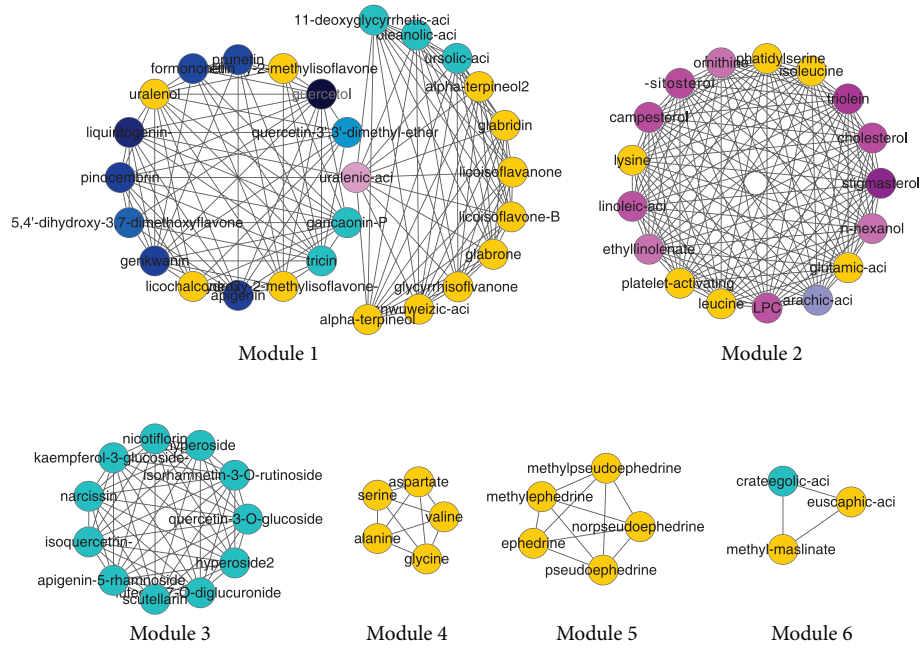


FIGURE 7: Modules of the ingredients network. The blue and purple nodes are in different modules in general, in accordance with the expectation that ingredients of different functions are mainly located in different modules. Then large modules should be in accordance with the main functions of key herbs. Module 1 is mainly composed of ingredients whose targets are not in the disease-related target clusters. Module 2 and Module 3 are composed of ingredients whose targets are mainly in the disease-related target Cluster 4 and Cluster 5, respectively.

which can contribute to the disease indirectly. Module 2 and Module 3 are composed of ingredients whose targets are mainly in the disease-related target Cluster 4 and Cluster 5, respectively; consequently they can restore the health state by acting on the disease-related targets.

To be detailed, we did further study and literature survey about the functions of the three main modules in Table 4.

The main function of Module 1 is related to steroid metabolism. In patients with steroid-resistant asthma, reduced steroid responsiveness is related to several molecular mechanisms. Nuclear translocation of glucocorticoid receptor (GR) $\alpha$ after binding corticosteroids is reduced, which might be due to phosphorylation of the GR activated by several kinases (p38 MAPK $\alpha$, p38 MAPK $\gamma$, and c-Jun N-terminal kinase 1). Furthermore, increased expression of GR$\beta$ competes with GR$\alpha$ and thus inhibits activated GR$\alpha$, ultimately leading to steroid resistance. Long-acting $\beta$2-agonists can increase steroid responsiveness by reversing phosphorylation of GR$\alpha$. Testosterone and 5$\alpha$-dihydrotestosterone caused nuclear localization of 5-lipoxygenase, which initiated the biosynthesis of leukotriene and lipid mediators involved in asthma. Consequently, ingredients in Module 1 can contribute to the cure of asthma by the steroid metabolism.

Ingredients in Module 2 were highly related to immune and inflammation processes and are core module for the therapy of asthma. Among the frequent pathways of Module 2, hyperactivation of EGFR signaling pathway was commonly involved in the mucous hypersecretion and initiated the activation of ERK1/2, PI3K, and Akt kinase in chronic inflammation of the airway [60]. In the pathway of angiotensin signaling via PYK2, PYK2 was essential for inflammatory cell migration and regulated airway inflammation, Th2 cytokine secretion, and airway hyperresponsiveness in the ovalbumin-sensitized mice during antigen challenge [61]. Vascular endothelial growth factor (VEGF) was secreted by human airway smooth muscle cells, and the level of VEGF was elevated by bradykinins through a protein kinase *C* and prostanoid-dependent mechanism [62]. The expression of VEGF and VEGFR in asthma patients increased accompanied by an increased number and size of blood vessels in asthmatic airways [63]. Interleukin-(IL-) 17 may inhibit the induction of tolerance to antigen through inducing IL-6 production, thereby suppressing the expansion of Foxp3-positive regulatory T (Treg) cells [64]. IL-5 is directly involved in recruiting eosinophils to the lung. Once recruited, eosinophils participate in the modulation of immune response, induction of airway hyperresponsiveness, and remodeling in asthma [65].

Function of module 3 is relevant to ion conduction and transport. The intracellular concentration of free ions regulates many cell functions such as secretion, contraction, motility, and transport processes. Ion channels including K and Ca channels modulated the activity of several structural and inflammatory cells and played an important role in the pathophysiology of asthma. These ion channels might serve as novel targets for the treatment of asthma [66]. Chloride channels are expressed on airway smooth muscle and influence airway smooth muscle force and cell length, which play an important role in the airway smooth muscle contraction and relaxation mechanisms. Activation of the ligand-gated chloride channel GABAA relaxed airway smooth muscle with the tachykinin and substance P. Activation of the glycine

Table 4: Module functions.

| Module | Aspect | Enriched items |
|---|---|---|
| 1 | GO process | Response to organic substance<br>Lipid metabolic process<br>Regulation of biological quality<br>Hormone biosynthetic process<br>Androgen metabolic process |
| | GO Molecular functions | Oxidoreductase activity<br>Acting on the CH-CH group of donors<br>Steroid dehydrogenase activity<br>NAD or NADP as acceptor<br>Catalytic activity |
| | GO localizations | Cell fraction<br>Insoluble fraction<br>Membrane fraction<br>Cytoplasmic part<br>Cell body fiber |
| | Pathways | Androstenedione and testosterone biosynthesis and metabolism<br>Immune response_Gastrin in inflammatory response |
| 2 | GO process | Developmental process<br>Regulation of cell death<br>Response to organic substance<br>Positive regulation of developmental process<br>Response to stress |
| | GO molecular functions | Regulatory region nucleic acid binding<br>Transcription factor binding<br>Protein binding<br>Regulatory region DNA binding |
| | GO localizations | Insoluble fraction<br>Cell projection<br>Dendrite<br>Neuron projection |
| | Pathways | EGFR signaling pathways<br>IL-17 signaling pathways<br>Immune response_C5a signaling<br>Immune response_IL-3 activation and signaling pathway<br>Immune response_IL-5 signalling<br>Immune response_IL-6 signaling pathway<br>Apoptosis and survival_Role of CDK5 in neuronal death and survival<br>Development_VEGF signaling via VEGFR2-generic cascades<br>Mucin expression in CF via IL-6<br>Mucin expression in CF via TLRs |
| 3 | GO process | Aminoglycoside antibiotic metabolic process<br>Synaptic transmission<br>Gamma-aminobutyric acid signaling<br>Inorganic anion transport<br>Multicellular organismal process |
| | GO molecular functions | Alcohol dehydrogenase (NADP+) activity<br>Ligand-gated channel activity<br>Benzodiazepine receptor activity<br>GABA receptor activity<br>Chloride transmembrane transporter activity<br>Passive transmembrane transporter activity |
| | GO localizations | Ion channel complex<br>Chloride channel complex<br>Neuronal cell body membrane<br>Cell body membrane<br>Synaptic membrane |
| | Pathways | Triacylglycerol metabolism p.1<br>Immune response_MIF-mediated glucocorticoid regulation |

Table 5: Module-herb relation.

| Module | Herbs |
|---|---|
| 1 | FHE, SAA, FEL, SC, and RL |
| 2 | PFL, PFS, SAA, Lum, PC, AGB, and RL |
| 3 | PFL, FHE, FEL, and RL |
| 4 | FHE |
| 5 | Lum, PC |
| 6 | FEL |

receptor was shown to relax airway smooth muscle with a selective neurokinin 2 receptor agonist [67].

Therefore, it can be inferred that different ingredients in the same module cooperate with each other to achieve certain effects; ingredients within each module act on targets with similar functions and play roles in related pathways. In the meantime, different modules with distinctive functions play different roles in the treatment to achieve overall effects by affecting different biological processes.

In addition, we were also interested in the relationship between modules and herbs, and we got the related herbs for each module as shown in Table 5 by finding out herbs which are connected with the ingredients of the module in the herb-ingredient network (Figure 5). The result suggests that the ingredients of a module are mainly from different herbs. This result, together with the herb-ingredient network, can reveal that although different herbs have distinctive ingredients, they can collaborate with each other through ingredients with similar curative effects.

*3.6. The Mechanism of the Treatment of Feature Zhengs Based on the Module Functions.* According to the network-based analyses of the ingredients of the key herbs, we infer that ingredients from different herbs can restore the healthy state by influencing multiple targets with different functions, and the ingredients share certain biological functions to collaborate with each other to obtain the therapeutic effects. By further mining the latent biology knowledge from the ingredient-network modules, the mechanism of the treatment of the feature Zhengs "FengXieFanFei," "FeiQiShiXuan," and "QiDaoLuanJi" was explained from three aspects.

(1) The treatment has effects on the steroid metabolism which play a role in the treatment of asthma.

(2) The treatment is highly related to immune and inflammation processes by influencing the pathways of EGFR, VEGF, Gn-RH, IL-17, and so forth, all of which play critical roles in asthma.

(3) Regulation of ion conduction and transport, which can promote relaxation of airway smooth muscle and modulate the activity of structural and inflammatory cells, respectively, is another critical part in the treatment for the feature Zhengs.

## 4. Conclusions

TCM experts have accumulated many TCM clinical cases which contain meaningful treatment experiences and rules. To uncover the mechanism of treatment of Zhengs, systematical analyses about the clinical cases for patients with CVA have been done. The results can be shown from the following six aspects.

(1) The feature Zhengs of CVA are "FengXieFanFei," "FeiQiShiXuan," and "QiDaoLuanJi."

(2) Eleven key herbs which not only play key roles by isolation analysis but also cooperate with each other frequently are SAA, Lum, PFL, PC, AGB, AT, FEJ, SC, PFS, RL, and FHE.

(3) There are 18 functional clusters based on 372 reliable potential targets which are targeted by more than 7 compounds of the key herbs.

(4) An herb-ingredient network was constructed, and we can catch sight of the composition features of herbs from the network.

(5) An ingredient network, in which each ingredient was assigned functional items based on the enrichment analyses of potential targets in respect to GOs and pathways, was also constructed. It can present the functional relations of ingredients as well as getting the latent interaction mechanism.

(6) Modules of the ingredient network which can show the latent collaboration among ingredients were identified, and main functions of the modules can help to illustrate the mechanism of the key herbs.

Herbal medicine is a complex system which can restore the state of patients back to a health level by influencing multiple bioprocesses [68]. The mechanism of the treatment of Zhengs which is highly related to the key herbs can be explained indirectly by analysis of the corresponding herbs.

In this work, we have discussed the functions of ingredients and targets of the key herbs and identified different target clusters and ingredient modules, which can provide evidence for explanations of the treatment of CVA. Since these key herbs are most commonly used for the treatment of the feature Zhengs "FengXieFanFei," "FeiQiShiXuan," and "QiDaoLuanJi," the mechanism of the treatment of these Zhengs must agree with the actions of these key herbs.

Based on the systematic analyses of key herbs, we have illustrated that the therapeutic effects of "FengXieFanFei," "FeiQiShiXuan," and "QiDaoLuanJi" were achieved by ingredients with similar functions in three main aspects as below.

(1) The treatment has impacts on the metabolic processes of steroid.

(2) The treatment is highly related to the immune and inflammation processes by influencing the pathways of EGFR, VEGF, Gn-RH, IL-17, and so on, all of which play critical roles in asthma.

(3) Except for the two main functions above, the treatment also has effects on the regulation of ion conduction and transport.

In general, compared to Western drugs, TCM therapy aims to correct maladjustments and restore the self-regulatory ability of the body by influencing targets with multiple pathogenic effects. This systematical study provides a new conceptual framework for multilevel explanations and scientific understanding for the mechanism of TCM treatment and thus can promote the scientific understanding of TCM theory. However, considering the insufficiency of complete collections of the compositions of herbs and the prediction of targets, the mechanism still requires further rigorous studies.

## Conflict of Interests

The authors declare that they do not have a direct financial relation with any commercial identity including the ones mentioned in the paper. None of the authors have a conflict of interests to declare.

## Authors' Contribution

Di Chen, Fangbo Zhang, and Shihuan Tang contributed equally to this work.

## Acknowledgments

This work was supported by the Special Research Foundation for Traditional Chinese Medicine (Grant no. 200907001-5), the National Science Foundation for Postdoctoral Scientists of China (Grant no. 2012M510733), and the National Science Foundation of China (Grant no. 81303152).

## References

[1] P. P. Song, J. J. Gao, N. Kokudo, and W. Tang, "Standardization of traditional Chinese medicine and evaluation of evidence from its clinical practice," *Drug Discoveries & Therapeutics*, vol. 5, no. 6, pp. 261–265, 2011.

[2] L. Guo, Y.-Y. Wang, Z.-B. Zhang, and J.-L. Zhang, "Origination and development of syndrome concept in traditional Chinese medicine," *Zhong Xi Yi Jie He Xue Bao*, vol. 4, no. 4, pp. 335–338, 2006.

[3] Z. B. Zhang and Y. Y. Wang, "Research on TCM syndrome nomenclature and classification: review and hypothesis," *Journal of Beijing University to Traditional Chinese Medicine*, vol. 26, no. 2, pp. 1–5, 2003.

[4] S. Li, "Framework and practice of network-based studies for Chinese herbal formula," *Zhong Xi Yi Jie He Xue Bao*, vol. 5, no. 5, pp. 489–493, 2007.

[5] M. Spinella, "The importance of pharmacological synergy in psychoactive herbal medicines," *Alternative Medicine Review*, vol. 7, no. 2, pp. 130–137, 2002.

[6] B. Li, X. Xu, X. Wang et al., "A systems biology approach to understanding the mechanisms of action of Chinese herbs for treatment of cardiovascular disease," *International Journal of Molecular Science*, vol. 13, no. 10, pp. 13501–13520, 2012.

[7] B. C. Shin, S. Kim, and Y. H. Cho, "Syndrome pattern and its application in parallel randomized controlled trials," *Chinese Journal of Integrative Medicine*, vol. 3, pp. 163–171, 2012.

[8] W. G. Meng, L. Shi, L. Y. Wu, L. Y. Lai et al., "Clinical research on treatment of migraine with pine needle moxibustion," *Zhongguo Zhen Jiu*, vol. 32, no. 6, pp. 519–522, 2012.

[9] Y.-H. Zhou, K.-M. Wei, L.-Y. He et al., "Multi-central clinical research into treating 80 cases of chronic thrombocytopenia with qi-supplementing and yin-nourishing therapy and western medicine," *Journal of Traditional Chinese Medicine*, vol. 31, no. 4, pp. 277–281, 2011.

[10] S. Li, "Network systems underlying traditional Chinese medicine syndrome and herb formula," *Current Bioinformatics*, vol. 4, no. 3, pp. 188–196, 2009.

[11] N. Nieto, "A systems biology approach for understanding the collagen regulatory network in alcoholic liver disease," *Liver International*, vol. 32, no. 2, pp. 189–198, 2012.

[12] S. Ekins, Y. Nikolsky, and T. Nikolskaya, "Techniques: application of systems biology to absorption, distribution, metabolism, excretion and toxicity," *Trends in Pharmacological Sciences*, vol. 26, no. 4, pp. 202–209, 2005.

[13] A. Bugrim, T. Nikolskaya, and Y. Nikolsky, "Early prediction of drug metabolism and toxicity: systems biology approach and modeling," *Drug Discovery Today*, vol. 9, no. 3, pp. 127–135, 2004.

[14] S. Ekins, E. Kirillov, E. A. Rakhmatulin, and T. Nikolskaya, "A novel method for visualizing nuclear hormone receptor networks relevant to drug metabolism," *Drug Metabolism and Disposition*, vol. 33, no. 3, pp. 474–481, 2005.

[15] J. Scheiber, B. Chen, M. Milik et al., "Gaining insight into off-target mediated effects of drug candidates with a comprehensive systems chemical biology analysis," *Journal of Chemical Information and Modeling*, vol. 49, no. 2, pp. 308–317, 2009.

[16] D. Johnson and L. M. Osborn, "Cough variant Asthma: a review of the clinical literature," *Journal of Asthma*, vol. 28, no. 2, pp. 85–90, 1991.

[17] H. Matsumoto, R. P. Tabuena, A. Niimi et al., "Cough triggers and their pathophysiology in patients with prolonged or chronic cough," *Allergology International*, vol. 61, no. 1, pp. 123–132, 2012.

[18] H. Matsumoto, A. Niimi, M. Takemura et al., "Features of cough variant Asthma and classic Asthma during methacholine-induced brochoconstriction: a cross-sectional study," *Cough*, vol. 5, no. 1, article 3, 2009.

[19] J. C. Martínez Alonso, A. Callejo Melgosa, M. J. Fuentes Gonzalo, and C. Martín García, "Rhinitis and Asthma due to ranitidine," *Journal of Investigational Allergology & Clinical Immunology*, vol. 16, no. 2, pp. 142–143, 2006.

[20] P. Sangsupawanich, V. Chongsuvivatwong, L. Mo-Suwan, and C. Choprapawon, "Relationship between atopic dermatitis and wheeze in the first year of life: analysis of a prospective cohort of Thai children," *Journal of Investigational Allergology & Clinical Immunology*, vol. 17, no. 5, pp. 292–296, 2007.

[21] S. W. Christensen, J. P. Bonde, and Ø. Omland, "A prospective study of decline in lung function in relation to welding emissions," *Journal of Occupational Medicine and Toxicology*, vol. 3, no. 1, article 6, 2008.

[22] I. Mohebbi, E. Hassani, S. Salarilak, and A. R. Bahrami, "Do bullae and emphysema increase risk of pneumothorax in silicosis?" *Journal of Occupational Medicine and Toxicology*, vol. 2, no. 1, article 8, 2007.

[23] M. Ashburner, C. A. Ball, J. A. Blake et al., "Gene ontology: tool for the unification of biology," *Nature Genetics*, vol. 25, no. 1, pp. 25–29, 2000.

[24] J. Q. Wu, Y. Chen, H. C. Zhang et al., "Characteristic of therapy used by professor CHAO En-xiang for treatment of pulmonary

system diseases," *China Journal of Traditional Chinese Medicine and Pharmacy*, vol. 22, no. 10, pp. 688–690, 2007.

[25] Y. L. Li, E. X. Chao, and S. W. L, "Cognition of cough variant Asthma from essence of disease," *China Journal of Traditional Chinese Medicine and Pharmacy*, vol. 21, no. 12, pp. 780–781, 2006.

[26] P. Lu, J. Li, S. H. Tang et al., "Development and application of traditional Chinese medicine inheritance support system," *Chinese Journal of Experimental Traditional Medical Formulae*, vol. 18, no. 9, pp. 1–4, 2012.

[27] S. Yu, Z. Guo, Y. Guan et al., "Combining ZHENG theory and high-throughput expression data to predict new effects of Chinese herbal formulae," *Evidence Based Complement and Alternative Medicine*, vol. 2012, Article ID 986427, 8 pages, 2012.

[28] S. Li, B. Zhang, D. Jiang, Y. Wei, and N. Zhang, "Herb network construction and co-module analysis for uncovering the combination rule of traditional Chinese herbal formulae," *BMC Bioinformatics*, vol. 11, no. 11, p. S6, 2010.

[29] J. Li, R. G. Wu, F. Y. Meng et al., "Synergism and rules from combination of Baicalin, Jasminoidin and Desoxycholic acid in refined Qing Kai Ling for treat ischemic stroke mice model," *PLoS ONE*, vol. 7, no. 9, Article ID e45811, 2012.

[30] S. Wang, Y. Hu, W. Tan et al., "Compatibility art of traditional Chinese medicine: from the perspective of herb pairs," *Journal of Ethnopharmacology*, vol. 143, no. 2, pp. 412–423, 2012.

[31] H. Z. Yang and Y. P. Gong, "Progress and thinking on the herb-pairs of Chinese medicine," *Zhongguo Zhong Xi Yi Jie He Za Zhi*, vol. 30, no. 2, pp. 218–220, 2010.

[32] R. Agrawal and R. Srikant, "Fast algorithms for mining association rules," in *Proceedings of the 20th International Conference on Very Large Databases*, 1994.

[33] P. Imming, C. Sinning, and A. Meyer, "Drugs, their targets and the nature and number of drug targets," *Nature Reviews Drug Discovery*, vol. 5, no. 10, pp. 821–834, 2006.

[34] M. A. Lindsay, "Finding new drug targets in the 21st century," *Drug Discovery Today*, vol. 10, no. 23-24, pp. 1683–1687, 2005.

[35] F. Sams-Dodd, "Target-based drug discovery: is something wrong?" *Drug Discovery Today*, vol. 10, no. 2, pp. 139–147, 2005.

[36] J. W. Godden, L. Xue, J. Bajorath et al., "Combinatorial preferences affect molecular similarity/diversity calculations using binary fingerprints and tanimoto coefficients," *Journal of Chemical Information and Computer Sciences*, vol. 40, no. 1, pp. 163–166, 2000.

[37] D. W. Huang, B. T. Sherman, and R. A. Lempicki, "Bioinformatics enrichment tools: paths toward the comprehensive functional analysis of large gene lists," *Nucleic Acids Research*, vol. 37, no. 1, pp. 1–13, 2009.

[38] M. E. Smoot, K. Ono, J. Ruscheinski, P.-L. Wang, and T. Ideker, "Cytoscape 2.8: new features for data integration and network visualization," *Bioinformatics*, vol. 27, no. 3, pp. 431–432, 2011.

[39] M. E. J. Newman, "Modularity and community structure in networks," *Proceedings of the National Academy of Sciences of the United States of America*, vol. 103, no. 23, pp. 8577–8582, 2006.

[40] M. Girvan and M. E. J. Newman, "Community structure in social and biological networks," *Proceedings of the National Academy of Sciences of the United States of America*, vol. 99, no. 12, pp. 7821–7826, 2002.

[41] J. P. Fratkin, "Improved outcomes when combining TCM with western interventions for cancer," *Acupuncture Today*, vol. 6, no. 9, p. 205, 2005.

[42] X. Zheng, X. Zhao, R. Yang, S. Wang, Y. Wei, and J. Zheng, "$\beta$2-Adrenoceptor affinity chromatography and its application in the screening of the active compounds from Semen Armeniacae Amarum," *Chinese Science Bulletin*, vol. 53, no. 6, pp. 842–847, 2008.

[43] W. C. W. Wong, A. Lee, A. T. Lam et al., "Effectiveness of a Chinese herbal medicine preparation in the treatment of cough in uncomplicated upper respiratory tract infection: a randomized double-blinded placedbo-control trail," *Cough*, vol. 2, p. 5, 2006.

[44] S. N. Xu, M. Y. Zhang, Y. M. Wang et al., "Antitussive, expectorant and antiAsthmatic effects of periostracum cicadae," *Chinese Pharmacological Bulletin*, vol. 23, no. 12, pp. 1678–1679, 2008.

[45] J. H. Chen, Z. H. Xia, and R. X. Tan, "High-performance liquid chromatographic analysis of bioactive triterpenes in Perilla frutescens," *Journal of Pharmaceutical and Biomedical Analysis*, vol. 32, no. 6, pp. 1175–1179, 2003.

[46] J.-H. Ju, L. Zhou, G. Lin, D. Liu, L.-W. Wang, and J.-S. Yang, "Studies on constituents of triterpene acids from Eriobotrya japonica and their anti-inflammatory and antitussive effects," *Zhongguo Yao Xue Za Zhi*, vol. 38, no. 10, pp. 752–757, 2003.

[47] M. Zhu, K. F. Lin, R. Y. Yeung, and R. C. Li, "Evaluation of the protective effects of Schisandra chinensis on Phase I drug metabolism using a CCl4 intoxication model," *Journal of Ethnopharmacology*, vol. 67, no. 1, pp. 61–68, 1999.

[48] C. H. Hsu, C. M. Lu, and T. T. Chang, "Efficacy and safety of modified Mai-Men-Dong-Tang for treatment of allergic Asthma," *Pediatric Allergy and Immunology*, vol. 16, no. 1, pp. 76–81, 2005.

[49] Y. P. Zhang, D. Zhao, L. Lin et al., "Clinical study on SuHuang ZhiKe capsule in treating 140 cases of cough variant Asthma," *China Journal of Traditional Chinese Medicine and Pharmacy*, vol. 22, no. 11, pp. 773–776, 2007.

[50] H. M. Li, X. L. Kang, X. Q. Li et al., "Studies on antitussive and antiAsthmatic action of suhuangzhike granules," *Chinese Journal of Experimental Traditional Medical Formulae*, vol. 14, no. 8, pp. 51–53, 2008.

[51] Z. D. Zhang, Y. Zhang, K. Q. Deng et al., "Effect of Suhuangzhike Decoction on immune function in patients with cough variant Asthma," *Journal of Beijing University of Traditional Chinese Medicine*, vol. 30, no. 9, pp. 637–639, 2007.

[52] A. Hamosh, A. F. Scott, J. S. Amberger, C. A. Bocchini, and V. A. McKusick, "Online Mendelian Inheritance in Man (OMIM), a knowledgebase of human genes and genetic disorders," *Nucleic Acids Research*, vol. 33, pp. D514–D517, 2005.

[53] E. A. Townsend, L. W. Meuchel, M. A. Thompson, C. M. Pabelick, and Y. S. Prakash, "Estrogen increases nitric-oxide production in human bronchial epithelium," *Journal of Pharmacology and Experimental Therapeutics*, vol. 339, no. 3, pp. 815–824, 2011.

[54] C. Donovan, X. Tan, and J. E. Bourke, "PPAR$\gamma$ ligands regulate noncontractile and contractile functions of airway smooth muscle: implications for Asthma therapy," *PPAR Research*, vol. 2012, Article ID 809164, 13 pages, 2012.

[55] G. L. Johnson and R. Lapadat, "Mitogen-activated protein kinase pathways mediated by ERK, JNK, and p38 protein kinases," *Science*, vol. 298, no. 5600, pp. 1911–1912, 2002.

[56] Y. S. Shin, K. Takeda, Y. Shiraishi et al., "Inhibition of Pim1 kinase activation attenuates allergen-induced airway hyperresponsiveness and inflammation," *American Journal of Respiratory Cell and Molecular Biology*, vol. 46, no. 4, pp. 488–497, 2012.

[57] V.-A. Oxelius, A.-M. Carlsson, and M. Aurivillius, "Alternative G1m, G2m and G3m allotypes of IGHG genes correlate with atonic and nonatopic pathways of immune regulation in children with bronchial Asthma," *International Archives of Allergy and Immunology*, vol. 115, no. 3, pp. 215–219, 1998.

[58] M. M. Marc, P. Korosec, M. Kosnik et al., "Complement factors C3a, C4a, and C5a in chronic obstructive pulmonary disease and Asthma," *American Journal of Respiratory Cell and Molecular Biology*, vol. 31, no. 2, pp. 216–219, 2004.

[59] M. van der Deen, E. G. E. de Vries, W. Timens, R. J. Scheper, H. Timmer-Bosscha, and D. S. Postma, "ATP-binding cassette (ABC) transporters in normal and pathological lung," *Respiratory Research*, vol. 6, article 59, 2005.

[60] J. Yang, Q. Li, X. D. Zhou, V. P. Kolosov, and J. M. Perelman, "Naringenin attenuates mucous hypersecretion by modulating reactive oxygen species production and inhibiting NF-$\kappa$B activity via EGFR-PI3K-Akt/ERK MAPKinase signaling in human airway epithelial cells," *Molecular and Cellular Biochemistry*, vol. 351, no. 1-2, pp. 29–40, 2011.

[61] Y. Duan, J. Learoyd, A. Y. Meliton, B. S. Clay, A. R. Leff, and X. Zhu, "Inhibition of Pyk2 blocks airway inflammation and hyperresponsiveness in a mouse model of Asthma," *American Journal of Respiratory Cell and Molecular Biology*, vol. 42, no. 4, pp. 491–497, 2010.

[62] A. J. Knox, L. Corbett, J. Stocks, E. Holland, Y. M. Zhu, and L. Pang, "Human airway smooth muscle cells secrete vascular endothelial growth factor: up-regulation by bradykinin via a protein kinase C and prostanoid-dependent mechanism," *The FASEB Journal*, vol. 15, no. 13, pp. 2480–2488, 2001.

[63] B. N. Feltis, D. Wignarajah, L. Zheng et al., "Increased vascular endothelial growth factor and receptors: relationship to angiogenesis in Asthma," *American Journal of Respiratory and Critical Care Medicine*, vol. 173, no. 11, pp. 1201–1207, 2006.

[64] H. Kawakami, T. Koya, H. Kagamu et al., "IL-17 eliminates therapeutic effects of oral tolerance in murine airway allergic inflammation," *Clinical and Experimental Allergy*, vol. 42, no. 6, pp. 946–957, 2012.

[65] S. S. Possa, E. A. Leick, C. M. Prado et al., "Eosinophilic inflammation in allergic Asthma," *Frontiers in Pharmacologyogy*, vol. 17, no. 4, p. 46, 2013.

[66] P. Bradding and H. Wulff, "The K+ channels KCa3.1 and Kv1.3 as novel targets for Asthma therapy," *British Journal of Pharmacology*, vol. 157, no. 8, pp. 1330–1339, 2009.

[67] E. A. Townsend, P. D. Yim, G. Gallos et al., "Can we find better bronchodilators to relieve Asthma symptoms?" *Journal of Allergy*, vol. 2012, Article ID 321949, 5 pages, 2012.

[68] C. Wang, Y. Wan, X. Luo et al., "Regulative mechanism of Chinese herbal medicine on cell signaling pathway in kidney," *Zhongguo Zhong Yao Za Zhi*, vol. 36, no. 1, pp. 85–91, 2011.

Hindawi Publishing Corporation
Evidence-Based Complementary and Alternative Medicine
Volume 2013, Article ID 402159, 4 pages
http://dx.doi.org/10.1155/2013/402159

*Review Article*

# Recent Highlights of Metabolomics in Chinese Medicine Syndrome Research

**Ai-hua Zhang, Hui Sun, Shi Qiu, and Xi-jun Wang**

*National TCM Key Laboratory of Serum Pharmacochemistry, Key Laboratory of Metabolomics and Chinmedomics, Department of Pharmaceutical Analysis, Heilongjiang University of Chinese Medicine, Heping Road 24, Harbin 150040, China*

Correspondence should be addressed to Ai-hua Zhang; metabonomics@126.com and Xi-jun Wang; metabolomics1@126.com

Received 5 August 2013; Accepted 2 October 2013

Academic Editor: Wei Jia



Chinese medicine syndrome (CMS, "ZHENG" in Chinese) is an understanding of the regularity of disease occurrence and development as well as a certain stage of a comprehensive response of patients with body condition. However, because of the complexity of CMS and the limitation of present investigation method, the research for deciphering the scientific basis and systematic features of CMS is difficult to go further. Metabolomics enables mapping of early biochemical changes in disease and hence provides an opportunity to develop predictive biomarkers. Moreover, its method and design resemble those of traditional Chinese medicine (TCM) which focuses on human disease via the integrity of close relationship between body and syndromes. In the systemic context, metabolomics has a convergence with TCM syndrome; therefore it could provide useful tools for exploring essence of CMS disease, facilitating personalized TCM, and will help to in-depth understand CMS. The integration of the metabolomics and CMS aspects will give promise to bridge the gap between Chinese and Western medicine and help catch the traditional features of CMS. In this paper, particular attention will be paid to the past successes in applications of robust metabolomic approaches to contribute to low-molecular-weight metabolites (biomarkers) discovery in CMS research and development.

## 1. Introduction

Metabolomics is a powerful new technology that allows for the assessment of global metabolic profiles in easily accessible biofluids and biomarker discovery in order to distinguish between diseased and nondiseased status information [1]. Combining metabolomic data with multivariate data analysis tools allows us to study alterations in metabolic pathways following different perturbations. Metabolite changes that are observed in diseased individuals as a primary indicator have been an important part of clinical practice. Most clinical chemistry tests available today rely on old technologies, and these tests are neither sensitive nor specific for any particular disease and traditional markers only increase significantly after substantial disease injury [2]. Therefore, more sensitive markers of disease are eagerly needed, particularly, for the early detection of disease, and highly sensitive and specific biomarkers as primary indicators are relatively more useful [3–5]. Discovery of clinically relevant biomarkers for diseases has revealed metabolomics has potential advantages that classical diagnostic approaches do not.

Traditional Chinese medicine (TCM) has been practiced for thousands of years and attracted worldwide interest, based on a holistic view that cure diseases through establishment of equilibrium in the human life [7]. The major advantage of TCM is treatment based on the treatment of differential syndrome (TDS, diagnosis, and treatment based on an overall symptoms and signs) [8]. Syndrome in TCM is the comprehensive analysis of clinical information gained by the four main diagnostic TCM procedures: observation, listening, questioning, and pulse analysis [9]. Currently lack of an easy-to-use and inexpensive sampling method and lack of an accurate and portable platform to facilitate early syndrome detection are the major limitations that have prevented people from recognizing the full potential of TCM and have seriously hampered the development of clinical diagnostics. Fortunately, the integrative approach of metabolomics is in line with the holistic concept and practices of TCM

and will gain a revolution in understanding of essence of CMS [10]. Some characteristic examples are presented to highlight the application of this platform to CMS research and development as well as some of the necessary milestones for moving TCM into mainstream health care.

## 2. Advantages of Metabolomics

Metabolomics has recently moved into one of the cornerstones of postgenomics for the quantitative analysis and unbiased identification of small molecule metabolites within an organism, processes important in clinical medicine. It can incorporate the most advanced technology to provide the ideal platform for the discovery of biomarkers regarding multifactorial diseases. The metabolites could yield important information about a person's health or disease. More specifically, metabolomics has a global and noninvasive analysis of biomarkers that are indicators of normal biological or pathogenic process, or response to therapeutic intervention, thereby helping to monitor treatment response [11]. Intimately, these large-scale analyses of metabolites are bound to novel mass spectrometry (MS) technology analyzers with the combination of hyphenated techniques [12]. Approaches of either HPLC or UPLC online with MS have recently been employed and became increasingly popular [13]. The most commonly used noninvasive techniques are an essential requirement; thus urine is particularly and ideally suited for large-scale research of metabolomic analysis even in small volume. Metabolites that can serve as diagnostic markers have also increased, as has the fact that these biomarkers may be useful in following and predicting disease progression or response to therapy, some of which may be molecular targets for therapeutic intervention [14]. Over the last few years, the progression made in metabolomics has provided insightful information on disease development and disease onset prediction [15].

## 3. Bringing Metabolomics into the Forefront of TCM

TCM is one of the rarely existing ancient traditional medicines that hold systematic theories as well as preventative and therapeutic methods for diseases in practice. Nowadays, there is strong evidence that the TCM has increasing popularity throughout the world, which especially shows great superiority in early intervention, combination therapies, disease control, personalized medicine, and so forth [16]. The focuses of TCM science are on the patient rather than disease. The syndrome is one of the most important concepts and ingredients in the theoretical and clinical research of TCM. TDS is basic principle of understanding and treatment of diseases in TCM. Syndrome, key term in TCM theory, is an outcome after a careful analysis of all symptoms and signs. Syndrome embodies the integrity status of the whole body condition in a specific time, space, environment, and pathogenic factors. These factors include the genetic, physiological, pathological, psychological, spiritual, social, and other aspects of the individuals. Disease treatment based on the syndrome differentiation is to determine the appropriate treatment. TCM treatment of disease does not primarily focus on the "the similarities and differences of disease" but rather focus on the difference of syndrome through TDS and better understanding of disease. The introduction of powerful new technologies should greatly accelerate the pace of personalized TCM. In this context, there are many new opportunities and challenges for the TCM research in postgenome era.

A syndrome is often understood in terms of the overall state of the body under the internal and external factors of the body combined with the environment, as well as changes with the course of development [17]. It is involved in multifactor and multilevel manners with the overall emergence of complex systems. Syndrome differentiation is the method of recognizing and diagnosing diseases or body imbalances by analyzing patient information based on TCM theories and experiences of doctors. The occurrence and development of a syndrome, which reflect pathological changes in some stages of disease development, inevitably affect human metabolism and change chemical substances in body fluids. From the perspective of systems biology, a syndrome may be a specific state in which protein networks and gene regulatory networks are "disturbed." Such disturbances may be reflected by changes in the endogenous composition, which can be secreted into the blood and urine [18]. Metabolomics incorporates a "top-down" strategy to reflect the terminal symptoms of a whole system caused by interventions in the holistic context, assesses holistic metabolic profiles in easily accessible biofluids, and facilitates biomarker discovery. The distinct features of syndrome and diagnostic model have constantly challenged the methodology. Many problems still exist in current studies, such as the standard of CM syndrome differentiation, the design methodology, and criteria to assess the efficacy of interventions. Metabolomics has been gradually introduced to CMS studies, making it more scientific.

Combining the metabolomics with in-depth investigations of CMS mechanisms will enable a revolution in our understanding of disease pathology and will advance TCM. Metabolomics studies living systems from whole systems instead of isolated parts and opens up a novel opportunity to reinvestigate TCM. Adoption of metabolomics approach would do much help for exploring the scientific connotation of CMS and revolutionizing personalized TCM. There are new signs that the pursuit of both TCM and metabolomics will be a priority for people and advances paving the way towards personalized health care.

## 4. Metabolomic Dissection of CMS

The key problem in the CMS research is how to establish a new approach to fit the potential law of CMS. Fortunately, the rapid development of metabolomics technology platforms provides a methodological basis for deep understanding of the essence of CMS. Metabolomics takes a global or system thinking of the human body and appears to be the holistic view of TCM. Presently, a growing body of evidence demonstrates that metabolomics has been used to explore

the particular metabolites and potential biomarkers and pathways of CMS, indicating that it is important to impact our understanding of the theory that is based on the evidenced TCM [19]. Particularly, for the early detection of disease, highly sensitive and specific biomarkers as primary indicators in biofluids are relatively more useful because those can be used for nonbiopsy tests. Analyzing and verifying the specifically early biomarkers of a disease, metabolomics enables us to better understand pathological processes and substance metabolic pathways. Compared with traditional diagnostic methods, even little changes of metabolites can help to detect early pathologic changes more sensitively.

With the increasing pace of modern life, many people have been suffering from liver diseases commonly complicated by jaundice syndrome (JS) that is a common disease in China. JS, a common and fatal disease requiring early diagnosis and treatment, mainly involves two subtypes of TCM syndromes, YangHuang (YAH) and YinHuang (YIH). YAH is related to the dysfunction of liver, spleen, stomach, and gall bladder and seems to be acute viral hepatitis. YIH is the body function decline caused by excessive metabolic activity, like the case of obstructive jaundice. Measuring levels of alanine aminotransferase, aspartate aminotransferase, and so forth in blood samples have been the main diagnostic standard for JS. However, sensitivity of these markers is relatively low. Fortunately, metabolomics has been used to explore the particular metabolites, potentially diagnostic and prognostic biomarkers and pathways of syndrome. In an article currently published in *Mol Cell Proteomics* [2012; 11(8):370-80], Wang and coworkers used UPLC-Q-TOF-HDMS combined with pattern recognition methods to investigate a comprehensive metabolome of JS in order to establish specific metabolites phenotype and generate a better understanding of the pathophysiology [20]. Results indicate that JS related metabolites play an essential role in glutamate metabolism, synthesis, and degradation of ketone bodies, alanine, and aspartate metabolism, which are tightly correlated with the genes of neurotransmitters, hormones, and cytokines in the metabolites interaction network. Interestingly, 44 distinct metabolites identified from these pathways are in various stages of progress at the JS. Furthermore, vitamin B6 metabolism, tryptophan metabolism, arginine, and proline metabolism were also the top functions listed by MetaboAnalyst for YAH patient. Significant changes associated with YAH disease, defined as metabolite changes in YAH versus controls, were identified for 40 metabolites that are potential candidates for biomarkers. Additionally, steroid hormone biosynthesis, primary bile acid biosynthesis, cysteine, and methionine metabolism were all related to YIH. It is noteworthy that 49 metabolites together are important for the host response to YIH through target metabolism pathways. The results not only indicated that metabolomics had sufficient sensitivity and specificity to distinguish JS from healthy controls but also contributed to a further understanding of disease mechanisms.

Understanding syndromes is a core research to develop more efficient therapeutic strategies and diagnostic criteria for patients. Clinical evidence has shown that patients with liver-stagnation and spleen-deficiency syndrome (LSS) that characterized by metabolic disorder of body fluid, and causing liver failure and weakness. It is difficult to get outcome immediately and not particularly effective in separating cases of LSS from other non-LSS disorders. Development of biomarkers with higher sensitivity and specificity is waiting to emerge. Recent advances in metabolomic technology made it possible to identify the metabolites in the clinical samples and thus extensive efforts are now attempted to search for the biomarkers. Metabolite profiling of urine samples collected from patients with LSS and healthy controls was performed by UPLC-Q-TOF-HDMS in conjunction with multivariate data analysis and ingenuity pathway analysis that were used to select the metabolites to be used for the noninvasive diagnosis of LSS [21]. Twelve urinary differential metabolites contributing to the complete separation of LSS patients from matched healthy controls were identified involving several key metabolic pathways. Of note, of the differential metabolites, 4 metabolite markers could provide the effective diagnosis for human LSS. A prediction model was developed to indicate LSS, and an accuracy of 93.0% was obtained and suggested that metabolomics is highly effective in aiding biomarker identification and thus implies a new strategy in the diagnosis of LSS. These observations support that metabolomics is an ideal approach to reveal the scientific and intrinsic connotation of TCM syndromes also opens new perspectives to resolve special TCM issues.

## 5. Conclusion and Future Perspectives

Metabolomics is the comprehensive assessment of endogenous metabolites and attempts to systematically identify and quantify metabolites from a biological sample. Small-molecule metabolites have an important role in biological systems and represent attractive candidates to understand disease phenotypes. One area of considerable interest in the field of metabolomics is to detect potential biomarkers associated with diseases, and the metabolic profiling could provide global changes of endogenous metabolites of patients. The future goals for metabolomics are the validation of existing biomarkers, in terms of mechanism and translation to man, together with a focus on characterizing the individual healthcare. Under the guidance of the TCM theory, the metabonomics approach can be used to evaluate clinical syndromes and identify potential biomarkers [22]. The integral metabolomics is the best to fit the holistic concept of multitargets and systems of TCM theory; therefore it may be one of the best methods to study the TCM science. Widespread use of this technique would significantly advance the field of TCM by bridging the gap between Chinese and Western medicine. It is conceivable that the application of metabolomic platforms will eventually lead to the reconciliation and integration of TCM with contemporary medicine and systems medicine. In summary, integration of metabolomics-based diagnostic principles into the TCM would make it possible to interpret and explore the essence of personalized TCM and might be the direction to enable a revolution for future health care, and also perhaps it is time to embrace the arrival of "TCM-OMICS" era in Chinese medicine research.

## Conflict of Interests

The authors have declared that they have no conflict of interests.

## Acknowledgments

This work was supported by grants from the Key Program of Natural Science Foundation of State (Grant no. 90709019, 81173500, 81373930, 81302905, 81102556, and 81202639), National Key Technology Research and Development Program of the Ministry of Science and Technology of China (Grant no. 2011BAI03B03, 2011BAI03B06, and 2011BAI03B08), Key Science and Technology Program of Heilongjiang Province, China (Grant no. GC06C501, GA08C303, and GA06C30101), Foundation of Heilongjiang University of Chinese Medicine (Grant no. 201209), and National Key Subject of Drug Innovation (Grant no. 2009 ZX09502-005).

## References

[1] J. K. Nicholson and J. C. Lindon, "Systems biology: metabonomics," *Nature*, vol. 455, no. 7216, pp. 1054–1056, 2008.

[2] T. Hyötyläinen, "Novel methodologies in metabolic profiling with a focus on molecular diagnostic applications," *Expert Review of Molecular Diagnostics*, vol. 12, no. 5, pp. 527–538, 2012.

[3] A. Sreekumar, L. M. Poisson, T. M. Rajendiran et al., "Metabolomic profiles delineate potential role for sarcosine in prostate cancer progression," *Nature*, vol. 457, no. 7231, pp. 910–914, 2009.

[4] G. Yan, A. Zhang, H. Sun et al., "Dissection of biological property of Chinese acupuncture point zusanli based on long-term treatment via modulating multiple metabolic pathways," *Evidence-Based Complementary and Alternative Medicine*, vol. 2013, Article ID 429703, 10 pages, 2013.

[5] A. H. Zhang, H. Sun, Y. Han et al., "Ultraperformance liquid chromatography-mass spectrometry based comprehensive metabolomics combined with pattern recognition and network analysis methods for characterization of metabolites and metabolic pathways from biological data sets," *Analytical Chemistry*, vol. 85, no. 15, pp. 7606–7612, 2013.

[6] A. H. Zhang, H. Sun, and X. J. Wang, "Recent advances in metabolomics in neurological disease, and future perspectives," *Analytical and Bioanalytical Chemistry*, vol. 405, no. 25, pp. 8143–8150, 2013.

[7] A. Zhang, H. Sun, and X. Wang, "Potentiating therapeutic effects by enhancing synergism based on active constituents from traditional medicine," *Phytotherapy Research*, 2013.

[8] K. Lan, G. Xie, and W. Jia, "Towards polypharmacokinetics: pharmacokinetics of multicomponent drugs and herbal medicines using a metabolomics approach," *Evidence-Based Complementary and Alternative Medicine*, vol. 2013, Article ID 819147, 12 pages, 2013.

[9] H. Sun, A. Zhang, and X. Wang, "Potential role of metabolomic approaches for Chinese medicine syndromes and herbal medicine," *Phytotherapy Research*, vol. 26, no. 10, pp. 1466–1471, 2012.

[10] X. Wang, A. Zhang, and H. Sun, "Future perspectives of chinese medical formulae: chinmedomics as an effector," *OMICS*, vol. 16, no. 7-8, pp. 414–421, 2012.

[11] C. Lu, X. Liu, X. Ding et al., "A metabolomics profiling study in hand-foot-and-mouth disease and modulated pathways of clinical intervention using liquid chromatography/quadrupole time-of-flight mass spectrometry," *Evidence-Based Complementary and Alternative Medicine*, vol. 2013, Article ID 647452, 10 pages, 2013.

[12] A. Zhang, H. Sun, P. Wang, Y. Han, and X. Wang, "Modern analytical techniques in metabolomics analysis," *Analyst*, vol. 137, no. 2, pp. 293–300, 2012.

[13] X. Wang, H. Sun, A. Zhang, P. Wang, and Y. Han, "Ultra-performance liquid chromatography coupled to mass spectrometry as a sensitive and powerful technology for metabolomic studies," *Journal of Separation Science*, vol. 34, no. 24, pp. 3451–3459, 2011.

[14] A. Zhang, H. Sun, and X. Wang, "Serum metabolomics as a novel diagnostic approach for disease: a systematic review," *Analytical and Bioanalytical Chemistry*, vol. 404, no. 4, pp. 1239–1245, 2012.

[15] B. Yang, A. Zhang, H. Sun et al., "Metabolomic study of insomnia and intervention effects of Suanzaoren decoction using ultra-performance liquid-chromatography/electrospray-ionization synapt high-definition mass spectrometry," *Journal of Pharmaceutical and Biomedical Analysis*, vol. 58, no. 1, pp. 113–124, 2012.

[16] A. Zhang, H. Sun, Z. Wang, W. Sun, P. Wang, and X. Wang, "Metabolomics: towards understanding traditional Chinese medicine," *Planta Medica*, vol. 76, no. 17, pp. 2026–2035, 2010.

[17] A. Zhang, H. Sun, and X. Wang, "Recent highlights of metabolomics for traditional Chinese medicine," *Pharmazie*, vol. 67, no. 8, pp. 667–675, 2012.

[18] X. Wang, H. Sun, A. Zhang, W. Sun, P. Wang, and Z. Wang, "Potential role of metabolomics apporoaches in the area of traditional Chinese medicine: as pillars of the bridge between Chinese and Western medicine," *Journal of Pharmaceutical and Biomedical Analysis*, vol. 55, no. 5, pp. 859–868, 2011.

[19] X. Wang, Q. Wang, A. Zhang et al., "Metabolomics study of intervention effects of Wen-Xin-Formula using ultra high-performance liquid chromatography/mass spectrometry coupled with pattern recognition approach," *Journal of Pharmaceutical and Biomedical Analysis*, vol. 74, pp. 22–30, 2013.

[20] X. Wang, A. Zhang, Y. Han et al., "Urine metabolomics analysis for biomarker discovery and detection of jaundice syndrome in patients with liver disease," *Molecular & Cellular Proteomics*, vol. 11, no. 8, pp. 370–380, 2012.

[21] A. Zhang, H. Sun, Y. Han et al., "Exploratory urinary metabolic biomarkers and pathways using UPLC-Q-TOF-HDMS coupled with pattern recognition approach," *Analyst*, vol. 137, no. 18, pp. 4200–4208, 2012.

[22] T. Wu, M. Yang, H. F. Wei, S. H. He, S. C. Wang, and G. Ji, "Application of metabolomics in traditional chinese medicine differentiation of deficiency and excess syndromes in patients with diabetes mellitus," *Evidence-Based Complementary and Alternative Medicine*, vol. 2012, Article ID 968083, 11 pages, 2012.

Hindawi Publishing Corporation
Evidence-Based Complementary and Alternative Medicine
Volume 2013, Article ID 302131, 7 pages
http://dx.doi.org/10.1155/2013/302131

*Research Article*

# Curative Effects of ZHENG-Based Fuzheng-Huayu Tablet on Hepatitis B Caused Cirrhosis Related to CYP1A2 Genetic Polymorphism

**Qing-Ya Li,[1,2,3] Zhi-Zhong Guo,[1,2] Xin Deng,[4] Lie-Ming Xu,[5] Yue-Qiu Gao,[5] Wei Zhang,[6] Xiao-Su Wang,[7] Dong-Ying Xue,[8] Yi-Yu Lu,[1] Ping Liu,[9] and Shi-Bing Su[1]**

[1] *Research Center for TCM Complexity System, Shanghai University of TCM, Shanghai 201203, China*
[2] *Key Laboratory of Viral Disease Prevention and Treatment of Traditional Chinese Medicine of Henan Province, Zhengzhou 450008, China*
[3] *Henan University of TCM, Zhengzhou 450008, China*
[4] *Ruikang Hospital of Guangxi University of TCM, Nanning, Guangxi 530011, China*
[5] *Shanghai Shuguang Hospital, Shanghai University of TCM, Shanghai 200021, China*
[6] *Shanghai Longhua Hospital, Shanghai University of TCM, Shanghai 201203, China*
[7] *Shanghai Yueyang Hospital, Shanghai University of TCM, Shanghai 200437, China*
[8] *Shanghai Putuo Hospital, Shanghai University of TCM, Shanghai 200060, China*
[9] *Shanghai University of TCM, Shanghai 201203, China*

Correspondence should be addressed to Shi-Bing Su; shibingsu07@163.com

Received 17 July 2013; Accepted 5 September 2013

Academic Editor: Shao Li



*Aim*. To investigate the correlation of Fuzheng-Huayu tablet (FZHY) efficacy on chronic hepatitis B caused cirrhosis (HBC) and single nucleotide polymorphisms (SNPs) of CYP1A2. *Methods*. After 111 cases of HBC with 69 excess, 21 deficiency-excess, and 21 deficiency ZHENGs (ZHENG, also called traditional Chinese medicine syndrome) were treated by FZHY for 6 months, clinical symptoms, Child-Pugh score, and ZHENG score were observed. Three of the SNPs in CYP1A2 gene were detected and analyzed using SNaPshot assay. *Results*. In ZHENG efficacy between effective and invalid groups, there was significant difference ($P < 0.001$). The ZHENG deficiency was significantly correlated with FZHY efficacy ($P < 0.05$). AA genotype of CYP1A2-G2964A was significantly different with GG genotype ($P < 0.05$) between CYP1A2 Genotypes and FZHY efficacy on ZHENG. More importantly, GA plus AA genotype of CYP1A2-G2964A was significantly different with deficiency ZHENG ($P < 0.05$) between CYP1A2 genotypes and FZHY efficacy on ZHENG. *Conclusion*. FZHY improved ZHENG score of HBC, and these efficacies may relate to CYP1A2-G2964A sites. It was suggested that CYP1A2-G2964A locus is probably a risk factor for ZHENG-based FZHY efficacy in HBC.

## 1. Introduction

Hepatitis B virus (HBV) infection is a major health problem in China. It is one of the important reasons for virus-related liver diseases, such as chronic hepatitis B (CHB), liver cirrhosis (LC), and hepatocellular carcinoma [1]. Worldwide, there are 350 million HBV-infected people who have 15–25% risk of dying from the HBV-caused LC or HCC [2]. Five-year survival rate of patients with severe CHB and its caused cirrhosis is about 50% [3]. Clinically, it lacks the effective drugs for the therapy of hepatitis B which caused cirrhosis (HBC) so far.

ZHENG, also known as traditional Chinese medicine (TCM) syndrome or TCM pattern, is a characteristic profile in clinical manifestations. Clinical treatments rely on the successful differentiation of ZHENG [4]. It has been reported that Fuzheng-Huayu tablet (FZHY), a Chinese herbal medicine formula, affected liver fibrosis [5–7]. Moreover, it was able to halt the progress of liver fibrosis through inhibiting the activation of hepatic satellite cells in animal

Table 1: Clinical data of HBC patients.

| | Patients (%) |
|---|---|
| Gender | |
| Male (%) | 79 (71.17) |
| Female (%) | 32 (28.83) |
| Mean age (yr) | 49.51 ± 10.05 |
| Child-Pugh classification | |
| A | 89 (80.18) |
| B | 20 (18.02) |
| C | 2 (1.80) |
| ZHENG classification | |
| Excess | 69 (62.16) |
| Deficiency-excess | 21 (18.92) |
| Deficiency | 21 (18.92) |

model [8]. Recent study has found that FZHY decreases the levels of HA and ZHENG scores and improves the life quality of HBC patients and the ZHENG differentiation is related to the FZHY treatment [9]. However, the mechanism of FZHY efficacy on HBC is still unclear.

The cytochrome P450 (CYP450) is a vast superfamily of haem-containing monooxygenases. The members of this ubiquitous superfamily play an important role in the metabolism and biosynthesis of a wide range of exogenous drug compounds [10]. Because variations of single nucleotide polymorphisms (SNPs) in human CYP450 genes cause different drug effects and even adverse effects, studies on SNPs of human CYP450 genes can be used for indicating the most possible genes associated with human diseases and relevant therapeutic targets, predicting the drug efficacy and adverse drug response, investigating individual gene specific properties, and then providing personalized and optimal clinic therapies [11]. CYP1A2 is an important member of the cytochrome P450 superfamily [12], and it has been reported that Chinese herbal formula is associated with CYP1A2 genotype [13].

In this study, the aim was to evaluate FZHY efficacy on HBC through the outcome assessment of clinical symptoms, ALT, AST, Child-Pugh score, and ZHENG score and investigate the relationship between the CYP1A2 SNPs and FZHY efficacy on HBC.

## 2. Materials and Methods

*2.1. Study Design.* The study was designed to be a multicenter study, as a clinical outcome assessment, and was carried out to evaluate the efficacy of FZHY, reported in accordance to the 2010 CORSORT statements. The patients were conducted at 6 centers including Longhua, Shuguang, Yueyang, and Putuo hospitals in Shanghai and Ruikang hospital and Guangxi hospital of TCM in Guangxi in China. One-hundred and eleven of HBC patients were given FZHY. It was evaluated to the FZHY efficacy between past and pre treatments through the outcome assessment of clinical symptoms, ALT, AST, Child-Pugh score, and ZHENG score. Moreover, the correlation of CYP1A2 SNPs and FZHY efficacy on HBC between effective and invalid groups was analyzed . The invalid cases were as a control compared with the effective group in FZHY treatment. The study was conducted according to the guidelines of the Declaration of Helsinki and the principles of Good Clinical Practice (China), and we obtained the approval of Medical Ethics Committee in Shanghai Shuguang Hospital. The clinical trial registration number was NCT00543426, which could be found in the website of clinicaltrials.gov.

*2.2. Patients and TCM Diagnosis.* To carry out the study with 127 participants in FZHY group, all patients signed the informed consent before treatment. In the process of followup, 16 patients in FZHY group were lost; thus, data from the other 111 patients in FZHY group were available for analysis.

All of the 111 patients were Chinese yellow race. Their ages were from 18 to 65 years (mean ± SD: 49.51 ± 10.05). There were 79 male cases (71.17%) and 32 female cases (28.83%). The clinical information of HBC patients such as symptoms and signs was collected from the above 6 hospitals, and then ZHENGs were classified into 69 excess, 21 deficiency-excess, and 21 deficiency ZHENGs (Table 1), according to define of diagnosis, and ZHENG differentiation of liver cirrhosis [14]. In order to ensure the repeatability and reliability of ZHENG and symptom diagnoses, all patients were diagnosed by 3 senior TCM physicians separately in the same condition, and the final diagnosis was made by a TCM botanic physician. It was brung into the further study when the diagnoses were consistent.

*2.3. Interventions.* FZHY (SFDA approval no: Z20050546) were prepared and provided by Shanghai Sundise Medicine Technology Development Co., Ltd. (Shanghai, China). There was the same appearance and smell and 0.4 g per tablet in FZHY. The quality control and preparing standardization of FZHY were established and enforced according to previous report [15].

127 patients were conducted at 6 centers. One-hundred and eleven of HBC patients were given FZHY, every day 3 times oral, every time 1.6 g, for a total of takes of 6 months. The FZHY efficacy was evaluated between before and after treatments through the outcome assessment of clinical symptoms, ALT, AST, Child-Pugh score, and ZHENG score.

*2.4. Efficacy Evaluation.* The HBC patients were treated by FZHY for 6 months. The Child-Pugh scores of the HBC were recorded and calculated by rating the following 5 parameters including serum levels of bilirubin and albumin, prothrombin time, ascites and encephalopathy, and divided into class A (5-6 points), B (7–9 points) and C (10–15 points) [16, 17]. The efficacy evaluation of FZHY on HBC was as effective: decrease or no change of Child-Pugh score; invalid: increase of Child-Pugh score.

The efficacy evaluation of ZHENG was according to "Guideline for Clinical New Drug Research in Chinese Herbal Medicine" [18]. The standard of ZHENG outcome was as follows: ZHENG score as without, 0; light, 1; heavy, 2

Table 2: The gene position, polymorphism, and primer sequences of CYP SNPs.

| Gene position | Rs number | Polymorphism | Primer sequences |
|---|---|---|---|
| CYP1A2-733 | rs762551 | C/A | F: 5′-CTACTCCAGCCCCAGAAGTG-3<br>R: 5′-CTGATGCGTGTTCTGTGCTT-3′ |
| CYP1A2-2964 | rs2069514 | G/A | F: 5′-AACACAACGGGACTTCTTGG-3<br>R: 5′-GGCATGACAATTGCTTGAAT-3′ |
| CYP1A2-5347 | rs2470890 | T/C | F: 5′-ATCTACGGGCTGACCATGAA-3<br>R: 5′-CTTGGCCTCCTAAAATGCTG-3′ |

Table 3: Effects of FZHY on ALT, AST, Child-Pugh score, and ZHENG sore in HBC.

| Parameters | FZHY treatment (M ± Q) ($n$ = 111) | | $Z$ | $P^*$ |
|---|---|---|---|---|
| | Before | After | | |
| ALT (U/L) | 34.50 ± 31.75 | 33.00 ± 25.00 | −1.764 | 0.078 |
| AST (U/L) | 43.00 ± 19.62 | 41.00 ± 26.25 | −1.445 | 0.149 |
| Child-Pugh (score) | 5.00 ± 0.00 | 5.00 ± 0.00 | −0.536 | 0.592 |
| ZHENG (score) | 212.5 ± 100.5 | 111.00 ± 15.25 | −7.673 | **0.001** |

*Wilcoxon test.
The bold font emphasizes the result was statistically significant ($P < 0.05$).

points. The calculation formula: the efficacy index of ZHENG ($N$) = (before treatment score − after treatment score)/before treatment score × 100%. The efficacy evaluation standard of TCM syndrome: clinical cure: $N \geq 90\%$; excellent: $N < 90\% \sim >60\%$; effective: $N \leq 60\% \sim >30\%$; invalid: $N \leq 30\%$. In the this study, the effective was $N > 30\%$ including above clinical cure, excellent, and effective.

*2.5. Samples and DNA Extraction.* Blood samples were obtained from all subjects with informed consent and ethical review board approval in accordance with the tenets of the Declaration of Helsinki. Each subject donated 1 mL peripheral blood samples, which were collected in $K_2$EDTA tubes, and then the genomic DNA was isolated from each sample, using the TIANamp Blood DNA Kit (Tiangen Biotech, Beijing, China). Subsequently, the DNA was stored at −80°C for genotype analysis.

*2.6. SNaPshot Assay.* SNPs were genotyped using the ABI PRISM SNaPshot Multiplex Kit (ABI Co., Ltd, CA, USA) and ABI 3730 XL DNA Analyzer. All the analyses were performed as described previously [19]. The primer sequences (Table 2) were selected for amplification. SNaPshot analysis was conducted using an ABI PRISM SNaPshot Multiplex Kit (ABI). Amplification reactions were performed in a thermal cycler for 45 cycles of 20 s denaturing at 96°C, 5 s annealing at 50°C, and 30 s extension at 60°C. The amplified products were denatured at 95°C for 5 minutes and then separated by an ABI PRISM 3730 XL Genetic Analyzer. This analysis was performed using GeneMapper 4.0 Software.

*2.7. Statistical Analysis.* All clinical data were expressed as the mean ± SD. The Wilcoxon test was used for the evaluation of the FZHY efficacy on clinical symptom, ALT, AST, Child-Pugh score, and ZHENG sore in HBC. The correlation between genotypes and phenotypes was compared by the $\chi^2$ test. $P < 0.05$ was considered statistically significant in all tests.

## 3. Results

*3.1. Efficacy Evaluation of FZHY.* As shown in Table 3, the curative effect of FZHY on ALT, AST, Child-Pugh score, and ZHENG sore was detected in 111 HBC patients. The ALT, AST, Child-Pugh score, and ZHENG score were evaluated before and after drug therapy. There was significant difference ($P < 0.001$) between before and after FZHY treatment in ZHENG score. However, there it was not statistically significant ($P > 0.05$) between before and after FZHY treatment in ALT, AST, and Child-Pugh score.

As shown in Table 4, the correlation was analyzed between ZHENG and FZHY efficacy on 111 HBC patients. There were 67 effective cases and 44 invalid cases, with the total effective rate of 60.36%. Among them, there were 18 effective cases and 3 invalid cases, with the total effective rate of 85.71% in deficiency ZHENG, and there was statistically significance ($P < 0.05$), and OR was 3.940 (95% CI: 1.095, 14.173) compared to excess or deficiency-excess syndromes.

*3.2. Correlation between CYP1A2 Genotypes and FZHY Efficacy on Child-Pugh Scores in HBC.* After SNaPshot assay was carried out, CYP1A2-T5347C, CYP1A2-G2964A, and CYP1A2-C733A were analyzed to clarify the correlation between CYP1A2 SNPs and FZHY effect. As shown in Table 5, the Child-Pugh score was analyzed between before and after treatment groups, and there were 25 effective cases and 86 invalid cases, with the total effective rate of 22.52%. Moreover, in the Child-Pugh scores between effective and invalid groups, the frequency of CC, CT, and TT genotypes at CYP1A2-T5347C locus was 70.80% versus 75.00%, 25.00% versus 23.80%, and 4.20% versus 1.20%; the frequency of GG, GA, and AA genotypes at CYP1A2-G2964A locus was

Table 4: Correlation between ZHENG and FZHY efficacy on HBC.

| ZHENG classification | Effective (%) $n = 67$ | Invalid (%) $n = 44$ | $P^{\#}$ | OR | 95% CI |
|---|---|---|---|---|---|
| Excess | 39 (58.21) | 30 (68.18) | 0.611 | 0.854 | 0.464, 1.570 |
| Deficiency-Excess | 10 (14.93) | 11 (25.00) | 0.277 | 0.597 | 0.234, 1.524 |
| Deficiency | 18 (26.86) | 3 (6.82) | **0.044** | 3.940 | 1.095, 14.173 |

The bold font emphasizes the result was statistically significant ($P < 0.05$).

Table 5: Correlation between CYP1A2 genotypes and FZHY efficacy on Child-Pugh scores in HBC.

| Genotypes | Effective (%) $n = 25$ | Invalid (%) $n = 86$ | $P^{\#}$ | OR | 95% CI |
|---|---|---|---|---|---|
| CYP1A2-5347 | | | | | |
| CC | 17 (70.80) | 63 (75.00) | | | |
| CT | 6 (25.00) | 20 (23.80) | 0.844 | 0.899 | 0.312, 2.591 |
| TT | 1 (4.20) | 1 (1.20) | 0.393 | 0.270 | 0.016, 4.541 |
| CT + TT | 7 (29.20) | 21 (25.00) | 0.681 | 0.810 | 0.295, 2.221 |
| CYP1A2-2964 | | | | | |
| GG | 10 (41.70) | 46 (53.50) | | | |
| GA | 11 (45.80) | 30 (34.90) | 0.289 | 0.593 | 0.224, 1.567 |
| AA | 3 (12.50) | 10 (11.60) | 0.700 | 0.725 | 0.168, 3.121 |
| GA + AA | 14 (58.30) | 40 (46.50) | 0.306 | 0.621 | 0.249, 1.552 |
| CYP1A2-733 | | | | | |
| CC | 3 (12.50) | 9 (10.50) | | | |
| CA | 9 (37.50) | 38 (44.20) | 0.653 | 1.407 | 0.316, 6.277 |
| AA | 12 (50.00) | 39 (45.30) | 0.914 | 1.083 | 0.252, 4.656 |
| CA + AA | 21 (87.50) | 77 (89.50) | 0.777 | 1.222 | 0.304, 4.921 |

The bold font emphasizes the result was statistically significant ($P < 0.05$).

41.70% versus 53.50%, 45.80% versus 34.90%, and 12.50% versus 11.60%; the frequency of CC, CA, and AA genotypes at CYP1A2-C733A locus was 12.50% versus 10.50%, 37.50% versus 44.20%, and 50.00% versus 45.30%, respectively. However, there was no statistical significance ($P > 0.05$) between the two groups in the comparison of any genetic locus.

*3.3. Correlation between CYP1A2 Genotypes and FZHY Efficacy on ZHENG Scores in HBC.* As shown in Table 6, the ZHENG score was analyzed between before and after treatment groups, and there were 67 effective cases and 44 invalid cases, with the total effective rate of 60.36%. Moreover, in the efficacy index of ZHENG between effective and invalid groups, the frequency of GG, GA, and AA genotypes at CYP1A2-G2964A locus was 49.30% versus 52.30%, 44.80% versus 25.00%, and 4.50% versus 22.70%, respectively. There was significant difference ($P < 0.05$) in CYP1A2-G2964A locus at AA compared with GG genotype. OR was 4.783 (95% CI: 1.184, 19.321). The frequency of CC, CT, TT genotypes at CYP1A2-C5347T locus were 71.60% versus 72.70%, 25.40% versus 20.50% and 0 versus 4.50%, respectively. The frequency of CC, CA, AA genotypes at CYP1A2-C733A locus were 13.40% versus 6.80%, 40.30% versus 45.50% and 44.80% versus 47.70%, respectively. However, there were no statistically significant ($P > 0.05$) between the genotypes at CYP1A2-C5347T and -C733A sites and efficacy index of ZHENG.

Moreover, the correlation between genotype of CYP1A2 and ZHENG types in FZHY efficacy was further analyzed in HBC. As shown in Table 7, there also was significant relevance ($P < 0.05$) between GA plus AA genotype and the efficacy index of deficiency ZHENG at CYP1A2-G2964A sites.

## 4. Discussion

ZHENG, a profile of symptoms and signs as a series of clinical phenotypes, plays an important role in understanding the human homeostasis and guiding the applications of TCM treatment. All diagnostic and therapeutic methods in TCM are based on the differentiation of ZHENG, and this concept has been used for thousands of years in China [20]. The "Heat," "Cold," "Excess," and "Deficiency" are the four basic syndromes in TCM. In TCM practice, an experiential diagnosis and efficacy evaluation approach has been frequently used to classify Excess, Deficiency, and Deficiency-Excess syndromes in HBC patients [21]. In order to demonstrate whether ZHENG differentiation approach leads to a personalized treatment, we investigated FZHY efficacy on HBC through a pharmacogenetic evaluation.

CYP1A2 is an important member of the cytochrome P450 superfamily [12], which is cytochrome P450 family 1, subfamily A, polypeptide 2. Its protein content contributes with 13% of the total CYP protein in liver [22]. CYP1A2

Table 6: Correlation between CYP1A2 Genotypes and FZHY efficacy on ZHENG score in HBC.

| Genotypes | Effective (%) $n = 67$ | Invalid (%) $n = 44$ | $P^{\#}$ | OR | 95% CI |
|---|---|---|---|---|---|
| CYP1A2-5347 | | | | | |
| CC | 48 (71.60) | 32 (72.70) | | | |
| CT | 17 (25.40) | 9 (20.50) | 0.624 | 0.794 | 0.315, 2.000 |
| TT | 0 (0) | 2 (4.50) | | | |
| CT + TT | 17 (25.40) | 11 (25.00) | 0.947 | 0.971 | 0.402, 2.341 |
| CYP1A2-2964 | | | | | |
| GG | 33 (49.30) | 23 (52.30) | | | |
| GA | 30 (44.80) | 11 (25.00) | 0.146 | 0.526 | 0.220, 1.258 |
| AA | 3 (4.50) | 10 (22.70) | **0.030** | 4.783 | 1.184, 19.321 |
| GA + AA | 33 (49.30) | 21 (47.70) | 0.815 | 0.913 | 0.426, 1.959 |
| CYP1A2-733 | | | 0.527 | | |
| CC | 9 (13.40) | 3 (6.80) | | | |
| CA | 27 (40.30) | 20 (45.50) | 0.266 | 2.222 | 0.532, 9.275 |
| AA | 30 (44.80) | 21 (47.70) | 0.299 | 2.100 | 0.507, 8.694 |
| CA + AA | 57 (85.10) | 41 (93.20) | 0.261 | 2.158 | 0.550, 8.466 |

The bold font emphasizes the result was statistically significant ($P < 0.05$).

Table 7: Correlation between CYP1A2 genotype and ZHENG types in FZHY efficacy.

| Genotypes | Excess ZHENG | | $P^{\#}$ | Deficiency-Excess ZHENG | | $P^{\#}$ | Deficiency ZHENG | | $P^{\#}$ |
|---|---|---|---|---|---|---|---|---|---|
| | Effective (%) $n = 39$ | Invalid (%) $n = 30$ | | Effective (%) $n = 10$ | Invalid (%) $n = 11$ | | Effective (%) $n = 18$ | Invalid (%) $n = 3$ | |
| CYP1A2-5347 | | | | | | | | | |
| CC | 27 (69.23) | 20 (66.67) | | 8 (80.00) | 8 (72.73) | | 14 (77.78) | 2 (66.67) | |
| CT | 11 (28.21) | 5 (16.67) | 0.425 | 2 (20.00) | 3 (27.27) | 1.000 | 4 (22.22) | 1 (33.33) | 1.000 |
| TT | 0 (0) | 2 (6.67) | — | 0 (0) | 0 (0) | — | 0 (0) | 0 (0) | — |
| CT + TT | 11 (28.21) | 7 (23.33) | 0.788 | 2 (20.00) | 3 (27.27) | 1.000 | 4 (22.22) | 1 (33.33) | 1.000 |
| CYP1A2-2964 | | | | | | | | | |
| GG | 17 (43.59) | 15 (50.00) | | 7 (70.00) | 5 (45.45) | | 1 (5.56) | 2 (66.67) | |
| GA | 19 (48.72) | 7 (23.33) | 0.119 | 3 (30.00) | 3 (27.27) | 1.000 | 12 (66.67) | 1 (33.33) | 0.071 |
| AA | 3 (7.69) | 6 (20.00) | 0.454 | 0 (0) | 3 (27.27) | — | 5 (27.78) | 0 (0) | — |
| GA + AA | 22 (56.41) | 13 (43.33) | 0.420 | 3 (30.00) | 6 (54.55) | 0.387 | 17 (94.44) | 1 (33.33) | **0.041** |
| CYP1A2-733 | | | | | | | | | |
| CC | 5 (12.82) | 2 (6.67) | | 2 (20.00) | 1 (9.09) | | 2 (11.11) | 0 (0) | |
| CA | 14 (35.89) | 13 (43.33) | 0.426 | 6 (60.00) | 4 (36.36) | 1.000 | 8 (44.44) | 2 (66.67) | — |
| AA | 20 (51.28) | 13 (43.33) | 0.691 | 2 (20.00) | 6 (54.55) | 0.491 | 8 (44.44) | 1 (33.33) | — |
| CA + AA | 34 (87.18) | 26 (86.67) | 0.454 | 8 (80.00) | 10 (90.91) | 0.586 | 16 (88.88) | 3 (100.00) | — |

The bold font emphasizes the result was statistically significant ($P < 0.05$).

activity can be used to monitor the alteration of liver function in clinical practice [23]. Especially, CYP1A2 is involved in the metabolism of many drugs, environmental toxins, and endogenous substrates [24]. In contrast to exogenous factors such as smoking causing enzyme induction, to drug intake, and to dietary factors, the genetic influences on CYP1A2 enzyme activity has been shown [25]. It has been reported that CYP1A2 genotype is involved in the rate-limiting step in the metabolism of many drugs such as caffeine in myocardial infarction [26], theophylline in asthma [27], and clozapine in schizophrenia [28], as well as in the bioactivation of procarcinogens [29]. Besides, CYP1A2 phenotype is applied frequently in epidemiologic and drug-drug interaction studies [23].

Previous studies have shown that Chinese herbal formula, Erxian Soup, is associated with CYP1A2 genotype [13] and suggested that the male climacteric syndrome patients with CYP1A2-G2964A locus at GG genotype have higher efficiency and those with GA genotype have lower efficiency when treated with Erxian Soup. In this study, our results showed that ZHENG score are significantly decreased ($P < 0.001$) by FZHY treatment and suggested that FZHY

improves the life quality of HBC patients. Moreover, there was significant correlation between ZHENG classification and FZHY efficacy ($P < 0.05$). In ZHENG efficacy of FZHY between effective and invalid groups, there was significant difference in CYP1A2-G2964A locus with AA compared to GG genotype ($P < 0.05$), and there also was significant relevance between GA plus AA genotype and GG in deficiency ZHENG ($P < 0.05$). It was suggested that HBC patients with CYP1A2-G2964A locus at GG genotype might have the higher efficiency and those with AA genotype have lower efficiency when treated with FZHY. However, there were no statistically significant between FZHY efficacy and Child-Pugh score in the comparison of any genetic locus. The study provided a proof for the ZHENG efficacy evaluation of Chinese herbal formula, which would be helpful to the clinical application of FZHY personalized treatment in HBC patients.

Since Chinese herbal formula contains multiple compounds, its pharmacological effects are the overall performance of these compounds interaction. Though our results showed that CYP1A2 genotypes might respond to the comprehensive effects of FZHY with multiple compounds based on ZHENG phenotype in HBC patients, it is still difficult to understand which compounds of FZHY respond to CYP1A2 genotype. Further researches might demonstrate the correlation between the interactions of FZHY contented compounds and the genotype of CYP and/or other drug metabolic genes through genome-wide association studies in a large number of HBC patients.

## 5. Conclusion

In this study, the FZHY efficacy between before and after treatment for 6 months was evaluated as a clinical outcome assessment. FZHY therapy improved clinical symptoms and ZHENG score in HBC. The efficacy may be related to CYP SNPs at CYP1A2-G2964A loci, suggesting that there is a possibility of ZHENG-based FZHY efficacy on HBC predicted by CYP1A2 genetic polymorphisms.

## Conflict of Interests

All authors manifest that there is no conflict of interests.

## Acknowledgments

This work was supported by National Science and Technology Major Project of China (no. 2012ZX10005001-004), National S and T Major Project of China (no. 2009ZX09311-003), Shanghai Municipal Science and Technology Commission Project (12401900401), and E-institutes of Shanghai Municipal Education Commission (E 03008).

## References

[1] B. J. McMahon, "Epidemiology and natural history of hepatitis B," *Seminars in Liver Disease*, vol. 25, supplement 1, pp. 3–8, 2005.

[2] H. S. Margolis, M. J. Alter, and S. C. Hadler, "Hepatitis B: evolving epidemiology and implications for control," *Seminars in Liver Disease*, vol. 11, no. 2, pp. 84–92, 1991.

[3] F. E. De Jongh, H. L. A. Janssen, R. A. De Man, W. C. J. Hop, S. W. Schalm, and M. Van Blankenstein, "Survival and prognostic indicators in hepatitis B surface antigen-positive cirrhosis of the liver," *Gastroenterology*, vol. 103, no. 5, pp. 1630–1635, 1992.

[4] Q. Y. Li, Z. Z. Guo, J. Liang et al., "Interleukin-10 genotype correlated to TCM syndrome in hepatitis B-caused cirrhosis," *Evidence-Based Complementary and Alternative Medicine*, vol. 2012, Article ID 298925, 6 pages, 2012.

[5] Y.-Y. Hu, P. Liu, and C. Liu, "Investigation on indication of fuzheng huayu capsule against hepatic fibrosis and its non-invasive efficacy evaluation parameters: data analysis of liver biopsy of 50 patients with chronic hepatitis B before and after treatment," *Zhongguo Zhong Xi Yi Jie He Za Zhi*, vol. 26, no. 1, pp. 18–22, 2006.

[6] P. Liu, C. Liu, L.-M. Xu et al., "Effects of Fuzheng Huayu 319 recipe on liver fibrosis in chronic hepatitis B," *World Journal of Gastroenterology*, vol. 4, no. 1-6, pp. 348–353, 1998.

[7] P. Liu, Y.-Y. Hu, C. Liu et al., "Multicenter clinical study about the action of Fuzheng Huayu Capsule against liver fibrosis with chronic hepatitis B," *Zhong Xi Yi Jie He Xue Bao*, vol. 1, no. 2, pp. 89–102, 2003.

[8] C. M. Jiang, C. H. Liu, and C. Liu, "Inhibiting effect of Fuzhenghuayu Capsule on the activation of hepatic stellate cells in rats," *Chinese Journal of Integrated Traditional and Western Medicine*, vol. 11, no. 5, pp. 280–283, 2003.

[9] Y. N. Song, J. J. Sun, Y. Y. Lu et al., "Therapeutic effect of Fuzheng-Huayu tablet based traditional Chinese medicine syndrome differentiation on hepatitis B caused cirrhosis," *Evidence-Based Complementary and Alternative Medicine*, vol. 2013, Article ID 709305, 8 pages, 2013.

[10] D. W. Nebert and D. W. Russell, "Clinical importance of the cytochromes P450," *The Lancet*, vol. 360, no. 9340, pp. 1155–1162, 2002.

[11] Q. Chen, T. Zhang, J.-F. Wang, and D.-Q. Wei, "Advances in human cytochrome P450 and personalized medicine," *Current Drug Metabolism*, vol. 12, no. 5, pp. 436–444, 2011.

[12] D. R. Nelson, L. Koymans, T. Kamataki et al., "P450 superfamily: update on new sequences, gene mapping, accession numbers and nomenclature," *Pharmacogenetics*, vol. 6, no. 1, pp. 1–42, 1996.

[13] M. Yang, C. Y. Ding, X. Zhang et al., "Genetic association research between mutation in CYP1A2 gene and erxian soup response," *Chinese Journal of Information on TCM*, vol. 15, no. 7, pp. 12–14, 2008.

[14] Chinese Association of Integrative Medicine and Liver Disease Committee, "Guideline for the diagnosis and treatment of liver fibrosis with integrative. Medicine," *Zhong Xi Yi Jie He Xue Bao*, vol. 4, no. 6, pp. 551–555, 2006.

[15] Q.-L. Wang, J.-L. Yuan, Y.-Y. Tao, Y. Zhang, P. Liu, and C.-H. Liu, "Fuzheng Huayu recipe and vitamin E reverse renal interstitial fibrosis through counteracting TGF-$\beta$1-induced epithelial-to-mesenchymal transition," *Journal of Ethnopharmacology*, vol. 127, no. 3, pp. 631–640, 2010.

[16] E. Cholongitas, G. V. Papatheodoridis, M. Vangeli, N. Terreni, D. Patch, and A. K. Burroughs, "Systematic review: the model for end-stage liver disease—should it replace Child-Pugh's classification for assessing prognosis in cirrhosis?" *Alimentary Pharmacology and Therapeutics*, vol. 22, no. 11-12, pp. 1079–1089, 2005.

[17] E. Christensen, "Prognostic models including the Child-Pugh, MELD and Mayo risk scores—where are we and where should we go?" *Journal of Hepatology*, vol. 41, no. 2, pp. 344–350, 2004.

[18] X. Zheng, *Guideline for Clinical New Drug Research in Chinese Herbal Medicine*, Chinese Medical Science and Technology Press, Beijing, China, 2002.

[19] S. Filippini, A. Blanco, A. Fernández-Marmiesse et al., "Multiplex SNaPshot for detection of BRCA1/2 common mutations in Spanish and Spanish related breast/ovarian cancer families," *BMC Medical Genetics*, vol. 8, article 40, 2007.

[20] B.-E. Wang, "Treatment of chronic liver diseases with traditional Chinese medicine," *Journal of Gastroenterology and Hepatology*, vol. 15, pp. E67–E70, 2000.

[21] Y. N. Song, H. Zhang, Y. Guan et al., "Classification of traditional Chinese medicine syndromes in patient with chronic hepatitis B by SELDI-based protein-chip analysis," *Evidence-Based Complementary and Alternative Medicine*, vol. 2012, Article ID 626320, 10 pages, 2012.

[22] T. Shimada, H. Yamazaki, M. Mimura, Y. Inui, and F. P. Guengerich, "Interindividual variations in human liver cytochrome P-450 enzymes involved in the oxidation of drugs, carcinogens and toxic chemicals: studies with liver microsomes of 30 Japanese and 30 Caucasians," *Journal of Pharmacology and Experimental Therapeutics*, vol. 270, no. 1, pp. 414–423, 1994.

[23] M. S. Faber, A. Jetter, and U. Fuhr, "Assessment of CYP1A2 activity in clinical practice: why, how, and when?" *Basic and Clinical Pharmacology and Toxicology*, vol. 97, no. 3, pp. 125–134, 2005.

[24] M. Shou, K. R. Korzekwa, E. N. Brooks, K. W. Krausz, F. J. Gonzalez, and H. V. Gelboin, "Role of human hepatic cytochrome P450 1A2 and 3A4 in the metabolic activation of estrone," *Carcinogenesis*, vol. 18, no. 1, pp. 207–214, 1997.

[25] B. B. Rasmussen, T. H. Brix, K. O. Kyvik, and K. Brøsen, "The interindividual differences in the 3-demthylation of caffeine alias CYP1A2 is determined by both genetic and environmental factors," *Pharmacogenetics*, vol. 12, no. 6, pp. 473–478, 2002.

[26] M. C. Cornelis, A. El-Sohemy, E. K. Kabagambe, and H. Campos, "Coffee, CYP1A2 genotype, and risk of myocardial infarction," *Journal of the American Medical Association*, vol. 295, no. 10, pp. 1135–1141, 2006.

[27] Y. Obase, T. Shimoda, T. Kawano et al., "Polymorphisms in the CTP1A2 gene and theophylline metabolism in patients with asthma," *Clinical Pharmacology and Therapeutics*, vol. 73, no. 5, pp. 468–474, 2003.

[28] H. Balibey, C. Basoglu, S. Lundgren et al., "CYP1A21F polymorphism decreases clinical response to clozapine in patients with schizophrenia," *Bulletin of Clinical Psychopharmacology*, vol. 21, no. 2, pp. 93–99, 2011.

[29] D. L. Eaton, E. P. Gallagher, T. K. Bammler, and K. L. Kunze, "Role of cytochrome P4501A2 in chemical carcinogenesis: implications for human variability in expression and enzyme activity," *Pharmacogenetics*, vol. 5, no. 5, pp. 259–274, 1995.

Hindawi Publishing Corporation
Evidence-Based Complementary and Alternative Medicine
Volume 2013, Article ID 759748, 8 pages
http://dx.doi.org/10.1155/2013/759748

*Research Article*

# Traditional Chinese Medicine Diagnosis "*Yang-Xu Zheng*": Significant Prognostic Predictor for Patients with Severe Sepsis and Septic Shock

**Sunny Jui-Shan Lin,[1,2,3] Yung-Yen Cheng,[4] Chih-Hung Chang,[5,6,7] Cheng-Hung Lee,[2] Yi-Chia Huang,[2,8] and Yi-Chang Su[2,3]**

[1] *Department of Chinese Medicine, National Defense Medical Center, Tri-Service General Hospital, Taipei 11490, Taiwan*
[2] *Graduate Institute of Chinese Medicine, College of Chinese Medicine, China Medical University, Taichung 40402, Taiwan*
[3] *School of Chinese Medicine, College of Chinese Medicine, China Medical University, Taichung 40402, Taiwan*
[4] *Department of Internal Medicine, Nantou Hospital, Department of Health, Executive Yuan, Nantou 54062, Taiwan*
[5] *Rehabilitation Institute of Chicago, Chicago, IL 60611, USA*
[6] *Department of Physical Medicine and Rehabilitation, Northwestern University Feinberg School of Medicine, Chicago, IL 60611, USA*
[7] *Graduate Institute of Biostatistics, China Medical University, Taichung 40402, Taiwan*
[8] *Department of Traditional Chinese Medicine, Taichung Veterans General Hospital, Taichung 40705, Taiwan*

Correspondence should be addressed to Yi-Chang Su; juishan.lin@msa.hinet.net

Received 14 July 2013; Accepted 13 September 2013

Academic Editor: Shibing Su



Pathogenesis of sepsis includes complex interaction between pathogen activities and host response, manifesting highly variable signs and symptoms, possibly delaying diagnosis and timely life-saving interventions. This study applies traditional Chinese medicine (TCM) *Zheng* diagnosis in patients with severe sepsis and septic shock to evaluate its adaptability and use as an early predictor of sepsis mortality. Three-year prospective observational study enrolled 126 septic patients. TCM *Zheng* diagnosis, Acute Physiology and Chronic Health Evaluation (APACHE) II score, and blood samples for host response cytokines measurement (tumor necrosis factor-$\alpha$, Interleukin-6, Interleukin-8, Interleukin-10, Interleukin-18) were collected within 24 hours after admission to Intensive Care Unit. Main outcome was 28-day mortality; multivariate logistic regression analysis served to determine predictive variables of the sepsis mortality. APACHE II score, frequency of *Nutrient*-phase heat, and *Qi-Xu* and *Yang-Xu Zhengs* were significantly higher in nonsurvivors. The multivariate logistic regression analysis identified *Yang-Xu Zheng* as the outcome predictor. APACHE II score and levels of five host response cytokines between patients with and without *Yang-Xu Zheng* revealed significant differences. Furthermore, cool extremities and weak pulse, both diagnostic signs of *Yang-Xu Zheng*, were also proven independent predictors of sepsis mortality. TCM diagnosis "*Yang-Xu Zheng*" may provide a new mortality predictor for septic patients.

## 1. Introduction

Mortality of severe sepsis and septic shock remains elevated despite progress in therapy [1]. Diagnostic methods reliably identifying patients with a higher risk of death are urgently needed in order to provide timely treatment and improve cost-efficacy of intensive care [2]. Since reliable concepts and accurate measurements to rate mortality risk and stratify severity of septic patients are insufficient [3, 4], a classification system named PIRO was developed to stratify patients on the basis of their *predisposition*, the nature and extent of *insult/infection*, nature and magnitude of *response*, and degree of concomitant *organ dysfunction* [5, 6]. Multiple host and pathogen-associated characteristics are utilized in this system to predict outcome. Similar diagnostic concepts also exist in traditional Chinese medicine (TCM) *Zheng* diagnosis.

The integrity of the human body and its close interaction with the environment (e.g., infectious pathogens) are emphasized in TCM. Disease is considered as a common product of both pathogenic factors and maladjustment in the body [7]. While diagnosing patients, *Zheng* is an outcome after all signs and symptoms are analyzed. As disease progresses, *Zheng* may evolve, since signs and symptoms may change [8]. The TCM *Zheng* diagnosis implies both the subtype categorization and severity staging of disease progress, making TCM *Zheng* diagnosis feasible for adoption as a disease stratification tool in clinical practice [9].

Severe acute respiratory syndrome (SARS) is an infectious disease caused by a novel coronavirus. It is believed that complicated pathogenesis and severity of SARS arise from complex host responses against infectious agents [10]. During the SARS outbreak in China, 40–60% of infected patients received standard modern medical treatment integrated with Chinese medicine treatment [11]. While facing the challenge to treat SARS patients, TCM *Zheng* differentiation enables physicians to prescribe medicine in accordance with the process and nature of the illness [12]. The positive effects of this integrative treatment were reported by WHO and other review articles [11, 13–16].

Our study applied TCM *Zheng* diagnosis in patients with severe sepsis and septic shock to see whether such diagnosis can be adopted as an early predictor of mortality. We also wanted to probe for significant differences between septic patients with and without this predictive TCM *Zheng* with regard to APACHE II score, which measures the deteriorated general condition of patients [17], and some host response cytokines have been reported as closely related to sepsis mortality: tumor necrosis factor-$\alpha$ (TNF-$\alpha$), Interleukin-6 (IL-6), Interleukin-8 (IL-8), Interleukin-10 (IL-10), and Interleukin-18 (IL-18) [18–24]. We also explored each diagnostic sign of predictive TCM *Zheng* for possible adoption individually or in combination with other signs to predict mortality. These predictive signs can then be applied by Western physicians to timely recognize the septic patients at higher risk of death.

## 2. Materials and Methods

*2.1. Development of TCM Zheng Diagnosis for Severe Sepsis and Septic Shock.* First, literature review on TCM *Zhengs* for diagnosing infectious diseases in Chinese classical medicine was completed by the research team. Then four rounds of meetings were held to develop TCM *Zhengs* and diagnostic criteria to classify patients with severe sepsis and septic shock into stages of disease progress. Ten participating experts had both Western and Chinese professional training, medical licenses, more than ten years of clinical experience, and had worked in medical centers.

After several rounds of discussions, two major theories of infectious disease in TCM, *Treatise on Cold Damage Diseases* (*Shanghanlun,* 傷寒論) and *Treatise on Warm Heat Disease* (*Wenrelun,* 温熱論) became central topics. Experts integrated both these theories to outline pathogenesis of sepsis in TCM and develop TCM *Zhengs* via clinical observation of septic patients and reports of SARS treatment [11, 13–16]. Two main types of TCM *Zhengs* were finalized: pathogen excess (邪實證) and human body deficiency (正虛證) [25–27].

The pathogen-excess type manifests in early phases of sepsis, while both infectious agents and host inflammatory reaction are very active. *Qi*-, *Nutrient*-, and *Blood*-phase heat (氣分熱證, 營分熱證, 血分熱證) were three TCM *Zhengs* finalized in the pathogen-excess type. The *Defense*-phase heat (衛分熱證), appearing in very early stage of infection, was not selected since the observed population in our study had already been diagnosed as severe sepsis.

The human body-deficiency type manifests in late phases of sepsis, in which there is overexpression of inflammatory mediators and multiple impaired functions of body organs [28]. Along with disease progress, pathological heat in *Qi*-, *Nutrient*-, and *Blood*-phase consume *Qi*-, *Blood, Yin, and Yang*, four basic elements to maintain body functions in TCM perspective. Therefore, *Qi*-, *Blood*-, *Yin*-, and *Yang-Xu* (氣虛證, 血虛證, 陰虛證, 陽虛證) were the four TCM *Zhengs* finalized in human body-deficiency type. Finally, experts' opinions on the hypothesis of pathogenesis in TCM reached consensus. Figure 1 illustrates a hypothesis of possible transition directions and pathways of TCM *Zhengs* from bacterial or viral infection to human death. Diagnostic criteria of each TCM *Zheng* were modified and established from TCM literature, considering easiness to operate in the environment of an Intensive Care Unit (Table 1).

*2.2. Study Design and Subjects.* Prospective observational study was conducted in the medical intensive care units (MICU) of two local community hospitals in Central Taiwan (Nantou and Taichung Hospital, Department of Health, Executive Yuan) from April 2005 to December 2008. Both institutional review boards approved this study. Informed consent was obtained from patients or their family members. Patients who fulfilled diagnostic criteria of severe sepsis or septic shock [29] consecutively admitted to the MICU were enrolled. Those with immunodeficiency, concomitant immunosuppressive therapy, malignancy, pregnancy, severe peripheral vascular disease, or end-stage renal disease were excluded. The study in no way affected patient treatment. All patients had indwelling artery and central line catheters and were mechanically ventilated in pressure controlled modes under continuous analgesic sedation if required. Fluid administration of crystalloids and colloids, dopamine or noradrenaline to maintain mean arterial pressure >65 mmHg, and if needed, dobutamine to maintain cardiac index 4 L/min·m$^2$ were given as routine resuscitation therapy for hypotension (systolic blood pressure < 90 mmHg or a reduction of systolic blood pressure by 40 mmHg from baseline). After collection of blood and other suspected infected materials for microbiological analysis, all patients underwent empirical broad-spectrum antibiotic therapy, later adjusted according to culture results.

*2.3. Sample Size Calculation.* As there are few studies in literature on TCM *Zhengs*, sample size was calculated based

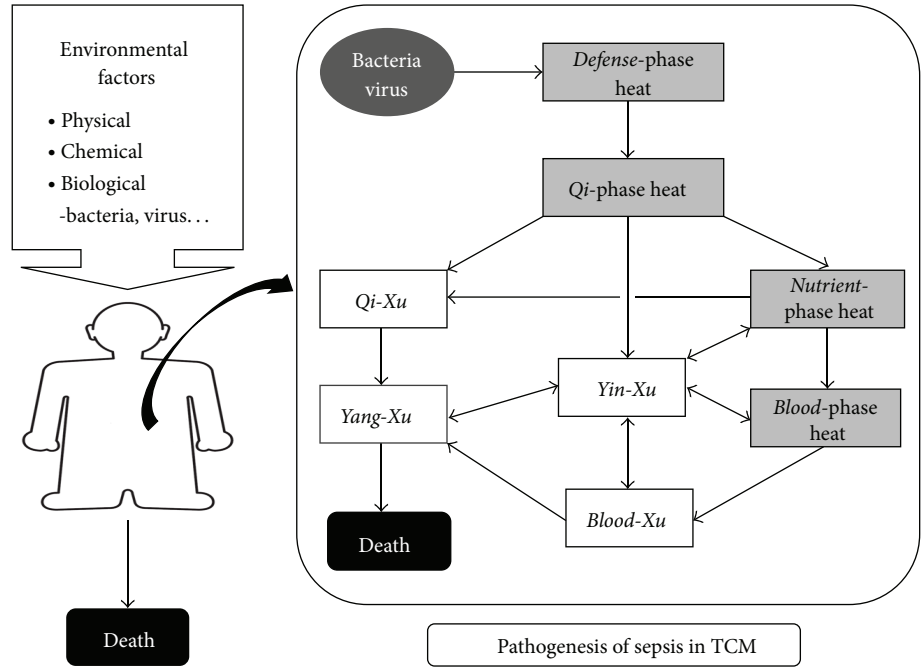


Figure 1: Hypothesis of pathogenesis of sepsis in traditional Chinese medicine. Solid rectangles denote "pathogen-excess type" TCM *Zhengs*. Void rectangles denote "human body-deficiency type" TCM *Zhengs*. Arrows denote possible transition directions and pathways of *TCM Zhengs*.

Table 1: Diagnostic criteria of traditional Chinese medicine (TCM) *Zhengs* in severe sepsis and septic shock.

| TCM *Zheng* | | Diagnostic criteria | | | |
|---|---|---|---|---|---|
| Type | *Zheng* | Body temperature | Signs[a] | Pulse | Tongue |
| Pathogen-excess type | *Qi*-phase heat | Fever (BT > 38°C) | Sweating<br>Thirsty<br>Nausea/vomiting<br>Abdominal distension<br>Abdominal pain<br>Constipation<br>Diarrhea | Rapid (HR > 100 beats/min) | With yellowish coating |
| | *Nutrient*-phase heat | | Delirium | | Red |
| | *Blood*-phase heat | | Hemorrhage[b]<br>Petechial or purpuric rash<br>Convulsion | | Dark-red crimson |
| Human body-deficiency type | *Qi-Xu*<br>*Yang-Xu*<br>*Blood-Xu* | — | Fatigue lethargy<br>Cool extremities edematous limbs<br>Pale | Weak<br>Threadlike | —<br>Light-red |
| | *Yin-Xu* | | Night sweating<br>Thirsty | | Red |

[a]Each *Zheng* was diagnosed when either sign appeared.
[b]Bleeding in any part of the body was included, except the skin.

on our pilot study. During our design stage, we determined that 35 patients in the group with and 53 in the group without *Yang-Xu Zheng* had to provide a power of 90% and 5% of two-sided type 1 error for prevalence of *Yang-Xu Zheng* of 40% in this population to differentiate proportions of patients who died. This was calculated by a two-sided proportion test ($z$ test) on the assumption that there was a 40% survival rate in the group with versus 75% survival rate in the group without *Yang-Xu Zheng*.

*2.4. Data Collection.* Whenever a patient diagnosed with severe sepsis or septic shock was admitted to MICU, the physician on duty informed our research team member on call (YYC), who was a specialist and chief of the MICU. Age,

gender, TCM *Zheng* diagnosis, and clinical and laboratory measurements for calculation of the APACHE II [17] and cytokine were collected by both reviewing the chart record and examining patients within 24 hours of admission to MICU, and this 24-hour period was considered as "Day 1" in our study. Ambient temperature was controlled at 24°C. To minimize potential observation bias, signs to diagnose TCM *Zhengs* were examined by only one attending physician (YYC) with both Western and Chinese professional training and medical licenses. Patient's survival or death (survivor versus nonsurvivor) in MICU was assessed during a follow-up of a 28-day interval.

*2.5. Cytokine Measurement.* Blood samples were collected from the arterial line for septic patients. Samples were immediately centrifuged in MICU at 1500 rpm for 10 minutes and separated plasma stored at −80°C. Plasma levels of TNF-$\alpha$, IL-6, IL-8, IL-10, and IL-18 were measured by enzyme-linked immunosorbent assay (ELISA) with a commercial kit (R&D systems, Minneapolis, MN) using the manufacture's protocol. All cytokine measurements were performed in the College of Chinese Medicine Laboratory at China Medical University by faculty blinded to clinical data. The samples were assayed with suitable controls for derivation of standard curves.

*2.6. Statistical Analysis.* For continuous variable, data are expressed as mean ± SD and for categorical variables, as numbers with corresponding percentages. Cytokine values were log-transformed to obtain proportionally constant variation and distributed normally. Comparisons between survivor and non-survivor groups were performed via Mann-Whitney *U* test. The Chi-square or Fisher's exact test was used for categorical variables. A multivariate logistic regression was conducted by including all potential variables associated with mortality (i.e., a full model) to assess joint predictive effect on sepsis mortality. Signs of the predictive TCM *Zheng* were analyzed by the full model of logistic regression for selection of independent predictive signs. Statistical calculations were performed using software package SPSS 14.0 (SPSS Inc., Chicago, IL). All comparisons were two-tailed, $P < 0.05$ regarded as statistically significant.

## 3. Results

*3.1. Characteristics of Study Subjects.* A total of 126 sepsis patients were consecutively enrolled: 71 survivors and 55 non-survivors (43.7%) who died within 6.6 ± 5.7 days after MICU admission. Mean age of each group was over 70 years. Male was predominant in the non-survivor group and as risk factor for mortality. Sepsis diagnosis at MICU admission showed no correlation with mortality. APACHE II score was significantly higher among non-survivors. Principal suspected infection source was the respiratory tract, followed by urogenital tract, most infection caused by gram negative bacteria. Six patients with intra-abdominal infection all died within twenty-eight days after admission (Table 2).

Table 2: Demographic and clinical characteristics of septic patients.

| Variable | Survivor ($n = 71$) | Nonsurvivor ($n = 55$) | $P$ value |
|---|---|---|---|
| Age (yr) | 74.7 ± 11.9 | 73.2 ± 16.6 | NS |
| Gender (male) | 38 (53.5%) | 39 (70.9%) | <0.05 |
| Survival time (days) | | 6.6 ± 5.7 | |
| Diagnosis at ICU admission | | | |
| Severe sepsis | 12 (16.9%) | 4 (7.3%) | NS[a] |
| Septic shock | 59 (83.1%) | 51 (92.7%) | NS |
| Severity scoring | | | |
| APACHE II | 28.5 ± 7.6 | 31.6 ± 7.7 | 0.02 |
| Source of infection[b] | | | |
| Respiratory tract | 38 (53.5%) | 26 (47.3%) | NS |
| Urogenital tract | 39 (54.9%) | 22 (40.0%) | NS |
| Liver and biliary tract | 2 (2.8%) | 4 (7.3%) | NS[a] |
| Intra-abdomen | 0 (0.0%) | 6 (10.9%) | <0.01[a] |
| Cutaneous/soft tissue | 5 (7.0%) | 1 (1.8%) | NS[a] |
| Others/unknown | 3 (4.2%) | 6 (10.9%) | NS[a] |
| Documented microbial agent[b] | | | |
| Gram positive | 12 (16.9%) | 11 (20.0%) | NS |
| Gram negative | 50 (70.4%) | 36 (65.5%) | NS |
| Fungus | 4 (5.6%) | 4 (7.3%) | NS[a] |

Survivor/nonsurvivor: septic patient alive/dead 28 days after admission to medical intensive care unit.
APACHE II: Acute Physiology and Chronic Health Evaluation II.
Continuous data are presented as Mean ± SD.
Categorical data are presented as number of patients (percentages).
Values have been calculated using Chi-square test and Mann-Whitney *U* test.
[a]Calculated using Fisher's exact test.
[b]Values total more than 100%, since patients could have more than one condition.
$P < 0.05$ statistically significant.
NS: not significant.

*3.2. Frequency of TCM Zhengs between Patients with Severe Sepsis and Septic Shock.* Among 126 septic patients, 16 were admitted with diagnosis of severe sepsis, the other 110 with septic shock. Frequency of *Qi-Xu Zheng* was the highest (**68.3%**), followed by *Yang-Xu Zheng* (**51.6%**). Frequency of three pathogen-excess types were between 35.7 and 40.5%. Only 6.3% and 4.8% of patients had *Blood-Xu Zheng* and *Yin-Xu Zheng*, respectively. There was no significance with regard to frequency of all TCM *Zhengs* between patients with severe sepsis or septic shock, although the percentage of *Nutrient*-phase heat and *Qi-Xu Zheng* was much higher in the patients with septic shock (Table 3).

*3.3. Frequency of TCM Zhengs between Survivors and Nonsurvivors.* Among three pathogen-excess types, only frequency of *Nutrient*-phase heat *Zheng* was significantly higher in the non-survivor group; in the human body-deficiency types, incidence of both *Qi*- and *Yang-Xu Zheng* was higher in non-survivors (Table 4).

Table 3: Frequency of TCM *Zhengs* between patients with severe sepsis and septic shock.

| TCM *Zheng*[a] | Total ($n$ = 126) | Severe sepsis ($n$ = 16) | Septic shock ($n$ = 110) | $P$ value[b] |
|---|---|---|---|---|
| Pathogen-excess type | | | | |
| *Qi*-phase heat | 47 (37.3%) | 5 (31.3%) | 42 (38.2%) | NS[c] |
| *Nutrient*-phase heat | 51 (40.5%) | 5 (31.3%) | 46 (41.8%) | NS[c] |
| *Blood*-phase heat | 45 (35.7%) | 5 (31.3%) | 40 (36.4%) | NS[c] |
| Human body-deficiency type | | | | |
| *Qi-Xu* | 86 (68.3%) | 9 (56.3%) | 77 (70.0%) | NS |
| *Yang-Xu* | 65 (51.6%) | 8 (50.0%) | 57 (51.8%) | NS |
| *Blood-Xu* | 8 (6.3%) | 1 (6.3%) | 7 (6.4%) | NS[c] |
| *Yin-Xu* | 6 (4.8%) | 1 (6.3%) | 5 (4.5%) | NS[c] |

Categorical data are presented as number of patients (percentages).
Values have been calculated using Chi-square test.
[a]Values total more than 100%, since patients could have more than one condition.
[b]Comparison between patient with severe sepsis and septic shock.
[c]Calculated using Fisher's exact test.
$P < 0.05$ statistically significant.
NS: not significant.

Table 4: Frequency of each TCM *Zheng* between the survivors and nonsurvivors.

| TCM *Zheng*[a] | Survivor ($n$ = 71) | Nonsurvivor ($n$ = 55) | $P$ value |
|---|---|---|---|
| Pathogen-excess type | | | |
| *Qi*-phase heat | 27 (38.0%) | 20 (36.4%) | NS |
| *Nutrient*-phase heat | 23 (32.4%) | 28 (50.9%) | 0.04 |
| *Blood*-phase heat | 22 (31.0%) | 23 (41.8%) | NS |
| Human body-deficiency type | | | |
| *Qi-Xu* | 41 (57.7%) | 45 (81.8%) | <0.01 |
| *Yang-Xu* | 23 (32.4%) | 42 (76.4%) | <0.01 |
| *Blood-Xu* | 5 (7.0%) | 3 (5.5%) | NS[b] |
| *Yin-Xu* | 5 (7.0%) | 1 (1.8%) | NS[b] |

Categorical data are presented as number of patients (percentages).
Values have been calculated using Mann-Whitney $U$ test and Chi-square test.
[a]Values total more than 100%, since patients could have more than one condition.
[b]Calculated using Fisher's exact test.
$P < 0.05$ being statistically significant.
NS: not significant.

*3.4. Independent Predictors for Sepsis Mortality.* Although frequency of *Qi-Xu Zheng* was also significantly higher in the non-survivor group, it was not included in multivariate analysis model due to its high collinearity with *Yang-Xu Zheng*. While site of infection also has prognostic value [6], intra-abdomen infection was excluded from multivariate analysis model because there was no case in the survivor group. Multivariate logistic regression was performed by including age, gender, APACHE II score, *Nutrient*-phase heat, and *Yang-Xu Zheng* in the model. Only *Yang-Xu Zheng* proved statistically significant in the full model, which had a prediction rate of 70.6% (Table 5). Next, in order to evaluate discrimination capacity of *Yang-Xu Zheng*, we compared APACHE II scores and plasma values of host reactive cytokine of TNF-$\alpha$, IL-6, IL-8, IL-10, and IL-18 between patients with and without *Yang-Xu Zheng*. APACHE II score and values of host reactive cytokines were all significantly higher in the septic patients with *Yang-Xu Zheng* (Table 6). Finally, five diagnostic signs of *Yang-Xu Zheng* were analyzed by multivariate logistic regression. Cool extremities and weak pulse emerged as significant portents for sepsis mortality in the full model, with prediction rate of 74.6% (Table 7).

## 4. Discussion

To our knowledge, this is the first study to evaluate whether TCM *Zheng* diagnosis can be adopted as an early predictor for sepsis mortality. Our prospective observational results indicate (1) *Yang-Xu Zheng* serves as an early predictor for sepsis outcome, since patients with it show higher APACHE II scores; and (2) in cases without it, these host response cytokines are reported as significantly lower: TNF-$\alpha$, IL-6, IL-8, IL-10, and IL-18. Furthermore, cool extremities and weak pulse, two diagnostic signs of *Yang-Xu Zheng,* were also cited as accurate predictors for sepsis mortality and can be adopted for use by Western physicians in their clinical practice.

The most challenging task of our study was to draw the hypothesis of pathogenesis of sepsis from TCM perspective. Experts debated whether to adopt the theory of *Zhang Zhongjing* (張仲景) or *Ye Tianshi* (葉天士) or to integrate both. The issue was resolved by in-depth literature review, along with discussion of clinical observations and experiences. All experts agreed to integrate these theories into pathogenesis of sepsis, since (1) both theories originate from *Huangdi's Internal Classic* (黃帝內經) [25–27] and (2) manifestations of septic patients cover signs and symptoms described in *Treatise on Cold Damage Diseases (Shanghanlun)* and *Treatise on Warm Heat Disease (Wenrelun)*.

Results show complexity of disease progress and TCM *Zheng* transitions in septic patients, who can manifest diverse TCM *Zhengs* simultaneously. The combination can be two *Zhengs* in the pathogen-excess type or human body-deficiency type, or one *Zheng* from pathogen-excess with

Table 5: Multivariate analysis of independent predictor for sepsis mortality.

| Variable | Prediction rate: 70.6% | | | | |
|---|---|---|---|---|---|
| | *B* | Wald | Relative risk | 95% CI | *P* value |
| Age | −0.01 | 0.77 | 0.99 | 0.96–1.02 | NS |
| Gender | 0.33 | 0.55 | 1.39 | 0.59–3.29 | NS |
| APACHE II | 0.03 | 1.11 | 1.03 | 0.98–1.01 | NS |
| *Nutrient*-phase *Zheng* | 0.31 | 0.51 | 1.36 | 0.58–3.16 | NS |
| *Yang-Xu Zheng* | 1.75 | 16.62 | 5.74 | 2.48–13.3 | <0.01 |

Multivariate logistic regression analysis was performed by "enter" method.
APACHE II: Acute Physiology and Chronic Health Evaluation II.
CI: confidence interval.
*P* value < 0.05 being statistically significant.

Table 6: APACHE II score and host reactive cytokine levels between septic patients with and without *Yang-Xu Zheng*.

| | With *Yang-Xu Zheng* ($n = 65$) | Without *Yang-Xu Zheng* ($n = 61$) | *P* value |
|---|---|---|---|
| Severity scoring | | | |
| APACHE II | 31.8 ± 7.8 | 27.8 ± 7.1 | <0.01 |
| Host reactive cytokine | | | |
| TNF-$\alpha$[a] | 1.6 ± 0.5 | 1.4 ± 0.5 | <0.01 |
| IL-6[a] | 3.3 ± 0.9 | 2.8 ± 0.8 | <0.01 |
| IL-8[a] | 2.5 ± 0.6 | 2.2 ± 0.5 | <0.01 |
| IL-10[a] | 2.3 ± 0.7 | 2.0 ± 0.7 | <0.01 |
| IL-18[a] | 2.9 ± 0.2 | 2.8 ± 0.3 | <0.01 |

APACHE II: Acute Physiology and Chronic Health Evaluation II.
Continuous data are presented as Mean ± SD.
Values have been calculated using Mann-Whitney *U* test.
TNF: tumor necrosis factor.
IL: interleukin.
[a]Based on log transformed values (pg/mL).
*P* < 0.05 statistically significant.
NS: not significant.

another from human body-deficiency type; this combination was most frequent. Predominant combination of *Zhengs* reflected both inflammatory reaction caused by the invading pathogen and impaired organ function resulting from cytokine storm and cardiovascular derangements [28].

In constructing the hypothesis of sepsis in TCM, we thought of *Yang-Xu* as the key pathological factor in determining mortality outcome, since *Yang* is energy to maintain body function. This was affirmed by finding *Yang-Xu Zheng* as an independent predictor of mortality. Although the Body Constitution Questionnaire (BCQ+) developed by our team aims at assessing *Yang-Xu* status of the body [30, 31], it is not fitting to measure the *Yang-Xu* status of septic patients in this study. BCQ+ measures the relatively stable physiological condition of the body, but signs and symptoms of sepsis vary quite rapidly under pathological interaction of pathogen virulence and host response [32].

Overwhelming host responses to pathogens may cause inappropriate inflammatory mediator secretion and a variety of acute insults leading to septic shock. Our study, comparing APACHE II score and the host response cytokines between patients with and without *Yang-Xu Zheng,* revealed that patients with *Yang-Xu Zheng* had significantly higher APACHE II scores and host response cytokine values. TCM diagnosis *Yang-Xu Zheng* can thus discriminate septic patients into two groups and help to identify septic patients with higher disease severity and impaired physiological function.

Likewise, cool extremities and weak pulse, both diagnostic signs of *Yang-Xu Zheng,* were found significant prognostic predictors of sepsis mortality. In this study, these diagnostic signs were observed in the postresuscitation phase of septic patients. Even under effects of fluid supplement and inotropic medication, all four distal extremities were still obviously cool to the examiner's hand. This finding concurs with reports from Kaplan et al. [33] and Lima et al. [34]. During examination of the radial artery (side without arterial line insertion), pulse was weak and blood flow easily blocked by fingertip compression. Pulse diagnosis enables TCM physicians to evaluate cardiac output and systemic vascular resistance approximately. In severe sepsis and septic shock, myocardial dysfunction and cardiovascular derangements often manifest [35]. Cool extremities and weak pulse, two signs of peripheral hypoperfusion, are easily assessed and can also be applied by Western physicians to identify septic patients at a higher risk of death within seconds.

In this study, only 6.3% and 4.8% of the patients were found to have *Blood-Xu Zheng* and *Yin-Xu Zheng*, respectively. This may be because (1) our patients were observed in post-resuscitation phase: fluid supplement treatment improved pathological status of *Yin-Xu* and *Blood-Xu*; Yan et al. also noted light tongue color instead of typical crimson tongue in SARS patients after fluid resuscitation [12]; and (2) TCM *Zheng* diagnosis was performed within the first 24 hours after admission: signs and symptoms of *Blood-Xu Zheng* and *Yin-Xu Zheng* did not develop in this period yet.

There are study limitations to note. First, our treatment of septic shock followed the standardized protocol of the hospital, which may not be universal. Since our patients were examined in post-resuscitation phase, effects of sedation and analgesics can not be ruled out. Yet this study provides information on MICU outcomes of patients admitted with severe sepsis and septic shock to local community hospitals in East Asia.

Table 7: Diagnostic signs of *Yang-Xu Zheng* as independent predictors of sepsis mortality.

| Variable | Prediction rate: 74.6% | | | | |
|---|---|---|---|---|---|
| | *B* | Wald | Relative risk | 95% CI | *P* value |
| Fatigue | 0.34 | 0.14 | 1.41 | 0.24–8.32 | NS |
| Lethargy | −1.35 | 2.96 | 0.26 | 0.06–1.21 | NS |
| Cool extremities | 1.94 | 17.94 | 6.97 | 2.84–17.12 | <0.01 |
| Edematous limbs | 0.51 | 1.36 | 1.66 | 0.71–3.92 | NS |
| Weak pulse | 1.35 | 5.64 | 3.86 | 1.27–11.77 | 0.02 |

Multivariate logistic regression analysis was performed by "enter" method.
CI: confidence interval.
$P < 0.05$ being statistically significant.

Second, we defined the first 24 hours after admission to MICU as the "Day 1" in our study. It was to be expected that there would be inherent lead-time bias in this study, with septic patients admitted from either the emergency department or inpatient ward. The lead-time bias may underlie observational differences between groups; we suggest that this does not reduce the value of our observations at the point at which decisions about the choice of further hemodynamic support were made.

Third, this study can be criticized for potential observer bias but is supported by other factors, such as both disease severity scores and cytokine values consistent with findings and outcomes.

Fourth, TCM *Zhengs* to diagnose the septic patients were analyzed and singled out from composite *Zhengs* in TCM literatures. Diagnostic criteria were selected after considering difficulties in clinical observation, so only the signs and symptoms that can be observed in the septic patients were included. Since diagnosis *Nutrient*-phase heat, *Qi-Xu*, and *Yang-Xu Zheng* significantly differed between survivors and non-survivors, TCM *Zhengs* and their diagnostic criteria still have the clinical feasibility. With frequency of *Nutrient*-phase heat, *Qi-Xu,* and *Yang-Xu Zheng* higher in non-survivors, further clinical study should evaluate TCM treatment for *Nutrient*-phase heat, *Qi-Xu,* and *Yang-Xu Zheng* in the patients with severe sepsis and septic shock.

## 5. Conclusions

Early identification of patients at high risk of death is a critical issue in management of sepsis. Highly variable signs and symptoms of sepsis emanate from the complex immune reaction and host response. Since TCM *Zheng* diagnosis is made after analyzing all signs and symptoms gathered, *Yang-Xu Zheng* serves as independent and significant prognostic predictor of patients with severe sepsis and septic shock. There were significant differences in APACHE II scores and plasma values of host response cytokine: TNF-$\alpha$, IL-6, IL-8, IL-10 and IL-18 between patients with and without *Yang-Xu Zheng*. These findings provide clinical evidence that TCM *Zheng* diagnosis can be applied to stratify severity and prognosis of septic patients.

## Conflict of Interests

All authors declare that there is no conflict of interests.

## Acknowledgments

This study was supported both by the Committee on Chinese Medicine and Pharmacy, Department of Health, Executive Yuan, Taiwan (Grant nos. CCMP95-RD-214, CCMP96-RD-209, and CCMP99-RD-207) and National Science Council (Grant no. NSC 98-2320-B-039-MY3). The authors wish to thank the entire team of MICU both at Nantou (Dr. Yi-Hsiang Lin, Dr. Tse-Hung Lin, and Dr. Chih-Hung Shih) and Taichung Hospital, Department of Health, Executive Yuan. They also thank Miss Yun-An Chen for cytokine measurement.

## References

[1] G. S. Martin, D. M. Mannino, S. Eaton, and M. Moss, "The epidemiology of sepsis in the United States from 1979 through 2000," *The New England Journal of Medicine*, vol. 348, no. 16, pp. 1546–1554, 2003.

[2] M. Zambon, M. Ceola, R. Almeida-de-Castro, A. Gullo, and J. Vincent, "Implementation of the surviving sepsis campaign guidelines for severe sepsis and septic shock: we could go faster," *Journal of Critical Care*, vol. 23, no. 4, pp. 455–460, 2008.

[3] S. L. Barriere and S. F. Lowry, "An overview of mortality risk prediction in sepsis," *Critical Care Medicine*, vol. 23, no. 2, pp. 376–393, 1995.

[4] R. Markgraf, G. Deutschinoff, L. Pientka, and T. Scholten, "Comparison of acute physiology and chronic health evaluations II and III and simplified acute physiology score II: a prospective cohort study evaluating these methods to predict outcome in a German interdisciplinary intensive care unit," *Critical Care Medicine*, vol. 28, no. 1, pp. 26–33, 2000.

[5] M. M. Levy, M. P. Fink, J. C. Marshall et al., "2001 SCCM/ESICM/ACCP/ATS/SIS international sepsis definitions conference," *Critical Care Medicine*, vol. 31, no. 4, pp. 1250–1256, 2003.

[6] S. M. Opal, "Concept of PIRO as a new conceptual framework to understand sepsis," *Pediatric Critical Care Medicine*, vol. 6, no. 3, pp. S55–S60, 2005.

[7] W. Y. Jiang, "Therapeutic wisdom in traditional Chinese medicine: a perspective from modern science," *Discovery Medicine*, vol. 5, no. 29, pp. 455–461, 2005.

[8] A. P. Lu, H. W. Jia, C. Xiao, and Q. P. Lu, "Theory of traditional chinese medicine and therapeutic method of diseases," *World Journal of Gastroenterology*, vol. 10, no. 13, pp. 1854–1856, 2004.

[9] K. L. Liang, R. S. Jiang, C. L. Lee, P. J. Chiang, J. S. Lin, and Y. C. Su, "Traditional Chinese medicine ZHENG identification provides a novel stratification approach in patients with allergic rhinitis," *Evidence-Based Complementary and Alternative Medicine*, vol. 2012, Article ID 480715, 9 pages, 2012.

[10] M. J. Cameron, J. F. Bermejo-Martin, A. Danesh, M. P. Muller, and D. J. Kelvin, "Human immunopathogenesis of severe acute respiratory syndrome (SARS)," *Virus Research*, vol. 133, no. 1, pp. 13–19, 2008.

[11] P. C. Leung, "The efficacy of Chinese medicine for SARS: a review of Chinese publications after the crisis," *The American Journal of Chinese Medicine*, vol. 35, no. 4, pp. 575–581, 2007.

[12] D. X. Yan, X. P. Yu, K. H. Shi, W. B. Song, H. Y. Zhang, and J. L. Wei, "Discussion about treatment of severe acute respiratory syndrome based on syndrome differentiation," *Journal of Chinese Integrative Medicine*, vol. 2, no. 4, pp. 241–244, 2004.

[13] SARS, "Clinical trials on treatment using a combination of traditional Chinese medicine and Western medicine," in *International Expert Meeting to Review and Analyse Clinical Reports on Combination Treatment for SARS*, WHO, Ed., World Health Organization, Beijing, China, 2003.

[14] J. Liu, E. Manheimer, Y. Shi, and C. Gluud, "Chinese herbal medicine for severe acute respiratory syndrome: a systematic review and meta-analysis," *Journal of Alternative and Complementary Medicine*, vol. 10, no. 6, pp. 1041–1051, 2004.

[15] M. M. Zhang, X. M. Liu, and L. He, "Effect of integrated traditional Chinese and Western medicine on SARS: a review of clinical evidence," *World Journal of Gastroenterology*, vol. 10, no. 23, pp. 3500–3505, 2004.

[16] X. Liu, M. Zhang, L. He, Y. P. Li, and Y. K. Kang, "Chinese herbs combined with Western medicine for severe acute respiratory syndrome (SARS)," *Cochrane Database of Systematic Reviews*, no. 1, Article ID CD004882, 2006.

[17] W. A. Knaus, E. A. Draper, D. P. Wagner, and J. E. Zimmerman, "APACHE II: a severity of disease classification system," *Critical Care Medicine*, vol. 13, no. 10, pp. 818–829, 1985.

[18] T. Calandra, J. D. Baumgartner, G. E. Grau et al., "Prognostic values of tumor necrosis factor/cachectin, interleukin-1, interferon-$\alpha$, and interferon-$\gamma$ in the serum of patients with septic shock," *Journal of Infectious Diseases*, vol. 161, no. 5, pp. 982–987, 1990.

[19] F. Riche, Y. Panis, M. J. Laisne et al., "High tumor necrosis factor serum level is associated with increased survival in patients with abdominal septic shock: a prospective study in 59 patients," *Surgery*, vol. 120, no. 5, pp. 801–807, 1996.

[20] R. T. Patel, K. I. Deen, D. Youngs, J. Warwick, and M. R. B. Keighley, "Interleukin 6 is a prognostic indicator of outcome in severe intra-abdominal sepsis," *The British Journal of Surgery*, vol. 81, no. 9, pp. 1306–1308, 1994.

[21] C. H. Wang, M. J. Gee, C. Yang, and Y. C. Su, "A new model for outcome prediction in intra-abdominal sepsis by the linear discriminant function analysis of IL-6 and IL-10 at different heart rates," *Journal of Surgical Research*, vol. 132, no. 1, pp. 46–51, 2006.

[22] S. M. El-Maghraby, M. M. Moneer, M. M. Ismail, L. M. Shalaby, and H. A. El-Mahallawy, "The diagnostic value of C-reactive protein, interleukin-8, and monocyte chemotactic protein in risk stratification of febrile neutropenic children with hematologic malignancies," *Journal of Pediatric Hematology/Oncology*, vol. 29, no. 3, pp. 131–136, 2007.

[23] S. Fujishima, J. Sasaki, Y. Shinozawa et al., "Serum MIP-1$\alpha$ and IL-8 in septic patients," *Intensive Care Medicine*, vol. 22, no. 11, pp. 1169–1175, 1996.

[24] A. Oberholzer, U. Steckholzer, M. Kurimoto, O. Trentz, and W. Ertel, "Interleukin-18 plasma levels are increased in patients with sepsis compared to severely injured patients," *Shock*, vol. 16, no. 6, pp. 411–414, 2001.

[25] Z. Z. Li, Y. H. Liu, K. H. Lai, and D. R. Tang, "Discussion on the relationship between exogenous febrile disease and epidemic febrile disease," *Chinese Journal of Basic Medicine in Traditional Chinese Medicine*, vol. 9, no. 3, pp. 13–16, 2003.

[26] M. S. Wu, "Relationship between febrile diseases and theory of epidemic febrile diseases," *Jiangsu Journal of Traditional Chinese Medicine*, vol. 26, no. 5, pp. 7–9, 2005.

[27] A. M. Chen, "Relationship between febrile diseases and epidemic febrile diseases," *Guiding Journal of Traditional Chinese Medicine and Pharmacy*, vol. 14, no. 2, pp. 8–9, 2008.

[28] H. Wang and S. Ma, "The cytokine storm and factors determining the sequence and severity of organ dysfunction in multiple organ dysfunction syndrome," *The American Journal of Emergency Medicine*, vol. 26, no. 6, pp. 711–715, 2008.

[29] "American college of chest physicians/society of critical care medicine consensus conference: definitions for sepsis and organ failure and guidelines for the use of innovative therapies in sepsis," *Critical Care Medicine*, vol. 20, no. 6, pp. 864–874, 1992.

[30] Y. C. Su, L. L. Chen, J. D. Lin, J. S. Lin, Y. C. Huang, and J. S. Lai, "BCQ+: a body constitution questionnaire to assess Yang-Xu—part I: establishment of a first final version through a Delphi process," *Forschende Komplementarmedizin*, vol. 15, no. 6, pp. 327–334, 2008.

[31] L. L. Chen, J. S. Lin, J. D. Lin et al., "BCQ+: a body constitution questionnaire to assess Yang-Xu—part II: evaluation of reliability and validity," *Forschende Komplementarmedizin*, vol. 16, no. 1, pp. 20–27, 2009.

[32] A. Lever and I. Mackenzie, "Sepsis: definition, epidemiology, and diagnosis," *The British Medical Journal*, vol. 335, no. 7625, pp. 879–883, 2007.

[33] L. J. Kaplan, K. McPartland, T. A. Santora, and S. Z. Trooskin, "Start with a subjective assessment of skin temperature to identify hypoperfusion in intensive care unit patients," *Journal of Trauma*, vol. 50, no. 4, pp. 620–627, 2001.

[34] A. Lima, T. C. Jansen, J. van Bommel, C. Ince, and J. Bakker, "The prognostic value of the subjective assessment of peripheral perfusion in critically ill patients," *Critical Care Medicine*, vol. 37, no. 3, pp. 934–938, 2009.

[35] O. Court, A. Kumar, J. E. Parrillo, and A. Kumar, "Clinical review: myocardial depression in sepsis and septic shock," *Critical Care*, vol. 6, no. 6, pp. 500–508, 2002.

Hindawi Publishing Corporation
Evidence-Based Complementary and Alternative Medicine
Volume 2013, Article ID 807801, 7 pages
http://dx.doi.org/10.1155/2013/807801

*Research Article*

# Efficacy of Crest Herbal Toothpaste in "Clearing Internal Heat": A Randomized, Double-Blind Clinical Study

**Jia-Xu Chen, Yue-Yun Liu, Shao-Xian Wang, and Xiao-Hong Li**

*School of Preclinical Medicine, Beijing University of Chinese Medicine, No. 11, Beisanhuan Donglu, Chaoyang District, P.O. Box 83, Beijing 100029, China*

Correspondence should be addressed to Jia-Xu Chen; chenjiaxu@hotmail.com

Received 19 June 2013; Revised 12 August 2013; Accepted 1 September 2013

Academic Editor: Shibing Su



*Objective*. Evaluation of the efficacy of Crest Herbal Crystal Toothpaste in "clearing internal heat." *Methods*. This was a randomized, double-blind, controlled parallel design clinical test of a product that was already on the market. 72 subjects were randomly assigned to control group (group A with Colgate Herbal Salty Toothpaste) or treatment group (group B with Crest Herbal Crystal Toothpaste) with ratio of 1 : 2. Subjects were instructed to brush with 1g toothpaste for 2 minutes each time, 2 times per day in a 4-aweek test period; measurement with the rating scale on the efficacy of "clearing internal heat" for the herbal toothpaste was done at baseline, 2 weeks, and 4 weeks of toothpaste usage. *Results*. The rating scale on efficacy of "clearing internal heat" for the herbal toothpaste reveals that the primitive points of 72-case intention-to-treat (ITT) analysis and 67-case per-protocol (PP) analysis for subjects in group A and subjects in group B were found to be reduced progressively with statistical significance ($P < 0.05$). The overall effective rates for group A and group B were, respectively, 62.50%, 56.25% (ITT) and 62.50%, 60.64% (PP). The statistical results indicated that the symptoms of fire-heat for both groups of subjects have been improved after application of toothpaste. *Conclusion*. The efficacy of Crest Herbal Crystal Toothpaste in "clearing internal heat" was confirmed by the trial as compared to Colgate Herbal Salty Toothpaste. And its efficacy was objectively evaluated by the rating scale on efficacy of "clearing internal heat."

## 1. Introduction

With the quickened pace of life and increased pressure of work for nowadays people, oral diseases such as toothache, sore, or bleeding gums occur very commonly. Most of these symptoms were considered "excessive internal heat" by traditional Chinese medicine (TCM). Meanwhile, as one of the daily necessities of oral cleaning agents, many types of herbal toothpaste claim to have the efficacy of "clearing internal heat." When consumers select toothpastes, their decisions were not only based on cleaning factors, but also on considerations for dental care and prevention of oral diseases. Because of cultural and geographical factors, herbal toothpastes with efficacy of "clearing internal heat" were estimated to have enormous market opportunities in China. Currently, there were a few reports [1, 2] on the efficacy of "clearing internal heat" by TCM for oral diseases, and effectiveness of herbal toothpastes has been found.

Traditional Chinese medical science paid extra attention to dental hygiene and prevention and treatment of diseases at early time. Totally eight categories were documented in the sections that involve oral diseases in Prescriptions for Universal Relief in Ming Dynasty (early at 15 centuries BC) [3], and ancient TCM doctors had already accumulated very abundant experiences in the prevention and treatment of oral diseases.

Crest Herbal Crystal Toothpaste, containing the essence scientifically extracted from the natural herbs of honeysuckle and mint with function of anti-inflammation and sterilization as well as heat-clearing and detoxication, is a kind of toothpaste of TCM exclusively manufactured by P&G Technology Co., Ltd, which has been identified to effectively remove bacteria in the mouth and freshen breath to prevent gum disease, therefore, keeping overall health for teeth and gums.

The purpose of this clinical trial was to scientifically evaluate the efficacy of Crest Herbal Crystal Toothpaste, using our reported rating scale (the 3rd edition) [4] with good reliability and validity on efficacy of "clearing internal heat" for the herbal toothpaste developed in prophase. The selected

positive control toothpaste was Colgate Herbal Salty Toothpaste with effect of "clearing internal heat," containing herbal essence, of which the main ingredients were honeysuckle and mint for tingly fresh breath and all day protection, soothing oral ailments like toothaches, mouth ulcers, and inflamed gums. The control product has been in the China market for a long time with the following claim: reducing internal heat. We therefore chose them as a comparison to the Crest brand.

## 2. Data and Methods

*2.1. Demographic Data.* All subjects were recruited by the Research Institute of Crest Oral Care, Beijing P&G Technology Co., Ltd., and the trial period was from August 26, 2009 to September 23, 2009. 72 subjects were randomly divided by ratio of 1 : 2 into control group with 24 subjects (group A) and test group with 48 subjects (group B). As it was the first time to evaluate the "clearing internal heat" efficacy of Crest herbal product, more data were needed to get a clear understanding relative to the control product, so 1 : 2 ratio recruiting was used in this study.

72 subjects were typical permanent residents in Beijing, among whom were 16 of males and 56 of females, aged between 19 and 55, with average age of 28, and randomly divided into two groups with the ratio of 1 : 2, and toothpaste A or toothpaste B was provided, respectively, where 24 subjects were arranged in group A and 48 subjects in group B. After unblinding, it was found that Colgate Herbal Salty Toothpaste was provided for group A, while Crest Herbal Crystal Toothpaste was for group B. The period of using the toothpaste was 4 weeks, collecting data of oral cavity and related symptoms of oral conditions for subjects after the end of the second week and the fourth week.

*2.2. Diagnostic Criteria and Inclusion and Exclusion Criteria*

*2.2.1. Diagnostic Criteria.* Diagnostic criteria for oral diseases of "syndrome of fire-heat" by TCM were formulated as referred to by Diagnostics of TCM edited by Chen and Wilson [5].

(1) Medical history: causative factors such as excessive spicy diet, tiredness, or excessive smoking and alcoholic drinking were found.

(2) Symptoms: they are recurrent attacks of toothache, swelling and aching of gum, gingival bleeding, oral ulcers, halitosis, bitter taste of mouth and dry pharynx, and so forth, often accompanied by sore throat, hydrodipsia, constipation, and yellow urine.

(3) Diagnosis: the patient has swelling and aching of gum, halitosis, red tongue, yellow coat, and red throat.

The above mentioned seven symptoms include toothache, swelling and aching of gum, gingival bleeding, aphthous stomatitis, halitosis, bitter taste of mouth, and dry pharynx; if the patients were with one of three (with three) or more they can be diagnosed as having "syndrome of fire-heat."

*2.2.2. Inclusion Criteria.* Inclusion Criteria encompass those who met the diagnostic criteria for oral diseases of "syndrome of fire-heat" by TCM; those who had no serious organic and mental diseases; those whose course of disease was within a month; those whose ages ranged from 18 to 55; those who had signed informed consent form (ICF).

*2.2.3. Exclusion Criteria.* The following subjects were excluded from this study: younger than 18 or older than 55; being pregnant or breast-feeding; being allergic to this toothpaste; used other brands of toothpastes for treatment; those who had complications from other diseases in cardiovascular system, cerebrovascular system, and hepatic, renal, and hematopoietic system as well as psychiatric patients.

*2.3. Clinic Trial Design.* We adopted a randomized, double-blind, single-center, and parallel control with positive toothpaste design for this study.

PROCPLAN procedure statement of SAS was used to design randomization of the trial. Statistical Analysis System (SAS) was software developed by North Carolina State University in 1966, with complete data access, data management, data analysis, and data presentation features. SAS was often used in the pharmaceutical industry for a variety of experimental studies, which could be done with simple programming. PROCPLAN procedure statement; of SAS was used to give a statement of randomized design. In this study, we gave a number of seeds randomly, and inputted statements meet the condition of this trail in the PROCPLAN procedure statement, then SAS outputted the therapeutic assignment corresponding to serial numbers from 01 to 72, which was, the randomized arrangement of treatments received by 72 subjects.

The requirement and design of blinding: verification toothpastes were packaged and provided by sponsor according to the randomization allocation table. The design of two-grade blind method was adopted, of which the first grade was the two treatments (group A or B randomly assigned) corresponding to each serial number from 01 to 72, while the second grade was the group (control group, treatment group) corresponding to A or B treatment. The allocation concealment of both grades was separately sealed up in duplicate for each, stored at the office of study site in the head organization and the sponsor. Two-grade unblinding was performed after cases collection. First of all, we clarified the code of two treatment groups corresponding to each serial number to perform statistical analysis and then identified the code of group (control group, treatment group) corresponding to each treatment group after completion of statistical analysis.

*2.4. Treatment Methods*

*2.4.1. The Name and Specification of Toothpaste Used in the Trial.* Test toothpaste, Crest Herbal Crystal Toothpaste, as mentioned in Section 1, had the role of removing oral bacteria, freshening breath, and keeping health of teeth and gums, which was manufactured by P&G Technology Co., Ltd. (a research agency belonging to Procter & Gamble Company, which was mainly responsible for daily consumer goods' research and development, especially in the "fabric and home care" and "oral care" areas) batch no. 90991864BA, specification: 120 g/tube.

Experimental Product (Not for sale. For subject's use only).
Study #: 2009OCC19.
Usage Instruction: Brush twice daily for two minutes.
Distributed by: Rui Wang, Beijing Health Tech Research Co., Ltd. Beijing, China 100086.
This product may contain Fluoride. Net Weight: ≤120 g.
Notes: Store at room temperature. Keep out of the reach of children. Do not swallow. In case of medical emergency, call Rui Wang, at a cell phone number.

Box 1: Description for package of toothpaste used in the trial.

Control toothpaste: the selected Colgate Herbal Salty Toothpaste contains herbal essence to make oral cavity healthy and fresh of which the main ingredients were honeysuckle and mint. It has been in China market for a long time with the exact effect of "clearing internal heat," which was manufactured by Colgate-Palmolive Co., Ltd. batch no. 9042CN11, specification: 120 g/tube.

*2.4.2. Package of Toothpaste.* White toothpaste tube of qualified hygiene was adopted as package material for Crest Herbal Crystal Toothpaste and Colgate Herbal Salty Toothpaste, and the label are listed in Box 1.

*2.4.3. The Randomized Blinding.* By using PROCPLAN procedure statement of SAS as mentioned in Section 2.3, we made randomly arrangements for treatments received by 72 subjects (test toothpaste or control toothpaste) that was to list the treatment allocation corresponding to serial numbers from 01 to 72.

*2.4.4. Allocation of Toothpaste.* We distributed toothpaste corresponding to the code specified randomly which is screened to include the qualified subjects and to distribute toothpaste by the administrator according to the proper order of subject's visit as well as the sequence of toothpaste's code. "Registration table for product release" should be filled by administrator of toothpaste in time.

*2.4.5. Check Off Toothpaste.* Whenever follow-up visit was made, the doctor should record the amount of toothpaste that the subject had received, used, and returned so as to determine the compliance of the subject in using the toothpaste.

*2.4.6. Preservation of Toothpaste.* The toothpastes used in the trial were preserved by designated person at dry drafty place under room temperature and distributed to the subjects according to the requirement of the trial design.

*2.4.7. Toothpastes Used in Combination*

(1) Except the toothpastes used for verification, other therapies related to the treatment of the diseases were not allowed to use during the observation period.

(2) If medicines or other therapies must be used for complicated diseases, then the drug names (or names of other therapies), dosage, frequency, and time of usage must be noted on the medical record for the trial in order to be used for analysis and report at summarization.

*2.4.8. Treatment and Observation Time for Subjects.* Inclusion of subject: subjects who met the inclusion criteria, being out of exclusion criteria, were included for observation.

Treatment methods: Crest Herbal Crystal Toothpaste was provided for test group, while Colgate Herbal Salty Toothpaste was provided for control group, and both groups were given 1 g/each time, bid. The subjects were instructed in correct brushing method (BASS brushing method, brushed teeth twice a day, morning and night, at least 2 minutes for tooth-brushing each time). (The subjects were required to be present at trial site receiving tooth-brushing instruction for 3 times every week.) All subjects spent 4 weeks (28 d) for treatment course.

The Bass brushing technique is scientifically proven to disrupt, disorganize, and remove the bad bugs that cause gum disease in our mouth. The Bass method, or Sulcular vibration brushing, or the 45-degree angle tooth brushing technique is a very effective method for germs or plaque removal next to and directly below the gum or gingival margin. The area at the gum-tooth margin is the most significant in the prevention of tooth decay and gum disease [6].

Observation time: the rating scale (the 3rd edition) [4] on efficacy of "clearing internal heat" for the herbal toothpaste was used before toothpaste application, at 2 w (14 d) of application and 4 w (28 d), respectively, for the subjects to fill for 3 times separately.

*2.5. Criteria of Efficacy*

*2.5.1. Measurement.* Rating scale (the 3rd edition) [4] on efficacy of "clearing internal heat" for the herbal toothpaste is one of the criteria.

*2.5.2. Criteria for General Efficacy Determination.* Refer to Guiding Principles for the New Drug Clinical Research of China Medicines (On trial) [7]. Symptomatic quantifying standards: 4-level method is adopted for grading: 0 point for absence of symptoms; 2 points for slight level; 4 points for mediate level; 6 points for severe level.

$N$ represents curative index: $N$ = ((accumulated points of symptoms before treatment − accumulated points of symptoms after treatment)/accumulated points of symptoms before treatment) × 100%.

Clinical cure: symptoms and signs disappeared after treatment, $N \geq 95\%$; marked improvement: most of symptoms

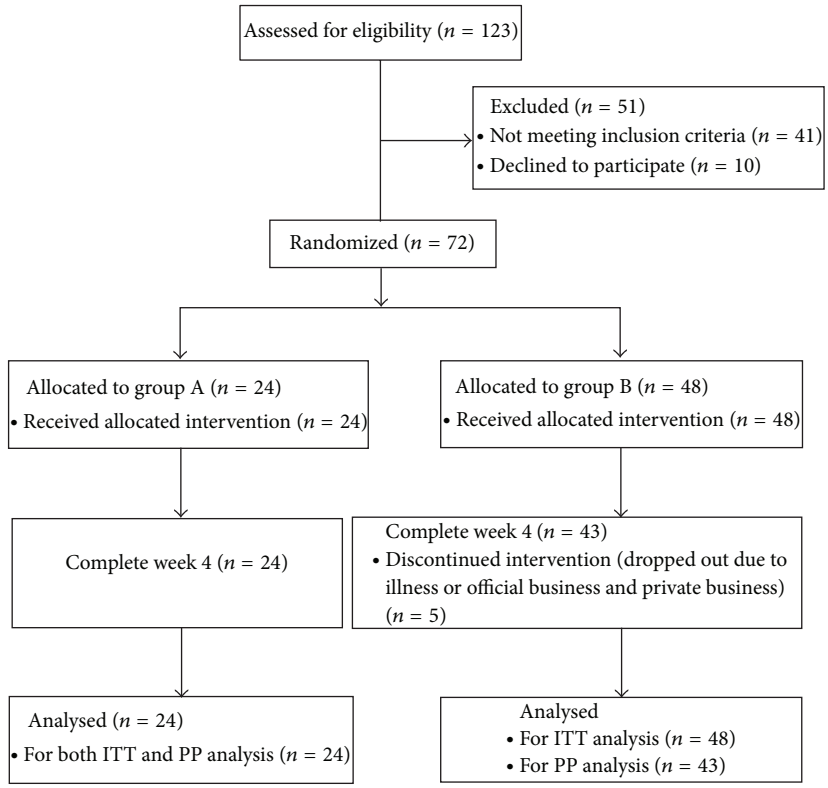


Figure 1: Participant flow through recruitment to trial completion.

and signs disappeared after treatment, 95% > $N \geq$ 70%; effective: a part of symptoms and signs disappeared after treatment, 70% > $N \geq$ 30%; ineffective: symptoms and signs did not disappear or aggravated after treatment, $N <$ 30%.

*2.5.3. Criteria of Efficacy Determination for Single Parameter.* $N$ represents curative index: $N$ = ((grade of symptoms before treatment − grade of symptoms after treatment)/grade of symptoms before treatment) × 100%.

Cure: $N = 1$; marked improvement: $1 > N = 2/3$ (67%); effective: $N = 1/3$ (33%) or $N = 1/2$ (50%); ineffective: $N = 0$ or $N < 0$.

### 2.6. Statistical Analysis

*2.6.1. Choice of Statistical Data for Evaluation of Curative Effect.* Intention-to-treat (ITT) analysis and per-protocol (PP) analysis was adopted. ITT analysis could prevent the poor prognosis patients excluded from the analysis and retain the advantages of randomization; PP analysis could reflect the actual results of completion of treatment by program and reduce the impact of interference or contamination.

Full analysis set: all randomized subjects were included, and those subjects without any observation data for follow-visits were rejected. For the data of subjects which did not include all results of entire treatment course, the result for latest observation must be carried forward to where the absence of verification data was found. The number of subjects at the endpoint of curative evaluation should be the same as that at the start of trial. PP set includes subjects who were consistent with the trial protocol, while the major variables were measurable, and no great violation to trial protocol was found.

ITT analysis was performed on 72 subjects, who were on full analysis set, of which 24 subjects were from group A and 48 subjects were from group B; 67 subjects were on PP set, of which 24 subjects were from group A and 43 subjects were from group B; 5 subjects dropped out due to illness or official business and private business.

In this study, the results would be better reflected when we performed the ITT and PP analysis at the same time. The closer the ITT and PP results are, the less the proportion of defaulter, the higher the quality of research, and the more credible the results will be.

*2.6.2. Statistical Method.* As for descriptive statistical analysis, qualitative indexes were described with percentage or constituent ratio, while quantitative indexes were described with mean ± standard deviation (SD). In comparative analysis between the two groups, we used Chi-square test, Fisher's exact test, and Wilcoxon rank sum tests. $t$ test was performed on quantitative data of normal distribution, and Wilcoxon rank sum test was done on data with skewed distribution data.

For demographic data analysis, Chi-square analysis was conducted to compare the sex ratio of two groups, and $t$ test was done to compare age and baseline inner heat level. For efficacy data analysis, normal test was done firstly to check if data fit in normal distribution, and then $t$ test or Wilcoxon

Table 1: Comparison of demographic data between the two groups (mean value ± standard deviation).

| Group | Sex (male/female) | Age ($X \pm SD$) | Grade of symptoms ($X \pm SD$) |
|---|---|---|---|
| Group A (24 subjects) | 7/17 | 28.42 ± 7.52 | 28.33 ± 6.79 |
| Group B (48 subjects) | 9/39 | 27.88 ± 6.99 | 26.25 ± 4.88 |
| $P$ value | 0.3162 ($X^2 = 1.0045$) | 0.6789 ($Z = 0.4140$) | 0.2337 ($Z = 1.1908$) |

rank sum test was done based on data property. Unified double-tailed test was used for hypothesis testing, while test statistics and the corresponding $P$ value were provided, and the statistical significance was confirmed if $P < 0.05$. EXCEL, Epidata 3.02, or SAS 8.2 statistical package was used in above analysis.

## 3. Results

A total of 123 subjects were assessed for eligibility, and 72 subjects were enrolled, 24 were randomised to group A and 48 to the control group B. Five randomly allocated participants in group B did not complete the study (see Figure 1).

*3.1. Comparison of Demographic Data.* Baseline characteristics are listed in Table 1. There was no significant difference between the two groups on sex, age, and level of fire-heat syndrome.

In Table 1, the difference of the demographic data such as sex, age and level of fire-heat syndrome among subjects between the two groups was not statistically significant ($P > 0.05$), which indicated the same baseline of two groups, and available comparability.

*3.2. Evaluation Result from the Rating Scale (the 3rd Edition) [4] on Efficacy of "Clearing Internal Heat" for the Herbal Toothpaste*

*3.2.1. Evaluation Result of Full Analysis Set for 72 Subjects in the Two Groups (Intention-to-Treat (ITT) Analysis).* It was shown in Table 2 that the mean value of syndrome of fire-heat has been reduced for both groups A and B, and there was no difference in curative effect between the two groups. Equivalence test was performed on the two groups at the same time, and the result 17.73 was between $Q = 13.84$~$25.24$, indicating that the two groups were equivalent in treatment effect.

*3.2.2. Per-Protocol (PP) Analysis for 67 Subjects of the Two Groups.* It was shown in Table 3 that the mean value of syndrome of fire-heat has been reduced for both groups A and B, and there was no difference in curative effect between the two groups. The result 17.40 was between $Q = 13.76$~$25.32$, indicating that the two groups were equivalent in treatment effect.

The results in Tables 2 and 3 indicated that from the rating scale (the 3rd edition) [4] on efficacy of "clearing internal heat" for the herbal toothpaste, the original accumulated points were found to be reduced progressively with statistical significance for subjects of both group A and group B after application of toothpaste, which suggested that symptoms of fire-heat have been improved for both groups after use of the toothpaste. The results were consistent with ITT and PP analysis.

Table 2: Comparison of original accumulated points among 72 subjects between the two groups before and after treatment (mean value ± standard deviation) (intention-to-treat (ITT) analysis).

| Group | Baseline | Week 2 | Week 4 |
|---|---|---|---|
| Group A (24 subjects) | 28.33 ± 6.79 | 21.75 ± 6.04* | 19.54 ± 6.19* |
| Group B (48 subjects) | 26.25 ± 4.88 | 20.02 ± 5.72* | 17.73 ± 5.48* |

Compare with the result before treatment in the group, $^*P < 0.05$.

*3.2.3. Evaluating the Curative Effect for the Two Groups after Treatment with the Rating Scale (the 3rd Edition) [4].* With effective rate ≥ 33%, it meant effective under this item; otherwise it was ineffective. It was shown in Table 4 that in group A, the effective rate of $Q5$, $Q7$, and $Q8$ was greater than 33%. In group B, the effective rate of $Q2 \sim Q8$ was greater than 33%. The overall effective rate of both groups was slightly lower than 33%, and no significant difference was found in curative effect between the two groups ($P > 0.05$).

It was shown in Table 5 that in group A, the effective rate of $Q5$, $Q7$, and $Q8$ was greater than 33%, which represented effectiveness, while the rest was lower than 33%, which represented ineffectiveness, and the overall effective rate was $31\% < 33\%$. In group B, the effective rate of $Q2 \sim Q8$ was greater than 33%, which represented effectiveness, while the rest was lower than 33%, which represented ineffectiveness, and the overall effective rate was $34\% > 33\%$. No significant difference was found in curative effect between the two groups ($P > 0.05$).

From the rating scale (the 3rd edition) [4] on efficacy of "clearing internal heat" for the herbal toothpaste, different data analysis was used in Tables 4 and 5, and the result indicated that the overall effective rate for both group A and group B was about 33%, which represented effectiveness.

*3.2.4. Comparison of Curative Effect of the Two Groups with the Rating Scale (the 3rd Edition) [4] after the Treatment.* Table 6 showed that effective rate in group A was slightly higher than that in group B (both values ≥30%), while the ineffective rate in group A was slightly lower than that in group B, and $P > 0.05$ by Wilcoxon rank sum test for both groups. No statistical significance was found, indicating there was no difference of overall curative effect between the two groups. The results were consistent with ITT and PP analysis.

Table 3: Comparison of original accumulated points among 67 subjects between the two groups before and after treatment (mean value ± standard deviation) (per-protocol (PP) analysis).

| Group | Baseline | Week 2 | Week 4 |
|---|---|---|---|
| Group A (24 subjects) | 28.33 ± 6.79 | 21.75 ± 6.04* | 19.54 ± 6.19* |
| Group B (43 subjects) | 26.34 ± 4.82 | 19.95 ± 5.50* | 17.40 ± 5.22* |

Compare with the result before treatment in the group, $^{*}P < 0.05$.

Table 4: Effective rate of full analysis set for 72 subjects in the two groups after treatment (%, ITT).

| | $Q1$ | $Q2$ | $Q3$ | $Q4$ | $Q5$ | $Q6$ | $Q7$ | $Q8$ | $Q9$ | $Q10$ | $Q11$ | (total) $Q$ |
|---|---|---|---|---|---|---|---|---|---|---|---|---|
| Group A (24 subjects) | 26% | 31% | 26% | 30% | 41% | 32% | 40% | 37% | 19% | 30% | 23% | 31% |
| Group B (48 subjects) | 29% | 36% | 41% | 33% | 39% | 35% | 33% | 38% | 23% | 12% | 22% | 32% |

Mean = −0.0058; SD = 0.078; $t = -0.2597$; $P > 0.05$.

Table 5: Effective rate of PP set for 67 subjects in the two groups after treatment (%, PP).

| | $Q1$ | $Q2$ | $Q3$ | $Q4$ | $Q5$ | $Q6$ | $Q7$ | $Q8$ | $Q9$ | $Q10$ | $Q11$ | (total) $Q$ |
|---|---|---|---|---|---|---|---|---|---|---|---|---|
| Group A (24 subjects) | 26% | 31% | 26% | 30% | 41% | 32% | 40% | 37% | 19% | 30% | 23% | 31% |
| Group B (43 subjects) | 31% | 38% | 43% | 35% | 43% | 36% | 33% | 39% | 24% | 15% | 22% | 34% |

Mean = −0.0225; SD = 0.077; $t = -1.006$; $P > 0.05$.

Table 6: Evaluating the overall effective rate of both groups with the rating scale (the 3rd edition) [4] after treatment (number of cases and %).

| Dataset | Group | Cure | Markedly effective | Effective | Ineffective | |
|---|---|---|---|---|---|---|
| FA set | Group A (24 subjects) | 0 (0) | 0 (0) | 15 (62.50) | 9 (37.50) | $z = -0.4613$ |
| (ITT) | Group B (48 subjects) | 0 (0) | 0 (0) | 27 (56.25) | 21 (43.75) | $P = 0.6446$ |
| PP set | Group A (24 subjects) | 0 (0) | 0 (0) | 15 (62.50) | 9 (37.50) | $z = -0.4613$ |
| (PP) | Group B (43 subjects) | 0 (0) | 0 (0) | 26 (60.64) | 17 (39.53) | $P = 0.6446$ |

(Full analysis) FA set $P = 0.6446$, PP set $P = 0.6446$.

## 4. Discussion

Oral diseases such as toothache, sore, or bleeding gums are very common, and most of them are regarded as "excessive internal heat" by TCM. The symptom of fire-heat is classified as deficiency and excess, where the fire in ZANG FU-organ is divided into stomach-fire, excessive heart fire, and hepatic fire. The formation of oral fire-heat symptom is related to the factors such as excessive spicy diet, tiredness, or excessive smoking and alcoholic drinking, as well as long-term depressed emotion leading to fire symptom [5]. However, in consideration of the manifestations of oral fire-heat symptom especially in young subjects, it mainly belongs to stomach-fire pattern manifestation such as toothache, swelling and aching of gum, gingival bleeding, oral ulcers, halitosis, bitter taste of mouth, and dry pharynx often accompanied by sore throat, hydrodipsia, constipation and yellow urine, and red tongue with thick yellow coat [5].

Based on the TCM theory, patients who suffered from oral fire-heat pattern could be easily diagnosed by a TCM doctor according to medical history and symptoms. However, such oral fire-heat pattern was often neglected by the patients, so we have developed a self-report rating scale (the 3rd edition) [4] (with good reliability and validity) to objectively evaluate oral fire-heat pattern. Crest Herbal Crystal Toothpaste, containing herbs of honeysuckle and mint with heat-clearing and detoxing, functions can protect teeth and gums. Honeysuckle, Flos Lonicerae, is a medically useful TCM herb, with the function of clearing heat and removing toxicity and of antibacterial activity [8]. Mint, *mentha haplocalyx*, is also commonly used in TCM, with the function of eliminating pathogen, in addition to fresh breath [8]. Also Colgate Herbal Salty Toothpaste with the efficacy of "clearing internal heat" is designated as positive control in the trial. Both herbal toothpastes with exotic herbal ingredients for tingly fresh breath and all day protection contain nature's best herbs which soothe oral ailments like toothaches, mouth ulcers, and inflamed gums.

Evaluation with the rating scale (the 3rd edition) [4] on efficacy of "clearing internal heat" for the herbal toothpaste indicated that no significant difference between Crest Herbal Crystal Toothpaste and the positive control was found in aspect of improving the accumulated points of oral fire-heat syndrome, for the subjects, level of oral fire-heat syndrome and overall effective rate. Meanwhile, we simultaneously observed the evaluation by the doctor with the symptoms grading scale of fire-heat pattern (SGS-FHP) for the herbal toothpaste, and the results also indicated that no significant difference between Crest Herbal Crystal Toothpaste and the positive control was found (this will be published in another report). This suggested that Crest Herbal Crystal Toothpaste has the equal efficacy of "clearing internal heat", while the availability of efficacy of "clearing internal heat" for Crest Herbal Crystal Toothpaste can be evaluated objectively by

the rating scale (the 3rd edition) [4] on efficacy of "clearing internal heat" for the herbal toothpaste.

## 5. Conclusion

This study confirms that the Crest Herbal Crystal Toothpaste has the effect of "clearing internal heat" with Colgate Herbal Salty Toothpaste as the on-market control. And the efficacy of Crest Toothpaste in "clearing internal heat" is evaluated by the rating scale (the 3rd edition) [4] on efficacy of "clearing internal heat" for the herbal toothpaste.

## Appendix

## The Rating Scale (the 3rd Edition) [4] on Efficacy of "Clearing Internal Heat" for the Herbal Toothpaste

Self-filling section: the following questions inquire about the common symptoms of traditional Chinese medicine during the last month. Answer every question by marking the appropriate box with a "√". Please according to your true feelings choose from one of the following answers.

| | 1 | 2 | 3 | 4 | 5 |
|---|---|---|---|---|---|
| | Never | Occasionally | Often | Very often | Always |
| How often was it, that you (your) | 1 | 2 | 3 | 4 | 5 |
| (1) feel dryness of throat; | □ | □ | □ | □ | □ |
| (2) feel thirsty and want to drink especially cold water; | □ | □ | □ | □ | □ |
| (3) feel bitter taste in mouth; | □ | □ | □ | □ | □ |
| (4) suffered from oral malodor (halitosis); | □ | □ | □ | □ | □ |
| (5) suffered from oral ulcer on mucosa or tongue; | □ | □ | □ | □ | □ |
| (6) suffered from swelling and aching of gums; | □ | □ | □ | □ | □ |
| (7) suffered from bleeding gums; | □ | □ | □ | □ | □ |
| (8) suffered from toothache; | □ | □ | □ | □ | □ |
| (9) suffered from lightly swelling, but no red or aching of gums; | □ | □ | □ | □ | □ |
| (10) suffered from loose teeth and inability to chew; | □ | □ | □ | □ | □ |
| (11) suffered from dry teeth (sticky feeling between the teeth and upper and lower lips). | □ | □ | □ | □ | □ |

Interview section: tongue body and tongue coating inspected and chose by TCM doctors.

(12) Tongue body: pale, pink, red, light purplish, deep red, or fissured.

(13) Tongue coating: thin and whitish, white, thin and yellowish, yellowish greasy, dryness, eroded, or less coating.

## Acknowledgments

This research was supported by Grants from China National Funds for Distinguished Young Scientists (no. 30825046), Program for Innovative Research Team in Beijing University of Chinese Medicine (2011CXTD-07), and Beijing Proctor & Gamble Technology Ltd. Co. It needs to be declared that there is no potential conflict of interests between them. The authors are grateful to Dr Min-Juan Wang who works at San Diego State University for her revision of English grammar and words. They would also like to thank Chun Li, Nan Wang, Jianqiong Peng, and Haizhen Cui for taking part in clinical data collection.

## References

[1] X. Pei, "Clinical application of chinese medicine in treatment of periodontal disease," *Journal of Modern Stomatology*, vol. 15, no. 2, pp. 151–152, 2001.

[2] H. Chen, X. Ding, X. H. Zhang, W. Zhang, Y. Li, and S. S. LEE, "In vitro antimicrobial potential of 5 chinese herbal toothpastes," *Chinese Journal of Microecology*, vol. 19, no. 4, pp. 352–353, 2007.

[3] L. Yang, "The historical materials of stomatological in Zhu Su's Pu ji Fang," *Chinese Journal of Medical History*, vol. 29, pp. 121–123, 1999.

[4] H. Zhao, S. X. Wang, X. H. Li, and J. X. Chen, "Development and evaluation of chinese medicine fire-heat syndrome scale in oral cavity for measuring chinese herb toothpaste," *Chinese Journal of Integrative Medicine*, vol. 19, no. 3, pp. 192–199, 2013.

[5] J. X. Chen and J. F. Wilson, *Diagnostics in Chinese Medicine*, Peoples Medical, Beijing, China, 1st edition, 2011.

[6] M. Poyato-Ferrera, J. J. Segura-Egea, and P. Bullón-Fernández, "Comparison of modified bass technique with normal toothbrushing practices for efficacy in supragingival plaque removal," *International Journal of Dental Hygiene*, vol. 1, no. 2, pp. 110–114, 2003.

[7] X. Y. Zheng, *Guiding Principles for the New Drug Clinical Research of China Medicines*, vol. 105, China Press of Traditional Chinese Medicine, Beijing, China, 2002.

[8] China Pharmacopoeia Committee, *Pharmacopoeia of the People'S Republic of China 2010*, vol. 1, China Medical Science Press, Beijing, China, 2011.

Hindawi Publishing Corporation
Evidence-Based Complementary and Alternative Medicine
Volume 2013, Article ID 248650, 12 pages
http://dx.doi.org/10.1155/2013/248650

*Research Article*

# Rheumatoid Arthritis with Deficiency Pattern in Traditional Chinese Medicine Shows Correlation with Cold and Hot Patterns in Gene Expression Profiles

**Minzhi Wang,[1] Gao Chen,[2] Cheng Lu,[1] Cheng Xiao,[3] Li Li,[1] Xuyan Niu,[1] Xiaojuan He,[1] Miao Jiang,[1] and Aiping Lu[1,4,5]**

[1] *Institute of Basic Research in Clinical Medicine, China Academy of Traditional Chinese Medicine, Beijing 100700, China*
[2] *School of Life Sciences, Hubei University, Wuhan 430062, China*
[3] *Sino-Japan Friendship Hospital, Beijing 100029, China*
[4] *School of Chinese Medicine, Hong Kong Baptist University, Kowloon, Hong Kong*
[5] *E-Institute of Shanghai Municipal Education Commission, Shanghai TCM University, Shanghai 201203, China*

Correspondence should be addressed to Miao Jiang; miao_jm@vip.126.com and Aiping Lu; aipinglu@hkbu.edu.hk

Received 28 April 2013; Revised 15 July 2013; Accepted 17 July 2013

Academic Editor: Shao Li



In our precious study, the correlation between cold and hot patterns in traditional Chinese medicine (TCM) and gene expression profiles in rheumatoid arthritis (RA) has been explored. Based on TCM theory, deficiency pattern is another key pattern diagnosis among RA patients, which leads to a specific treatment principle in clinical management. Therefore, a further analysis was performed aiming at exploring the characteristic gene expression profile of deficiency pattern and its correlation with cold and hot patterns in RA patients by bioinformatics analysis approach based on gene expression profiles data detected with microarray technology. The TCM deficiency pattern-related genes network comprises 7 significantly, highly connected regions which are mainly involved in protein transcription processes, protein ubiquitination, toll-like receptor activated NF-$\kappa$B regulated gene transcription and apoptosis, RNA clipping, NF-$\kappa$B signal, nucleotide metabolism-related apoptosis, and immune response processes. Toll-like receptor activated NF-$\kappa$B regulated gene transcription and apoptosis pathways are potential specific pathways related to TCM deficiency patterns in RA patients; TCM deficiency pattern is probably related to immune response. Network analysis can be used as a powerful tool for detecting the characteristic mechanism related to specific TCM pattern and the correlations between different patterns.

## 1. Introduction

Rheumatoid arthritis (RA) is a common autoimmune disease with a prevalence of over 1% of the population worldwide [1]. This inflammatory disease is characterized by chronic inflammation and progressive impair in joints and immunity disorder [2, 3]. Inflammatory cell infiltration in synovial membrane plays a crucial role in the pathogenesis of RA, including CD4+ T cells, which are activated in joint sites [4–7]. Activated CD4+ T cells can promote IL-17 producing and enhance immune activity, and other cytokines like IL-2, IL-4, and IL-10 are also secreted by CD4+ T cells, and these will either upregulate or downregulate immune reaction in RA patients [8–10]. Circulating CD4+CD161+ T cells are now regarded to be a potential biomarker of RA disease activity [11]. Thus, it is believed that studies on this subset of T cells can promote better understandings of joint immune response and inflammation in RA.

Patients with RA vary considerably in terms of their clinical manifestations and outcome [12]. Some of the complementary and alternative medical systems, such as traditional Chinese medicine (TCM), take a different approach in diagnosing and treating RA. In TCM, patients with RA are further stratified according to their symptoms, a pattern (also called Zheng or syndrome) diagnosis will be determined for a subgroup of the patients, and then specific therapy will be prescribed based on these pattern classifications [13]. In

RA patients, cold, hot, and deficiency patterns were regarded as 3 major pattern classifications in clinical practice [14]; in our previous study, the correlation between cold and hot patterns in TCM and gene expression profiles in RA has been explored [15]. MAPK signaling, Wnt signaling, and insulin signaling pathways were revealed to be related to TCM hot pattern; purine metabolism was related to both TCM hot and cold patterns; alanine, aspartate, and tyrosine metabolisms were related to TCM cold pattern, and histidine metabolism and lysine degradation were related to TCM hot pattern [15]. Interestingly, other studies also detected the functions of general cold/hot pattern-related genes [16, 17], and in some specific diseases, such as gastritis [18], further found the imbalanced network biomarkers for traditional Chinese medicine syndrome in gastritis patients [19]. These results indicated that different pattern could be regarded as a consequence of biological networks comprising hundreds of thousands of gene expressions changed in various affected tissues and immune effector cells; thus, the functional gene network analysis might be a useful tool in exploring the biological fundamentals of pattern classification in RA.

As another key pattern diagnosis among RA patients, deficiency pattern can lead to a specific treatment principle of "tonifying the deficiency" in clinical management. Therefore, the elucidation of the underlying mechanism of deficiency pattern in RA in the context of gene expression profile should not only open out mechanism of classical TCM theory on pattern classification but also enriche current research on complex diseases.

Yet the study on deficiency pattern should be different from that on cold/hot pattern, and for that the hot and cold patterns are typical, these two types of patterns can be easy to be classified in each patient in clinical practice. The deficiency pattern summarizes another set of clinical manifestations, and in most cases it is accompanied with hot or cold pattern (resulting in cold-deficiency pattern, or hot-deficiency pattern). Thus in order to achieve better understanding on deficiency pattern and the comparison with cold/hot pattern, in this study we concentrated on the symptom sets by factor analysis which contribute to pattern classification and then we try to explore the significantly related genes to these symptom sets. This analysis method has been successfully used in our previous study on cold and hot patterns [15].

Therefore, on the basis of previous study, further analysis aiming at exploring the characteristic gene expression profile of deficiency pattern and its correlation with cold and hot patterns in RA patients is underscored. In the present study, a genome-wide expression technology and systems biology approach were combined to reveal the characteristic gene expression profile of deficiency pattern and its correlations with cold and hot patterns in RA patients.

## 2. Materials and Methods

*2.1. Patients.* A total of 33 female RA patients from the China-Japan Friendship Hospital and 12 healthy female volunteers from the China Academy of Chinese Medical Science in Beijing, aged 18 to 70 years old, participated in the study. RA patients were eligible to participate if they had met the American College of Rheumatology (ACR) criteria for RA for at least one year, with functional classes of I, II, or III [20]. Patients with cold/hot/deficiency pattern, or combination pattern (hot deficiency or cold deficiency), were recorded with whole clinical manifestations according to TCM theory using a questionnaire, a tongue examination, and pulse diagnosis by 3 appointed TCM practitioners [14, 21]. Patients were included in the study only if the 3 practitioners reported consistent results. Healthy females without any diagnosed diseases were included as controls.

Patients who had continuously received nonsteroidal anti-inflammatory corticosteroid drugs for more than 6 months or who had received these medicines within one month were excluded from the study. Patients with severe cardiovascular, lung, liver, kidney, mental, or blood system diseases and women who were pregnant, breastfeeding, or planning pregnancy in the next 8 months were excluded from the study. A complete joint function and biochemical function evaluation was available for all participants in the study. The study was granted by the local Ethical Committee for Clinical Research, and each patient signed informed consent before enrollment.

*2.2. Sample Preparation.* For the microarray, 8 mL of venous blood was collected in anticoagulation tubes from each of the 45 participants before breakfast. CD4+ T cells were extracted and purified using the RosetteSep Human CD4+ T Cell Enrichment Cocktail (StemCell Technologies, Inc., Vancouver, Canada) [22]. Total RNA was isolated from the CD4+ T cells using the Trizol extraction method (Invitrogen, Carlsbad, Canada), as described by the manufacturer. mRNA was amplified linearly using the MessageAmp aRNA Kit (Ambion, Inc., Austin, USA), in accordance with the instructions of the manufacturer. cRNA was purified using an RNeasy Mini Kit (QIAGEN, Hilden, Germany) based on a standard procedure.

*2.3. Microarray Assay.* Total RNA was extracted using TRIZol reagent from CD4+ T cells according to the manufacturer's instruction. Probes were verified for amplification yield and incorporation efficiency by measuring the DNA concentration at 280 nm, Cy3 incorporation at 550 nm, and Cy5 incorporation at 650 nm. For each color, 10 pmol incorporated dye was fragmented and resuspended in 500 $\mu$L hybridization solution. Samples were hybridized to dual-color human Whole Genome Microarray (University of British Columbia, Canada) that contained four arrays of probes representing around 23,232 well-characterized transcripts. The arrays were hybridized in microarray hybridization chambers overnight at 42°C. After washing, the slides were scanned with GenePix 4000B scanner.

All nonflagged array elements for which the fluorescent intensity in each channel was 1.5 times greater than the local background were considered well measured. The ratio values were log-transformed (base 2) and stored in a table (rows, individual cDNA clones; columns, single mRNA species). cDNA spots that fulfilled the intensity criteria on at least 80% of the microarrays were analyzed. Data for the remaining

genes were centered by subtracting (in log space) the median observed value to remove any effect of the amount of mRNA in the common reference pool.

### 2.4. Statistics and Functional Analysis

*2.4.1. TCM Pattern Classification and Correlation Analysis.* Since clinical manifestation is the key information for TCM pattern classification, and in most cases the deficiency pattern is accompanied with hot or cold pattern, in this study, 58 clinical manifestations were listed for recording before blood collection based on TCM theory. Then factor analysis was applied for clustering the clinical manifestations into 3 different sets based on the TCM pattern diagnosis. The 3 factors contributed significantly to the cold, hot, and deficiency pattern diagnoses, respectively; furthermore, clinicians proved that the symptoms in each factor were the most common ones for diagnosing the relative pattern in real TCM clinical practice. Therefore, the factors were regarded as the representatives of the 3 patterns and employed in further correlation analysis. The TCM patterns-related genes were selected with correlation analysis (coefficient $> 0.5$ or $< -0.5$, and $P < 0.05$ as significant). All data were analyzed on an SAS9.1.3 statistical package (Order no. 195557), and a cluster analysis was performed using Cluster 3.0 and Tree View software.

*2.4.2. Microarray Statistics.* The data were normalized to correct for technical variations among individual microarray hybridizations using the two-step procedure described in detail by Jarvis and colleagues. The signal intensity of each expressed gene was globally normalized (LOWESS) using the R statistics program [23]. Any ratio between two groups (RA and healthy control) of more or less than 1 : 1.5 was taken as the differential gene expression criteria. Statistical significance was tested using the Student's $t$-test ($P < 0.05$). Changes greater than 1.5-fold (cold or hot or deficiency pattern to control group) were recorded as upregulations, and those less than 1.5-fold (cold or hot or deficiency pattern to control group) were recorded as downregulations. Other fold changes for gene expression were recorded as normal expression. Changes in gene expression (1.5-fold change) were required in more than 50% of the patients. A chi-squared test was used for these comparisons ($P < 0.05$) and to identify similar and different genes in the deficiency pattern and cold/hot pattern groups of differentially expressed genes. Gene assemblages related to the 3 symptom sets (as 3 patterns) were obtained using correlation analysis.

*2.4.3. Protein-Protein Interaction Analysis and Network Illustration.* The information on human protein-protein interactions was obtained from databases, including Biomolecular Interaction Network Database (BIND), The General Repository for Interaction Datasets (BioGRID), Database of Interacting Proteins (DIP), Human Protein Reference Database (HPRD), Database system and analysis tools for protein interaction data (IntAct), and Molecular Interactions Database (MINT), and was complemented with curated relationships parsed from the literature using Agilent Literature Search [24]. These datasets are mostly based on experimental evidence. We did not include data that were deemed to be of lower quality. The protein-protein interaction network was visualized using cytoscape [25].

Table 1: Basic information of enrolled patients.

| Index | Value range | Mean ± SD |
|---|---|---|
| Age (years) | 25–55 | 42.8 ± 9.9 |
| Duration of RA (month) | 1–240 | 57.4 ± 56.9 |
| X-ray score | 0–2 | 0.18 ± 0.47 |
| Rheumatoid factor | 0–673 | 135.6 ± 177.0 |
| Erythrocyte sedimentation rate (mm/h) | 4–140 | 43.9 ± 35.6 |
| C-reactive protein (mg/L) | 0–185 | 13.0 ± 34.1 |

*2.4.4. Highly Connected Clusters of the Integrated Network.* The database and the literature data mining networks were integrated, and then IPCA was used to analyze the characteristics of the network. The IPCA algorithm can detect densely connected regions in the interactome network [26]. Interactomes with a score greater than 2.0 and at least four nodes were taken as significant predictions in this study.

*2.4.5. Gene Ontology Analysis.* To identify the function of each cluster generated by IPCA individually, GO clustering analysis was performed with the proteins described in all subnetworks. For this purpose, the latest version of Biological Network Gene Ontology (BiNGO) tool [27] was used to statistically evaluate groups of proteins with respect to the existing annotations of the Gene Ontology Consortium. The degree of functional enrichment for a given cluster was quantitatively assessed ($P$ value) by hypergeometric distribution, implemented in BiNGO tool. The 10 GO biological categories with the smallest $P$ values were selected as significant.

## 3. Results

*3.1. The Identification of Deficiency Pattern.* In the 33 enrolled patients (12 with cold pattern and 21 with hot pattern), 18 were diagnosed with deficiency pattern and 15 with non-deficiency pattern. Among the 18 patients with deficiency pattern, 8 were diagnosed with cold-deficiency pattern and 10 with hot-deficiency pattern. No typical deficiency pattern was individually diagnosed. The basic clinical information of the enrolled patents was listed in Table 1. The clinical manifestations of RA patients were clustered into three sets with factor analysis, which were corresponding to the cold, hot, and deficiency patterns in TCM, respectively. Deformity, inhibited bending and stretching in limbs, pain occurring or worsening at night, pain occurring or worsening during moodiness, and numbness were categorized in TCM deficiency pattern (as listed in Table 2). The symptom sets for cold and hot patterns are the same as those reported in our previous cold and hot patterns in RA study (data not shown) [14].

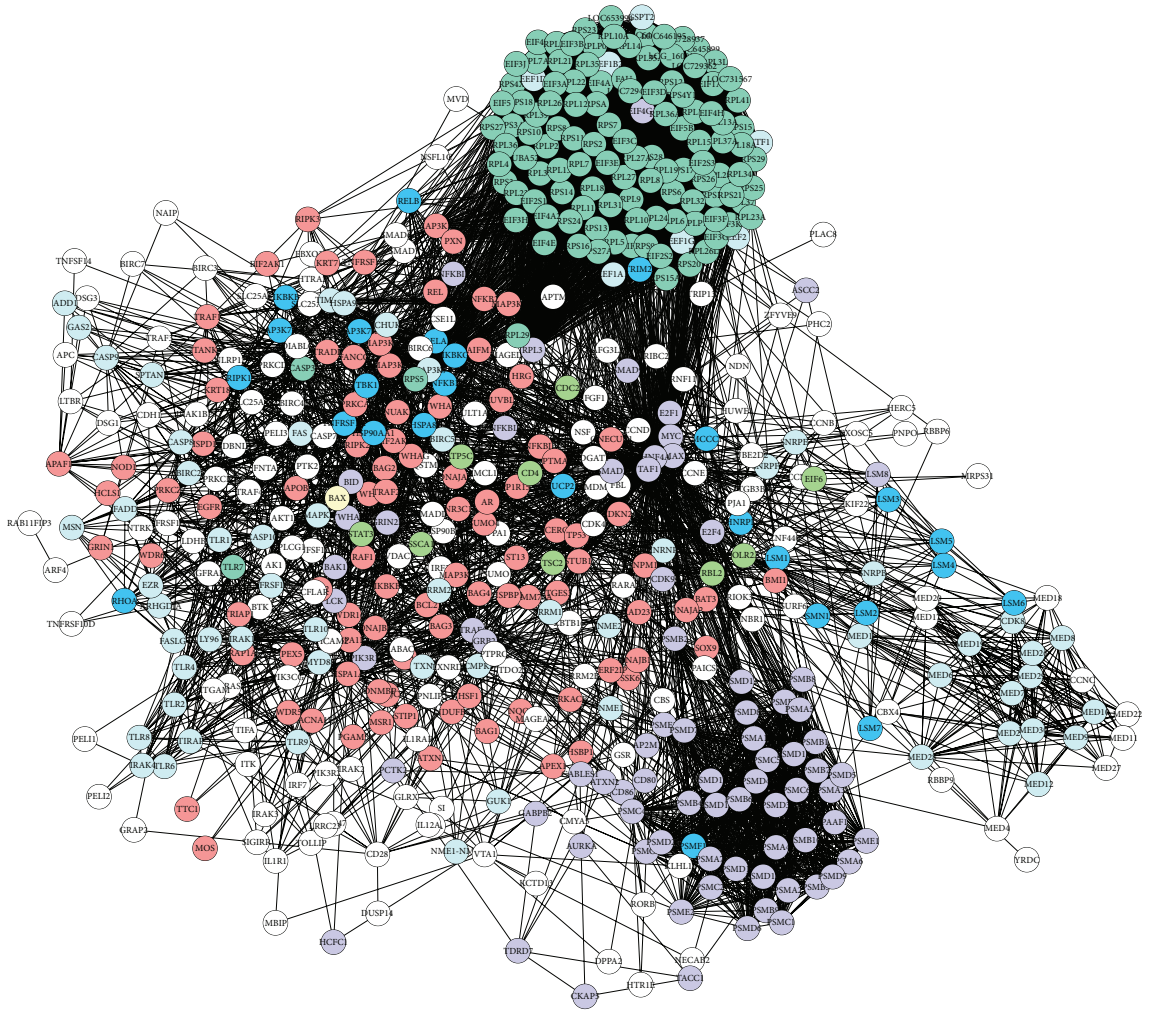

Figure 1: Protein-protein interaction (PPI) network for deficiency pattern-related genes. Cycles represent nodes. All edges represent interactions between the nodes. The green nodes represent cold pattern-related molecules; plum stands for hot pattern-related molecules; light blue stands for deficiency pattern; yellow stands for both cold and hot patterns; bluish green stands for both cold and deficiency patterns; deep blue stands for both hot and deficiency patterns; dark blue stands for cold, hot, and deficiency patterns.

Table 2: The factor related to deficiency pattern obtained in factor analysis after oblique PROMAX rotation*.

| Clinical symptoms | Factor loading |
|---|---|
| Deformity | 0.81 |
| Inhibited bending and stretching in limbs | 0.69 |
| Pin occurring or worsening at night | 0.63 |
| Pain occurring or worsening during moodiness | 0.58 |
| Numbness | 0.40 |

*The data in the table are factor loadings obtained after oblique PROMAX rotation. The factor loading represents the correlation power of the symptom with the factor. A loading value of more than 0.20 suggests that there is correlation of the articular manifestation with the factor.

*3.2. The TCM Deficiency Pattern and Its Functional Gene Networks.* The TCM RA deficiency pattern-related genes were selected using correlation analysis. All related genes were listed in Table 3.

To further refine the biological functions of these genes, protein and protein interaction analysis was applied based on the genes listed in Table 3, and the molecular networks for those genes were built up (Figure 1). In the network, the nodes represent proteins and the edges represent interactions between the proteins. More importantly, during the process of analysis, cold and hot patterns related differential genes (data not shown) were marked in the deficiency pattern network if those cold or hot pattern-related genes were included in the network in order to clarify the potential relations among deficiency pattern and cold/hot pattern in RA. Seven significantly, highly connected regions were proposed by IPCA, and these subnetworks of highly connected regions were visualized by cytoscape (Figure 2).

The subnetworks of highly connected regions and functions of the nodes are mainly involved in protein transcription processes, protein ubiquitination, toll-like receptor activated nuclear factor $\kappa$B (NF-$\kappa$B) regulated gene transcription and apoptosis, RNA clipping, NF-$\kappa$B signal, nucleotide

Table 3: TCM deficiency pattern related genes in RA*.

| Name | ID | Coefficient value | *P* value |
|---|---|---|---|
| Hypothetical gene CG018 | NM_052818 | 0.61 | 0.0045 |
| Homo sapiens cDNA FLJ11557 fis, clone HEMBA1003083 | AK021619 | 0.59 | 0.0011 |
| Hypothetical protein FLJ10769 | NM_018210 | 0.58 | 0.0057 |
| Homo sapiens cDNA: FLJ23020 fis, clone LNG00943 | AK026673 | 0.55 | 0.0027 |
| Cytochrome c-1 | NM_001916 | 0.53 | 0.0116 |
| Phosphoprotein associated with glycosphingolipid-enriched microdomains | NM_018440 | 0.53 | 0.002 |
| Tumor necrosis factor receptor superfamily, member 10b | AF016266 | 0.53 | 0.012 |
| Hematological and neurological expressed 1 | NM_016185 | 0.53 | 0.0015 |
| Homo sapiens cDNA FLJ13721 fis, clone PLACE2000450 | AK023783 | 0.53 | 0.0044 |
| HSPC041 protein | NM_016099 | 0.53 | 0.0016 |
| KIAA0826 protein | AB020633 | 0.52 | 0.0046 |
| Small fragment nuclease | NM_015523 | 0.52 | 0.0169 |
| Protein phosphatase 2A 48 kDa regulatory subunit | NM_013239 | 0.51 | 0.0096 |
| HSPC160 protein | NM_014182 | 0.51 | 0.0051 |
| Mitochondrial ribosomal protein L11 | NM_016050 | −0.5 | 0.0046 |
| Hypothetical protein MDS025 | NM_021825 | −0.51 | 0.0028 |
| KIAA1270 protein | AB033096 | −0.56 | 0.0104 |
| DKFZP586D0824 protein | BC013934 | −0.56 | 0.0008 |
| Lin-7b protein; likely ortholog of mouse LIN-7B; mammalian LIN-7 protein 2 | NM_022165 | −0.64 | 0.0019 |

*The genes were selected with correlations analysis (coefficient value >0.5 or < −0.5, and $P < 0.05$).

metabolism-related apoptosis, and immune response processes. Particularly the articular manifestations in deficiency pattern were related to toll-like receptor activated NF-$\kappa$B regulated gene transcription and apoptosis (Figure 2(c)) and nucleotide metabolism-related apoptosis (Figure 2(f)).

*3.3. TCM Deficiency Pattern-Related Central Subnetwork Analysis and Its Correlations with Cold and Hot Patterns.* The deficiency pattern-related central subnetwork was analyzed by IPCA, and the functions of genes involved in the central subnetwork were presented in Table 4. The central subnetwork and functions of the nodes are mainly involved in NF-$\kappa$B and macromolecule metabolic processes. The central subnetwork was visualized by cytoscape (Figure 3(a)). Most nodes in this network are dark blue, bluish green, plum and deep blue, which indicate that the major biological mechanism of TCM deficiency pattern is closely correlated with cold and hot patterns.

Then the network modules of deficiency, cold, and hot patterns are combined (Figure 3(b)), and through network analysis, the correlations among deficiency, cold, and hot patterns are revealed. There are 3 green-predominant modules which represent cold pattern-related mechanism, and functions of these modules are mainly involved in ubiquitylation, RNA clipping, and JAK-STAT cascade signaling; 1 plum-predominant module represents hot pattern related mechanism with function of insulin signaling; 3 light blue-predominant modules are deficiency pattern related, with functions of toll-like receptor activated NF-$\kappa$B regulated gene transcription and apoptosis, and nucleotide metabolism related apoptosis; 1 yellow-predominant module is related to both cold and hot patterns with function of JAK-STAT signaling-related apoptosis; 1 bluish green-predominant module is related to both cold and deficiency patterns with function of protein translation process; 2 deep blue-predominant modules denote the mechanism relevant to both hot and deficiency pattern, with functions of NF-$\kappa$B signaling and mRNA clipping; 1 dark blue-predominant module is related to cold, hot, and deficiency patterns, with the functions of ubiquitylation and apoptosis.

Table 4: Description of central subnetwork biofunctions related to deficiency pattern in RA.

| Description | *P* value |
|---|---|
| Translational elongation | $9.4409E-19$ |
| Cellular protein metabolic process | $7.6789E-13$ |
| Cellular macromolecule metabolic process | $2.2814E-11$ |
| Cellular macromolecule biosynthetic process | $9.7307E-11$ |
| Macromolecule biosynthetic process | $1.3144E-10$ |
| Macromolecule metabolic process | $5.9427E-10$ |
| Cellular metabolic process | $1.0405E-09$ |
| Gene expression | $1.8878E-09$ |
| Primary metabolic process | $4.6891E-09$ |
| Activation of NF-$\kappa$B-inducing kinase activity | $1.4532E-08$ |

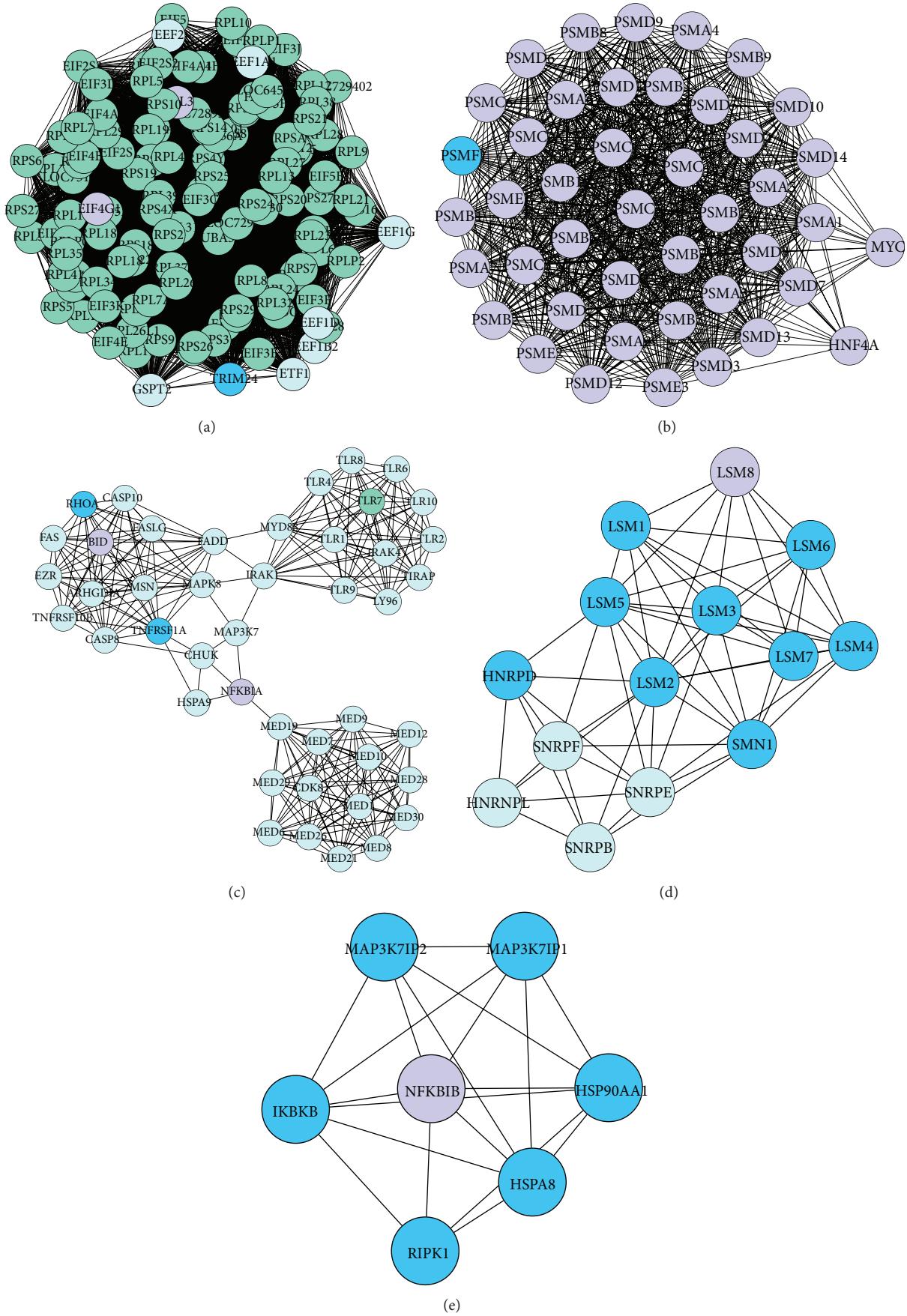


Figure 2: Continued.

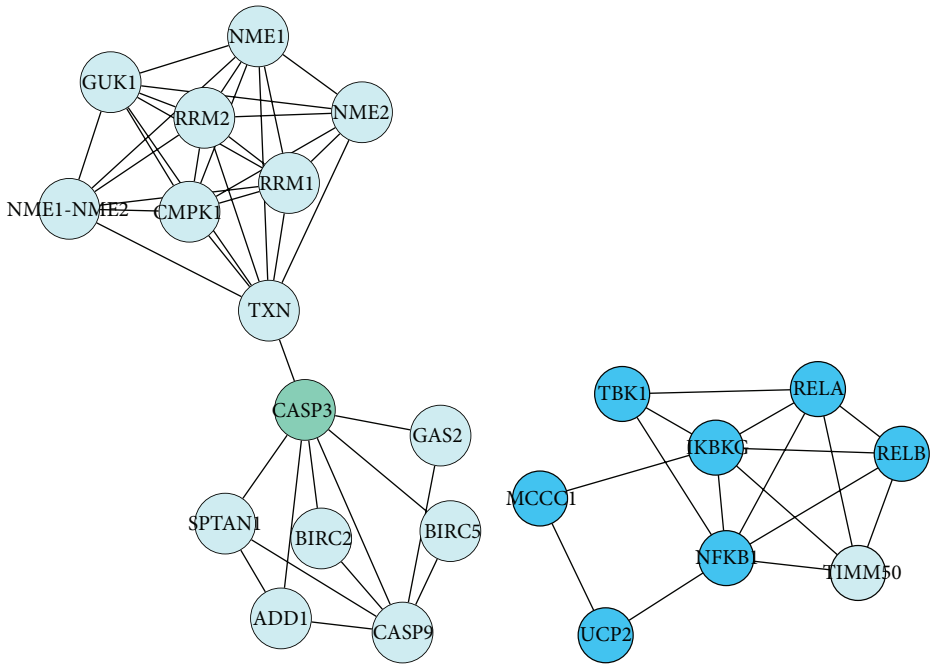


Figure 2: The subnetworks made up of highly connected regions and functions of the nodes in TCM deficiency pattern-related genes. Cycles represent nodes. All edges represent interactions between the nodes. Clusters with score >2 were considered to be significant (it represents the log of the probability that the network was found by chance).

## 4. Discussion

The major findings in this study include revealing the characteristics of TCM deficiency pattern and the correlations between deficiency pattern and cold/hot pattern in gene expression profile. To date, this is the first study to explore the distinct and common features among three basic patterns in RA patients at a genome-wide level.

From the view of both biomedicine and TCM, the clinical manifestations in RA patients are diverse and complex, which pose challenges on diagnostic study. For example, it has been pointed out that, besides some common articular symptoms, bone destruction or erosion-related symptoms can start early or later from disease onset, which can result in loss of physical function [28]. Given the tight correlation between physical disability and loss of social and economic opportunities in patients with RA [29], treatment options which are capable of profoundly interfering with joint damage would appear to be of greater value under the framework of biomedical theory [30].

In TCM clinical practice, the symptoms of RA can be classified into different groups, and based on this classification, pattern diagnosis can be determined and guides the therapy selection [13]. The cold, hot, and deficiency patterns are key patterns in RA patients, and they can be identified individually or concomitantly, such as deficiency-cold, deficiency-hot, or intermingled cold and hot patterns. The pattern classification can be regarded as a further subgrouping of patients, with the aim of a more precise individualized treatment. Thus, with the ultimate aim to preserve functional status and joint architecture in RA patients, better understanding and characterization of the underlying mechanism of TCM pattern classification in RA patients have been an important goal in RA research in the present years.

Given the complexity of pattern differentiation in clinical practice, another distinctive point in this study is that we selected symptom factors, instead of the typical patients with some specific patterns, as representatives of TCM patterns in the correlation analysis. The significant predominance of this method lies in that we can avoid the confusion resulting from multiple-patterns diagnosis occurring in one patient and the disagreement of different clinicians. Aiming at the major symptom sets which contribute to a pattern would better concentrate on the pattern diagnosis itself and the comparison with other concomitant patterns. This method has been successfully used in our previous study on correlation between cold and hot patterns in gene expression profile [14]. With cold feeling in joints and pain relieved with warming which are important for TCM cold pattern differentiation and hot feeling and pain relieved with cooling which are important for TCM hot pattern differentiation [14], this classification has been verified with factor analysis [31]. For TCM deficiency pattern identification, deformity and inhibited bending and stretching in limbs are key manifestations, and generally these symptoms clinically occur in the later stage of disease or later than other common articular symptoms such as pain with cold or hot feeling and swelling. Thus, in most cases, deficiency pattern is believed as result of prolonged disease or delayed treatment. Of course in some aged patients, deficiency pattern can be identified from the disease onset because of the weak general state of health. What is more, the deficiency pattern is often diagnosed and

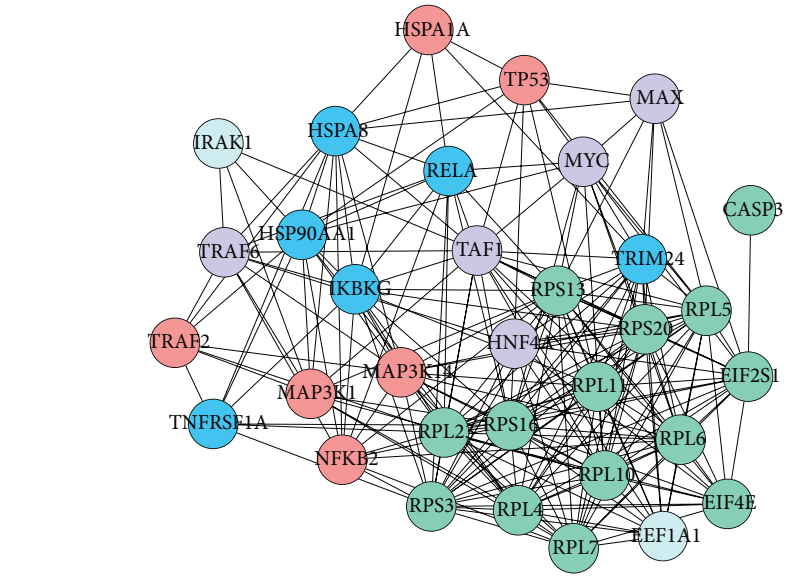


(a)

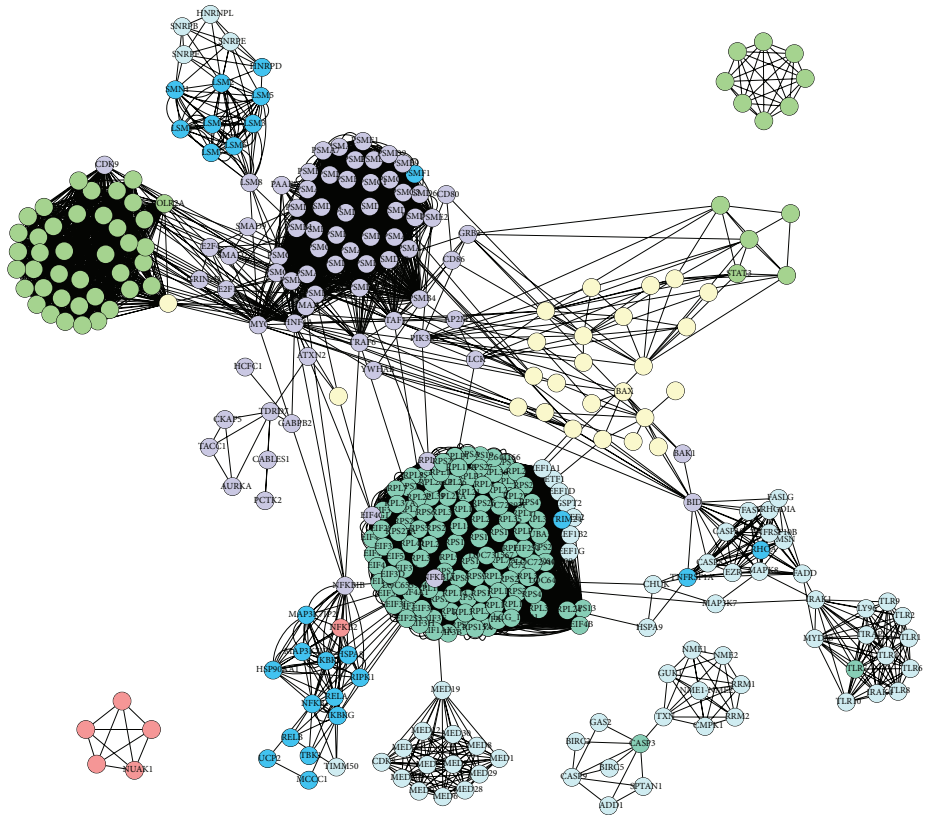

(b)

Figure 3: (a) Central PPI subnetwork related to deficiency pattern in RA. (b) PPI network from combined modules of cold, hot, and deficiency patterns-related genes. Cycles represent nodes. All edges represent interactions between the nodes. The green nodes represent cold pattern-related molecules; plum stands for hot pattern-related molecules; light blue stands for deficiency pattern; yellow stands for both cold and hot patterns; bluish green stands for both cold and deficiency patterns; deep blue stands for both hot and deficiency patterns; dark blue stands for cold, hot, and deficiency patterns.

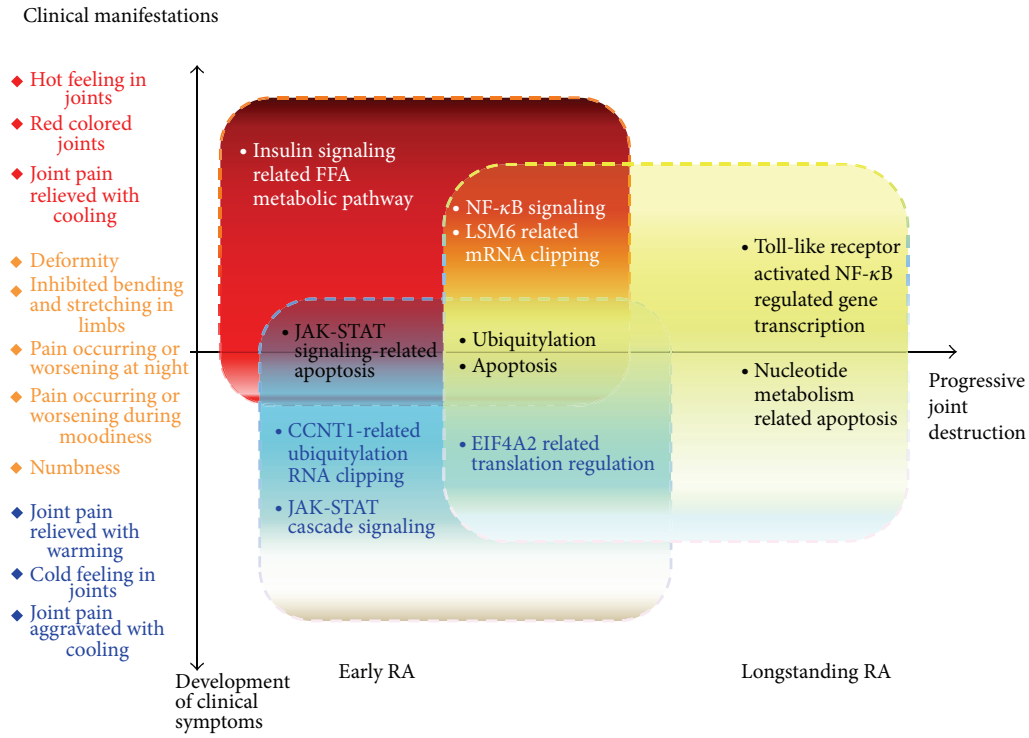


Figure 4: Correlations and characteristics among TCM deficiency, cold, and hot patterns in RA concerning pathways and clinical manifestations. Blue square denotes cold pattern, red square represents hot pattern, and yellow square indicates deficiency pattern.

complicated with cold or hot pattern in clinical practice. These diagnostic principles are in line with the corresponding understandings of RA in biomedicine, also accordant with our findings in this study.

The articular manifestations in deficiency pattern of RA patients were found to be related to protein transcription processes, protein ubiquitination, toll-like receptor activated NF-$\kappa$B regulated gene transcription and apoptosis, RNA clipping, NF-$\kappa$B signal, nucleotide metabolism-related apoptosis, and immune response processes. In particular, toll-like receptor activated NF-$\kappa$B regulated gene transcription and apoptosis and nucleotide metabolism-related apoptosis were specifically responsible for deficiency pattern identification.

NF-$\kappa$B is a set of multifunctional transcriptional factors that regulate expression of genes involved in numerous normal cellular activities [32–34]. They were activated in many inflammatory and neoplastic conditions in which their expression may be stimulated by proinflammatory cytokines [35, 36]. NF-$\kappa$B regulated the expression of cytokines and mediated autocrine, self-amplifying cycles of cytokine release, and NF-$\kappa$B activation leading to maintenance of inflammatory reactions beyond the initial stimulus in RA [36, 37]. Since discovery of the requirement of NF-$\kappa$B for basal and cytokine-induced osteoclast formation in the mid-1990s, many studies have been focused on the role of NF-$\kappa$B in bone [38–40]. NF-$\kappa$B plays predominant roles both in skeletal development, endochondral ossification, osteoclast, and osteoblast functions [39, 41] and in synovial cells of RA [42, 43]. In the synovial cells of patients with RA, activation of the NF-$\kappa$B pathway resulted in the transactivation of a multitude of responsive genes that contribute to the inflammatory phenotype, including TNF-$\alpha$ from macrophages, matrix metalloproteinase from synovial fibroblasts, and chemokine that recruit immune cells to the inflamed pannus. In short, inhibition of NF-$\kappa$B pathway is believed to be a potential therapeutic target in RA [44].

Toll-like receptor is one of the key functions of innate immune system, which can recognize both exogenous pathogen-associated molecular patterns (PAMPs) and endogenous molecules created upon tissue injury, sterile inflammation, and degeneration [45]. Endogenous toll-like receptor ligands were called as damage-associated molecular patters (DAMPs), including endogenous molecules released by activated and necrotic cells and extracellular matrix molecules [46]. The molecule family had many members. Synovial tissues from RA joints expressed toll-like receptor 2 predominantly at attachment sites and invaded cartilage and bone, mostly in synovial fibroblasts, but not in macrophages, in which expression was enhanced not only by IL-1$\beta$ and TNF-$\alpha$ but also by LPS [47]. In synovia of patients with early stage RA, increased expression of toll-like receptors 3 and 4 was demonstrated as well as that of toll-like receptors 2, 3, and 4 in long-lasting RA synovitis [48]. This finding might provide a potential and partially explanation on why deficiency pattern can be identified in both later and early stages of RA. Toll-like receptor activation triggers intracellular signaling pathways that lead to the induction of inflammatory cytokines, type I IFNs, and upregulation of costimulatory molecules leading to the activation of the adaptive immune response [49]. Toll-like receptor activation can promote angiogenesis in various inflammatory settings in response to both exogenous and endogenous ligands [50]. Crucially, further investigation

showed that toll-like receptors were important modulators of mesenchymal stem cells; which played great role in bone formation and bone remodeling, and important regulators in angiogenesis [51, 52]. These findings could partially explain why this pathway is tightly related to TCM deficiency pattern identification, which is based on the onset of joint deformity and inhibited bending and stretching in limbs symptoms.

Since the deficiency pattern is often diagnosed and complicated with cold or hot pattern in clinical practice of TCM, it is of tantamount importance to understand the correlations between deficiency pattern and cold/hot pattern. In our study, the network analysis provides some clues about answering this question. The clinical manifestations and relevant pathways of TCM cold, hot, and deficiency patterns in RA are presented in Figure 4. The results further support our previous findings that different patterns were related to different pathways; on the other hand, it is also indicated that some pathways were shared in different patterns, which might be the underlying mechanism of shared symptoms in different patterns or intermingled patterns. Our data also imply that the identification of the underlying mechanism of and correlations among the TCM patterns might contribute to better understanding of pathogenesis of RA.

However, several potential limitations in our study should not be neglected. Firstly, the typical RA patients with single deficiency pattern are hard to be identified, and in most cases deficiency pattern occurs accompanied with other patterns such as hot or cold pattern. Thus the symptom sets of these patterns acquired by factor analysis were adopted in the gene expression analysis, which might result in some indeterminateness and variance, although this method has been successfully applied in previous study on cold and hot patterns in RA patients. Secondly, our study population is relatively small, and some bias might exist; for example, all enrolled patients are female, despite the exploration of distinct pathways of each TCM pattern and their correlations. Further study of larger sample size is needed in the future. In addition, there exist other TCM patterns in RA patients besides cold, hot, and deficiency patterns, and the neglecting of these patterns might have potential impact on our results.

## 5. Conclusions

Toll-like receptor activated NF-$\kappa$B regulated gene transcription and apoptosis and nucleotide metabolism-related apoptosis pathways are potential specific pathways related to TCM deficiency pattern in RA patients, and TCM deficiency pattern is probably related to immune response. Network analysis can be used as a powerful tool for detecting the distinct and common characteristics among different patterns in RA patients at molecular level. These findings are also able to contribute to the pathogenesis study in RA in light of systems biology.

## Conflict of Interests

All the authors declare that they do not have any conflict of interests to disclose regarding this paper.

## Authors' Contribution

Minzhi Wang and Gao Chen contributed to this work equally.

## Acknowledgments

This research is supported in part by the projects from the National Natural Science Foundation of China (Grant no. 30825047 and no. 30902003), the projects from the China Academy of Chinese Medical Sciences (nos. Z0218 and Z0252), and the E-Institutes of Shanghai Municipal Education Commission (no. E03008).

## References

[1] M. C. Hochberg and T. D. Spector, "Epidemiology of rheumatoid arthritis: update," *Epidemiologic Reviews*, vol. 12, pp. 247–252, 1990.

[2] I. E. M. Bultink, M. Vis, I. E. van der Horst-Bruinsma, and W. F. Lems, "Inflammatory rheumatic disorders and bone," *Current Rheumatology Reports*, vol. 14, pp. 224–230, 2012.

[3] H. Takayanagi, "Osteoimmunology and the effects of the immune system on bone," *Nature Reviews Rheumatology*, vol. 5, no. 12, pp. 667–676, 2009.

[4] G. Carbone, A. Wilson, S. A. Diehl, J. Bunn, S. M. Cooper, and M. Rincon, "Interleukin-6 receptor blockade selectively reduces IL-21 production by CD4 T cells and IgG4 autoantibodies in rheumatoid arthritis," *International Journal of Biological Sciences*, vol. 9, no. 3, pp. 279–288, 2013.

[5] J. A. G. van Roon, J. W. J. Bijlsma, and F. P. J. G. Lafeber, "Diversity of regulatory T cells to control arthritis," *Best Practice and Research*, vol. 20, no. 5, pp. 897–913, 2006.

[6] C. M. Weyand, E. Bryl, and J. J. Goronzy, "The role of T cells in rheumatoid arthritis," *Archivum Immunologiae et Therapiae Experimentalis*, vol. 48, no. 5, pp. 429–435, 2000.

[7] M. Toh and P. Miossec, "The role of T cells in rheumatoid arthritis: new subsets and new targets," *Current Opinion in Rheumatology*, vol. 19, no. 3, pp. 284–288, 2007.

[8] S. Oh, A. L. Rankin, and A. J. Caton, "$CD4^+CD25^+$ regulatory T cells in autoimmune arthritis," *Immunological Reviews*, vol. 233, no. 1, pp. 97–111, 2010.

[9] N. Komatsu and H. Takayanagi, "Autoimmune arthritis: the interface between the immune system and joints," *Advances in Immunology*, vol. 115, pp. 45–71, 2012.

[10] L. Himer, A. Balog, B. Szebeni et al., "Th17 cells in rheumatoid arthritis," *Orvosi Hetilap*, vol. 151, no. 25, pp. 1003–1010, 2010.

[11] J. Miao, J. Geng, K. Zhang et al., "Frequencies of circulating IL-17-producing $CD4^+CD161^+$ T cells and $CD4^+CD161^+$ T cells correlate with disease activity in rheumatoid arthritis," *Modern Rheumatology*. In press.

[12] D. Van Der Woude, A. Young, K. Jayakumar et al., "Prevalence of and predictive factors for sustained disease-modifying antirheumatic drug-free remission in rheumatoid arthritis: results from two large early arthritis cohorts," *Arthritis and Rheumatism*, vol. 60, no. 8, pp. 2262–2271, 2009.

[13] C. Lu, X. Niu, C. Xiao et al., "Network-based gene expression biomarkers for cold and heat patterns of rheumatoid arthritis in traditional chinese medicine," *Evidence-based Complementary and Alternative Medicine*, vol. 2012, Article ID 203043, 17 pages, 2012.

[14] C. Lu, Q. Zha, A. Chang, Y. He, and A. Lu, "Pattern differentiation in traditional chinese medicine can help define specific indications for biomedical therapy in the treatment of rheumatoid arthritis," *Journal of Alternative and Complementary Medicine*, vol. 15, no. 9, pp. 1021–1025, 2009.

[15] M. Jiang, C. Xiao, G. Chen et al., "Correlation between cold and hot pattern in traditional Chinese medicine and gene expression profiles in rheumatoid arthritis," *Frontiers of Medicine in China*, vol. 5, no. 2, pp. 219–228, 2011.

[16] T. Ma, C. Tan, H. Zhang, M. Wang, W. Ding, and S. Li, "Bridging the gap between traditional Chinese medicine and systems biology: the connection of Cold Syndrome and NEI network," *Molecular BioSystems*, vol. 6, no. 4, pp. 613–619, 2010.

[17] S. Li, Z. Q. Zhang, L. J. Wu, X. G. Zhang, Y. D. Li, and Y. Y. Wang, "Understanding ZHENG in traditional Chinese medicine in the context of neuro-endocrine-immune network," *IET Systems Biology*, vol. 1, no. 1, pp. 51–60, 2007.

[18] B. Jiang, X. Liang, Y. Chen et al., "Integrating next-generation sequencing and traditional tongue diagnosis to determine tongue coating microbiome," *Scientific Reports*, vol. 2, p. 936, 2012.

[19] R. Li, T. Ma, J. Gu, X. Liang, and S. Li, "Imbalanced network biomarkers for traditional Chinese medicine Syndrome in gastritis patients," *Scientific Reports*, vol. 3, p. 1543, 2013.

[20] F. C. Arnett, S. M. Edworthy, D. A. Bloch et al., "The American Rheumatism Association 1987 revised criteria for the classification of rheumatoid arthritis," *Arthritis and Rheumatism*, vol. 31, no. 3, pp. 315–324, 1988.

[21] W. Y. Jiang, "Therapeutic wisdom in traditional Chinese medicine: a perspective from modern science," *Discovery Medicine*, vol. 5, no. 29, pp. 455–461, 2005.

[22] C. Lu, C. Xiao, G. Chen et al., "Cold and heat pattern of rheumatoid arthritis in traditional Chinese medicine: distinct molecular signatures indentified by microarray expression profiles in CD4-positive T cell," *Rheumatology International*, vol. 32, no. 1, pp. 61–68, 2012.

[23] Y. H. Yang, S. Dudoit, P. Luu et al., "Normalization for cDNA microarray data: a robust composite method addressing single and multiple slide systematic variation," *Nucleic Acids Research*, vol. 30, no. 4, p. e15, 2002.

[24] A. Vailaya, P. Bluvas, R. Kincaid, A. Kuchinsky, M. Creech, and A. Adler, "An architecture for biological information extraction and representation," *Bioinformatics*, vol. 21, no. 4, pp. 430–438, 2005.

[25] P. Shannon, A. Markiel, O. Ozier et al., "Cytoscape: a software Environment for integrated models of biomolecular interaction networks," *Genome Research*, vol. 13, no. 11, pp. 2498–2504, 2003.

[26] M. Li, J. Chen, J. Wang, B. Hu, and G. Chen, "Modifying the DPClus algorithm for identifying protein complexes based on new topological structures," *BMC Bioinformatics*, vol. 9, article 398, 2008.

[27] S. Maere, K. Heymans, and M. Kuiper, "BiNGO: a Cytoscape plugin to assess overrepresentation of Gene Ontology categories in Biological Networks," *Bioinformatics*, vol. 21, no. 16, pp. 3448–3449, 2005.

[28] K. W. Drossaers-Bakker, M. de Buck, D. van Zeben, A. H. Zwinderman, F. C. Breedveld, and J. M. Hazes, "Long-term course and outcome of functional capacity in rheumatoid arthritis: the effect of disease activity and radiologic damage over time," *Arthritis and Rheumatism*, vol. 42, no. 9, pp. 1854–1860, 1999.

[29] V. Strand and D. Khanna, "The impact of rheumatoid arthritis and treatment on patients' lives," *Clinical and Experimental Rheumatology*, vol. 28, no. 3, pp. S32–S40, 2010.

[30] S. Li, B. Zhang, D. Jiang, Y. Wei, and N. Zhang, "Herb network construction and co-module analysis for uncovering the combination rule of traditional Chinese herbal formulae," *BMC Bioinformatics*, vol. 11, no. 11, article S6, 2010.

[31] Y. He, A. Lu, Y. Zha, and I. Tsang, "Differential effect on symptoms treated with traditional Chinese medicine and western combination therapy in RA patients," *Complementary Therapies in Medicine*, vol. 16, no. 4, pp. 206–211, 2008.

[32] S. T. Smale, "Dimer-specific regulatory mechanisms within the NF-κB family of transcription factors," *Immunological Reviews*, vol. 246, no. 1, pp. 193–204, 2012.

[33] S. Basak, M. Behar, and A. Hoffmann, "Lessons from mathematically modeling the NF-κB pathway," *Immunological Reviews*, vol. 246, no. 1, pp. 221–238, 2012.

[34] M. Kaileh and R. Sen, "NF-κB function in B lymphocytes," *Immunological Reviews*, vol. 246, no. 1, pp. 254–271, 2012.

[35] P. Yde, B. Mengel, M. H. Jensen, S. Krishna, and A. Trusina, "Modeling the NF-κB mediated inflammatory response predicts cytokine waves in tissue," *BMC Systems Biology*, vol. 5, article 115, 2011.

[36] S. S. Makarov, "NF-KB in rheumatoid arthritis: a pivotal regulator of inflammation, hyperplasia, and tissue destruction," *Arthritis Research*, vol. 3, no. 4, pp. 200–206, 2001.

[37] G. van Loo and R. Beyaert, "Negative regulation of NF-κB and its involvement in rheumatoid arthritis," *Arthritis Research and Therapy*, vol. 13, no. 3, article 221, 2011.

[38] R. Jin, J. A. Sterling, J. R. Edwards et al., "Activation of NF-κ B signaling promotes growth of prostate cancer cells in bone," *PloS ONE*, vol. 8, no. 4, 2013.

[39] B. F. Boyce, Z. Yao, and L. Xing, "Functions of nuclear factor κb in bone," *Annals of the New York Academy of Sciences*, vol. 1192, pp. 367–375, 2010.

[40] D. V. Novack, "Role of NF-κB in the skeleton," *Cell Research*, vol. 21, no. 1, pp. 169–182, 2011.

[41] K. B. Marcu, M. Otero, E. Olivotto, R. M. Borzi, and M. B. Goldring, "NF-κB signaling: multiple angles to target OA," *Current Drug Targets*, vol. 11, no. 5, pp. 599–613, 2010.

[42] Y. Woo, B. Yoon, J. Jhun et al., "Regulation of B cell activating factor (BAFF) receptor expression by NF-κB signaling in rheumatoid arthritis B cells," *Experimental and Molecular Medicine*, vol. 43, no. 6, pp. 350–357, 2011.

[43] P. A. Beavis, B. Gregory, P. Green et al., "Resistance to regulatory T cell-mediated suppression in rheumatoid arthritis can be bypassed by ectopic foxp3 expression in pathogenic synovial T cells," *Proceedings of the National Academy of Sciences of the United States of America*, vol. 108, no. 40, pp. 16717–16722, 2011.

[44] R. E. Simmonds and B. M. Foxwell, "Signalling, inflammation and arthritis: NF-κB and its relevance to arthritis and inflammation," *Rheumatology*, vol. 47, no. 5, pp. 584–590, 2008.

[45] M. Takagi, "Toll-like receptor—a potent driving force behind rheumatoid arthritis," *Journal of Clinical and Experimental Hematopathology*, vol. 51, pp. 77–92, 2011.

[46] G. Srikrishna and H. H. Freeze, "Endogenous damage-associated molecular pattern molecules at the crossroads of inflammation and cancer," *Neoplasia*, vol. 11, no. 7, pp. 615–628, 2009.

[47] R. Seibl, T. Birchler, S. Loeliger et al., "Expression and regulation of Toll-like receptor 2 in rheumatoid arthritis synovium," *American Journal of Pathology*, vol. 162, no. 4, pp. 1221–1227, 2003.

[48] C. Ospelt, F. Brentano, Y. Rengel et al., "Overexpression of toll-like receptors 3 and 4 in synovial tissue from patients with early rheumatoid arthritis: toll-like receptor expression in early and longstanding arthritis," *Arthritis and Rheumatism*, vol. 58, no. 12, pp. 3684–3692, 2008.

[49] S. Akira and K. Takeda, "Toll-like receptor signalling," *Nature Reviews Immunology*, vol. 4, no. 7, pp. 499–511, 2004.

[50] T. Saber, D. J. Veale, E. Balogh et al., "Toll-like receptor 2 induced angiogenesis and invasion is mediated through the tie2 signalling pathway in rheumatoid arthritis," *PLoS ONE*, vol. 6, no. 8, Article ID e23540, 2011.

[51] Y. Ding, N. Song, and Y. Luo, "Role of bone marrow-derived cells in angiogenesis: focus on macrophages and pericytes," *Cancer Microenvironment*, pp. 1–12, 2012.

[52] T. Saber, D. J. Veale, E. Balogh et al., "Toll-like receptor 2 induced angiogenesis and invasion is mediated through the tie2 signalling pathway in rheumatoid arthritis," *PLoS ONE*, vol. 6, no. 8, Article ID e23540, 2011.

Hindawi Publishing Corporation
Evidence-Based Complementary and Alternative Medicine
Volume 2013, Article ID 540957, 10 pages
http://dx.doi.org/10.1155/2013/540957

*Research Article*

# Metabolic Signatures of Kidney *Yang* Deficiency Syndrome and Protective Effects of Two Herbal Extracts in Rats Using GC/TOF MS

**Linjing Zhao,[1,2] Hongbing Wu,[1] Mingfeng Qiu,[1] Wei Sun,[3] Runmin Wei,[1] Xiaojiao Zheng,[1] Yiting Yang,[3] Xue Xin,[1] Haimiao Zou,[1] Tianlu Chen,[4] Jiajian Liu,[4] Lina Lu,[1] Jing Su,[1] Chungwah Ma,[3] Aihua Zhao,[4] and Wei Jia[4]**

[1] *School of Pharmacy, Shanghai Jiao Tong University, Shanghai 200240, China*
[2] *College of Chemistry and Chemical Engineering, Shanghai University of Engineering Science, Shanghai 201620, China*
[3] *Infinitus (China) Company Ltd., Guangzhou 510665, China*
[4] *Center for Translational Medicine, and Shanghai Key Laboratory of Diabetes Mellitus, Department of Endocrinology and Metabolism, Shanghai Jiao Tong University Affiliated Sixth People's Hospital, Shanghai 200233, China*

Correspondence should be addressed to Chungwah Ma; william_ma@infinitus.com.cn and Aihua Zhao; zhah@sjtu.edu.cn

Received 25 April 2013; Revised 4 August 2013; Accepted 6 August 2013

Academic Editor: Aiping Lu



Kidney *Yang* Deficiency Syndrome (KDS-*Yang*), a typical condition in Chinese medicine, shares similar clinical signs of the glucocorticoid withdrawal syndrome. To date, the underlying mechanism of KDS-*Yang* has been remained unclear, especially at the metabolic level. In this study, we report a metabolomic profiling study on a classical model of KDS-*Yang* in rats induced by hydrocortisone injection to characterize the metabolic transformation using gas chromatography/time-of-flight mass spectrometry. WKY1, a polysaccharide extract from *Astragalus membranaceus* and *Lycium barbarum*, and WKY2, an aqueous extract from a similar formula containing *Astragalus membranaceus*, *Lycium barbarum*, *Morinda officinalis*, *Taraxacum mongolicum*, and *Cinnamomum cassia presl*, were used separately for protective treatments of KDS-*Yang*. The changes of serum metabolic profiles indicated that significant alterations of key metabolic pathways in response to abrupt hydrocortisone perturbation, including decreased energy metabolism (lactic acid, acetylcarnitine), lipid metabolism (free fatty acids, 1-monolinoleoylglycerol, and cholesterol), gut microbiota metabolism (indole-3-propionic acid), biosynthesis of catecholamine (norepinephrine), and elevated alanine metabolism, were attenuated or normalized with different degrees by the pretreatment of WKY1 or WKY2, which is consistent with the observations in which the two herbal agents could ameliorate biochemical markers of serum cortisone, adrenocorticotropic (ACTH), and urine 17-hydroxycorticosteroids (17-OHCS).

## 1. Introduction

The theory of *Yin-Yang* is a conceptual framework used for observing and analyzing the material world in ancient China. This philosophical approach has also been adopted for the studies of traditional Chinese medicine (TCM) syndrome and the guidance clinical diagnosis, treatment, and prevention for thousands of years. Kidney *Yang* Deficiency Syndrome (KDS-*Yang*) was firstly documented in Huangdi Neijing, an earliest systematic monograph in TCM. Modern research has shown that damages and functional disorders of hypothalamic-pituitary-target gland axis, including adrenal, thyroid, and gonad, are the main pathological mechanism for forming KDS-*Yang* [1]. Over the past half century, more than 20 experimental models with a variable range of clinical manifestations similar to those observed in KDS-*Yang* human have been developed [2]. It is one of classical methods of establishing KDS-*Yang* to inject animals with high dose

of exogenous glucocorticoid, such as hydrocortisone, which would induce adrenocortical insufficiency after abrupt withdrawal administration [2]. This animal model mimicked the pathological state of suppression of hypothalamic-pituitary-adrenal (HPA) axis to some extent in KDS-*Yang* human and contributed greatly to important advances in the current understanding of the underlying mechanisms of KDS-*Yang* as well as treatments [3–5].

Metabolomics, a new omics technique defined as quantitative measurement of time-related multiparametric metabolic response of multicellular systems to pathophysiological stimuli or generic modification [6], has recently developed into an increasingly important tool and has been successfully used in revealing the essence of syndrome and therapeutic effect of TCM. Recently, an increasing number of publications have described the applications of metabolomic approach in evaluating the curative effect and mechanism of traditional medicine in KDS-*Yang* [7–10]. Gong et al. [7] investigated the metabolic profile of hydrocortisone-induced KDS-*Yang* in rats and the intervention effects of *Morinda officinalis* based on nuclear magnetic resonance (NMR). Lu et al. [8] studied the metabonomic characters of KDS-*Yang* rats and the therapeutic effects of *Drynaria fortune* (Kunze) J. Sm. using ultra-performance liquid chromatography coupled with mass spectrometry (UPLC/MS). Li et al. [9] described the serous metabonomic study on *Epimedium brevicornum* Maxim. treated KDS rats and its therapeutic basis using UPLC/MS. Subsequently, an integrated plasma and urinary metabolomics method by UPLC/MS were also developed to reveal the intervention effects of *Epimedium koreanum* Nakai on KDS-*Yang* rats [10]. Also, in our previous study, the urinary metabolic profiles using gas chromatography coupled with mass spectrometry (GC/MS) characterized the biochemical fingerprints of a physiopathologic status similar to KDS in TCM, and the intervention of *Herba Cistanches* could cause a systemic recovery from the hydrocortisone-induced metabolic perturbation in rats [11, 12].

WKY1 and WKY2 are two TCM formulas designed for strengthening kidney *Yang*. WKY1 is a crude compound polysaccharide extracted from *Astragalus membranaceus* and *Lycium barbarum*. The combination of these two medicinal plants as a formula is derived from the *Royal Formulary of Yang Spring*, which is part of an ancient health preserving book, "The Life Documentary of Emperor Qianlong." The rationale for the use of this two-plant formula is to strengthen *Yang* and *Qi* with *Astragalus membranaceus*, while replenishing the *Yin* with *Lycium barbarum* fruits, according to the *Royal Formulary*. The clinical use of the formula is believed to achieve a satisfactory effect of replenishing the kidney deficiency, and therefore, may particularly be effective for chronic colitis and diarrhea generally resulting from the KDS-*Yang*. WKY2 is a mixture of an aqueous extract from a similar Chinese herbal formula, including *Astragalus membranaceus*, *Lycium barbarum*, *Morinda officinalis, Taraxacum mongolicum, and Cinnamomum cassia presl*. The additional three herbs were used in this formula to further strengthen the lung and spleen and thus synergize with the first two herbs to enhance the clinical efficacy of KDS-*Yang*-derived conditions such as chronic diarrhea. Based on our pilot study in dozens of volunteers, the two herbal formulas both showed promising protective effects against KDS-*Yang*.

In this study, a serous metabolic profiling approach based on gas chromatography time-of-flight mass spectrometry (GC/TOF MS) was explored to characterize the metabolic signature of the KDS-*Yang* rats. The protective effects of WKY1 and WKY2 against the metabolic alteration were also investigated with this strategy. The finding of metabolic pathways will be helpful to understand the essence of KDS-*Yang* and the underlying mechanism of the two herbal treatments.

## 2. Materials and Methods

*2.1. Chemicals and Reagents.* HPLC grade methanol, chloroform, and pyridine were purchased from Merck Chemicals (Darmstadt, Germany). Hydrocortisone solution for injection (0.5%) was purchased from Shanghai Xinyi Pharmaceutical Co. (Shanghai, China). *L*-2-chlorophenylalanine was purchased from Intechem Tech. Co. Ltd. (Shanghai, China). BSTFA (1% TMCS), heptadecanoic acid, and methoxyamine were purchased from Sigma Aldrich (St. Louis, MO, USA). All aqueous solutions were prepared with ultrapure water produced by a Milli-Q system (18.2 MΩ, Millipore, Bedford, MA, USA).

*2.2. Herbal Preparation.* The five raw herbs, including *Astragalus membranaceus, Lycium barbarum, Morinda officinalis, Taraxacum mongolicum, and Cinnamomum cassia presl*, were purchased from Chinese mainland and were authenticated on the basis of morphological and chemical analysis in accordance with the Chinese Pharmacopoeia (data not shown).

WKY1 was produced by water extraction and ethanol precipitation as described previously [13]. In brief, *Astragalus membranaceus* and *Lycium barbarum* mixed at a certain proportion were boiled in 10-fold water for 1.5 h. At the end of 1.5 h boiling, the water extract was collected and the residue was reboiled in 8-fold water for 1 h. The blending supernatant was concentrated in a vacuum rotary evaporator, and then pooled and mixed with ethanol (final concentration 75% v/v) to precipitate the polysaccharide-enriched fraction. The precipitate was separated from the supernatant and vacuum-dried at 40°C to obtain WKY1 (moisture content <7.0%). WKY2 is composed of WKY1 and the powder of an aqueous extract, which was obtained from *Morinda officinalis, Taraxacum mongolicum, and Cinnamomum cassia presl*. For the aqueous extract preparation, three crude herbs were mixed according to proportion and boiled in 10-fold water for 1.5 h. The mixture was cooled to room temperature and filtered. The residue was then refluxed with additional 6-fold water for 1 h. The supernatant was pooled, concentrated under reduced pressure, and then sprayed into dry powder. According to proportion, the spray-drying powder and WKY1 were mixed for obtaining WKY2 (moisture content <5.0%). The total polysaccharide contents of WKY1 and WKY2 were 34.5% (w/w) and 22.6% (w/w), respectively, as determined by the phenol-sulphuric acid method [14].

*2.3. Experimental Design and Sample Collection.* The handling of all animals in this study was conformed to the national guidelines and performed at the Center for Laboratory Animals, School of pharmacy, Shanghai Jiao Tong University (SJTU). All the experimental protocols were approved by the Animal Ethics Committee of SJTU. A total of 28 eight-week-old male Sprague-Dawley rats (200 ± 20 g) were commercially obtained from Shanghai Laboratory Animal Co. Ltd. (SLAC, Shanghai, China), housed individually in stainless steel wire mesh cages, and provided with a certified standard rat chow and tap water ad libitum. Room temperature and humidity were regulated at 21 ± 1°C and 60 ± 10%, respectively. A 12/12-h light-dark cycle was set, with lights on at 8 a.m. After 2 weeks of acclimatization in metabolic cages, rats were randomly divided into four groups, 7 in each group: control group (C), which received daily the same volume of saline as the other groups from days 1 to 15; model group (M), which received saline daily from days 1 to 15, then 5% hydrocortisone solution at 50 mg/kg of body weight with i.p. injection from days 16 to 22; WKY1 pretreatment group (WKY1), which received daily WKY1 (30 g/L aqueous suspension) by oral administration at dose of 0.18 g/kg of body weight (equal to 30 times dose of clinic dosage) from days 1 to 15, then 5% hydrocortisone solution daily with i.p. injection at 50 mg/kg from days 16 to 22; and WKY2 pretreatment group (WKY2), which received WKY2 (30 g/L aqueous suspension) at daily oral dose of 1.01 g/kg of body weight (equal to 30 times dose of clinic dosage) from days 1 to 15, then 5% hydrocortisone solution daily at 50 mg/kg with i.p. injection from day 16 to 22. Sera and urine samples were collected at day 25, on the 3rd day after hydrocortisone withdrawal, and stored at −80°C, pending for biochemical and metabolomic analysis.

*2.4. Behavioral Observation and Hormone Level Measurement.* The weighed chow and water were added into the container of each metabolism cage and the residual food and water were measured daily, respectively. The 24 h urine volume and weekly body weight were recorded, and the general behavior or activity changes of rats were also observed. The serum cortisone, ACTH, and 24 h urine 17-OHCS were measured using ELISA kits (Groundwork Biotechnology Diagnosticate Ltd., San Diego, CA, USA). Data from the serum biochemistry determination were expressed as mean ± SD. Statistical analysis was conducted using the Student's two-tailed, unpaired $t$-test. A $P$ value of less than 0.05 was considered statistically significant.

*2.5. Preparation of Samples and Analysis by GC/TOF MS.* Sera samples were derivatized and subsequently analyzed by GC/TOF MS following our previously published protocols [15]. A 100 $\mu$L aliquot of serum sample was spiked with two internal standards (10 $\mu$L of *L*-2-chlorophenylalanine in water, 0.3 mg/mL; 10 $\mu$L of heptadecanoic acid in methanol, 1 mg/mL) and vortexed for 10 s. The mixed solution was extracted with 300 $\mu$L of methanol/chloroform (3 : 1) and vortexed for 30 s. After standing for 10 min at −20°C, the samples were centrifuged at 10,000 rpm for 10 min. An aliquot of 300 $\mu$L supernatant was transferred to a glass sampling vial to vacuum-dry at room temperature. The residue was derivatized using a two-step procedure. First, 80 $\mu$L of methoxyamine (15 mg/mL in pyridine) was added to the vial and kept at 30°C for 90 min followed by 80 $\mu$L of BSTFA (1%TMCS) at 70°C for 60 min. Each 1 $\mu$L aliquot of the derivatized solution was injected in spitless mode into an Agilent 6890N gas chromatography coupled with a Pegasus HT time-of-flight mass spectrometer (Leco Corporation, St Joseph, MI, USA). Separation was achieved on a DB-5MS capillary column (30 m × 250 $\mu$m I.D., 0.25 $\mu$m film thickness; (5%-phenyl)-methyl-polysiloxane bonded and crosslinked; Agilent J&W Scientific, Folsom, CA) with helium as the carrier gas at a constant flow rate of 1.0 mL/min. The temperature of injection, transfer interface, and ion source were set to 270°C, 260°C, and 200°C, respectively. The GC temperatures programming was set to 2 min isothermal heating at 80°C, followed by 10°C/min oven temperature ramps to 180°C, 5°C/min to 240°C, and 25°C/min to 290°C, and a final 9 min maintenance at 290°C. Electron impact ionization (70 eV) at full scan mode ($m/z$ 30–600) was used, with an acquisition rate of 20 spectrum/second in the TOF MS setting.

*2.6. Data Processing and Statistical Analysis.* The acquired MS files from GC/TOF MS analysis were exported in NetCDF format by ChromaTOF software (v3.30, Leco Co., CA, USA). CDF files were extracted using custom scripts (revised MATLAB toolbox HAD) [15, 16] in the MATLAB 7.1 (The MathWorks, Inc., USA) for data pretreatment procedures such as baseline correction, denoising, smoothing, and alignment; time-window splitting; and peak feature extraction (based on multivariate curve resolution algorithm) [17]. The resulting three-dimensional data set, including sample name, peak retention time, and peak intensity, was imported into the SIMCA-P 11.5 Software package (Umetrics, Umea, Sweden) for data analysis according to our previous publication [18]. Multivariate statistical analysis (partial least-squares-discriminant analysis, PLS-DA) was performed. Meanwhile, significantly expressed features between groups were calculated using a Student's $t$-test ($P < 0.05$). The fold change shows the relative intensity ratio of the differential or representative metabolites between control and model groups with or without WKY1/WKY2 treatments. Additionally, metabolites were annotated by comparing the mass fragments with those of mass spectral in NIST MS databases 2.0 (NIST, Gaithersburg, MD, USA) with a similarity of more than 70% and further verified by the available reference standards.

## 3. Results and Discussion

*3.1. Hormone Level and Behavioral Presentation.* The blood cortisone, ACTH, and 24 h urine 17-OHCS, which were widely admitted as diadynamic criteria of KDS-*Yang* in clinic of TCM [19], were carried out to assess the success of hydrocortisone-induced KDS-*Yang* model. The results showed that these three hormones levels, as well as body weight, water intake, and 24-h hour urinary excretion, were significantly decreased ($P < 0.05$) in the model group

Table 1: Hormone variation and behavioral investigation results on the 3rd day after hydrocortisone withdrawal with or without WKY1/WKY2 pretreatments.

| Groups | Cortisone (ng/mL) | ACTH (pg/mL) | 17-OHCS ($\mu$mol/L) | Body weight (g) | Food consumption (g) | Water intake (mL) | Urine volume (mL) |
|---|---|---|---|---|---|---|---|
| Control group | 220.78 ± 105.78 | 633.43 ± 111.1 | 433.81 ± 15.64 | 371.9 ± 7.2 | 14.8 ± 1.3 | 48.9 ± 4.3 | 40.6 ± 5.9 |
| Model group | 139.21 ± 40.79** | 447.14 ± 126.5* | 398.91 ± 29.13** | 349.0 ± 12.0** | 13.4 ± 1.1 | 36.3 ± 4.5** | 18.4 ± 6.0** |
| WKY1 group | 161.84 ± 87.27 | 632.98 ± 50.65 | 400.6 ± 16.59 | 356.6 ± 15.6* | 15.1 ± 2.5 | 42.3 ± 5.9* | 27.9 ± 8.4** |
| WKY2 group | 206.51 ± 71.64 | 993.26 ± 17.46** | 416.79 ± 12.78 | 357.4 ± 12.4* | 14.9 ± 2.1 | 34.8 ± 4.6** | 20.4 ± 2.8** |

*$P < 0.05$, **$P < 0.01$ compared with control group (two-tailed Student's $t$-test).

compared to those in the control group on day 25 (Table 1), confirming the suppression of HPA axis and the establishment of KDS-*Yang* model on the 3rd day after hydrocortisone withdrawal (50 mg/kg·d for 7 consecutive days). In addition, the model rats showed the signs of exhaustion, such as reduced activity, idleness, slow response, tending to cluster, and depilate. These pathological changes were in well accordance with those in KDS-*Yang* patients. Pretreatment with WKY1 or WKY2 significantly attenuated the alterations of cortisone and 17-OHCS levels. It was somewhat surprising that the ACTH level significantly increased in the WKY2 group compared with the control group, suggesting that WKY2 might effectively stimulate the anterior pituitary to release ACTH. We also found that the rats in WKY1 and WKY2 treatment groups were more active and curious than the model rats.

*3.2. Metabolic Variation of KDS-Yang Induced by Hydrocortisone.* Typical GC/TOF MS total ion current (TIC) chromatograms of serum samples obtained from the control and model rats are illustrated in Figures 1(a) and 1(b). Some obvious differences could be visually inspected between the two groups. A total of 241 peaks were obtained from the GC/TOF MS spectra, and 99 metabolites were identified with NIST 05 standard mass spectral databases with a similarity >70%, further verified by the available reference standards. The multiple pattern recognition PLS-DA scores plot constructed with all the GC/TOF MS data was utilized to depict the general variation between control and model groups (Figure 1(c)). Obvious separations were observed with the stable cumulative modeled variation and good prediction capability with the first two components (component number = 3, $R^2X = 0.420$, $R^2Y = 0.993$, and $Q^2 = 0.778$). The results suggested that the perturbation of serum metabolome occurred in rats on the 3rd day after hydrocortisone withdrawal. The metabolites responsible for the differentiation of metabolic profiles between the two groups were obtained based on a multivariate statistics variable importance in the projection (VIP) threshold of 1.0 from the PLS-DA model. Univariate statistical analysis and Student's $t$-test were performed on metabolites identified from GC/TOF MS analysis of sera samples to evaluate their significance. Fold change was calculated by comparing those metabolites in the model group to the controls. The identified differential metabolites were selected based on the criteria of VIP > 1.0, $P < 0.05$, and fold change (FC) >1.2 or <0.8. A total of 13 differentially expressed metabolites between the control and model groups are listed in Table 2, including decreased lactic acid, acetylcarnitine, glyceraldehyde, histidine, palmitic acid, indole-3-propionic acid, linolic acid, oleic acid, stearic acid, lactose, arachidonic acid, and 1-monolinoleoylglycerol, and increased alanine in the model group compare with the controls. Besides, serum norepinephrine and cholesterol levels tended to decrease in the model group compared to the controls (Table 2).

The metabolic profiling was able to reveal the protective effects of WKY1 or WKY2 on the serum metabolic pattern of KDS-*Yang*. The 3-dimensional PLS-DA scores plots, derived from all variables based on GC/TOF MS spectral data of the control, model, and WKY1 or WKY2 treatment groups on the 3rd day after hydrocortisone withdrawal, are illustrated in Figure 2. The modeling parameters were $R^2X(\text{cum}) = 0.510$, $R^2Y(\text{cum}) = 0.927$, $Q^2(\text{cum}) = 0.537$ (Figure 2(a)), and $R^2X(\text{cum}) = 0.502$, $R^2Y(\text{cum}) = 0.952$, and $Q^2(\text{cum}) = 0.504$ (Figure 2(b)), respectively. It could be clearly observed that the two treatment groups were both much closer to the control group than the model group. Among the 15 metabolites responsible for KDS-*Yang* induced by hydrocortisone withdrawal, 13 in WKY1 treatment group except histidine and linolic acid and 14 in WKY2 treatment group except linolic acid had no significant variation ($P > 0.05$) relative to controls on the 3rd day after hydrocortisone withdrawal (Table 2).

We further selected 30 representative metabolites in model rats compared to controls based on the FC and VIP values (FC >1.2 or <0.8 and VIP >1.0). Among these, 16 metabolites in the WKY1 groups, and 16 metabolites in WKY2 group showed significant alterations in FC relative to those in the model group (see Table S1 in Supplementary Material available online at http://dx.doi.org/10.1155/2013/540957). The heatmap generated with the 30 metabolites also indicated less significant fluctuation of metabolite levels in FC relative to controls in both WKY1 and WKY2 groups (Figure 3). To be exact, 17 out of the 30 representative metabolites in WKY1 group and 13 out of the 30 metabolites in WKY2 group were insignificant (in FC, $0.8 < FC < 1.2$) relative to controls, as shown in Table S1. These results indicated that pretreatment with WKY1 or WKY2 could effectively attenuate or normalize the metabolic perturbation with different degrees in rats induced by hydrocortisone.

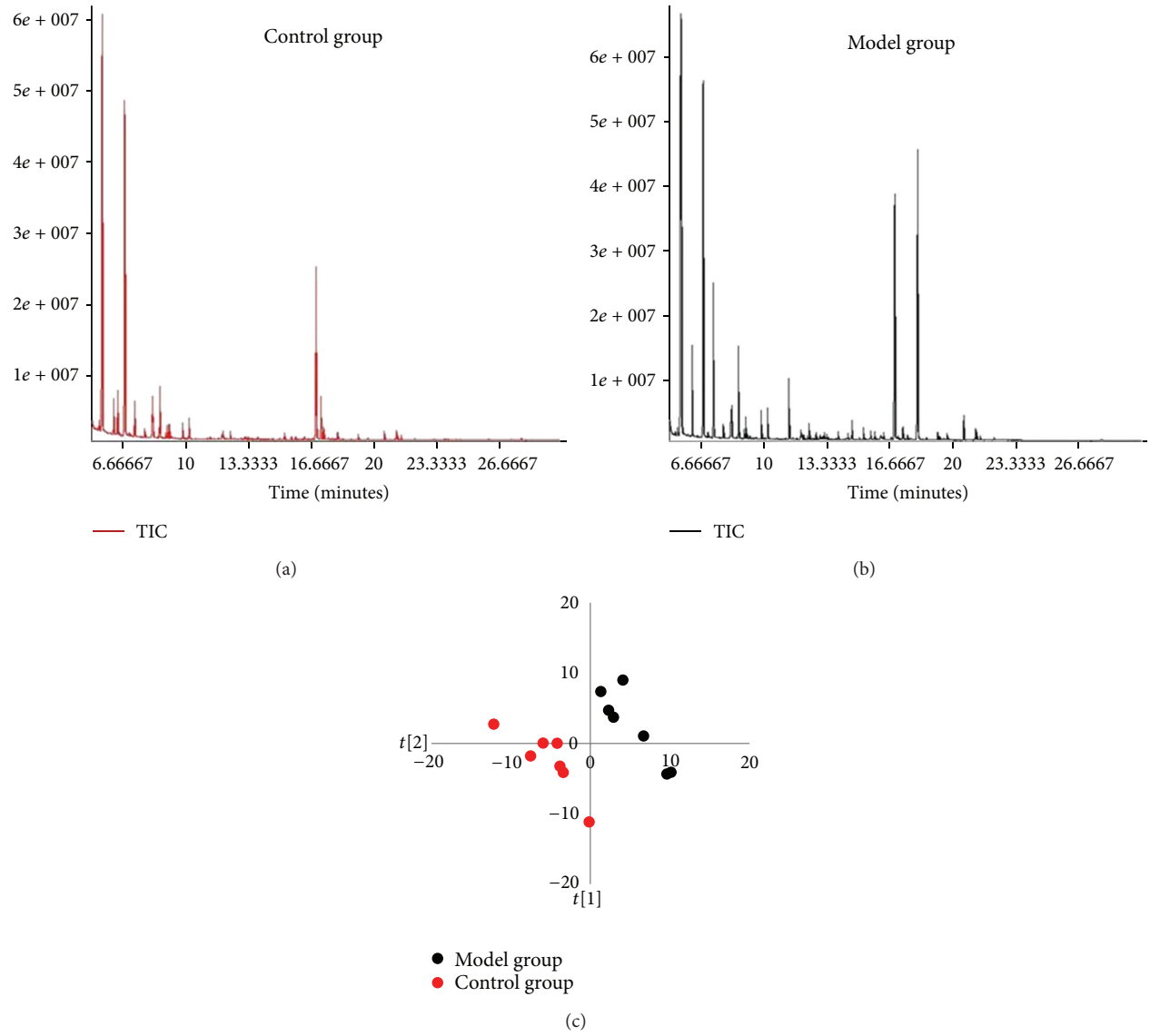


Figure 1: Visualization of biochemical effects of hydrocortisone-induced KDS-*Yang* in rats using a metabolic profiling approach. Typical GC/TOF MS spectra of serum samples from control group (a) and model group (b). (c) Metabolic profiles depicted by PLS-DA sores plot of GC/TOF MS spectral data from serum samples ($n = 7$, each dot denotes an individual rat).

*3.3. Metabolomic Pathways Associated with KDS-Yang and WKY1/WKY2 Treatments.* KDS-*Yang* is one of the elementary syndrome patterns in TCM and closely linked to multiple disordered metabolic pathways. In our study, the model was established through abrupt withdrawal administration after exposure to a high dosage of hydrocortisone for 7 consecutive days in rats. The serum metabolic profiling revealed that the global metabolic perturbation on the 3rd day after hydrocortisone withdrawal, a key time point of KDS-*Yang* study [2], has obviously occurred in model the group characterized by the 15 differentially expressed metabolites listing in Table 2. According to the theory of drugs counterevidence in TCM, most of these metabolites were identified as the important biomarkers associated with KDS-*Yang*, because of their insignificant differential levels in WKY1 or WKY2 pretreatment groups (Table 2). The key biomarkers included lactic acid, acetylcarnitine, glyceraldehyde, lactose, palmitic acid, stearic acid, oleic acid, arachidonic acid, 1-monolinoleoylglycerol, cholesterol, alanine, indole-3-propionic acid, and norepinephrine. Their alterations were associated with multiple metabolic perturbations, including energy metabolism, lipid metabolism, amino acid metabolism, gut microbiota metabolism, and biosynthesis of catecholamine, as summarized in Figure 4.

Based on the principle of TCM, *Yang* can keep metabolic rate in a normal level to satisfy the normal physiological activities of the human body [20]. In our study, the serum metabolic profiling analysis from KDS-*Yang* rats indicated a significant downregulation in metabolic activities. As illustrated in Table 2, many metabolites related to energy metabolism showed a decreased metabolic tendency in KDS-*Yang* rats compared with controls, such as lactic acid,

Table 2: List of differential serum metabolites in M group on the 3rd day after hydrocortisone withdrawal, and $P$ values in M, WKY1, and WKY2 groups compared to controls.

| Metabolites | Formula | RT (min) | VIP[a] | FC[b] | $P$[c] | | |
|---|---|---|---|---|---|---|---|
| | | | | | M | WKY1 | WKY2 |
| Lactic acid | $C_3H_6O_3$ | 5.54 | 1.43 | 0.58 | 0.043 | 0.545 | 0.312 |
| Alanine | $C_3H_7NO_2$ | 6.19 | 1.40 | 1.21 | 0.036 | 0.535 | 0.916 |
| Acetylcarnitine | $C_9H_{17}NO_4$ | 6.39 | 1.42 | 0.62 | 0.034 | 0.172 | 0.076 |
| Glyceraldehyde | $C_3H_6O_3$ | 6.77 | 1.46 | 0.80 | 0.033 | 0.085 | 0.080 |
| Histidine | $C_6H_9N_3O_2$ | 17.29 | 1.83 | 0.58 | 0.002 | 0.004 | 0.050 |
| Palmitic acid | $C_{16}H_{32}O_2$ | 19.16 | 1.35 | 0.76 | 0.047 | 0.450 | 0.603 |
| Indole-3-propionic acid | $C_{11}H_{11}NO_2$ | 19.63 | 1.37 | 0.56 | 0.038 | 0.676 | 0.303 |
| Linoleic acid | $C_{18}H_{32}O_2$ | 21.18 | 1.46 | 0.61 | 0.021 | 0.009 | 0.007 |
| Oleic acid | $C_{18}H_{34}O_2$ | 21.23 | 1.37 | 0.61 | 0.035 | 0.070 | 0.139 |
| Stearic acid | $C_{18}H_{36}O_2$ | 21.42 | 1.63 | 0.70 | 0.008 | 0.448 | 0.162 |
| Arachidonic acid | $C_{20}H_{32}O_2$ | 22.15 | 1.47 | 0.61 | 0.024 | 0.382 | 0.113 |
| 1-Monolinoleoylglycerol | $C_{21}H_{38}O_4$ | 22.36 | 1.71 | 0.23 | 0.004 | 0.556 | 0.158 |
| Norepinephrine | $C_8H_{11}NO_3$ | 22.61 | 1.28 | 0.61 | 0.065 | 0.417 | 0.947 |
| Lactose | $C_{12}H_{22}O_{11}$ | 23.63 | 1.48 | 0.50 | 0.027 | 0.433 | 0.114 |
| Cholesterol | $C_{27}H_{46}O$ | 27.85 | 1.33 | 0.69 | 0.066 | 0.811 | 0.716 |

[a]VIP was obtained from PLS-DA model (Figure 1(c)).
[b]FC with a value >1 indicates a relatively higher concentration while a value <1 means a relatively lower concentration present in M group as compared to the controls.
[c]$P$ value of Student's $t$ test.

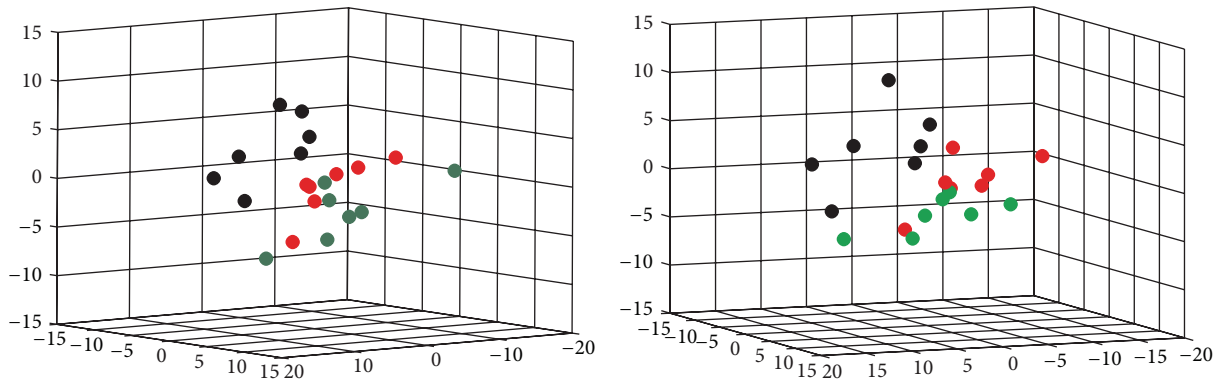


Figure 2: Visualization of biochemical effects of hydrocortisone-induced KDS-*Yang* in rats pretreated with WKY1 (a) and WKY2 (b) using a metabolic profiling approach depicted by a 3D PLS-DA scores plot of GC/TOF MS spectral data from serum samples ($n$ = 7; control group, red dot; model group, blank dot; WKY1 treatment group, dark green dots; and WKY2 treatment group, bright green dots; each dot denotes an individual rat).

acetylcarnitine, glyceraldehyde, and lactose. Lactic acid is a predominant source of carbon atoms for glucose synthesis by gluconeogenesis. The regulation of hepatic gluconeogenesis is an important process in the adjustment of the blood glucose level. The serum lactic acid level was observed to significantly decrease statistically in model rats compared with those in the controls, suggesting an inhibitory glycolysis in the KDS-*Yang*. Furthermore, serum acetylcarnitine level in rats exposed to hydrocortisone was significantly decreased relative to controls. Acylcarnitines are synthesized by carnitine acyl transferases from acylCoA and carnitine. Carnitine induces fatty acid $\beta$-oxidation in the liver [21, 22] and acylcarnitines are substrates for oxidation processes in mitochondria [23]. The decreased level of acetylcarnitine in our study indicated that KDS-*Yang* might be related to the impaired mitochondrial function, compatible with the notion that the lack of glucocorticoids selectively inhibits free fatty acids (FFAs) oxidation [24]. The changes of metabolites were consisted in the state of "exhaustion" in KDS-*Yang* rats, as evidenced by the signs of decreased activity, raritas clothing hair, tendency to cluster, dropped appetite, and weight loss (Table 1). The upregulation of lactate and acetylcarnitine was presented in the two pretreatment groups compared with those in the model group, indicating that WKY1 or WKY2 was able to

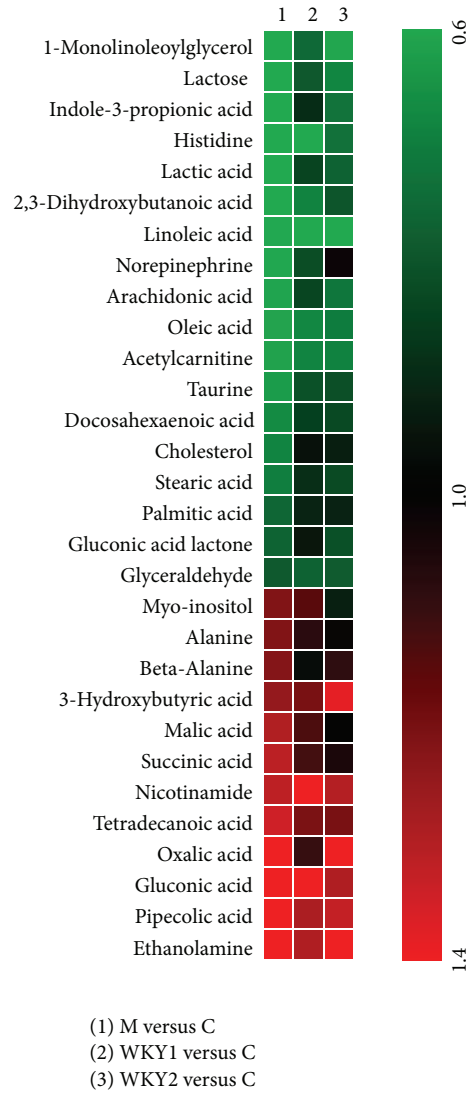


Figure 3: The heatmap of model group; two prophylactic treatment groups (WKY1 and WKY2) compared with controls. Shades of red represent fold increase compared with control, green shades represent fold decrease compared with control, respectively.

efficaciously ameliorate the altered energy metabolism and enhance the mitochondria function.

Glucocorticoid excess could cause insulin resistance [25] and cortisol could promote lipolysis [26, 27], rendering it possible that increased levels of FFAs in the circulation may contribute to the observed insulin resistance. Consistently, our data clearly showed that some FFAs, such as palmitic acid, stearic acid, oleic acid, linolic acid, and arachidonic acid, as well as 1-monolinoleoylglycerol significantly decreased in model groups. These results are in agreement with the studies that inhibition of the rise of glucocorticoids could significantly depress plasma FFAs at exhaustion in rodents [28] and that acute cortisol withdrawal could dramatically increase insulin sensitivity in the clinical research [29]. Meanwhile, cholesterol was also found at lower level in model rats. It has been reported that lipoprotein lipase is a key enzyme in the regulation of serum cholesterol, and the activity of the enzyme is increased by glucocorticoids [30]. The decreased cholesterol level in the model group was presumably due to lower activity of lipoprotein lipase, which was caused by the lack of glucocorticoids in KDS-*Yang*. WKY1 and WKY2 effectively attenuated or normalized the alteration of 1-monolinoleoylglycerol, cholesterol, and some FFAs (palmitic acid, stearic acid, oleic acid, and arachidonic acid), suggesting the inhibitory effects of the two herbal medicines on lipid metabolism dysfunction.

According to TCM theory, *Yang* also refers to a cluster of material resources containing excitement and promotion [31]. Our study found that the rats in model group showed the state of lack of vitality, slow reaction, listlessness, and lethargy. It has also been reported that the women with menopausal syndrome of kidney *Yang* deficiency were accompanied by many negative depressive emotions compared with healthy persons [32]. It might be associated with the metabolic dysfunction of some amino acids. In the present study, the serum level of alanine was significantly greater in the model group compared to the controls. It is in agreement with the study that there was a significant positive correlation between the severity of the depression and the plasma levels of alanine [33]. And further, alanine is also an important intermediate regulator in glucose metabolism. Normal blood alanine is transported to liver via glucose-alanine cycle to generate pyruvate which is also an important source for gluconeogenesis [34]. The significantly increased alanine level in model rats indicated that the glucose-alanine cycle was probably impaired in KDS-*Yang*. The normalized expression level of alanine in the WKY1 and WKY2 treatment groups suggests that the two agents' interactions are possibly involved in the glucose-alanine cycle and closely associated with amino acids metabolism.

Chronic diarrhea is another typical signal of KDS-*Yang* patients. However, to date, the pathogenesis has been poorly understood. In our study, the serum level of indole-3-propionic acid (IPA) in rats exposed to hydrocortisone was significantly decreased compared to controls. IPA is a deamination product of tryptophan formed by symbiotic bacteria in the gastrointestinal tract of mammals. The metabolite could be regarded as the characteristic biomarkers of KDS-*Yang* associated with the impaired gut microflora. IPA has been found to protect against oxidative damage caused by carcinogens and other peroxidative agents in animals [35, 36]. The significantly decreased serum IPA level in model rats could help to explain the manifestation of watery diarrhea in rats exposed to hydrocortisone, which was in line with the recent research in which the increased oxidative stress may be responsible for the pathogenesis of diarrhea-related bowel diseases [37]. WKY1 and WKY2 could greatly inhibit the decrease of IPA in serum, suggesting the protective action of WKY1 and WKY2 on gut microbiota metabolism.

In the present study, the decreased serum norepinephrine level in KDS-*Yang* rats was observed. Norepinephrine is an important neurotransmitter secreted by the adrenal medulla. The decreased serum norepinephrine could ascribe to the downregulation of catecholamine biosynthetic pathway in

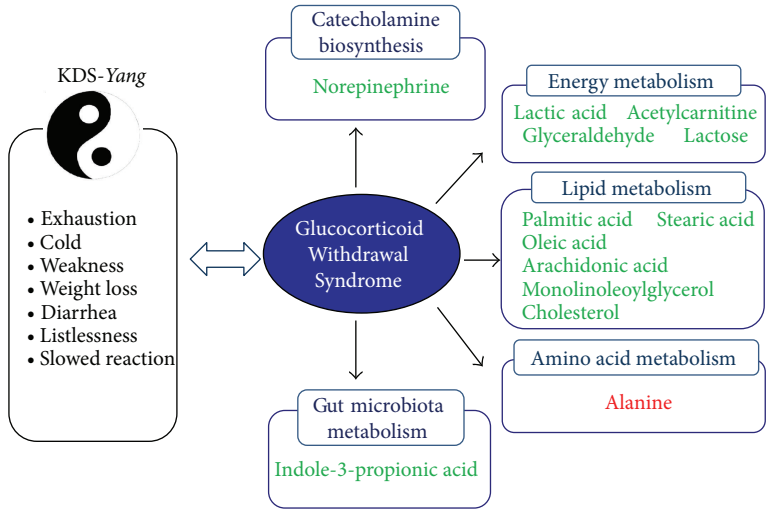


FIGURE 4: Metabolomic pathways associated with KDS-*Yang* induced by hydrocortisone withdrawal. Green: down-regulated metabolites; Red: up-regulated metabolites.

KDS-*Yang* status. The result was compatible with the previous experiments in which the levels of norepinephrine in the blood of patients with *Yang* hyperactivity syndrome were higher than those of healthy people [38]. So, it is believed that the sympathetic nervous system suppression is an important pathological progress of KDS-*Yang*, and the levels of norepinephrine might be thought to be a vitally important diagnostic biomarker for KDS-*Yang*. The normalized expression level of norepinephrine in the two treatment groups suggests the protective effect of WKY1 and WKY2 on catecholamine pathways.

Our results revealed that the interventions in energy metabolism, lipid, amino acid, gut microbiota metabolism, and biosynthesis of catecholamine might be the critical factors for WKY1 or WKY2 to prevent the experimental KDS-*Yang* rats suffering from the disorder of metabolism. And further, some differences were shown between the two prophylactic treatment groups. To be exact, lactose, lactic acid, 1-monolinoleoylglycerol, stearic acid, arachidonic acid, cholesterol, and IPA levels in sera samples of WKY1 group appeared more similar as normal, while the serum levels of alanine and norepinephrine in WKY2 group were much closer to control levels than those in WKY1 group (Figure 3; Table S1). The results suggested that the preventive effect of WKY1, the crude compound polysaccharides obtained from *Astragalus membranaceus* and *Lycium barbarum,* was superior to the aqueous extract of *Morinda officinalis, Taraxacum mongolicum,* and *Cinnamomum cassia presl* on energy metabolism, lipid metabolism, and gut microbiota metabolism. And, WKY2 was more effective on amino acid metabolism and catecholamine pathways than WKY1, possibly related to the aqueous extract of three additional herbs. Further studies of the two original herbal agents are necessary to develop plant-derived therapeutic medicines for the prevention and treatment of the metabolic dysfunction from KDS-*Yang*.

## 4. Conclusion

In the paper, a serum metabolomic profiling approach based on GC/TOF MS has been developed to investigate the specific physiopathologic state of KDS-*Yang* in rats induced by hydrocortisone withdrawal. Some potential biomarkers, such as lactic acid, acetylcarnitine, some FFAs, alanine, indole-3-propionic acid, and norepinephrine, were found and identified. The metabolic shifts of these metabolites could help explain the clinical manifestation of KDS-*Yang* and further reveal the alterations in energy metabolism, lipid, amino acid, gut microbiota metabolism, and biosynthesis of catecholamine induced by hydrocortisone. Two innovative herbal agents of WKY1 and WKY2 could attenuate or normalize the metabolic transformation with different degrees on these metabolic pathways.

## Abbreviations

| | |
|---|---|
| 17-OHCS: | 17-hydroxycorticosteroids |
| ACTH: | Adrenocorticotropic hormone |
| FFAs: | Free fatty acids |
| GC/MS: | Gas chromatography coupled with mass spectrometry |
| GC/TOF MS: | Gas chromatography coupled with time-of-flight mass spectrometry |
| HC: | Hydrocortisone |
| HPA axis: | Hypothalamic-pituitary-adrenal axis |
| IPA: | Indole-3-propionic acid |
| KDS-*Yang*: | Kidney-*Yang* Deficiency Syndrome |
| NMR: | Nuclear magnetic resonance |
| PLS-DA: | Partial least squares discriminant analysis |
| TCM: | Traditional Chinese medicine |
| UPLC/MS: | Ultra Performance liquid chromatography coupled with mass spectrometry. |

## Authors' Contribution

Linjing Zhao, Hongbing Wu, and Mingfeng Qiu contributed equally to this work.

## Acknowledgment

This study was financially supported by Infinitus (China) Company Ltd., a member of LKK Health Products Group.

## References

[1] Z. Shen, "The location of deficiency syndrome of kidney Yang," *Chinese Medical Journal*, vol. 112, no. 11, pp. 973–975, 1999.

[2] Q. Chen, *Experimental Methodology of Pharmacological Research in Traditional Chinese Medicine*, People's Health Publishing House, Beijing, China, 1993.

[3] H. Cao, S. T. Wang, L. Y. Wu, X. T. Wang, and A. P. Jiang, "Pharmacological study on Tianxiong (tuber of Aconitum carmichaeli Debx.), a Chinese drug for reinforcing the kidney yang retail in Hong Kong market," *China Journal of Chinese Materia Medica*, vol. 26, no. 6, pp. 369–372, 2001.

[4] J. Yang, Y. Wang, Y. Bao, and J. Guo, "The total flavones from Semen cuscutae reverse the reduction of testosterone level and the expression of androgen receptor gene in kidney-yang deficient mice," *Journal of Ethnopharmacology*, vol. 119, no. 1, pp. 166–171, 2008.

[5] C. M. Wang, S. Y. Xu, S. Lai et al., "*Curculigo orchioides* (Xian Mao) modifies the activity and protein expression of CYP3A in normal and Kidney-Yang Deficiency model rats," *Journal of Ethnopharmacology*, vol. 144, no. 1, pp. 33–38, 2012.

[6] J. K. Nicholson and I. D. Wilson, "Understanding 'global' systems biology: metabonomics and the continuum of metabolism," *Nature Reviews Drug Discovery*, vol. 2, no. 8, pp. 668–676, 2003.

[7] M. Gong, W. Ye, Y. Xie et al., "Metabonomic study of intervention effects of Morinda officinalis on 'kidney-yang deficiency syndrome'," *China Journal of Chinese Materia Medica*, vol. 37, no. 11, pp. 1682–1685, 2012.

[8] X. Lu, Z. Xiong, J. Li, S. Zheng, T. Huo, and F. Li, "Metabonomic study on 'Kidney-Yang Deficiency syndrome' and intervention effects of Rhizoma Drynariae extracts in rats using ultra performance liquid chromatography coupled with mass spectrometry," *Talanta*, vol. 83, no. 3, pp. 700–708, 2011.

[9] F. Li, X. Lu, H. Liu, M. Liu, and Z. Xiong, "A pharmacometabonomic study on the therapeutic basis and metabolic effects of Epimedium brevicornum Maxim. on hydrocortisone-induced rat using UPLC-MS," *Biomedical Chromatography*, vol. 21, no. 4, pp. 397–405, 2007.

[10] D. Huang, J. Yang, X. Lu et al., "An integrated plasma and urinary metabonomic study using UHPLC-MS: intervention effects of *Epimedium koreanum* on 'Kidney-Yang Deficiency syndrome' rats," *Journal of Pharmaceutical and Biomedical Analysis*, vol. 76, pp. 200–206, 2013.

[11] M. Chen, L. Zhao, and W. Jia, "Metabonomic study on the biochemical profiles of a hydrocortisone-induced animal model," *Journal of Proteome Research*, vol. 4, no. 6, pp. 2391–2396, 2005.

[12] Y. Qiu, M. Chen, M. Su et al., "Metabolic profiling reveals therapeutic effects of Herba Cistanches in an animal model of hydrocortisone-induced 'kidney-deficiency syndrome'," *Chinese Medicine*, vol. 3, article 3, 2008.

[13] C. H. Cho, Q. B. Mei, P. Shang et al., "Study of the gastrointestinal protective effects of polysaccharides from *Angelica sinensis* in rats," *Planta Medica*, vol. 66, no. 4, pp. 348–351, 2000.

[14] M. Dubois, K. A. Gilles, J. K. Hamilton, P. A. Rebers, and F. Smith, "Colorimetric method for determination of sugars and related substances," *Analytical Chemistry*, vol. 28, no. 3, pp. 350–356, 1956.

[15] Y. Qiu, G. Cai, M. Su et al., "Serum metabolite profiling of human colorectal cancer using GC-TOFMS and UPLC-QTOFMS," *Journal of Proteome Research*, vol. 8, no. 10, pp. 4844–4850, 2009.

[16] P. Jonsson, J. Gullberg, A. Nordström et al., "A strategy for identifying differences in large series of metabolomic samples analyzed by GC/MS," *Analytical Chemistry*, vol. 76, no. 6, pp. 1738–1745, 2004.

[17] P. Jonsson, A. I. Johansson, J. Gullberg et al., "High-throughput data analysis for detecting and identifying differences between samples in GC/MS-based metabolomic analyses," *Analytical Chemistry*, vol. 77, no. 17, pp. 5635–5642, 2005.

[18] Y. Ni, M. Su, Y. Qiu et al., "Metabolic profiling using combined GC-MS and LC-MS provides a systems understanding of aristolochic acid-induced nephrotoxicity in rat," *FEBS Letters*, vol. 581, no. 4, pp. 707–711, 2007.

[19] Z. Y. Shen, "Study on localization of kidney-yang deficiency," *Zhongguo Zhong Xi Yi Jie He Za Zhi*, vol. 17, no. 1, pp. 50–52, 1997.

[20] S. Lin and S. J. Feng, "Reviews of kidney-Yang deciency syndrome," *Hebei Journal of Traditional Chinese Medicine*, vol. 33, no. 3, pp. 463–465, 2011.

[21] I. B. Fritz, "Action of carnitine on long chain fatty acid oxidation by liver," *The American Journal of Physiology*, vol. 197, no. 2, pp. 297–304, 1959.

[22] I. B. Fritz and K. T. Yue, "Effects of carnitine on acetyl-CoA oxidation by heart muscle mitochondria," *The American Journal of Physiology*, vol. 206, no. 3, pp. 531–535, 1964.

[23] J. Bremer, "Carnitine in intermediary metabolism. The metabolism of fatty acid esters of carnitine by mitochondria," *The Journal of Biological Chemistry*, vol. 237, no. 12, pp. 3628–3632, 1962.

[24] K. R. Short, J. Nygren, M. L. Bigelow, and K. S. Nair, "Effect of short-term prednisone use on blood flow, muscle protein metabolism, and function," *The Journal of Clinical Endocrinology & Metabolism*, vol. 89, no. 12, pp. 6198–6207, 2004.

[25] G. Dimitriadis, B. Leighton, M. Parry-Billings et al., "Effects of glucocorticoid excess on the sensitivity of glucose transport and metabolism to insulin in rat skeletal muscle," *Biochemical Journal*, vol. 321, part 3, pp. 707–712, 1997.

[26] C. H. Gravholt, R. Dall, J. S. Christiansen, N. Møller, and O. Schmitz, "Preferential stimulation of abdominal subcutaneous lipolysis after prednisolone exposure in humans," *Obesity Research*, vol. 10, no. 8, pp. 774–781, 2002.

[27] C. Djurhuus, C. H. Gravholt, S. Nielsen et al., "Effects of cortisol on lipolysis and regional interstitial glycerol levels in humans," *American Journal of Physiology*, vol. 283, no. 1, pp. E172–E177, 2002.

[28] T. L. Sellers, A. W. Jaussi, H. T. Yang, R. W. Heninger, and W. W. Winder, "Effect of the exercise-induced increase in glucocorticoids on endurance in the rat," *Journal of Applied Physiology*, vol. 65, no. 1, pp. 173–178, 1988.

[29] J. J. Christiansen, C. B. Djurhuus, C. H. Gravholt et al., "Effects of cortisol on carbohydrate, lipid, and protein metabolism:

studies of acute cortisol withdrawal in adrenocortical failure," *The Journal of Clinical Endocrinology & Metabolism*, vol. 92, no. 9, pp. 3553–3559, 2007.

[30] J. R. Mead, S. A. Irvine, and D. P. Ramji, "Lipoprotein lipase: structure, function, regulation, and role in disease," *Journal of Molecular Medicine*, vol. 80, no. 12, pp. 753–769, 2002.

[31] G. R. Sun, *Basic Theory of Traditional Chinese Medicine*, China Press of Traditional Chinese Medicine, Beijing, China, 2006.

[32] B. J. Wu, Y. Wang, Y. X. Liu, and F. Wang, "Characteristics of memory functional impairment in women with menopausal syndrome of kidney yang deficiency and yin deficiency types," *Chinese Journal of Clinical Rehabilitation*, vol. 10, no. 39, pp. 18–20, 2006.

[33] H. Mitani, Y. Shirayama, T. Yamada, K. Maeda, C. R. Ashby Jr., and R. Kawahara, "Correlation between plasma levels of glutamate, alanine and serine with severity of depression," *Progress in Neuro-Psychopharmacology and Biological Psychiatry*, vol. 30, no. 6, pp. 1155–1158, 2006.

[34] C. A. Nichol and F. Rosen, "Changes in alanine transaminase activity related to corticosteroid treatment or capacity for growth," *Advances in Enzyme Regulation*, vol. 1, pp. 341–361, 1963.

[35] M. Karbownik, M. Stasiak, A. Zygmunt, K. Zasada, and A. Lewiński, "Protective effects of melatonin and indole-3-propionic acid against lipid peroxidation, caused by potassium bromate in the rat kidney," *Cell Biochemistry and Function*, vol. 24, no. 6, pp. 483–489, 2006.

[36] M. Karbownik, E. Gitto, A. Lewiñski, and R. J. Reiter, "Relative efficacies of indole antioxidants in reducing autoxidation and iron-induced lipid peroxidation in hamster testes," *Journal of Cellular Biochemistry*, vol. 81, no. 4, pp. 693–699, 2001.

[37] N. Şengül, S. Işık, B. Aslım et al., "The effect of exopolysaccharide-producing probiotic strains on gut oxidative damage in experimental colitis," *Digestive Diseases and Sciences*, vol. 56, no. 3, pp. 707–714, 2011.

[38] H. Liao, D. P. Li, Q. Chen et al., "Observation on therapeutic effect of "reducing south and reinforcing north" needling method on hypertension of type of yang-hyperactivity due to yin-deficiency," *Chinese Acupuncture & Moxibustion*, vol. 26, no. 2, pp. 91–93, 2006.